Monolith

100% Hemp and Lime

Tom Boom

Master's Thesis | Building Technology

MSc. Architecture, Urbanism and Building Sciences

True innovation potential lies in reinventing
how we build with natural, traditional materials:
introducing them to modern manufacturing,
without changing their essence.

MSc. Architecture, Urbanism and Building Sciences | Building Technology

Faculty of Architecture and the Built Environment

Delft University of Technology

Mentors	Dr. Olga Ioannou
	Prof. Dr. Martin Tenpierik
Delegate Examiner	Dr. Daniel Hall

Acknowledgments

Thank you to Olga and Martin, thank you to everyone at GroupA Architecten, thank you to everyone else at the Keilepand, thank you to Evelyne and Mathieu from EXIE, thank you to Boudewijn and Maarten from YOMABOUW, thank you to Alex from Woodwave, thank you Kirsten and Robbin from Quooker, thank you to Andre from FactoryLab, thank you to Fred. Thank you to Joost, Merijn, Ruben, Hidde and Max.
Thank you to Folkert.
Thank you to my family.

Tom Boom
Rotterdam, June 2025

Abstract

Modern wall systems are constructed by overlayering toxic, petrochemical materials. Hempcrete can replace this complex stack as a monolithic wall that serves structure, insulation, moisture buffering, acoustic damping and fire resistance in one single material. Hemp shiv and a lime binder form a self-supporting mass whose performance depends parameters like density, compaction methods, binder-to-hemp ratio and shiv orientation. Under a 75% end-of-life recycling scenario, hempcrete removes a net 14 kg CO_2-equivalent per functional unit from the atmosphere, making it a carbon-negative building material. Field observation on a full-scale hempcrete wall show that the manufacturing workflow is still artisanal, subjective and weather-dependent, leading to high labour demands and unreliable wall performance.

This research aims to produce a self-standing and insulating hempcrete wall with predictable performance. An experiment is set up, varying manufacturing parameters: layer height, compaction factor, orientation and binder type. Layers thinner than 10cm and compaction above 50% prevented interlayer density gradients, preserving hygrothermal properties and providing a safe mechanical margin. Top-down compaction increased compressive strength exponentially, but showed big settlement. Monolithic hempcrete still needs extra stability. Strategies proposed in this research include altering mix design, section geometry or integrating natural reinforcements. However, life-cycle recalculations show a carbon-neutral ceiling: further increasing density, binder ratio or wall thickness should be done with care, to keep the overall emissions net-negative.

Keywords

Hempcrete, hemp-lime composite, monolithic architecture, biobased, regeneration, prefabrication, automated manufacturing

Fig 0.1 Hempcrete panel sample

Content

Introduction

Literature & Field Research

The Basics

The Material

The Manufacturing

Automating Hempcrete

Experiment Design

Ramming

Sample Production

Testing

Drying Test

Hotbox Test

Compressive Test

4 Point Bending Test

Discussion & Conclusion

Bibliography

Appendix

Introduction

This chapter sets the research context, introduces hempcrete and outlines the project's method, structure and research questions

Fig 1.1 Hempcrete close up

Monolithic Architecture

Monólithos

The word monolith finds its origin in the ancient Greek words: μόνος (mónos) meaning “single” or “one,” and λίθος (líthos) meaning “stone.” Put together (monólithos), the term literally means “one stone,” which is why it is used for any structure or object made from a single, solid piece of material. Well known geological monoliths are Uluru/Ayers Rock in Australia or the Stonehenge in England. The church of Saint George in Ethiopia (figure 1.2) is carved out of solid rock, representing one of the most early and basic architectural monoliths.

According to Sturgis & Davis (2013), in modern engineering and construction, monolithic architecture refers to structures constructed from a single continuous material, forming a unified and solid mass, instead being composed of separate components, like bricks or panels.

Earth

Natural materials as cob and earth and have been built with for ages: casting thick layers into simple timber formwork, producing walls that were both structural and the envelope in one seamless pour. The adobe builders of the Ait-Ben-Haddou village in Morocco (figure 1.3) combined earth, straw and gravel that cured into a single rock-like mass. No joints or additional material layers were required: strength, thermal mass and moisture buffering all come from a unified, locally sourced material. The earth was dug from below the foundations and carried in tubs to the formwork. No transport, no chemicals, zero waste.

Fig 1.2 Church of Saint George, Lalibela, Ethiopia

Fig 1.3 Monolithic Earth Architecture, Ait-Ben-Haddou, Marocco

Fig 1.3 Monolithic Earth Architecture, Ait-Ben-Haddou, Marocco

Overconsumption

The straightforward, monolith construction method of early earth buildings gave them durability and minimal environmental impact while still delivering the enough performance.

In construction today, this simplicity is lost. In the search for more and more performance, cross sections of modern buildings are made up by overlaying membranes, foams, vapour barriers, difficult connections, adhesive layers and increasingly complex technical installations. These are very material intensive and can often not be separated at end of life, resulting in waste that is being incinerated (examples in figures 1.5 & 1.6).

One century ago

Looking back only a century ago, the increase in material use per person then and nowadays is striking. Around 1900, materials like concrete and synthetic insulations were not produced and used at all. But today, they dominate construction.

In the early 20th century, the material use and design of homes were simple and practical. Houses were constructed using solely locally sourced materials. Installations were minimal, typically limited to basic light fixtures, chimneys, and shared neighborhood facilities. Research by HCVA (2024) reveals how material use per inhabitant has changed over time. For a typical household around 1900, the material breakdown per person included only a small variety of materials, including bricks, wood, cement, plaster, paint and glass (figure 1.4).

The average living space per person was about 13 m^2 around that time. Carbonlab (2024) calculated the contribution of the used material to CO_2 emissions per square meter: 388 $kgCO_2eq/m^2$.

Key contributors were bricks and roof tiles. When recalculated to emissions per person living in the house, this results in 3978 kg, comparable to the emissions from driving a car once around the world (figure 1.4).

Nowadays

Since 1900, the shift in living standards has enormously increased environmental impact of our buildings. Today, the average living space per person has increased to 41 m^2, resulting in emissions per person equivalent to 4.5 car trips around the world. (Carbonlab, 2024). Traditional materials like brick and wood, once used for load-bearing structures, are now only mostly used for facades only (ibid.).

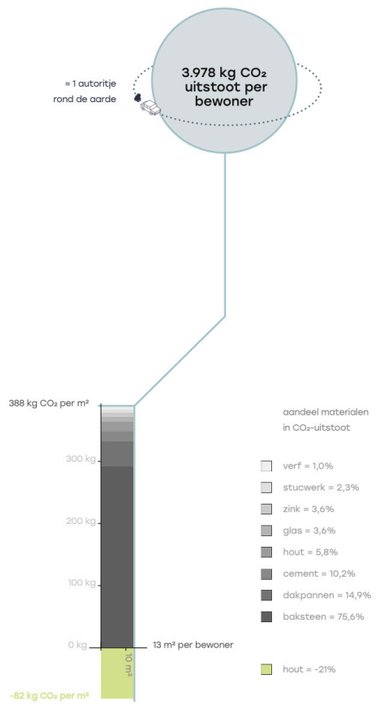

Fig 1.4 Material use, single-family row house, around 1900

Fig 1.5 PVC pipe with PUR-foam insulation stuck to it

Fig 1.6 Various kinds of insulation boards with aluminium and plastic layers attached

Petrochemical Industry

IBN Germany (n.d.) categorizes materials into three groups: mineral, biobased and synthetic. In short, mineral materials, like stone, concrete and brick, are extracted from the earth and have been foundational in construction for centuries. Biobased materials, such as wood and straw, are derived from renewable resources and have been combined with minerals for their natural insulation properties and the ability to regulate indoor temperatures. The third, synthetics, have only been here since the petrochemical revolution.

Synthetic Materials

Synthetic materials are artificially created through chemical processes rather than being naturally sourced. After the Second World War, synthetic materials experienced an exponential rise in usage (Carbonlab, 2024). Their production rapidly overtook biobased and mineral materials and has since remained dominant in construction. This shift was largely driven by the demand for cost-effective, scalable building solutions in a post-war world. Synthetic products offered lightweight, durable and seemingly energy-efficient solutions for modern buildings.

However, their rise has come with significant environmental and health concerns. Synthetic materials are often associated with high embodied energy. The blind assumption that "any extra energy consumed for production will be worthwhile for the energy savings further down the line" (Sparrow & Stanwix, 2014), does not add up.

Research from the Centre for Alternative Technology (2010) adds that many synthetic solutions consume more energy in their production than they save over 20 to 30 years to use.

Toxic Insulations

And it is not only energy consumption that is the issue, the production and use of synthetic materials releases harmful volatile organic compounds (VOCs) and other toxic chemicals, such as fire retardants, into indoor air. Combined with the airtight construction techniques required to maximize their efficiency, this can lead to poor indoor air quality (USEPA, 2024). To solve this problem, active mechanical ventilation and heat recovery systems are often installed, further increasing the buildings lifetime energy consumption (Hens, 2012).

Vapour permeability

The cheap availability of synthetic materials, which are usually not vapour permeable, resulted in poorly considered 'insulation' work on older buildings (Sparrow & Stanwix, 2014). The use of inappropriate materials often stopped the naturally breathing wall from working properly and resulted in damage to the structure. No moisture was able to freely pass in and out of the building fabric as water vapour.

Since our buildings are being made more airtight and insulated, in an effort to reduce greenhouse gas emissions, there is concern that higher humidity levels could cause health problems if they are not correctly ventilated (Sharpe et al., 2015) (Hall et al., 2013).

This makes it important to maximize buildings ability to buffer moisture. There is also evidence to show that using water vapour impermeable insulation layers (like in figure 1.7) without a full understanding how they will affect the moisture balance in the building, could lead to mould growth and structural damage (Künzel, 1998).

Fig 1.7 Oil refineries producing the raw material for petrochemical insulation materials

Fig 1.8 Worker insulation a home with toxix polyurethane foam, wearing a protective suit and mask against VOCs

Introduction to Hempcrete

Natural materials

A different path is possible: one that replaces the complex, petrochemical, non-breathable facade layers for a monolithic wall, grown from natural materials. These have a proven track record over thousands of years in providing healthy buildings, made from nothing more than earth, plant fibres and a mineral binder.

Such materials meet every benchmark Sparrow and Stanwix (2014) set for truly future-proof construction. They:

- are sourced locally,
- renew quickly,
- require little manufacturing energy,
- offer good thermal performance,
- contain no toxins and
- can return harmlessly to the soil at end-of-life (Elnagar et al., 2024).

While storing a lot of carbon, slow-growing hardwoods such as oak, are not able to renew themselves quickly enough to be a sustainable resource. But fast-growing, annual crops, like hemp, meet very item on the list above.

Carbon capture and renewability

"Research suggests hemp is twice as effective as trees at absorbing and locking up carbon, with 1 hectare of hemp reckoned to absorb up to 22 tonnes of CO_2 per year, more than any woodland."

- Jeremy Plester, 2022

Modern monolith

Hemp, harvested every 4 months, supplies the insulating part of a modern monolith, while lime being the mineral binder providing structural rigidity and durability. Together they form hempcrete: a vapour-open, carbon-storing biocomposite that needs no additional foams, plastic membranes or chemical fire retardants (Ingrao et al., 2015).

The hemp and lime are mixed with water and cast in-situ into a formwork to form a wall. After firmly compacting the mixture, the formwork can be taken off, allowing the lime to cure by carbonation: hardening out by reacting with CO_2 from the air. When the wall's service life ends, the hemp shiv can biodegrade or be reused, and the lime has carbonated back to stone, closing the material loop.

Returning to such regenerative, monolithic architecture would let modern construction regain the simplicity that early earth buildings achieved, while delivering present-day comfort and performance. In this way, the waste, pollution and complexity of multi-layered envelopes can be avoided.

Hempcrete construction

Efforts by the European Union and the Dutch Government to encourage the development of a regenerative economy, led to a growing interest in building with hempcrete (BKZ, 2023). An example is the Voorst Town Hall in Twello, completed in 2023, which is currently the Netherlands' largest hemp-lime facade (Figure 1.9). Even bigger scale is anticipated at Quooker's new factory, where a 1200 m² hempcrete plinth is scheduled for completion in late 2025 (Figure 1.11).

Fig 1.9 Town Hall Voorst: Hempcrete facade

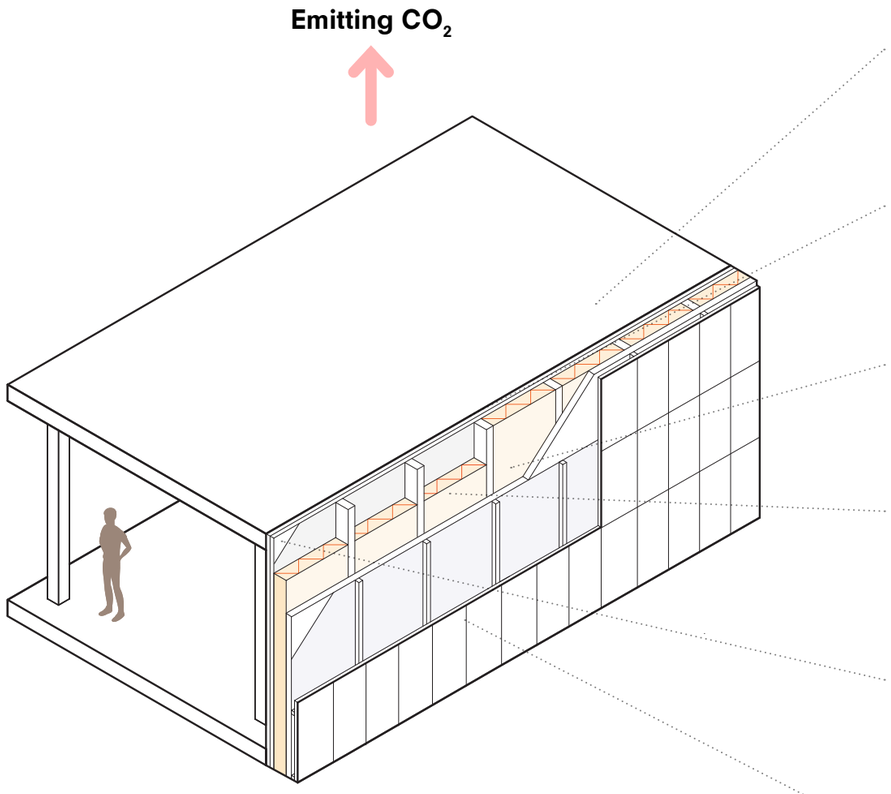

Fig 1.10 Layered wall system: Each layer only serving one function and emitting carbon during production and at end of life

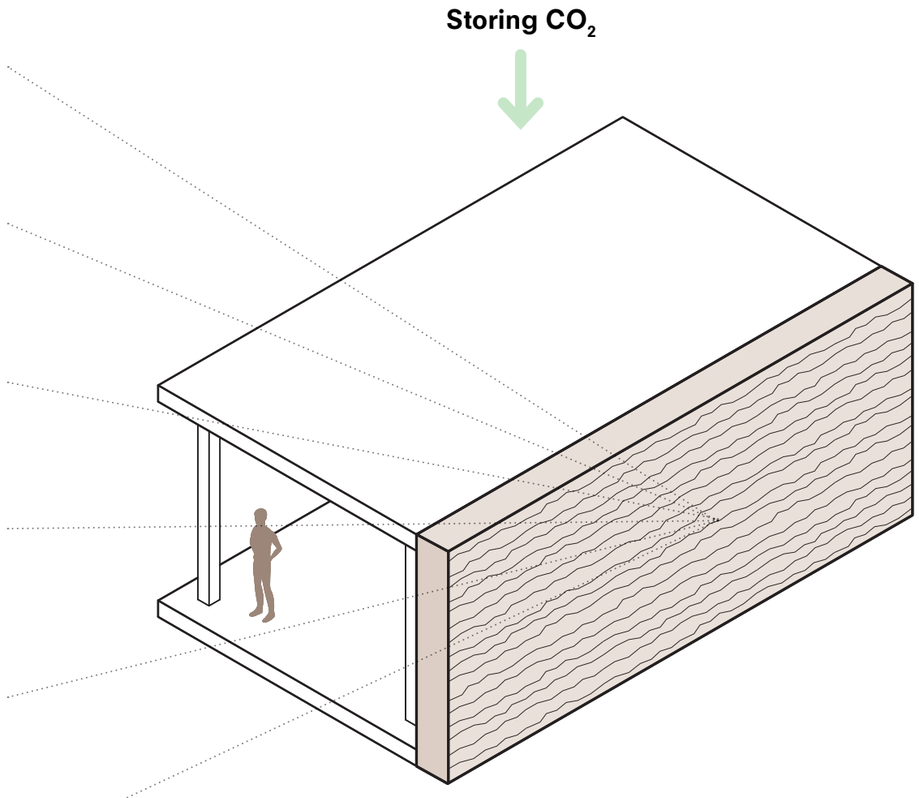

Fig 1.11 Monolithic Hempcrete wall: serving all functions in one material while storing carbon during its life cycle

Structural
support

Insulation
thermal

Moisture
regulation

Acoustic
damping

Fire
resistance

Finishing
durability

Petrochemically Based	Hemp Based
40% of all green house gas emissions are produced by the construction industry	**91 kg** of CO_2-eq is sequestered in one cubic meter of hempcrete
1.2 million barrels of oil are used to heat homes per day in the Europe	**50-80%** energy use reduction for heating and cooling in hemp structures
100.000 additional barrels of oil are used by the construction sector	**22 tonnes** of CO_2 is absorbed by one hectare of industrial hemp
12 kg of toxic pesticides are used by farmers per hectare each season	**0** toxic pesticides or fertilisers are required by farming industrial hemp
2.3 billion tonnes of construction waste was generated in 2020 wordwide	**0%** on-site waste with hempcrete

Fig 1.12 Petrochemically based vs. hemp based construction material comparison

Petrochemicals vs Hemp

A comparison between the environmental impacts of petroleum and hemp based construction products is shown in figure 1.10. Petroleum-based building products bring a long list of environmental problems. They are made from non-renewable oil, take a lot of energy to produce, and leave behind toxic pollutants. Comparable hemp-based products do the opposite: they need less process energy and they store carbon.

Hempcrete is a good example. Most of the wall is hemp shiv, a plant material that can be grown close to the site. Hemp is easy to farm and needs hardly any pesticides because its dense canopy keeps weeds down (Van der Werf, 2004). Making lime does release CO_2. Yet several studies still rate hempcrete lower in impact than standard wall systems. The reason is twofold. First, the hemp plant takes up a lot of CO_2 while it grows (Ingrao et al., 2015). Second, the lime binder pulls some of its own CO_2 emissions back from the air as it cures (Bing et al., 2023). Put together, these effects mean a hemp-lime wall causes far environmental harm than a wall built with petrochemical insulation.

Fig 1.13 Impression of Quooker Factory

Method

Problem Statement

The supply of industrial hemp in Europe has risen more than six-fold since 1993 (Tilstra & Beatrice, 2024). It is pushed forward through EU and Dutch policies and initiatives such as Building Balance, that link farmers, processors and builders (BKZ, 2023). However, the construction industry still leans on petrochemical insulations. Bisschop et al. (2023) argue contractors prioritize material quality, and more importantly: the ability to demonstrate that quality. In other words: materials with a proven, standardized method of use.

Currently, the construction of hempcrete walls is limited to a small group of hemp-lime-building specialists, who rely on subjective techniques and work largely “by feel” (Risinger, 2020). The workflow is slow, labour-intensive and hard to quality-check. This reliance on non-standardized methods makes it challenging to scale hempcrete as a widely accepted building material and create enough demand to match the growing hemp supply. Unless the hempcrete manufacturing workflow is modernized and scalable, the sector will miss a chance to replace complex, polluting multi-layered facade systems with monolith hempcrete walls.

Objective

The goal of this research is to produce a self-standing and insulating hempcrete wall element in a way that reliable material performance is secured.

Because reliable data on hempcrete performance is still rare, the study begins at the purest material level. First, it examines the fundamentals of the raw mix itself, in pure form, when no machinery is involved. Next, it looks at the current workflow to see how that process affects the material’s performance in full scale hempcrete walls. Only after this foundation is laid does the project move to automation. An experiment then explores how hempcrete’s performance changes when critical manufacturing parameters are varied.

Scope

This study uses only pure mixtures of hemp shiv and hydrated lime; mixes containing additives, stabilisers, or reinforcement in any form are not considered. It evaluates hygrothermal and mechanical performance within the Dutch Bouwbesluit 2012 framework. Details of the experimental set-up appear in chapter 6, while the individual test methods are described in chapters 8-11.

Research Questions

Main research question

How can a monolithic hempcrete wall be manufactured in a way that reliable material performance is ensured?

Subquestions

- What key fundamentals of hempcrete define its overall material performance?
- How do current manufacturing techniques (in-situ and prefab) affect the performance of hempcrete walls?
- How does varying manufacturing parameters affect the hygrothermal and mechanical performance of a hempcrete wall element?

Research Outline

This research consists out of three parts, building up to research how a hempcrete wall element can be manufactured by using an automated system.

Part A: Literature & field research

The first part combines a literature review with field research to gain an understanding of both the fundamental performance of the material and its currents manufacturing methods.

It starts with introducing the basics of a hemp-lime build, describing its raw components and how they interact. Afterwards a deeper dive is done into the behaviour of hempcrete in relation to its porosity, anisotropy and hygrothermal and mechanical properties. Then, on-site insights observed while building a hempcrete wall in practice are described. Manufacturing areas where automation could offer improvements are noted.

Part B: Experiment

An experiment was designed that explores how varying parameters in the manufacturing process (such as compaction factor, layer height, and orientation) influence hempcrete’s performance.

A series of samples were produced and tested on key hygrothermal and mechanical properties. They specific methodologies are provided separately for each test. This experiment builds directly upon the insights gained from the literature and field research in part A.

Part C: Discussion and Conclusions

Lastly, test results are interpreted and corralations between the experiment variables and sample performance are drawn. Afterwards, their broader implications are reflected on.

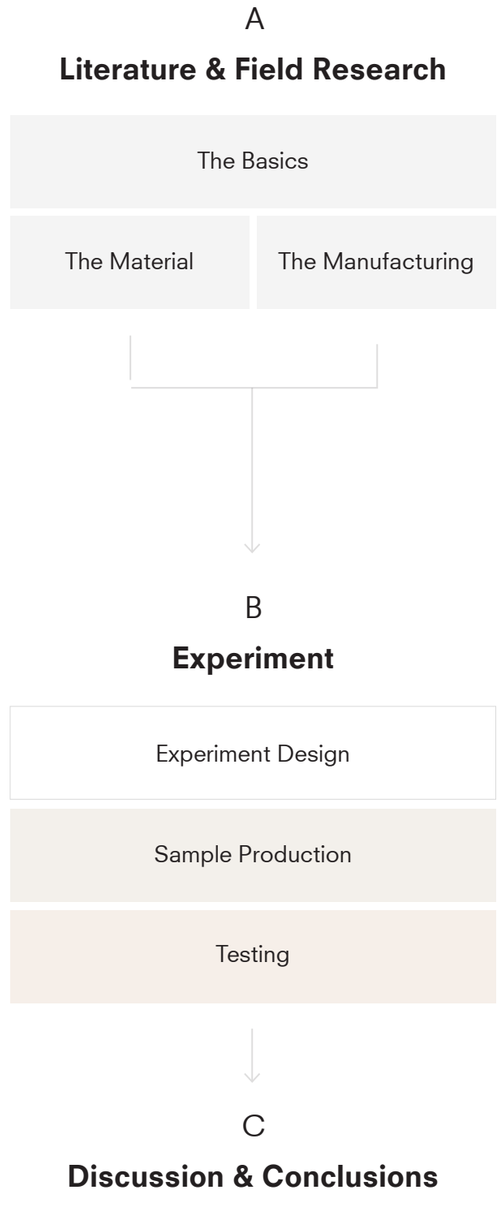

Fig 1.14 Research Framework

The Basics

This chapter outlines the fundamentals of hempcrete, focusing on the cultivation of the hemp plant, the extraction of lime, and the core construction principles of a hemp-lime building system.

Fig 2.1 Two buckets of freshly mixed hempcrete

Industrial Hemp

The hemp plant is extremely versatile. Almost every part of the plant is used for high value applications. The hemp used for making hempcrete is the so called industrial hemp; *Cannabis Stativa L*. It is named industrial hemp to distinguish it from the narcotic "brother" used to produce the cannabis drug. However, industrial hemp is grown specifically for its high yields of strong fibers, and does only contain low amounts of THC, the active psychoactive ingredient in the cannabis drug. (Dhondt & Munthu, 2021).

History of Hemp

Growing and using industrial hemp as a crop is a far from recent development. Cannabis Stativa is one of the earliest domesticated plants. It is thought that the plant originated in China, with evidence of its cultivation back to the Neolithic period. The most early used of hemp were pottery, textiles, fibers for clothing, ropes and sails, paper, mortars and plasters and also as a food source (Robinson, 1995). Of the more than 200 products made from hemp today, many are still produced using very traditional techniques (Mears et al., 2020).

The word "canvas" even finds its origin in the word cannabis, meaning "fabric made from hemp" Ancient civilizations such as the Egyptians, Greeks and Romans highly valued hemp for its utility, with records showing its importance for trade, lifestyle and empire expansion (Robinson, 1995).

In Europe, hemp cultivation has a long history, first introduced by the Romans and later encouraged by English kings. Its strategic importance was shown during Napoleon Bonaparte's failed invasion of Russia, where he wanted to destroy Russian hemp supplies that were being used by the British Navy, his enemy at the time (Robinson, 1995).

The plant's use went further than only practical applications. Hemp has long been used in religious ceremonies and as a recreational drug. This association led to a prohibition of all hemp strains in most Western countries during the early 20th century. Hemp was classified as a narcotic, and its cultivation, whether for psychoactive purposes or industrial uses, was banned worldwide (Sparrow & Stanwix, 2014).

From the 1930s, efforts began to develop hemp strains with minimal THC, and countries slowly started regulating cultivating industrial hemp. Today, industrial hemp (with less than 0.2% THC; compared to 10–15% in drug-producing varieties) is legal and widely grown.

Growing Hemp

The hemp plant grows extremely fast, reaching heights of four meters within four months. It has a thin and hollow stem, with a diameter from 4 to 20 mm (Sparrow & Stanwix, 2014). One hectare of hemp cultivated for its fibers and shivs can yield 6 to 15 tons of dry plant biomass per harvest. At least half the plant consists of shivs, 20 to 30% of fibers and the remaining is dust and shivs too small to process (ibid.).

Because the plant has very long and sturdy roots, it can penetrate deep into the soil and is able to grow on relatively poor soils and in nearly all climates. Hemp cultivation requires little to no chemical fertilizers or pesticides and even enriches the soil (van der Werf & Turunen, 2008). After harvest 20 to 40% of the crop remains in the field. These are the roots, leaves and tops. The nutrients left behind are valuable for cultivating the next crop (Hempflax, nd.).

Fig 2.2 Cannabis Stativa L.

Fig 2.3 Young hemp field at the Quooker building site, Ridderkerk

Fig 2.4 Close up of a single hemp plant

The Plant

Fibers

The hemp fibers are obtained from the bast, or outer layer of the stem. Hemp fibers are lightweight, strong and have great tensile properties. They are long and flexible, ranging from about 1.2m to 2.1m in length (Sparrow & Stanwix, 2014). Therefore, they are used in numerous applications, such as building and insulation materials (mostly insulation mats), as well as in the automotive and paper industries.

Shivs

The inner woody core of the hemp stem is called the ‘shiv’ (or ‘shive’ or ‘hurd’). These short, woody fragments appear once the outer fibers are removed from the stem. They have a high water absorption capacity. Due to their high porosity and specific pore structure, they can absorb and release 2 to 4 times their weight in water (Arnaud & Gourlay, 2012). Traditionally, the shivs were mostly considered a byproduct, because hemp cultivation used to be focused on the more in-demand fibers.

Seeds

Both the seeds themselves and hemp seed oil coming from it, are used in the food, cosmetics, and leather industries. They are rich in protein, healthy fats, vitamins and minerals. The seeds are also processed into birdseed and other animal feed (Hempflax, n.d.). The hemp plant in its whole state can be used as a biofuel by combustion.

Shivs

In hempcrete, only the shivs are used. Certain requirements are set for the shivs, including their length, color and degree of retting.

Degree of retting

After harvesting the hemp stalks, the fibers are separated from the stem through a retting process. The mowed stems are laid out in rows in the field to dry and ret. Under the influence of UV radiation and alternating wet and dry conditions, the ‘pectin’ (a chemical found in plants, which binds the shivs and the fibers together) breaks down. Both the quality and the color of the shivs are affected by the degree of retting (Snauwaert & Ghekiere, 2011).

Shiv length

Shivs measuring between 10 and 25 mm are favorable for achieving a good matrix structure in cast-in-place hempcrete (Sparrow & Stanwix, 2014). However, several studies on hempcrete using small shivs (3 to 9 mm) have shown that compressive strength increases with smaller shives (Arnaud & Gourlay, 2012) (Niyigena et al., 2018). Too small shivs must be avoided, because they can absorb too much of the mixing water and disrupt the curing process of the mixture.

Colour

Hemp shivs should have a light beige-gray colour. Deviating colours indicate shivs that are not suitable for hempcrete construction. Green indicates that the hemp was not fully grown, brown indicates a drying issue in the field and a blackish colour indicates mould (Arnaud & Gourlay, 2012). The is no research found about potential changes in mechanical properties based on the colour of the hemp shivs.

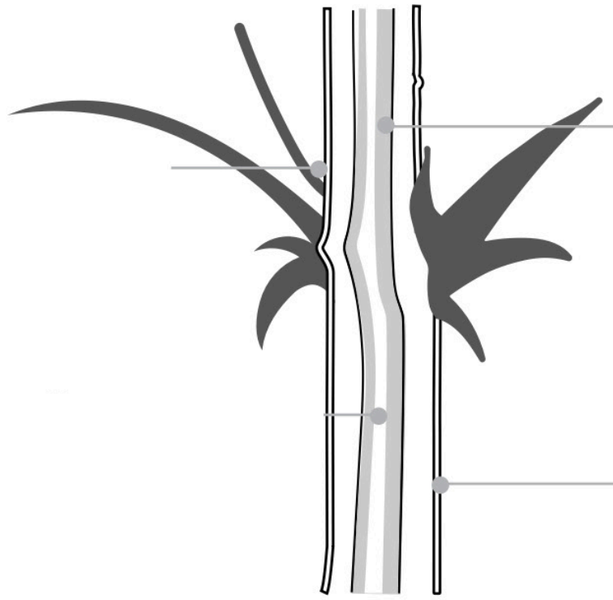

Flowers

- Psycho-actives
- Cosmetics

Seeds

- Food (protein source)
- Oil
- Lubricants
- Ink

Shivs

- Mulch
- Fiberboard
- **Hempcrete**

Fibers

- Netting
- Canvas
- Carpet
- Clothes
- Bio composites
- Insulation

Stalks

- Biofuel
- Paper products
- Cardboard

Fig 2.5 Hemp Plant structure and uses

Lime

This research aims to find an alternative to toxic, synthetic, petrochemical-based building products, so that our buildings can be built using only natural, non-toxic and healthy materials. It is clear that using hemp positively contributes to this goal. The lime in the hempcrete mix also positively contributes to the health of the space and its direct environment.

Lime is the collective name for a number of minerals, substances that occur in pure form in nature. It originates from sources of calcium carbonate ($CaCO_3$), such as rocks or shells. These have been used extensively as a building material throughout history.

In the hempcrete mix, lime acts as a binder. It 'sticks' to the silica of the hemp hurds. Because of its naturally high pH, lime acts as a natural fighter against mould and fungus, making it an antimicrobial material (Knapen et al, 2020). It completely coats each hemp shiv, preventing mould from building up in humid conditions.

Other etymological terms such as kalk (Dutch) and calce (Italian) refer directly to the description of glue (Mears et al., 2020).

Fig 2.6 Supercalco 97 by Carmeuse

Air Lime (Hydrated Lime)

Lime is mainly sourced from limestone quarries. To transform natural limestone, or $CaCO_3$ into a binder ready for construction, the raw material is heated in an oven to a temperature of 750-900°C. This causes it to chemically change: Carbon dioxide (CO_2) is released, and calcium oxide (CaO) is left behind. CaO is better known as *quicklime*, a highly reactive, bright white powdery substance.

When mixing quicklime with water, a process called "slaking", calcium hydroxide is produced ($Ca(OH)_2$). This is referred to as *hydrated lime*. (Van Balen et al., 2003). Other common names are slaked lime, putty lime or air lime.

Air lime comes as a fine powder or lime paste and forms the basis for the binder used in hempcrete. It will harden slowly by 'carbonation', a reaction with the CO_2 from the air (idem.). This entire cycle, from raw material to hardened binder, is referred to as the 'lime cycle'.

Hydraulic Lime

The setting of air lime via carbonation is a very slow process. Therefore, it is not suitable for all applications. Stonemasons found out that different types of limestone (depending on the purity of the material) produce different types of building lime. They started experimenting with this and so introduced many lime variations (Sparrow & Stanwix, 2014).

Hydraulic lime is produced from limestone containing a certain percentage (10-25%) of clay. These either occur naturally or are added. A lime is produced that is able to set relatively quickly on exposure to water (hydration), instead of slowly on exposure to air only.

Pozzolans

The carbonisation process is slow because the concentration of CO_2 in the air is low and the diffusion of CO_2 through the lime progresses slowly, always from the surface inward (Van Balen et al., 2003).

To speed up the process, small amounts of additive binders (or pozzolans) are often added. Some examples of pozzolans are volcanic ashes (such as pozzolana, found in Pozzuilo, which inspired for the name), crushed clay brick dust or pulverized fly ash. (Knapen et al., 2020). When adding these pozzolans to air lime, it can cause a hydraulic effect like that of naturally occurring hydraulic lime.

Choice of Lime in Hempcrete

Air lime and hydraulic lime differ in properties. In its most pure form, air lime has high vapour permeability but low stiffness (Arnaud & Gourlay, 2012).

To improve these drawbacks, small amounts of hydraulic components or pozzolans are added to hempcrete binder mixes. These must be carefully balances and tested (Knapen et al., 2020).

Mechanical strength

Because of the slow carbonation process of the lime binder in hempcrete, it can take more than a year to achieve its final mechanical properties (Colinart et al., 2012). For cast-in situ hempcrete, it is important that it quickly reaches a compressive strength sufficient to support its own weight. This ensures that the formwork can be removed shortly after casting, allowing the drying and further curing of the hempcrete wall to proceed. Most commercial limes available satisfy this requirement

Breathability

Another key issue is the vapour permeability of lime, and the way in which this helps the building to keep a good health (Sparrow & Stanwix, 2014).

Therefore, strong hydraulic binders, being far less vapour permeable are not recommended for use in hempcrete. The slow carbonation process of air lime or lightly hydraulic lime gives better results than the rapid reaction of strong hydraulic limes.

Lime and Water

The third, and last component of hempcrete is mixing water. Although it is expected to evaporate out of the mix during drying, mixing water is essential for both air and hydraulic lime during curing. It gives the hempcrete a certain consistency and cohesion, which is needed for casting in-situ.

The amount of water and the method of adding it during the preparation of hempcrete are crucial for both the workability and the performance of hempcrete. On the one hand, sufficient water must be added to allow complete curing and to make the mixture workable. On the other hand, an excess of water should not thin the binder to the point that the binder becomes too weak to support the hempcrete's own weight (Sparrow & Stanwix, 2014).

The thermal performance is also influenced by the presence of moisture. During its drying phase, hempcrete temporarily has less effective insulation properties. The thermal conductivity of a non-dried wall is higher than that of a dry hempcrete wall (Collet & Pretot, 2014). Too much excess water also results in longer drying times (Colinart et al., 2012).

Drying

Not only the curing, but also the drying of hempcrete is a slow process, therefore, drying conditions should be optimised to improve the curing and prevent mould formation.

It is important not to confuse the drying and curing processes. Curing occurs through hydration reactions of the (hydraulic components) of the binder with water, as well as through carbonation. For carbonation to occur, CO_2 must penetrate through the exterior of the hempcrete. In very humid conditions, the diffusion of CO_2 is hindered, but very dry conditions are also unfavourable for carbonation. Once carbonation occurs, the excess moisture must evaporate. Drying helps the carbonation reaction, giving hempcrete its final strength. Therfore, the amount of mixing water plays a big role in the drying and curing process (Colinart et al., 2012).

Additives

To improve curing speed, additives, including both hydraulic and organic components, as well as pozzolans, are added to the hempcrete mix. (Sparrow & Stanwix, 2014). Some additives retain water. This ensures that sufficient water remains available for the curing reaction. Others improve the accessibility of air (and thus CO_2) within the hempcrete (ibid.).

Natural pigments can be added to the hempcrete mix al well, to add colour to individual layers and make them stand out. These are derived from natural minerals or plant-based sources.

Fig 2.7 Limestone quarry in Northern France

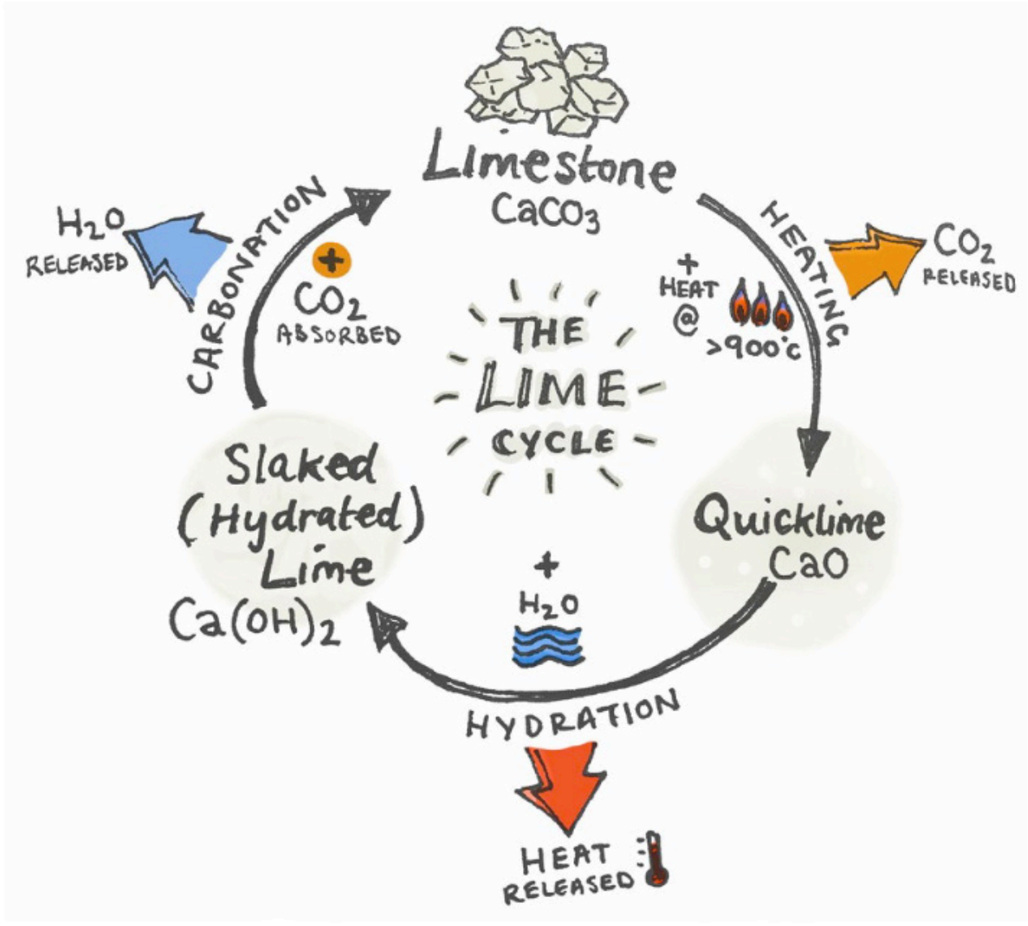

Fig 2.8 The lime cycle

The Lime Cycle

Figure 2.8 summarizes the lime cycle, the chemical process that describes extracting limestone from the ground, heating it in a oven, boiling it in water to allow slaking to occur and producing a lime putty that can be transformed back into solid limestone by carbonisation.

First, limestone is mined from the earth and crushed at the quarry. At this point, the limestone is safe to touch. Afterwards, the rubble pieces are baked in ovens. When they come out, they become dangerous to handle. This baking process releases carbon dioxide into the atmosphere. Although harming the earth, this process is needed to transform limestone into lime. The baking colours the lime a chalky white and halves its original weight.

The lime is then cooked in a pool of water, a process known as slaking. This transforms the once solid lime into a thick liquid. The resulting substance, lime putty, is safe to touch and can be used to produce air lime powders. It can be mixed with materials to choice, and when exposed to CO_2 again (e.g. from ambient air), it slowly transforms back into solid limestone, closing the lime cycle.

Limestone
$CaCO_3$

Fig 2.9 Limestone

Quicklime
CaO

Fig 2.10 Quicklime

Air Lime
$Ca(OH)_2$

Fig 2.11 Air lime

Hempcrete
$CaCO_3$

Fig 2.12 Hempcrete

The Mix

Fig 2.13 Freshly mixed, wet and fluffy Hempcrete

Cast-in-Situ

Hempcrete is a versatile material suitable for both new construction and renovation projects. It can be applied in walls, floors, roofs, and as plaster. To meet specific performance requirements, its composition and thickness can be adjusted to achieve desired levels of insulation and structural strength. Hempcrete can be applied through various construction methods, including spraying, forming into blocks, or as insulation infill for cavity walls. This research focuses specifically on the use of hempcrete as a cast-in-situ material for exposed facades.

As of today, the workflow of casting in situ is very manual. The hemp shivs, lime and water are mixed in a horizontal pan mixer according to prescribed quantities. The mixture is then carried in buckets to the formwork, where it is rammed in by hand. On the exterior wall, it must be firmly tamped; on the interior wall, it should be looser, ensuring the material can breathe optimally while still supporting its own weight (Junte, 2020). Skilled workers are needed who understand the material and technique, and detailing the work with this material is quite challenging. In short, it's slow and very labour intensive process.

Self-Supportive

Before exploring the properties of cast-in-situ hempcrete, it is important to know that while hempcrete is self-supporting, it lacks enough compressive strength and stiffness to serve as a structural load-bearing material (de Bruijn et al., 2009). This means there is always the need for an exterior load bearing structure. Additionally, an internal frame is typically incorporated to provide stability against horizontal loads acting on the facade.

Fig 2.14 Building of a Hempcrete wall: Cast-in-situ around a wooden stud frame using a formwork

Fig 2.15 Exposed hempcrete facade. Formwork is removed, studs account for load

The Material

This chapter explains how the hemp–lime mixture develops its unique properties, how variations in its composition affect its hygrothermal and mechanical performance, and what its environmental impacts are.

Fig 3.1 Hemporete closeup

Porosity

Pores

Hempcrete is highly porous, with 60-90% of its volume consisting of interconnected pores, which are present in the cellular structure of the hemp shives, between the shives, and in the lime matrix (Nguyen et al., 2010). Due to this porous structure, hempcrete is highly hygroscopic and thus can absorb, store and release moisture from its environment (Collet et al., 2013).

The pores are also responsible for the insulating properties of hempcrete. Its thermal performance strongly depends on the amount of air voids in the cured mixture (Nguyen et al., 2010) (Collet & Pretot, 2014). Conventional, synthetic insulation materials, have a more favorable thermal conductivity value than hempcrete, but it are its pores that gives the material a unique combination of properties that make the material an attractive choice.

Phase Shift

For example, the porous nature of hempcrete gives it interesting thermal inertia. A hempcrete wall can store heat and gradually release it back into a room (Sparrow & Stanwix, 2014), leveling out temperature fluctuations inside. In summer, the outside heat can be transferred to the indoor space with a certain delay, improving the summer comfort of the building. This is called the phase shift, which can take up to 16 hours, depending on the density of the mixture (ibid.).

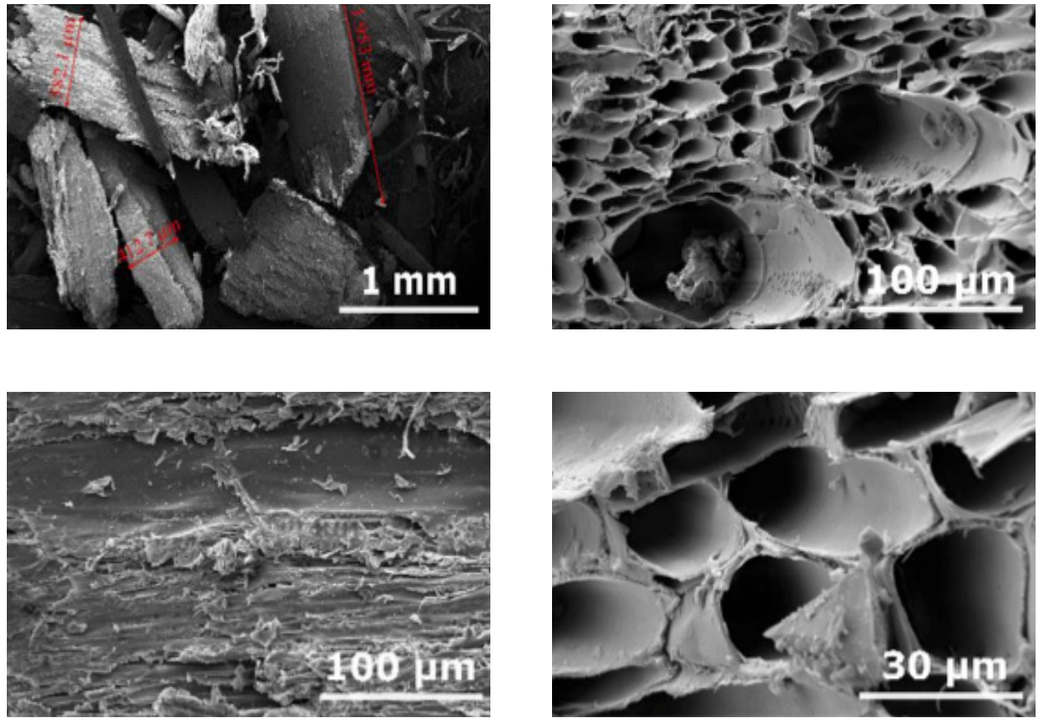

Fig 3.2 Microscopic cross-sectional analysis of hempcrete

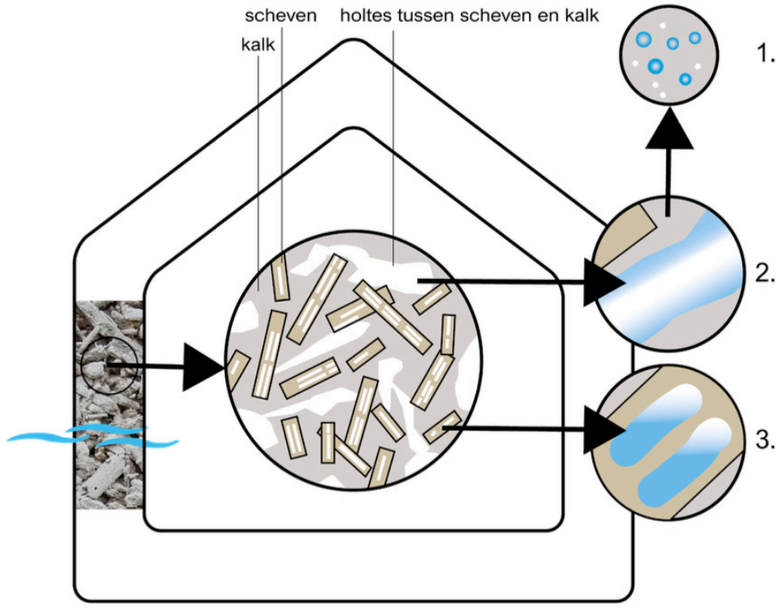

Fig 3.3 Air voids in hempcrete, 1: pores within the lime matrix, 2: pores in between the shivs, 3: pores within the shivs

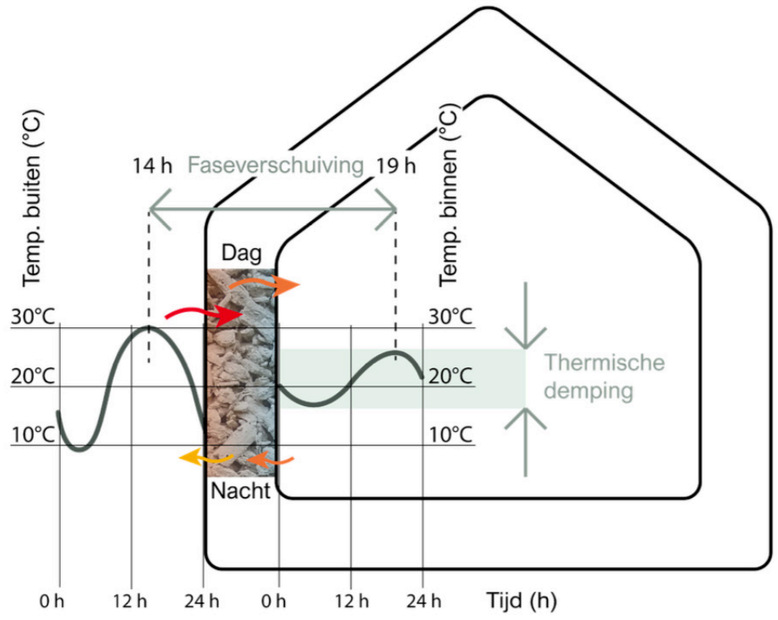

Fig 3.4 Thermal inertia and phase shift in a hempcrete wall

Anisotropy

Hempcrete is a non-uniform material. Its performance depends not only on the mix and compaction but also on how the hemp shiv particles and the pores are arranged inside the wall. These shivs are naturally anisotropic, meaning their shape and structure cause them to behave differently depending on the direction of force or heat (Williams et al., 2016).

Shiv orientation

During in-situ casting, and when compacting the mix from above, the shivs tend to lie flat, stacking up in horizontal layers. From above, they appear randomly oriented, but in section, they follow the layer direction closely. If the material would be compacted from another direction, the path of force or heat will pass through the shivs differently. As a result, the orientation of these shivs, determined during compaction, has a direct effect on both mechanical and thermal performance. This behaviour further explored in the experiment phase of this research.

Literature supports this anisotropic behaviour. Brzyski et al. (2021) observed that hemp particles are much longer than they are wide and due to this geometry, they tend to align perpendicular to compaction. Similar to wood, hemp shivs conduct heat better along their length than across (ibid.). This means thermal conductivity depends on the direction of heat flow relative to the shiv orientation.

Compaction direction

The direction from where the mix is compacted also affects how pores are formed, influencing its behaviour regarding to moisture and heat. Studies into the anisotropy of hempcrete show that compressive loads perpendicular to the compaction direction result in stiffer material with less deformation, and flexural strength is also higher in this orientation. (Nguyen et al., 2010) (Williams et al., 2016).

In short, both hygrothermal and mechanical behaviour of hempcrete is direction-dependent, and therefore shaped by the manufacturing method. This becomes especially relevant when looking at methods here layers might be installed in orientations different from how they were cast.

Figure 3.4 shows an illustration of hemp shivs oriented perpendicular and parallel to compressive loads (gray arrow) and moisture and heat flows (brown arrow). Figure 3.4 shows randomly oriented hemp shivs in the uncompacted part of the hempcrete sample, and flatter orientation in compacted part.

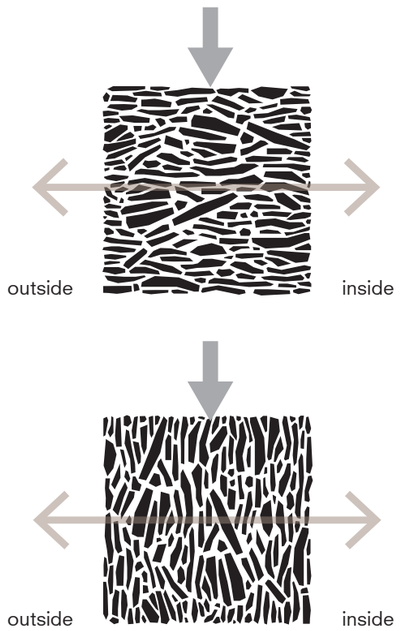

Fig 3.5 Shiv orientation

Fig 3.6 Left part: compacted hempcrete, shivs oriented flat, right part: uncompacted: shivs randomly oriented

Hygrothermal Behaviour

Hygrothermal properties include the characteristics that determine how air, moisture and heat move through the hemp-lime wall. Good hygrothermal design is essential to make sure the building is energy efficient, prevents moisture-related issues, and guarantees a comfortable and healthy indoor climate (Knapen et al., 2020).

Hempcrete and Moisture

Within a building, moisture can exist in various forms. Water vapour is present in both indoor and outdoor air, while liquid water can come from sources as rain or condensation (both internally and on the outer surface). The open-pore structure of hempcrete allows moisture to be transported through its pores (Evrard, 2008). The extent to which moisture moves through these pores is determined by the materials vapour permeability, moisture storage capacity and capillary water absorption.

Vapour permeability

In practice, hempcrete walls are always constructed vapour permeable, or often referred to as vapour open or ‘breathable’. Its only consists of materials that are all open for vapour to pass through, allowing a certain amount of water vapour to through the wall. Moisture that got in the construction is able to dry out more easily. Most hempcrete mixtures show a μ-value between 1 and 3, similar to other vapour permeable materials such as wood fiberboards, cellulose and mineral wool (Knapen et al., 2020).

Breathable walls?

Vapour permeable, but always airtight.

The term ‘breathable’ may mistakenly suggest that air can pass through these walls. However, all building walls, including those made with hempcrete, must always be sufficiently airtight to prevent significant energy losses and moisture issues.

μ-value

The vapour diffusion resistance factor is a dimensionless material property that indicates how many times more difficult it is for water vapour to move through the material compared to a layer of air of the same thickness. Lower μ-value means the material is more vapour permeable.

Hygroscopicity

Building materials react differently to the humidity of their surroundings, depending on their nature. Hygroscopic materials can absorb water vapour from the air and can store a certain amount of moisture without being in direct contact with liquid water. Because of the many pores in the hemp shivs and lime binder, hempcrete is highly hygroscopic. This means it can absorb and retain significant amounts of moisture from the air (Amziane & Arnaud, 2013).

Moisture buffering

For hempcrete to benefit from moisture-buffering properties, it must not only be able to store moisture, but also absorb it quickly enough.

Hempcrete has an excellent moisture-buffering capacity (Collet et al., 2013). This means it responds quickly to changes in indoor humidity. When the air becomes more humid, the wall absorbs more moisture, storing it within the material. Also, when the air becomes dryer, the wall releases the stored moisture back into the room. This process helps stabilize indoor humidity levels (Evrard, 2008).

Capillary water absorption

In addition to water vapour, liquid water can also be present in a hempcrete wall, coming from sources such as construction moisture, condensation, leaks and rain. Measurements by Knapen et al. (2020) show that hemp-lime can transport large amounts of water in a short time due to its high capillary water absorption capacity.

This means that when a hempcrete outer wall is exposed to a water source, such as insufficient protection against rain, it can quickly absorb and transport water through the wall. Excessive water absorption must be avoided (Piot et al., 2017), as it negatively impacts the wall’s thermal performance and increases the risk of degradation, which can occur with all plant-based materials (Sparrow & Stanwix, 2014).

Hempcrete and Heat

Thermal conductivity

Thermal performance of a wall is strongly dependant on the thermal conductivity of the material. Research by Collet & Pretot (2014) and Jami et al. (2019) into the thermal conductivity of in-situ placed hempcrete show a λ-value between 0.06 and 0.18 W/mK, for a density ranging from 200 to 800 kg/m³. The λ-value of synthetic, conventional insulation materials is lower, meaning that hempcrete must be thicker to achieve the same thermal resistance.

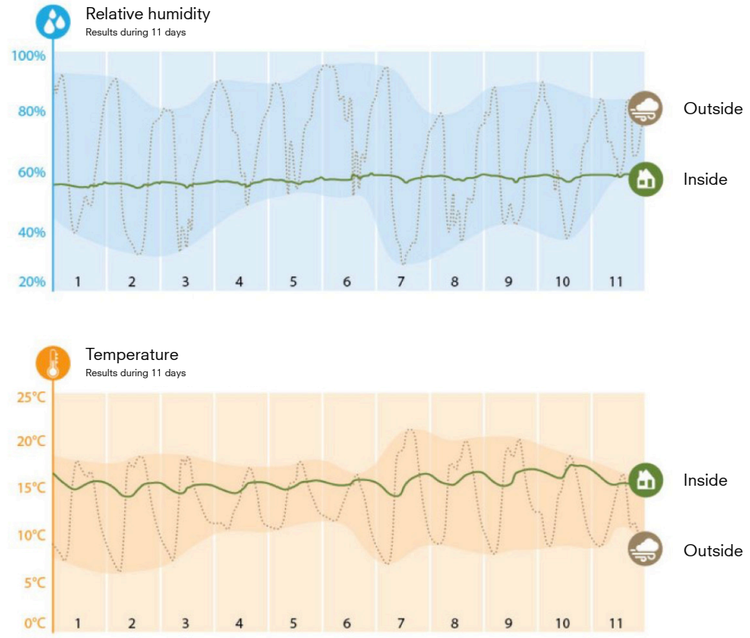

Fig 3.7 Top: Stabalised indoor humidity levels, bottom: Storing heat and gradually releasing it back

λ-value

Thermal conductivity of a material is a property that indicates how much heat flows through the material under a constant heat flow, for a thickness of 1 meter and a temperature difference of 1°C (unit: W/mK). The lower this value, the less heat is lost though the material, and the better it will insulate.

The λ-value of hempcrete increases with a higher material density. Differences also exist between mixtures and manufacturing methods. This is because density is influenced by various factors, such as the degree of compaction, the ratio of hemp shivs, binder and water in the mix, the type of binder and additives, and the size and type of hemp shivs (Jami et al., 2019). Currently, there is no declared λ-value for cast-in-place hemp-lime. Since these mixtures are formed on-site and compacted manually, there can be significant variation in the actual λ-value in practical applications. Different mix ratios or compaction levels will influence the λ-value (Sparrow & Stanwix, 2014).

Shiv direction

Hemp shivs, like wood, have properties that change depending on their orientation, meaning they are anisotropic. Heat flows more easily along the length of the shivs. When hempcrete is compacted, the shivs tend to lie horizontally, and this effect increases with more compaction. In a hempcrete wall, most shivs are oriented from the inside to the outside. Because heat moves through the wall in the same direction as the shivs' length, the wall's insulation might be less effective.

Moisture and the λ-value

When a material absorbs moisture, its insulating capacity decreases. This is because water conducts heat about 20 times more efficiently than the still air within the pores (Collet & Pretot, 2014).

Because of hempcrete's high hygroscopic properties, it absorbs significant amounts of moisture even in environment with low relative humidity. While this benefits indoor moisture buffering, it means that the material insulates less effectively in practice compared to its dry state (Evrard, 2008). If the material becomes fully saturated with water, the λ-value can increase by a factor 4 to 5 (ibid.). Therefore, it is crucial to protect the wall from becoming excessively wet, so making sure it is protected against driving rain.

Thermal inertia

The thermal inertia of a material measures how much heat it can store during changes in heat flow. A wall with high thermal inertia will delay the effect of outdoor temperature peaks inside the building (this is the 'phase shift') and reduce the impact of temperature fluctuations. In other words, it describes the ability of a material to absorb heat from the nearby air and release it again slowly when the air cools down. In old buildings, burning wood was the way to heat, and the thick walls allowed the heat produced by the fire during the day to be slowly absorbed by the wall materials and just as slowly released again during the night (Sparrow & Stanwix, 2014). In summer, it absorbs and holds the heat from the sun during the day to release it at night.

Hempcrete has a low diffusivity, meaning temperature peaks move slowly through the wall. As a result, heat from the external environment is transferred to the interior very gradually. This phase shift can take up to 15 hours, depending on the thickness of the wall (ibid.).

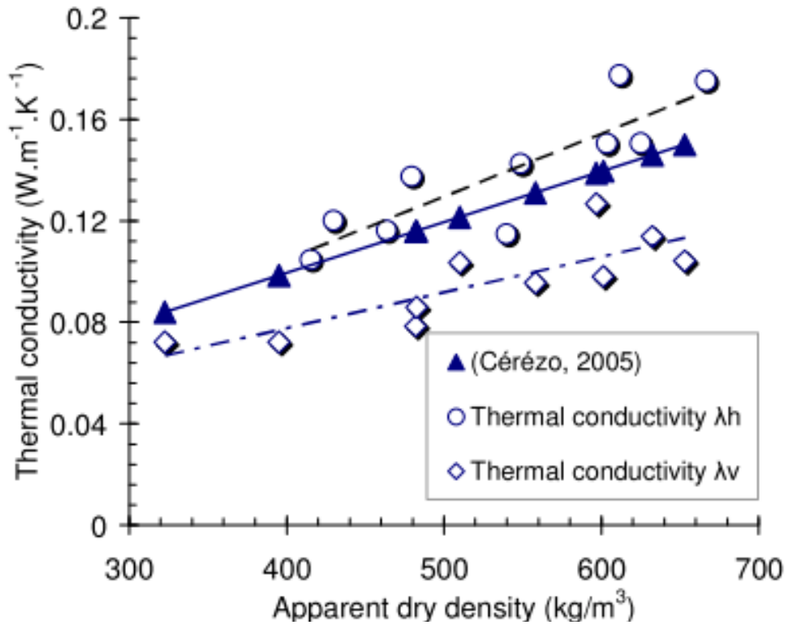

Fig 3.8 Thermal conductivity vs. dry density

Summary Hygrothermal Behaviour

Breathable and moisture-regulating

Hempcrete is a vapour permeable material with excellent moisture buffering capacities. This helps smooth out temporary peaks in humidity.

Highly insulating

Although, compared to conventional insulation materials, hempcrete has a higher λ-value, meaning it must be applied in a thicker layer to achieve the same thermal resistance.

High phase shift

Hempcrete has an interesting thermal inertia, which high phase shift contributes to the inside climate. It's thermal inertia is higher than many other insulation materials, but lower than concrete and bricks.

Mechanical Behaviour

Hempcrete is regarded as self-supporting but can not be used as a load bearing structure. Its mechanical properties depend heavily on the amount of binder and its final density. It takes around three months for freshly cast hempcrete to gain most of its compressive strength. Due to the slow carbonation process, it can take more than a year to gain its final strength (Walker et al., 2014).

Hempcrete in Compression

Compressive strength refers to a material's ability to resist being compressed without breaking or deforming. Because hempcrete is made with natural hemp and can be produced in different ways, its compressive strength varies. Compared to concrete, hempcrete has much lower compressive strength and can not be used as a load-bearing material by itself. Several factors contribute to this limited strength, including the way the hemp shivs are arranged, the flexibility of the hemp particles, the type of binder used, and the material's high porosity (Walker et al., 2014).

The compressive strength of hempcrete is influenced by several factors, including the type of binder, the binder-to-hemp ratio (B/H), the water-to-binder ratio (W/B), curing conditions, particle size, and the method of production. Most studies report compressive strengths below 1 MPa. However, its strength increases over time due to carbonation. Hempcrete cured in outdoor conditions often shows higher compressive strength than samples cured indoors, and some studies have reported outlying values. For example, compressive strengths of 4.74 MPa were achieved by Sassoni et al. (2014). However, these high compressive strengths often include stabilizers, like cement.

Hempcrete in Bending

Flexural strength describes a material's ability to resist bending forces. In experiments by Murphy et al. (2010), the development of flexural strength was studied over time for different hemp contents. Samples with lower hemp content gained strength more quickly, while samples with higher hemp content had lower load-bearing capacity but showed more ductile, flexible failure behavior.

Research also shows that the size and shape of hemp shivs influence hempcrete's shear strength. Smaller particles allow better compaction, while a variation of shapes, rigidity, and surface textures of the shivs increase internal friction and overall stability (Brzyski et al., 2021). Hempcrete is known for its flexibility, meaning it can deform under stress without breaking. In compression tests by Chabannes et al. (2017), hempcrete samples showed high ductility and did not fail even under increasing loads.

Its unique combination of flexible hemp shivs and a stiff binder gives hempcrete the ability to absorb large deformations without cracking. This means it can absorb much energy during lateral stresses.

Fig 3.9 Compressive strength and flexural strength vs. dry density

Summary Mechanical Behaviour

Self-supportive but non load bearing

Hempcrete has limited compressive strength, making it self supportive but non load bearing.
The choice of binder, ratio of binder to hemp and the orientation and size of the shivs strongly affect mechanical performance.

High flexibility

Hempcrete behaves in a ductile manner, allowing it to deform under high stress without breaking.

Other Behaviour

Hempcrete and Sound

A distinction must be made between sound absorption and sound insulation when discussing the acoustic properties of hempcrete.

Sound absorption indicates the extent to which sound in a room is absorbed. Because of its open pore structure, hempcrete itself has good sound absorption. However, plastering it will decrease the final sound absorption of the total.

Sound insulation refers to how much sound is blocked from passing through a wall. A hempcrete wall without a finishing layer has very low sound insulation. Even with a plastered layer, the sound insulation remains limited because of hempcrete's relatively low density.

Sound absorption

The absorption of porous materials is mainly influenced by open porosity and flow resistance, and secondly by tortuosity and characteristic length. These are acoustic material parameters that describe the irregularity of the pore structure (Knapen et al., 2020). The thickness of the porous material also has impact.

The open porosity of hempcrete ranges between 60% and 90%. (Nguyen et al., 2009) and depends mainly on the density of the final material. The structure of hempcrete is characterized by dual porosity: meso-pores (~1 mm) between particles and the micro-pores in the hemp particles (~10-60 µm) and binder particles (~1 µm). Only the bigger meso-pores contribute to acoustic absorption.

The sound absorption coefficient α is highly dependent on frequency. The absorption of hempcrete typically reaches its maximum in mid-frequency range. For example, Isohemp's (nd.) blocks with a thickness of 12 cm achieve an absorption of value $\alpha_w = 0.85$. Sound absorption will improve with greater thickness, a lower density (due to higher porosity) and a higher binder to hemp ratio

Sound insulation

The sound insulation of hempcrete walls is, due to the low density, relatively limited. Only hempcrete variants with a density above 500 kg/m^3 are suitable when minimum sound insulation must be guaranteed (Glé et al., 2018). For unfinished walls, sound insulation is determined by porosity and flow resistance (in a addition to the wall thickness) rather than density. According to Glé et al. (2018), a 20 cm thick hempcrete wall can achieve a sound reduction index (Rw) of approximately 22–32 dB in its unfinished state, and 39–40 dB once finished. Similar sound insulation values have been reported for hempcrete blocks of the same thickness (Isohemp, 2022).

Hempcrete and Fire

A materials fire reaction describes how combustible a building material is and its role in the cause and spread of a fire. A material's fire reaction is classified under the European system, based on its flammability (main class A1 to F), smoke production (class s1 to s3) and potential to produce flaming drops (class d0 to d2).

Fire reaction tests on Isohemp hempcrete blocks resulted in a B-s1, d0 classification (ATG, 2020) (Isohemp, 2020). This means the product does not cause flash over, but can contribute to fire development. It produced transparent smoke and no framing droplets during the first 10 minutes.

Whether hempcrete can be used without additional fire safety measures depends on the specific requirements for the situation. Fire reaction requirements vary based on factors like the building type, room function, and user characteristics (e.g., whether occupants are self-reliant or sleeping). For example, hempcrete can not be used without additional measures for walls in evacuation routes for non-self-reliant occupants or communal kitchens.

Hempcrete and Durability

Hempcrete is generally considered as a durable material that withstands most factors causing degradation in traditional building materials. Its durability is influenced by several factors:

Resistance to degradation

Hempcrete's relatively large pores prevent salt crystallization. This reduces degradation caused by salt exposure (Jami et al., 2019).

The high alkalinity of lime creates an environment that is disliked by insects and moulds. The material also lacks nutrients, so limited microorganisms will grow (ibid.). Moreover, due to its permeable and hygroscopic properties, hempcrete can withstand repeated absorption and release of moisture for almost unlimited periods of time. For this it is very important that appropriate finishing layers are used to prevent moisture entrapment within the wall (Sparrow & Stanwix, 2014).

Freeze-thaw

The freeze-thaw performance of hempcrete depends on the binder's hydraulic properties. Hydraulic binders perform better under freezing conditions, while hydrated lime-based binders show more degradation and weight loss (Walker et al., 2014).

Summary Other Behaviour

Sound-absorbing

Hempcrete absorbs sound well due to its porous structure. Its sound insulation is limited because of low density.

Fire-resistant

Hempcrete is classified as B-s1, d0, meaning limited fire contribution, low smoke, and no flaming droplets, but extra fire measures may be needed depending on building use and occupant needs.

Mould-resistant

Hempcrete is considered durable, resisting salt, mould, insects, and moisture cycles, though its freeze-thaw performance depends on the type of binder used.

Varying the Mix

The previous sections show that the material properties of hempcrete vary broadly in the literature, depending on its exact composition. Both in terms of components used and their proportions and the method of application.

Mix Ratios

Since the proportions of the components in a hempcrete mix impact the materials performance, it is imporant to consider these ratios when selecting a hempcrete mixture for a specific application (Sparrow & Stanwix, 2014).

B/H ratio

For example, the binder-to-hemp (B/H) ratio affects the materials thermal insulation (λ-value) (Collet & Pretot, 2014) and compressive strength (Nguyen et al., 2009). A higher hemp content results in a lighter mix, with a lower density, that insulates better but has lower compressive strength. Which means that for a wall construction, the ideal binder-to-hemp ratio will be typically higher than for a floor, but lower than for a roof. Floors require a stronger mix, while roofs can use a less load-bearing composition. A lighter mix, due to its higher porosity, also has better sound- absorption properties (Kinnane et al., 2016).

W/B ratio

Another important factor is the water-to-binder (W/B) ratio, which affects the workability, setting, and strength of the mix. A higher W/B ratio improves workability but leads to increased porosity, which may reduce compressive strength and durability (Walker et al., 2014). On the other hand, a lower W/B ratio typically results in a denser, stronger mix but can make placement more difficult.

Compaction Effects

The hygrothermal, mechanical, and acoustic properties of hempcrete are influenced not only by its mix proportions but also by the level of compaction during placement.

Lower compaction increases open porosity, which improves thermal conductivity (λ-value), moisture buffering capacity (MBV), and water vapour permeability (Holcroft & Shea, 2015). While thermal conductivity also varies with humidity, compaction has a greater impact (Collet & Pretot, 2014). Higher compaction reduces porosity, which lowers sound absorption (Glé et al., 2018) but increases compressive strength (Nguyen et al., 2010) (Arnaud & Gourlay, 2012). However, the denser structure also slows down drying and carbonation (Colinart et al., 2012; Evrard, 2008).

Fig 3.10 Hempcrete (left) and its components: hemp shivs (middle) and lime (right)

Environmental Impact

Although almost unnecessary to emphasize, the construction sector plays a major role in environmental degradation. It consumes 50% of all raw materials, over a third of global energy use and is responsible for nearly 40% of total CO_2 emissions (International Energy Agency, 2022). Stricter energy performance requirements are helping to lower the operational energy use in buildings. This makes the environmental impact of construction materials increasingly important. Choosing low-impact and renewable materials with low embodied energy is now essential. Therefore it is important to know the environmental impact of hempcrete.

Life cycle assessment

Comparing life-cycle assessments (LCAs) of hemp-lime is hard because each study uses its own set of assumptions:

- Recipes vary (hemp-to-binder ratio, binder type),
- Production methods differ (cast in place, blocks, panels),
- Local factors (transport distance, electricity mix, waste rules) differ

(Pretot et al., 2014) (Ingrao et al., 2015).
These differences mean that numbers from separate studies cannot be compared and combined directly.

Low impact crop

Even with these different assumptions, two points appear constantly in literature. First, hemp is a low-impact fiber crop: it needs little land, water, and energy compared with many other fibers (van der Werf & Turunen, 2008). It contains no VOCs (volatile organic compounds) which would otherwise be emitted after end of life. This makes it a healthy material, both for the user and environment.

Carbon negativity

Second, most hemp-lime mixes have a far lower overall environmental footrpint compared to common mineral or petrochemical insulations, even after counting the CO_2 released when making lime (Ingrao et al., 2015). Some authors even find a net-negative carbon balance because the CO_2 taken up during hemp growth and later re-absorbed as the lime cures can outweigh all other emissions (Pretot et al., 2014). But this result only holds for their exact setup again; change the mix, transport, or end-of-life scenario and the negativity can flip.

Summary Environmental Impact

CO_2 negative footprint

Hempcrete is able to have a carbon-negative footprint, as it absorbs more CO_2 during hemp growth and lime carbonation than is emitted during its production.

Biobased

Hempcrete is a biobased material, made primarily from renewable plant-based resources and a natural binder

Healthy: free from VOCs

Hempcrete is a healthy material, as it contains no VOCs and does not release harmful emissions at end of life.

EPD EXIE

To keep the environmental aspects of this research clear and comparable, all further arguing will use one thoroughly documented source: the Belgian environmental product declaration (EPD) for EXIE's loose-fill hemp-lime insulation "CaNaDry" (B-EPD, 2024). A modification is shown in figure 3.11 on the next pages.

EXIE is a Belgian company based in Herzele, specializing in hemp cultivation and the production of hempcrete. They offer two types of premixed hemp-lime products:

CaNaDry

A lightweight, dry hemp-lime mix primarily used as an infill insulation material across all building layers. It has a dry density of approximately 175 kg/m³ and a binder-to-hemp (B/H) ratio of 0.54.

CaNaCrete

EXIE's version of traditional hempcrete, this mix includes pre-added water and is designed for semi-structural applications. It has a dry density of around 275 kg/m³ and a B/H ratio of 1.09.

Only CaNaDry has an Environmental Product Declaration (EPD) available, and will therefore be used as the reference product.

Fuctional Unit

The CaNaDry EPD is built around one functional declared unit (FU): 42.53 kg of hemp lime mix. (about 0.243 m³ at a dry density of 175 kg/m³). This is sufficient to insulate 1 m² of wall to R_c value of 4.5 m²·K/W (Belgian standard). Packaging is included and a 75 year reference service life is assumed. For easy comparison to other densities, every GWP result in the EPD is converted to GWP per kg.

Scenarios

The GWP results of the EPD are separated into two scenarios:

Standard scenario

This is based on the regulatory practice in Belgium. Organic construction waste that can not be cleanly separated is normally sent to incineration plants rather than landfilled. The B-EPD standard scenario follows that default route.

Although CaNaDry is theoretically 100% reversible when vacuumed out cleanly, the standard scenario assumes no selective recovery at demolition. All 42.5 kg per m² therefore leave the site as mixed construction waste and follow the generic split (95% burned, 5% landfill).

75% reuse scenario

That is why a second scenario is introduced, in which 75% of the loose fill is vacuum recovered and fed back into a new hemp lime product However, today, there is not enough evidence that this scenario could replace the standard.

Stages A-C1 stay the same as in the standard scenario, the differences appear in the end of life steps and the credits beyond the system boundary (C2-D). It gains the most in waste processing stage C3. Only 25% of the hemp is now burned, so far less biogenic CO_2 is released there.

The rest of that CO_2 is accounted for in stage D, as required by the biogenic carbon-balance rule. Because the reused material is not burned for energy, its benefit shows up as "avoided production" of new raw materials, cutting impacts from extraction and manufacturing.

Phase	Module		What happens?	Standard scenario GWP total (kg CO_2-eq) Per FU	Standard scenario GWP total (kg CO_2-eq) Per kg	75% Reuse scenario GWP total (kg CO_2-eq) Per FU	75% Reuse scenario GWP total (kg CO_2-eq) Per kg
A1–A3 **Product**	A1	Raw materials	Biogenic carbon sequestration in the hemp + Lime extraction and processing	- 22.10	- 0.52	- 22.10	- 0.52
	A2	Transport	Diesel trucks/machinery of raw material to factory	+ 1.14	+ 0.027	+ 1.14	+ 0.027
	A3	Manufacturing	Electricity + diesel generator for mixing and packaging	+ 0.17	+ 0.004	+ 0.17	+ 0.004
A4–A5 **Production**	A4	Transport	Field to production site: 50–100 km with EURO 6 trucks	+ 0.80	+ 0.019	+ 0.80	+ 0.019
	A5	Installation	2% material loss + disposal of the plastic bags	+ 0.56	+ 0.013	+ 0.56	+ 0.013
B1–B7 **Use**	B1	Use	Carbonation of the lime binder over 75 years (50% of its emssions during processing)	- 4.28	- 0.10	- 4.28	- 0.10
	B2	Maintenance	-	-	-	-	-
	B3	Repair	-	-	-	-	-
	B4	Replacement	-	-	-	-	-
	B5	Refurbishment	-	-	-	-	-
	B6	Operational energy use	-	-	-	-	-
	B7	Operational water use	-	-	-	-	-
C1–C4 **End of Life**	C1	Deconstruction	Diesel machinery	+ 0.18	+ 0.004	+ 0.18	+ 0.004
	C2	Transport	Transport to sorting centre (diesel)	+ 1.00	+ 0.024	+ 0.25	+ 0.01
	C3	Waste processing	**Standard:** 95% incineration of hemp, 5% landfill **Reuse:** 75% reuse of hempcrete, 25% incineration	+ 37.3	+ 0.88	+ 9.33	+ 0.22
	C4	Disposal	Landfilling residues	+ 0.13	+ 0.003	+ 0.03	+ 0.0004
			Cradle to Grave Result	**+ 14.9**	**+ 0.35**	**- 13.9**	**- 0.33**
D **Beyond Building Life Cycle**		Reuse/recovery/recycling potential of the next lifecycle	**Standard:** Heat and power energy recovery from burning the hemp shivs **Reuse:** CO_2 discount for next lifecyle + retour transport	- 3.99	- 0.09	+ 15.70	+ 0.37
			Cradle to Cradle Result	**+ 10.9**	**+ 0.26**	**+ 1.79**	**+ 0.04**

Fig 3.11 B-EPD of EXIE's CaNaDry

Product Phase (A1-A3)

This stage is heavily negative in both cases (-20,79 $kgCO_2eq/FU$, or about -86 kg/m^3). This is thanks to the biogenic storage in the hemp: -38.5 $kgCO_2eq/FU$. The CO_2 emitted by the lime extraction and calcination is 16.4 $kgCO_2eq/FU$. Making the net product strongly carbon negative (storing 22.1 $kgCO_2eq/FU$ or 91 $kgCO_2eq/m^3$. The end-of-life scenario determines whether the system stays net negative or not.

Use phase (B1)

Although very slow and thus spread over 75 years, the carbonisation of the lime binder adds another carbon negativity to the combined material.

Standard scenario

This scenario is dominated by C3: burning 95% of the hemp shiv releases the biogenic CO_2 that was captured during growth.

75% reuse scenario

Here only 25% of the shiv is burned, so C3 drops sharply, turning the A-C subotal (Cradle to Grave result) negative.

Carbon balance bookkeeping

The Belgian norms state that any CO_2 counted as "stored" earlier has to re-appear later. So, even though the 31.9 kg (75%) of reused hemp still holds its carbon, the EPD adds the same amount of CO_2 in Module D, as if it was burned, to keep the books balanced.

In short, when D is not regarded and it is assumed that 75% of the material can be reused in a next life cycle, CaNaDry is a carbon negative material, sequestering about 57 kg CO_2 eq per cubic meter.

Life Cycle Analysis

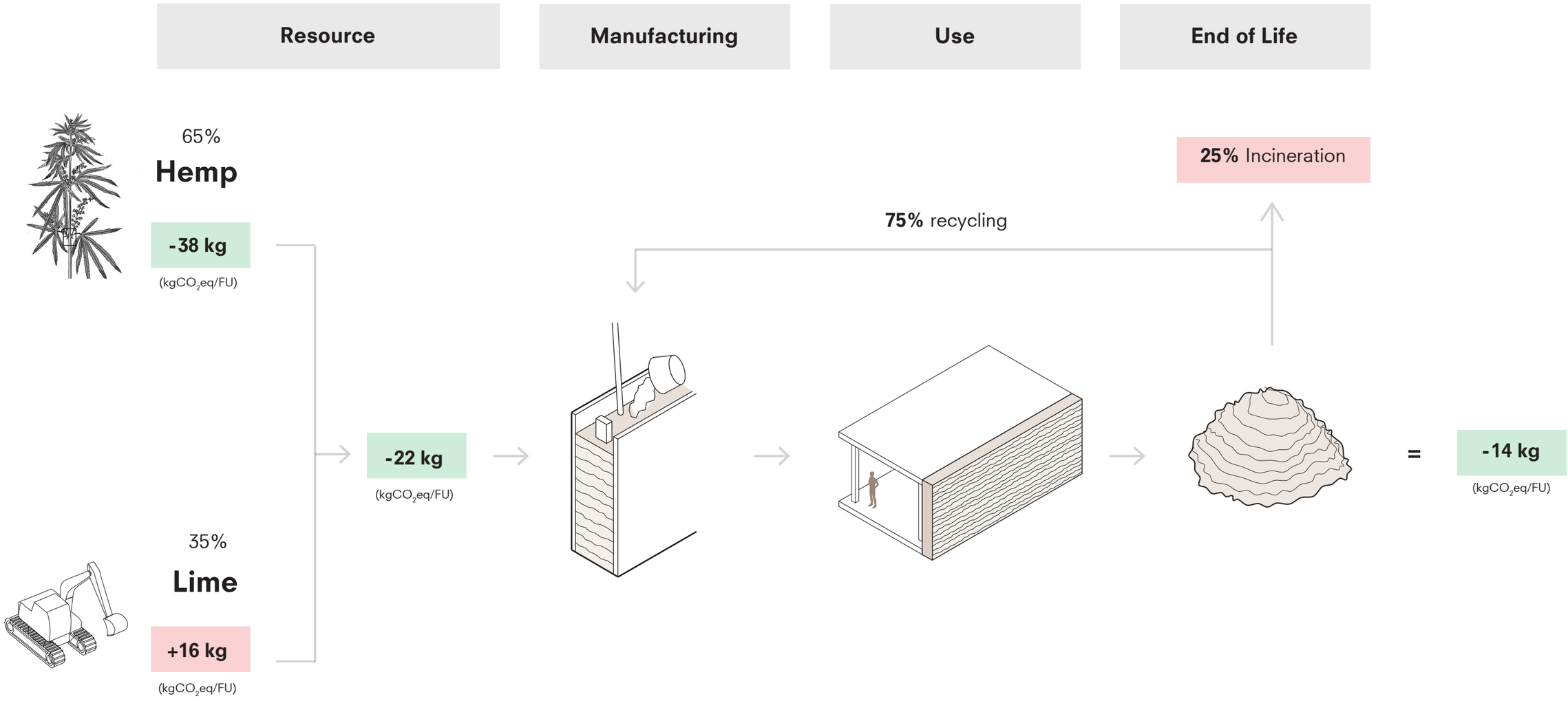

Fig 3.12 Schematic Life Cycle Analysis of EXIE's CaNaDry

Design for Disassembly

The B-EPD (2024) also includes information on the reversibility of the CaNaDry. This is according to the standard Belgian EPD format, where the reader is expected to tick the the answer option that applies.

For comparison, the table is filled in for both CaNaDry and CaNaCrete; the hempcrete system that is researched in this work.

In short, the cast in situ CaNaCrete is not fully reversible like loose CaNaDry, but is does offer a middle ground option: down cycling the demolished wall with fresh hemp lime instead of landfilling or incinerating it.

Although the granulate is light, both initial removal and crushing the material needs mechanical handling. Disassembly would also cause damage to the studs, and possible finishes.

Fig 3.14 Site visit at EXIE in Herzele, Belgium. Big bags of CaNaDry stacked on top of eachother

Description	Type of fixing	Level of reversibility	Simplicity of disassembly	Speed of disassembly	Ease of handling (size and weight)	Robustness of material	Damage to other elements	Comments
CaNaDry Loose-fill hemp-lime insulation tipped into floors, roofs and wall cavities; no extra fixings.	poured	0%	simple (no specific dismanling tools required)	very speedy	easy manual - one worker	material resists well during disassembly	no damage	Vacuum extraction keeps material clean. Exie offers 25 % buy-back of uncontaminated material.
CaNaCrete Monolithic hemp-lime mix placed between formwork and left to harden into a solid wall.	loose laid	25%	needs common power tools	moderate	manual but heavy - two workers	moderate risk of damage	minor cosmetic damage	Recovered hemp-lime granulate can replace part of new shiv/binder after sieving; energy use must be managed.
	clipped	50%	needs specialised tools	slow	needs lifting equipment	fragile	significant damage	
	screwed	75%	destructive removal					
	nailed	100%						
	glued							
	mortared							
	welded							
	bolted							
	other							

Fig 3.13 Disassembly table

Material: Conclusion

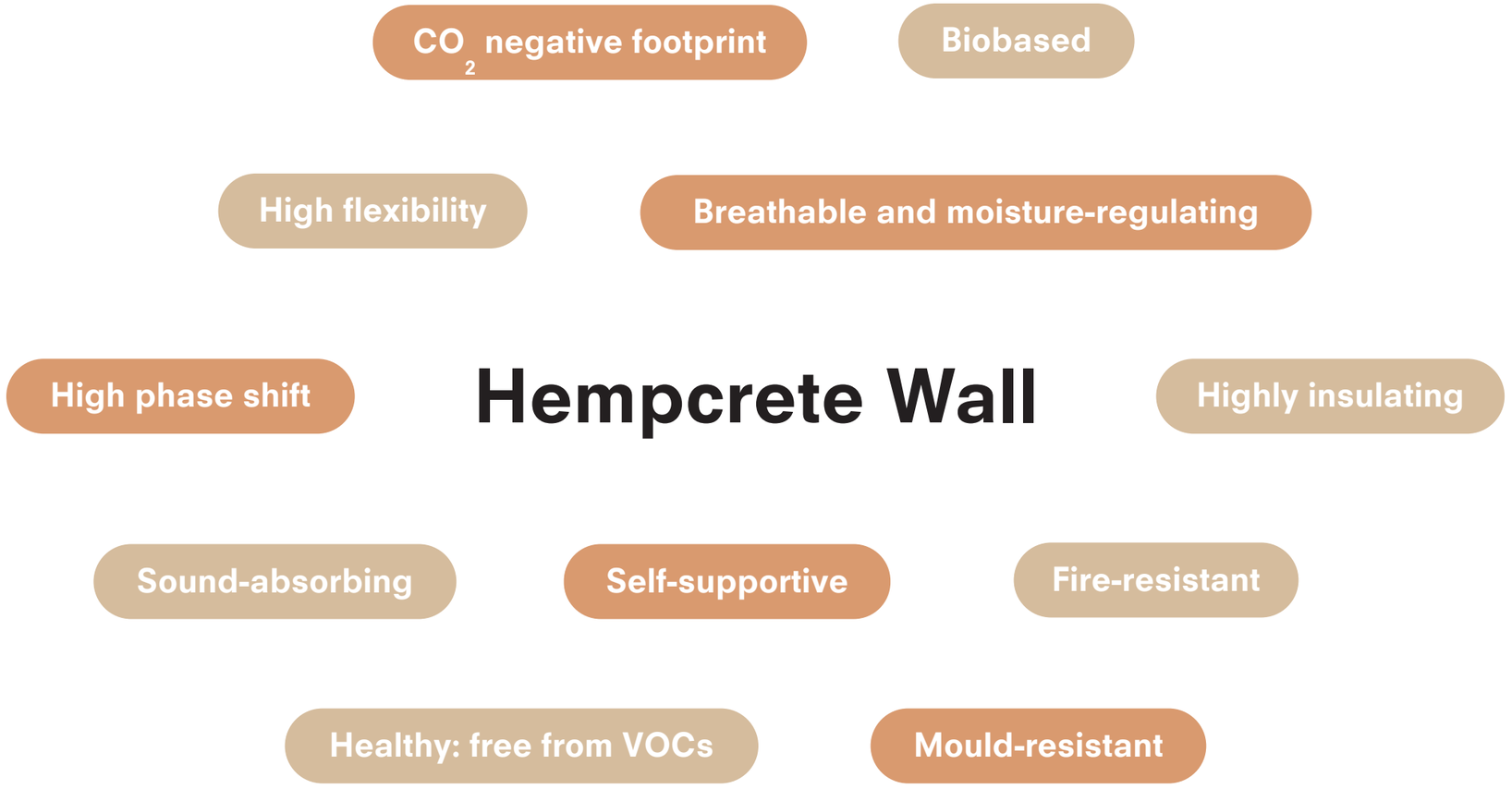

Fig 3.15 Hempcrete wall properties

Properties

Hempcrete combines hemp shiv with a lime binder to create a breathable, moisture-regulating thermal insulation that is able to even out indoor humidity and temperature peaks. Because its thermal conductivity (λ) is higher than that of mineral wool or foam, thicker walls are needed to reach the same R-value. However, the mix's thermal inertia and high phase shift still stabilise indoor temperatures better than light-weight insulations (though not as much as concrete or brick).

Structurally, hempcrete is self-supporting but not load-bearing: compressive strength, ductility, and acoustic absorption all depend on the binder type, binder-to-hemp ratio, and shiv size and orientation.

Fire-class B-s1,d0 means the material contributes little to fire and smoke but may require extra measures in safety-critical locations. Durability tests show good resistance to salts, mould, insects, and wet–dry cycles.

Environmentally, hempcrete can be carbon-negative because the CO_2 captured during hemp growth and later lime carbonation outweighs production emissions. Its VOC-free ingredients make it a healthy, low-toxicity choice.

The Manufacturing

This chapter presents field research on in-situ hempcrete manufacturing, identifies key workflow challenges and explores automation via prefabricated blocks, elements, and robotic rammed-earth systems.

Fig 4.1 Manually ramming a hempcrete interior wall

Building a Hempcrete Wall

Field research

The following section describes field research conducted over two working days with the Dutch biobased contractor YOMABOUW, during which a hempcrete wall was cast on-site at a daycare center in Amsterdam. The aim was to observe practical challenges in the in-situ manufacturing workflow, from mixing to curing of the wall.

Summary

On-site casting begins with preparing the hemp-lime mix directly in the workplace. Strictly measured proportions of hemp shiv, lime binder and water are combined until a wet, earthy mixture is obtained. Workers place this mix by hand into timber formwork surrounding a timber load-bearing frame, then compact each lift with a wooden rammer. After the first setting reactions occur, the formwork can be removed, so the wall can dry and cure. With basic guidance from YOMABOUW, even untrained workers were able to perform the casting with minimal instruction. Seven people were working simultaneously over these two days, with tasks differing from mixing the hempcrete, walking the mixing tubs to the formwork, and ramming the material into a solid wall.

This method offers high form flexibility (each pour takes the shape of its mould) but also needs carefully built formwork by skilled carpenters to achieve clean edges. Layered casting leaves visible horizontal lines. To emphasize these natural layers, strong pigmentation was used, altering per layer (figure 4.3).

Fig 4.2 Hemp shivs, lime and mixing tubs on site

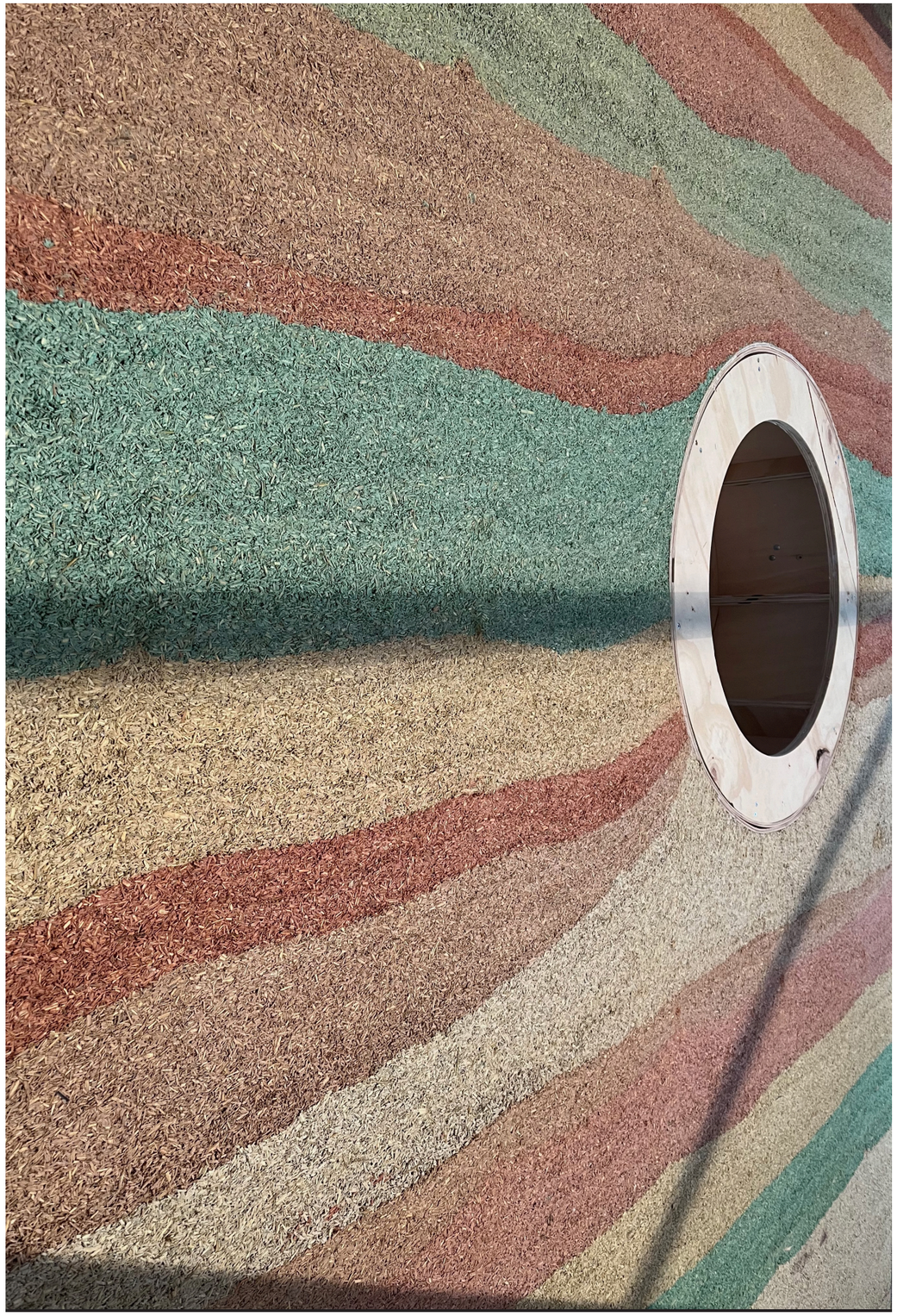

Fig 4.3 Close up of the finished, pigmented hempcrete wall

Fig 4.4 Mixing and filling the tubs

Consistent mix quality and uniform placement are essential for both aesthetics and wall performance. The on-site work was found to be very labour intensive, and slow drying delays the moment when the wall reaches intended thermal resistance. Prior decisions on anchoring points, reinforcements, cables and piping must be made before casting, since heavy fixings cannot be added later.

Artisanal Workflow

Observation

The manufacturing process included the following manual steps:

1. Making the timber frame
2. Mounting and bracing the formwork
3. Manually weighing and mixing hemp, lime binder, water and pigment (figure 4.4)
4. Transporting batches of wet mix in buckets
5. Placing the mix into the formwork by hand (figure 4.6)
6. Ramming and lightly compacting each layer with a wooden stick (figure 4.7)
7. Stripping and repositioning formwork for the next layer

Consequence

This artisanal workflow limited daily throughput, introduced variability between workers and shifts, and increased the risk of errors or delays as tiredness of the workers grew.

Subjective Compaction

Observation

Compaction was performed manually with a wooden 2x3 stick to increase surface durability. The force applied varied by worker strength and fatigue. As shifts progressed, compaction became weaker, and the top of freshly placed mix began to dry out before sufficient consolidation.

Consequence

Inconsistent packing and surface drying produced voids and uneven density, compromising durability and creating potential weak spots in the finished wall.

Minimum Coverage

Observation

When using a timber frame as the load-bearing structure for an in-situ cast hempcrete wall, the hempcrete fully or partially encases the frame. Based on years of practical experience, it is generally assumed that the minimum coverage over the studs should be at least (0.5 × stud thickness) + 5 cm, with an absolute minimum of 7 cm, in order to ensure adequate adhesion and to prevent cracking.

Consequence

When wall height rises, stud thickness rises as well. Achieving the minimum cover leads to very thick walls and exceptionally high thermal resistance (often exceeding R 4.7 m²K/W), resulting in material overuse and unnecessary waste. This is calculated in figure 4.5 for a 40cm wall.

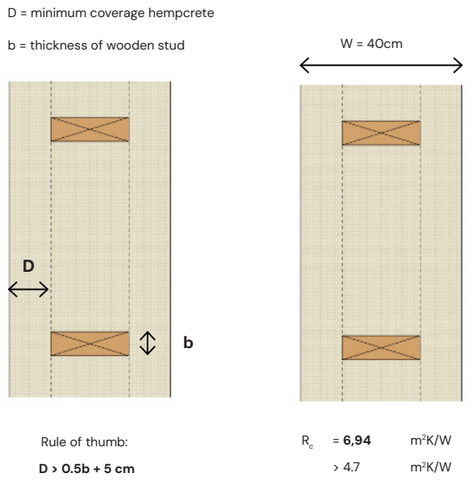

Fig 4.5 Cross section of studs and their minimum coverage

Fig 4.6 Manually placing the hempcrete in the formwork

Fig 4.7 Manually tamping the sides with a wooden stick

Density Gradient

Observation

Workers poured thick lifts to speed construction. However, compaction effort decreased toward the mould walls and the bottom of each layer. The upper portions saw greater rammer force, aligning hemp shivs more horizontally, while lower regions remained loosely packed. This created a vertical density gradient within layers, also seen in other project during site visits (figure 4.8) Such variation highlights the limits of manual in-situ casting and suggests advantages for prefabrication, where layer thickness and compaction force can be strictly controlled.

Consequence

A clear gradient in density and shiv orientation formed within each layer, possibly leading to non-uniform thermal conductivity and mechanical strength across the wall's height.

Uncontrolled Curing Conditions

Observation

After casting, the wet lime requires extensive time to harden. On average, finishing work can only begin after about three months (Sparrow & Stanwix, 2014). Because all manufacturing occurs in situ, exterior wall curing is subject to ambient weather. Variations in temperature and humidity make hardening unpredictable, and cracks on crucial parts of the facade (such as at door and window frames) occur (figure 4.7).

Consequence

Unpredictable hardening might delay finishing work, complicates scheduling, and makes it difficult to guarantee performance under strict building regulations.

Fig 4.8 Cracks at window frame

Fig 4.9 Uncontrolled layer height and clear density gradient

Prefabrication

The field research with YOMABOUW revealed several challenges when manufacturing hempcrete walls in-situ. Prefabrication seems like a logical approach to these challenges.

Prefabrication moves much of the work into a factory setting, where environmental conditions and production parameters are controlled. This reduces weather dependency, improves material consistency, and shortens on-site drying times. Although factory-made components would cost more upfront than cast-in-place hempcrete, they require far less labour and can be installed more rapidly.

Prefab Blocks

Prefabricated hempcrete blocks are one of the most established systems on the market. In a factory, raw hemp shiv, binder and water are automatically dosed, mixed, and pressed into uniform blocks (figure 4.10). After an indoor drying phase, blocks cure outdoors under a shed for 10–15 weeks, depending on their thickness, see figure 4.11 (Isohemp, n.d.).

On site, these blocks are laid like masonry units in non-load-bearing walls (figurer 4.12). A lime-based mortar bonds the blocks, and accessories such as integrated lintels with reinforced-concrete cores are available to simplify openings.

Fig 4.10 IsoHemp's hempcrete blocks at their factory in Fernelmont, Belgium

The IsoHemp Hempro system, for example, uses U-shaped blocks as lost formwork for cast-in-place reinforced concrete beams and columns, eliminating the need for a separate frame (figure 4.13).

Because production is automated, blocks have uniform density and moisture content before delivery. This allows finishing layers to be applied sooner, and the thermal resistance of the wall to be achieved more quickly. Placement requires some training but is less labour intensive than casting on site. Only basic tools are needed, and the blocks can be easily cut to size during installation.

However, the rigid block format makes irregular shapes more difficult than with casting. Unlike in situ hempcrete, heavy fixtures can be fastened directly into the blocks when suitable anchors are used (Isohemp, n.d.).

Prefab Elements

In addition to blocks, fully prefabricated wall panels are available. These panels consist of a timber frame filled with hempcrete at the factory. A dry but still uncured hemp-lime mix is machine-blown into a timber frame that is clad on one or both sides with vapour permeable material (DunAgro, n.d.). The material is lightly moistened during this process to initiate the setting of the lime binder. After an drying, panels can be shipped to site, ready for assembly.

Integration of electrical systems, plumbing and other technical installations make sure that on-site work only includes positioning, fixing and finishing the panels. Workers construct walls, floors and roofs in a fraction of the time required for cast-in-place methods. As with blocks, the prefab elements offer consistent density, predictable performance, and freedom from weather-related delays.

Fig 4.11 IsoHemp's drying facility

Fig 4.12 Stacked IsoHemp block wall, non load bearing

Fig 4.13 IsoHemp worker filling the U shaped blocks of the Hempro system with concrete

Fig 4.14 Prefab hempcrete system, shipped to site on a trailer

Fig 4.15 Elements installed on site, unfinshed

Fig 4.16 Cast-in situ hempcrete wall. Project by HOP Architects and YOMABOUW

Fig 4.17 Cast-in situ hempcrete wall. Project by Giesen Architects and YOMABOUW

Automation

By manufacturing hempcrete blocks or elements off-site in controlled factory settings, producers can regulate moisture content, optimize curing conditions and reduce the reliance on skilled on-site labour. Also, prefabricated hempcrete elements can be delivered to the construction site a more predictable and logistically manageable form (Isohemp, nd).

Yet, prefabrication has its drawbacks. Although prefabricated hempcrete products can serve as a highly effective insulation layer, this often comes at the cost of the unique aesthetic qualities that define monolithic hempcrete (figure 4.16 and 4.17). Prefab blocks and elements need to be clad or finished, hiding the raw textural layers of hemp and lime that give it its natural character. The manufacturing workflow may be more economic, but it misses the look and feel of a biobased hempcrete wall. As a result, current use of hempcrete for exterior wall construction is not living up to its full potential. This research tries to retain the material's natural aesthetic while ensuring consistent performance.

Robotic Rammed Earth

To explore automated production methods, the study also examined rammed earth, a monolithic material formed layer by layer in reusable formwork, much like cast-in-place hempcrete. The rammed earth sector has already pioneered a range of prefabricated wall solutions. Several of these innovative systems are described in the following section.

Fig 4.17 Worker using a pneumatic rammer to construct a rammed earth wall

Fig 4.18 FInished monolithic rammed earth walls

Industry Examples

The manufacturing technique of rammed earth walls seems similar: placing a moist mixture into formwork in similar horizontal layers and compacting it into a dense, cohesive mass (Minke, 2013).

Research into the automation of rammed earth walls shows that a stronger focus on simple construction and natural materials doesn't have to conflict with the use of innovative digital fabrication technologies (Kloft et al., 2019). If successful, robotic fabrication processes could bring the use of traditional and low-tech materials like hemp and lime to new levels of performance and expression.

Three robotic rammed earth manufacturing workflows are regarded for their guide in hempcrete compaction. Below is a comparison, summarising their key technical features and how they differ in formwork strategy, compaction method and product handling.

'Roberta' by Martin Rauch

(Lehm ton Erde Baukunst, Schlins, Austria)
This system includes a semi-automated, linear production line with reusable formwork sections up to 20 m long and 2.8 m high (Gomaa et al., 2023). Formwork (dis)assembly is machine-driven, and a conveyor belt automatically delivers fresh earth mix into each section. A dedicated compaction unit travels along the formwork, ramming each lifted layer to the target density.

After compaction, a cutting machine slices continuous walls into transportable panels (ibid.). Figures 4.23 and 4.24 show the prefabricated and cut rammed earth wall elements after placing them on the building site. After stacking them, workers finish the gaps with fresh rammed earth mixtures.

Fig 4.19 "Roberta" Machine by Martin Rauch

Fig 4.20 Robotic Arm by ERNE AG

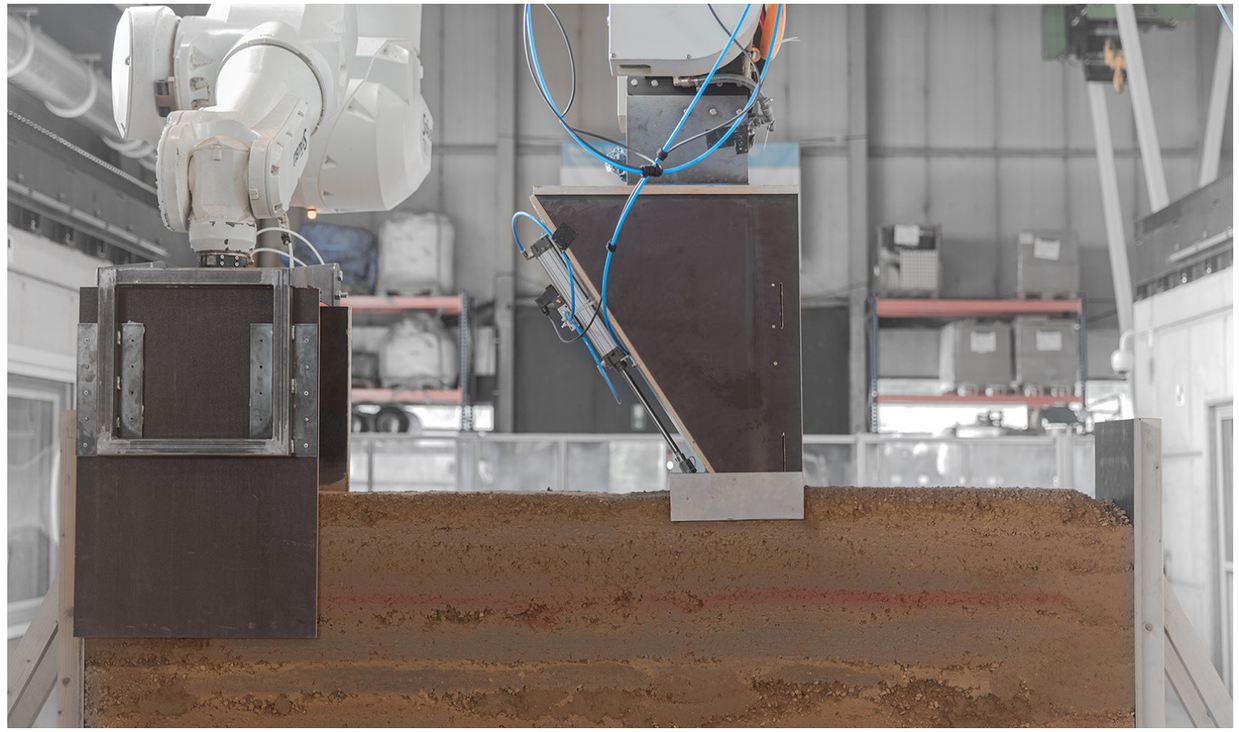

Fig 4.21 Fully CNC controlled material feeding and ramming by Kloft

Robotic Rammed Earth

(ITE, TU Braunschweig, Germany)

This prototype uses an integrated slip-form system where the formwork itself is mounted on a robotic gantry and moves upward with each lift. (Gosslar & Kloft, 2023). Earth mix is fed automatically as the robot manages and steers both formwork movement and compaction. Its custom compaction tool at the end of the robot arm applies precise, repeatable pressure. Layer heights are reduced to 5 cm, compared to 10–15 cm layers that YOMABOUW uses. This minimizes formwork loads and ensures uniform density (Schmitz et al., 2024). Since this technique is not commercially available, no full scale walls have been developed yet.

Stampflehm Tamping Robotic Arm

(ERNE AG Holzbau, Stein, Switzerland)

This system uses a reinforced, quick to assemble timber formwork of a standard size for each element (Gomaa et al., 2023). A six-axis industrial arm has a pneumatic rammer at its end. It is able to densely compact each layer, and can work with complex forms. Finished wall elements are cured under a cover, then stacked and sealed with clay mortar on-site (ibid.).

Robotic Hempcrete

All three systems demonstrate that traditional earth construction can be elevated through digital fabrication. The workflows differ in the degree of integration between formwork, feeding and compaction, as well as in their production scale. From early semi-automated lines (Roberta), to research prototypes (TU Braunschweig) to fully industrialized prefabrication (ERNE AG Holzbau).

The next part of this research investigates whether a similar technique could also be applied to ramming hempcrete wall elements.

Fig 4.22 Finished prefab rammed earth elements

Fig 4.23 Workers finishing the gaps between the elements

Automating Hempcrete

Main Objective

As described in the previous chapter, compared to the current manual workflow for rammed earth, mechanical automation increases workflow speed and enables ramming consistency. When applied to hempcrete manufacturing, this could prevent premature cracking and weak spots due to density gradients in the layer. It would improve material performance.

That is why the main objective of this research is:

to manufacture a monolithic hempcrete wall in a way that reliable performance is ensured

Due to constrains in using a ramming machine, for the scope of this research, the automated ramming has been simulated manually. This may seem incomparable to the use of a machine: these can deliver consistent and high force, while measuring and applying consistent human force is difficult.

For this reason, instead of measuring and regulating the force or pressure, compaction was measured as the percentage reduction in layer height. This factor can be directly translated into robotic control parameters.

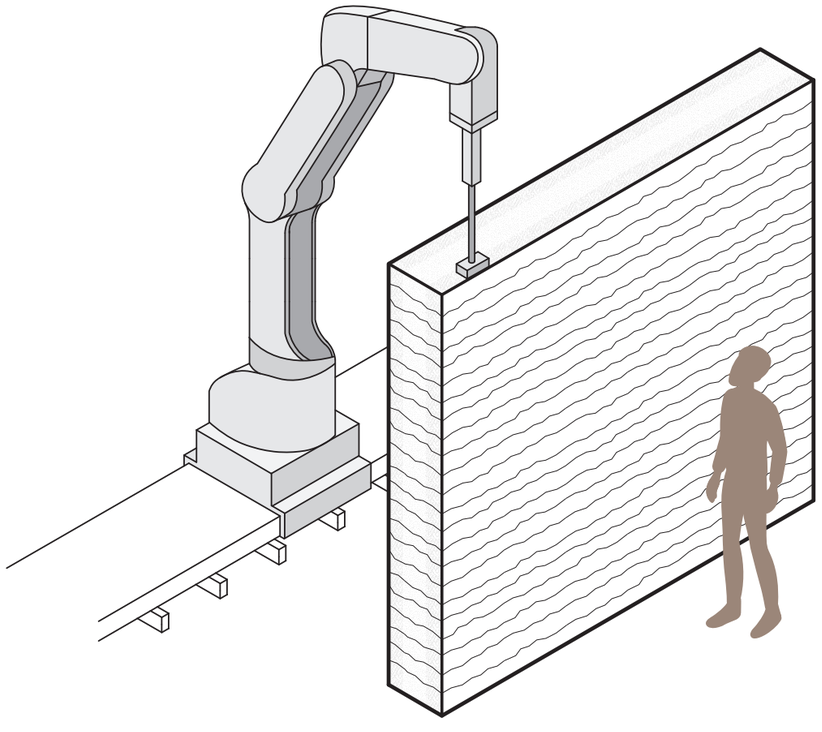

Fig 5.1 Concept: A rail-mounted robotic arm equipped with a pneumatic rammer to produce hempcrete wall elements.

Method

An experiment was set up that sits in between material characterization and manufacturing methods. It examines how varying parameters in the manufacturing system influences the wall's material performance, and based on these results loops back to make an estimate of the best manufacturing method.

A variety of samples were made, which were tested on hygrothermal and mechanical properties.

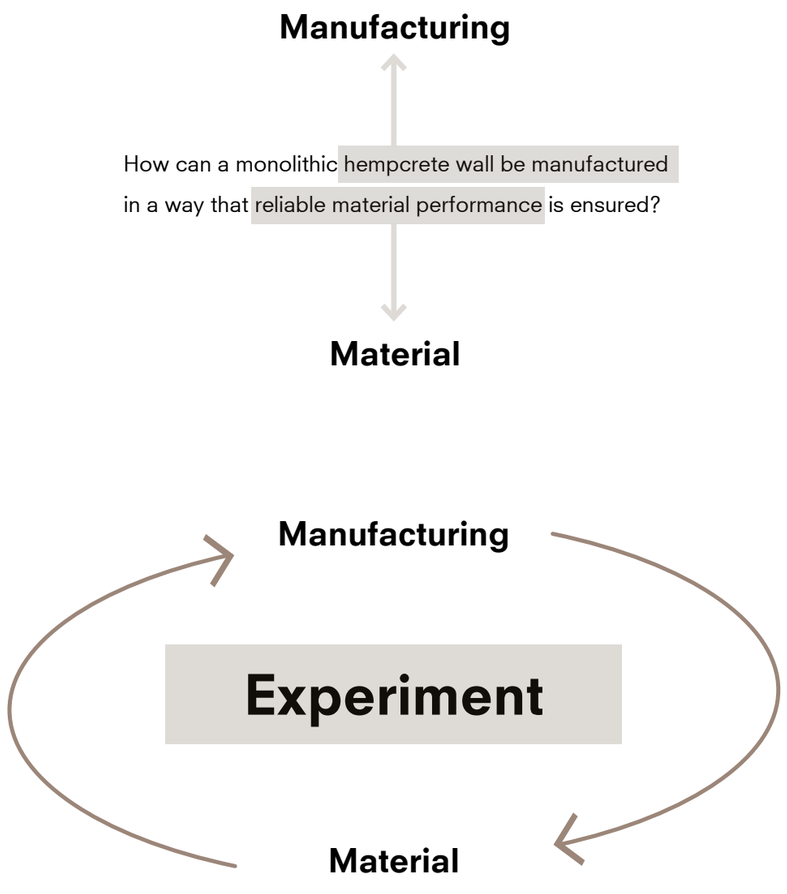

Fig 5.2 Method of experiment

Experiment Design

This chapter describes the considerations that informed the experiment's design. It also presents the experiments' setup.

Fig 6.1 Close up of column samples A2

Material Selection

The first step was to determine the material compostion of the hempcrete. The big variety of hemp-lime binders and mix ratios found in the literature makes researching hempcrete as a general material nearly impossible. To keep the scope manageable and observe whether binder type influences the material properties, two hempcrete recipies are used in this experiment:

- Air lime binder (EXIE)
- Mix of air and hydraulic binder (IsoHemp)

CaNaCrete (EXIE)

CaNaCrete is a factory-blended “wet” hemp lime mixture, delivered in 1.2 m3 big-bags. EXIE mixes its own cultivated hemp shiv, a high purity air lime binder (CL90-S), water and additives on order. Because air lime hardens only by carbonation from ambient air, the mix can be pre-wetted without the risk of quickly setting in the big-bag. When any hydraulic binders would be used, it would arrive as a solid limestone block.

CaNaCrete is installed on-site with the same placement techniques as traditional hand-mixed hempcrete. It saves time and labor by eliminating the need for mixing equipment. It also ensures consistent mix proportions, making it ideal for experimental studies. To prevent premature drying and carbonation inside the bag, the material must be placed within 10 days of delivery.

Hempbag + Prokalk Lime (IsoHemp)

To isolate the influence of the binder on material performance, a mixture of Isohemp’s hemp shiv and the proprietary Prokalk Lime binder is used. Prokalk is a purpose-designed binder for the on-site production of hempcrete. The product combines hydraulic lime with air lime in a single, ready-to-use formulation. It comes with clear proportioning instructions, allowing for the on-site mixing of batches without the risk of dosing errors.
Because hydration initiates setting almost immediately, the fresh mix must be processed within 30 minutes after mixing to avoid premature curing.

Fig 6.2 Used materials, LTR: EXIE CaNaCrete, Isohemp shivs, Prokalk Lime and natural clay-derived pigment “Rouge Venitien”

Hemp Shivs

The industrial hemp shivs supplied are untreated (un-coated) and mechanically cleaned and sieved. Isohemp shiv is finer and less dense than the EXIE batch. A visual inspection revealed a color difference: EXIE shivs appear darker grey-brown, whereas IsoHemp shivs are pale yellow. A lighter color is generally associated with shorter retting and fresher shivs, indicating a higher quality (Knapen et al., 2020).

EXIE grows, harvests and processes its hemp on their own farmland in Herzele, Belgium. The hemp used by IsoHemp is grown in Bar-sur-Aube, France and processed at the manufacturers facility (Léonard, 2014).

Commercial product	Particle size (mm)	Oven-dry bulk density (kg/m3)	Manufacturer	Origin
CaNaCrete	2 - 30	110	EXIE	Herzele, Belgium
Hempbag	2 - 25	100	IsoHemp	Bar-sur-Aube, France

Table 6.1 Material selection: Hemp shivs

Binders

Two limes compositions were used to contrast a pure air lime matrix with a mixed air + hydraulic lime matrix. The binder pre-mixed into CaNaCrete is Carmeuse SuperCalco 97. This is a very pure, hydrated calcium lime, standard classified as CL90-S. It relies entirely on atmospheric carbonisation (CO_2 uptake from the surrounding air). Pure air lime is characterised by high vapor-openness, but slow strength gain (Van Balen et al., 2003).

Prokalk Lime contains 54% natural hydraulic lime (NHL3.5). Its hydraulic components react with added process water, giving it a faster initial set. Because hydraulic limes are less vapour-permeable, hybrid lime systems typically dry slower. Considering the additional firing in for hydraulic limes, using CaNaCrete is expected to result in a reduced carbon footprint compared to the Isohemp mix. However, no full LCA data for these specific products were found by the authors.

Commercial product	Type of lime	Composition	Bulk density (kg/m3)	Manufacturer	Origin
Supercalco 97	Air lime	>97% Calcium-hydroxide (CL90-S)	520	Carmeuse	Seilles Quarry, Belgium
ProKalk Lime	Mix of air and hydraulic lime	46% air lime (CL90-S) + 54% hydraulic lime (NHL3.5)	700	IsoHemp	?, France

Table 6.2 Material selection: Binders

Process Water

Adding process water is essential for both air and hydraulic limes. The hemp shivs and binders are mixed with water to give the mixture a certain consistency and cohesion needed for in-situ casting. The mass-based water-to-binder ratios (W/B) are given in table 6.3. CaNaCrete was delivered with all process water incorporated: no additional water was needed on-site. The Isohemp mix had to be manually hydrated, using buckets with tap water of about 15 °C.

Additives

Pozzolans

In both mixes, pozzolanic materials are used as additives to provide a stronger initial bond, improve frost and water resistance and help retain mix water during curing. This ensures a proper binding process of the components. For reasons of confidentiality, the exact nature and dosage of these additives is kept secret by the manufacturers.

Since this additive is already premixed through the CaNaCrete and in the Isohemp formulation, it is excluded from the mix-design ratios in table 6.3.

Pigment

A powdered natural pigment, “70 Rouge Vénitien”, was used as a visual tracer. It was added to every second layer during casting, creating alternating red colored layers. This was done to verify layer thickness and uniformity of compaction during testing. A variety of dosages was used to showcase aesthetic possibilities of the material.

The used powder is an inorganic clay-derived pigment containing 25-65% iron oxides (Pigmentshop, 2025). The dosed quantities are so small they are excluded from the mix-design ratios in table 6.3.

Mix Design

The mix-proportioning of both mixes is reported in table 6.3. The supplier recipes are translated into two dimensionless ratios for easy comparison with hemp-lime mixtures found in the literature: Binder-to-hemp mass ratio (B/H) and water-to-binder mass ratio (W/B).

Isohemp’s mix has roughly 45% more binder per unit fiber, which also explaints its higher manufacturer declared dry bulk density. CaNaCrete has a higher W/B ratio, making it a very workable mix. However, excess water must evaporate before significant carbonation can occur, so the mixture dries more slowly and gains strength later.

Mix	Description	Hemp Shivs	Binder	Water	B/H*	W/B*	Dry bulk density (kg/m³)	Manuf.
CaNaCrete	“Wet” premix, in 1.2 m³ big-bag based on air lime	110 parts	120 parts	240 parts	**1.09**	**2.00**	275 +/- 2.5%	EXIE
Hempbag + ProKalk Lime	On-site mix, based on air + hydraulic lime	200L (25kg)	40kg	50L	**1.60**	**1.25**	300 +/- 10%	IsoHemp

**W/B = water ÷ binder, B/H = binder ÷ hemp (both by mass)*

Table 6.3 Mix design ratios

Fig 6.3 Bigbag of EXIE CaNaCrete (back), IsoHemp Hempbag + ProKalk (front)

Fig 6.4 Adding pigment to the mix

Manufacturing Considerations

Previous chapter describes the two hempcrete compositions used in this reseach. When aiming to automate the materials manufacturing and thus prefabricate a hempcrete wall element off-site, several considerations came up. These are described in the following chapter.

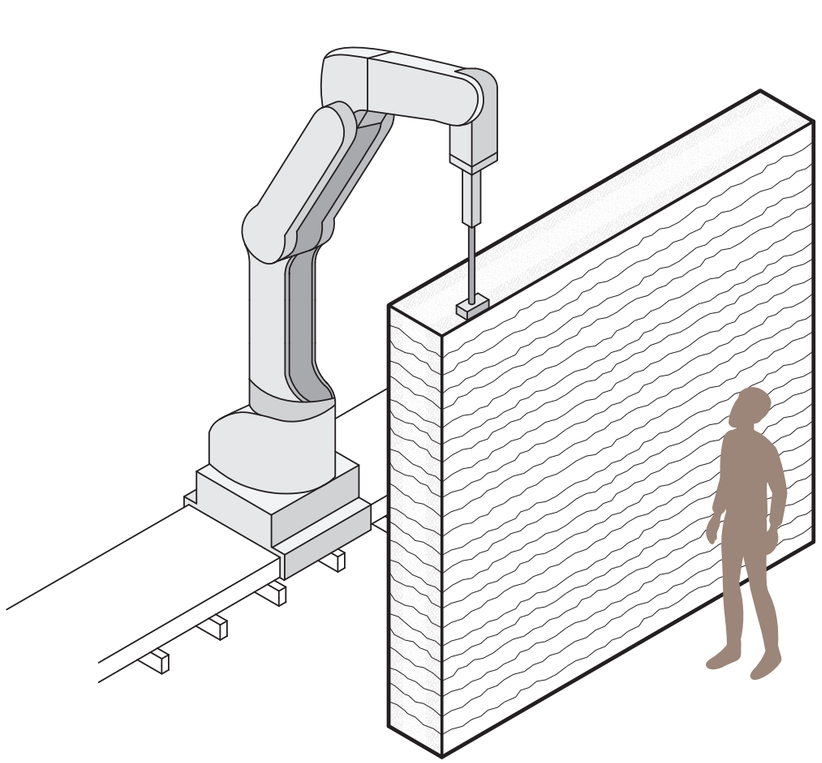

Fig 6.5 Concept: A rail-mounted robotic arm equipped with a pneumatic rammer to produce hempcrete wall elements.

Monomateriality

The first consideration is to eliminate the supporting timber frame and use multi-density compaction instead. This follows the following logic:

Eliminate timber stud frame

As described in chapter 4, in current hempcrete construction an internal timber stud frame accounts for loads applied to the wall. At least 7 cm of hempcrete must cover each stud to prevent cracking. As the wall height increases, the dimensions of the stud grow. Combined with the mandatory hempcrete coverage, this results in hempcrete wall sections being unnecessarily thick and often thermally over-dimensioned. To assess the need for this interal frame, at first, “pure” hemp and lime needs to be researched.

Multi-density compaction

Field observations (chapter 4) show that builders ram the exterior face of a hempcrete wall harder than the interior. This heavier compaction is mostly done for durability, not for rigidity. This is done very inconsistently, leading to density differences within the layer which eventually cause cracks.

A machine could turn this necessary compaction into an advantage by densifying the exterior face in a controlled and repeatable way. It could even allow this zone to take over part of the wall’s rigidity. To make this work, the machine needs exact instructions on how far it must ram inwards from each face. In other words, the depth of the high density zones, and therefore the size of the rammer head, need to be specified.

Leaving the interior zone less compacted will improve the wall’s insulation. However, it is not yet known how thick that low density core must be to satisfy thermal requirements, as well as the residual insulation values of the denser zones.

Monolithic Composite

Treating a monolithic hempcrete wall as a multi-density zoned “sandwich” wall sounds contrasting. However, that is exactly one of the considerations of this research. Densified exteriors enclose a lighter core, turning a monomaterial into a composite by density alone.

This experiment investigates how this multi-density compaction will affect performance of the wall. A series of hempcrete samples with varied density profiles are tested on mechanical strength and thermal resistance. These results will give an indication of how the pure hempcrete, without the help of additional binders or an internal frame, behaves when its density is controlled from the outside in.

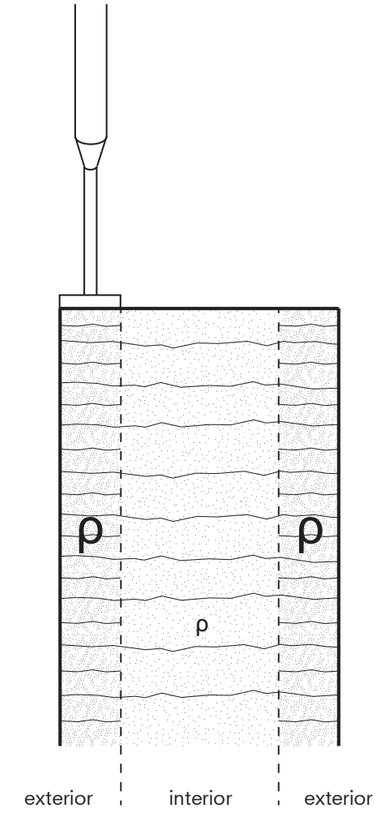

Fig 6.6 Three zone ramming concept

Layering and Orientation

Second, the walls layer height and orientation are reconsidered. Hempcrete is traditionally rammed top down. This creates horizontal layers that remain in this orientation once the wall cures in situ. Prefabrication would break this constraint: once cured, an element compacted top down at the factory can be rotated into any orientation before it is installed on site.

Layer orientation

Chapte 3.2 describes that hemp shiv particles on themselves are anisotropic. This means the direction of the hemp shiv in the element influences its materials properties. During ramming, the more force is applied to a layer, the more the shivs tends to line up perpendicular to the direction of compacting. Looking from above, densely compacted shivs lie flat but are pointing in random directions. This means that shiv orientaion always follows layer orientaiton. Rotating the element after curing, changes the way loads and heat flows intersect its micro structure of aligned shivs. This observation is illustrated in figur 6.7.

Layer height

On site observations (chapter 4) showed that hemp lime builders often pour thick layers of hemp to increase workflow speed. Since the compaction force decays against the mould walls, the top of a thick layer ends up denser (and the shivs more aligned) than the bottom. Both result in varying material performance inside the layer. Prefabrication opens the chance to both speed up the workflow and precisely control layer thickness.

This experiment investigates how layer thickness and orientation will influence density and particle alignment. Samples varying in initial layer height and compaction orientation are produced and tested on mechanical strength and thermal resistance.

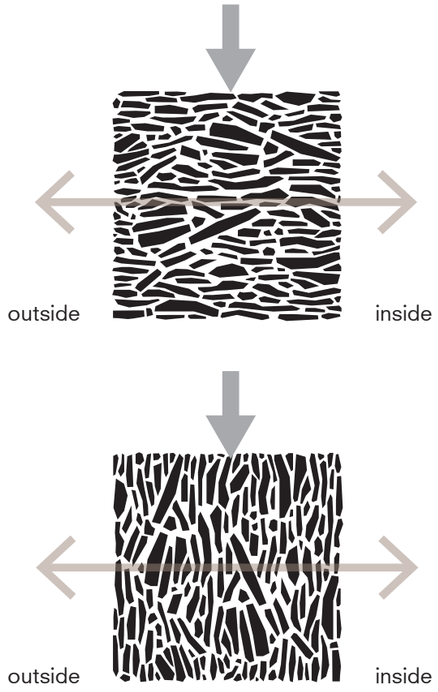

Fig 6.7 Load (gray) or thermal path (brown) oriented parallel or perpendicular to layer and shiv orientation.

Fig 6.9 Cross section of compressed sample, torn by hand. The shivs are stacked horizontally, but the orientation of their long axes remain randomly distributed in the plane.

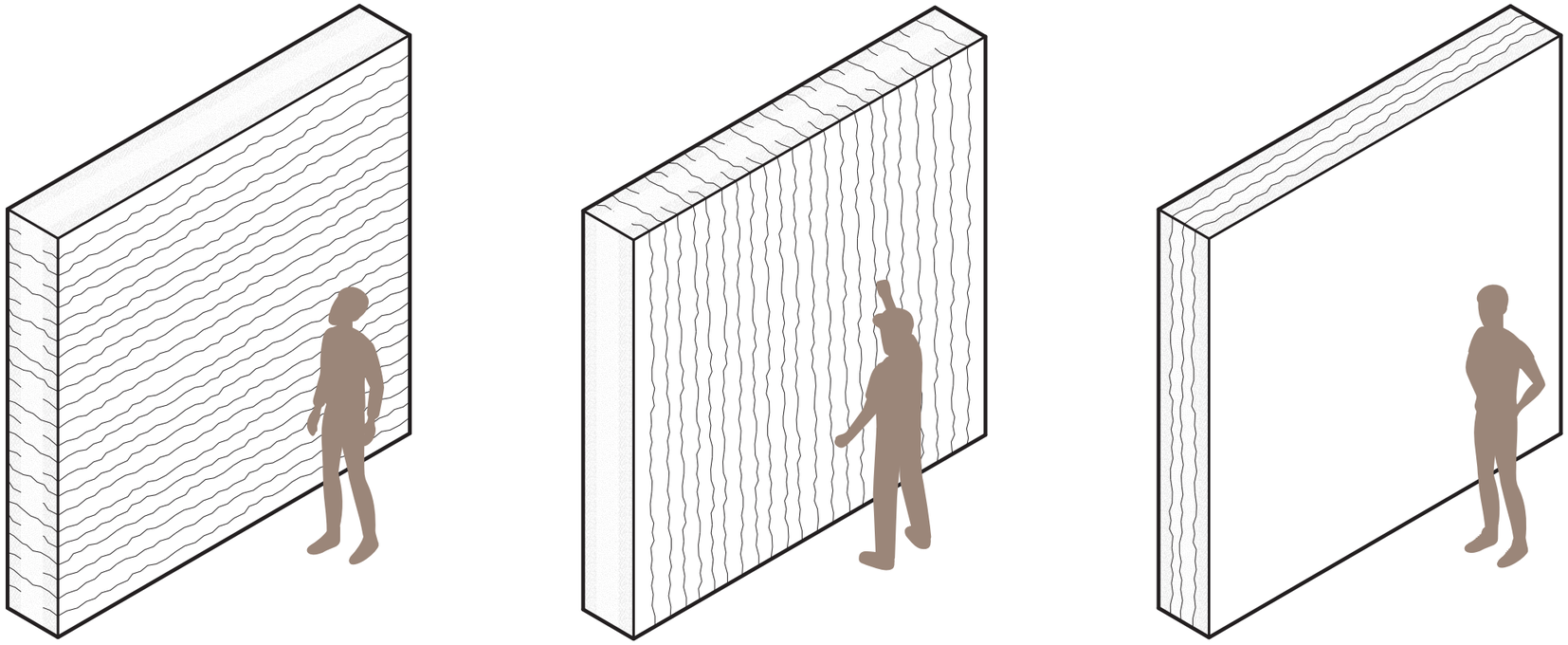

Fig 6.8 Orientations regarded in this experiment, LTR: Top compaction, side compaction, front compaction

Transportation

Also, transportation limits are considered. Once production moves off site, the prefab elements have to be lifted and moved. Their mechanical performance limits in what way this can be done. A review of rammed earth practice (chapter 4) pointed to two promising options; lifting straps passed beneath the panel and barrier clamps that grip the element through distributed clamping force.

Giving a substantiated suggestion asks for data on hempcrete's capacity in compression and bending. This experiment therefore identifies those properties to judge whether the elements can be handled in their bare state, without additional frames or anchors.

Environmental Impact

Lastly, the environmental impact of hempcrete is condisered. Changing the manufacturing method affects its carbon footprint. Both manual and prefabricated block production are often claimed to result in a CO_2-negative product. It is important to understand to what extent, and in which life cycle stages, automation influences the environmental performance of the material.

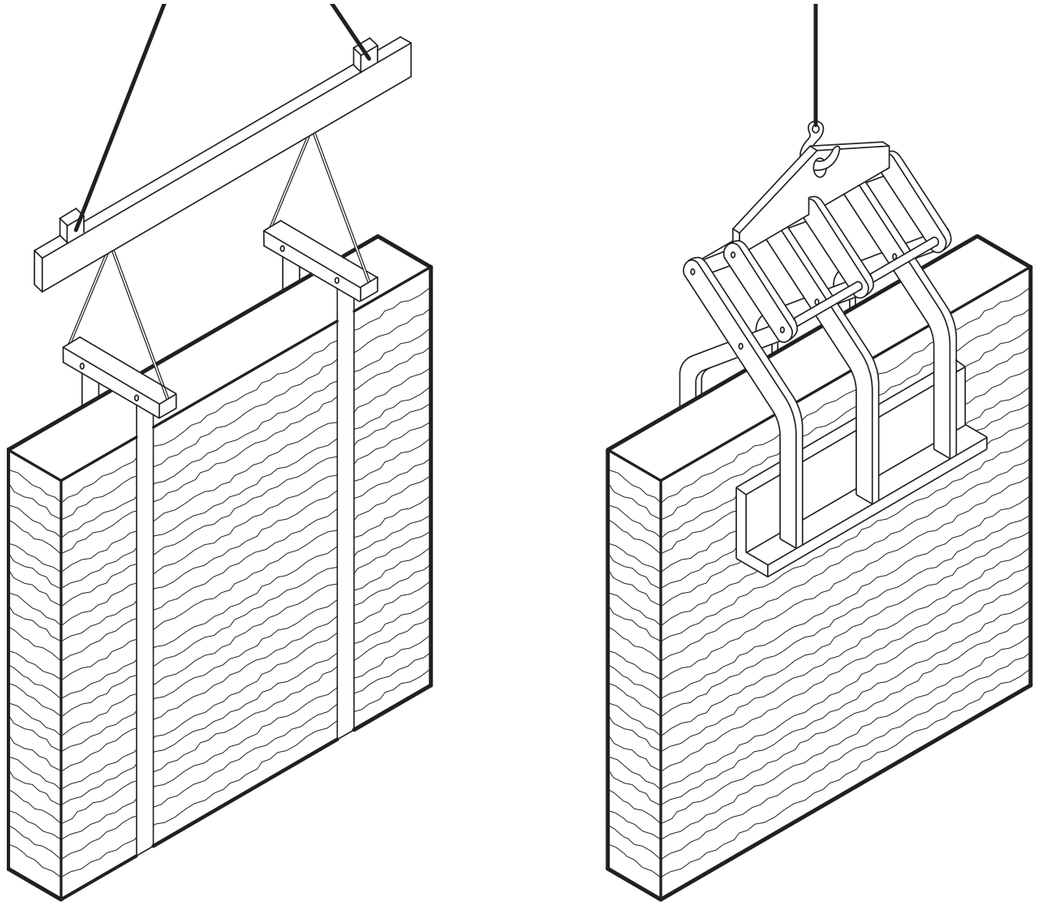

Fig 6.10 Suggested transporting systems. Left: lifing straps, right: barrier clamps

Fig 6.11 Craning Rammed Earth blocks into place on site

Experiment Setup

As found in the literature, hempcretes density (and therefore its hygrothermal and mechanical properties) are influenced by a broad range of material and manufacturing related factors.

Four of the considerations discribed in the previous section are turned into the experiments variables:

- The binder used in the mixture (B);
- The percentual reduction of layer thickness, the so called 'compaction factor' (C);
- The initial layer thickness put in the formwork, before tamping (L_i) and
- The orientation of compaction (O)

The corresponding values for each variable are shown in table 6.4.

Variables

Symbol	Variable	Values				Unit
L_i	Initial layer thickness (before compaction)	5	10	20	30	(cm)
C	Compaction Factor (reduction of layer thickness)	10	33	50	60	(%)
O	Orientation of compaction	Top	Side	Front	-	-
B	Binder used in mixture	Air lime	Mixed lime	-	-	-

Table 6.4 Input variables with corresponding values

Initial layer thickness (L_i)

The thickness of a single layer placed in the formwork, before tamping. Thicker layers are expected to cause a density gradient: a non-uniform density distribution (top vs. bottom) within the layer. This potentially creates thermal bridges and mechanically weaker points. Thinner layers are expected to improve homogeneity but would result in a longer production time.

The variable boundaries are defined by combining three sources:

- The manufacturers' stated maximum layer heights.
- Values cited in the literature.
- Limits observed when working on hemp-lime constructing projects in practice.

Compaction factor (C)

The compaction factor describes the percentage reduction of the material layer during tamping. A higher C gives a denser mixture, resulting in lower porosity. This is expected to result in higher thermal conductivity and higher mechanical strength since there it includes more binder per unit hempcrete (Nguyen et al., 2009).

A preliminary compaction test (described in chapter 7.3) defined the variable boundaries:

- C_{min} = 10%: The least compaction that is needed to still give the hemp and lime enough bond for a coherent initial set.
- C_{max} = 60%: The maximum manually achievable percentage reduction.

The variable values were chosen within this range so that the resulting densities are spread evenly.

Orientation of compaction (O)

This experiment tests whether the orientation of a prefab hempcrete element has influence on its thermal and mechanical bahaviour. It might create directional flows of heat along the grain of the shiv and weak spots at the interface between layers, where layers of shiv delaminate.

Figure 6.12 illustrates that changing the orientation of a hempcrete wall element alters whether the layers, and therefore shiv particles lie parallel or perpendicular to heat flow paths and load directions. This is expected to influence its thermal and mechanical performance. In this experiment, three orientations are considered: top, side and front compaction.

Binder used in mixture (B)

As discussed in material selection, two mixtures are used and compared: One based on an air lime binder, one based on a mix of air and hydraulic lime binder.

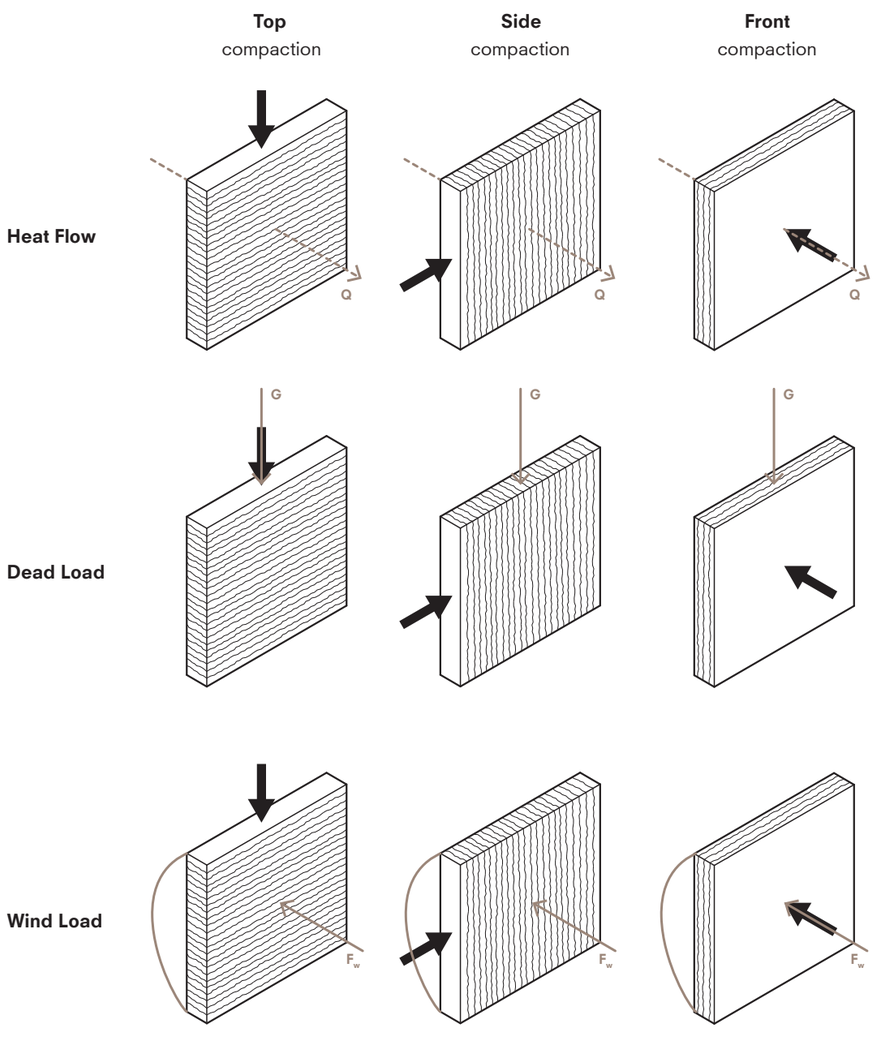

Fig 6.12 Compaction orientations (black arrows), heat flow and load directions (brown arrows)

Sweeps

A full factorial of all variables would give 96 unique configurations. These were not all considered. 13 representative configurations were chosen and grouped into four experiment sweeps, each isolating one variable (S1 - S4). (Table 6.5) The entire experiment design of this research is summarized in figure 6.13.

Experiment	Description	Isolated variable	Fixed variables	Configurations
E1	Compaction Sweep	C (10 - 60%)	L_i = 10cm O = Top B = Air lime	A0, A1, A2, A3
E2	Layer height Sweep	L_i (5 - 30cm)	C = 50% O = Top B = Air lime	A6, A2, A4, A5
E3	Orientation Sweep	O (Top / Side / Front)	C = 50% L_i = 5cm B = Air lime	A6, A7, A8
E4	Binder Sweep	B (Air lime vs Mixed lime)	C = 50%, 60% L_i = 5, 10 O = Top, Side	A2, A3, A6, A7 M9, M10, M11, M12

Table 6.5 Experiment matrix

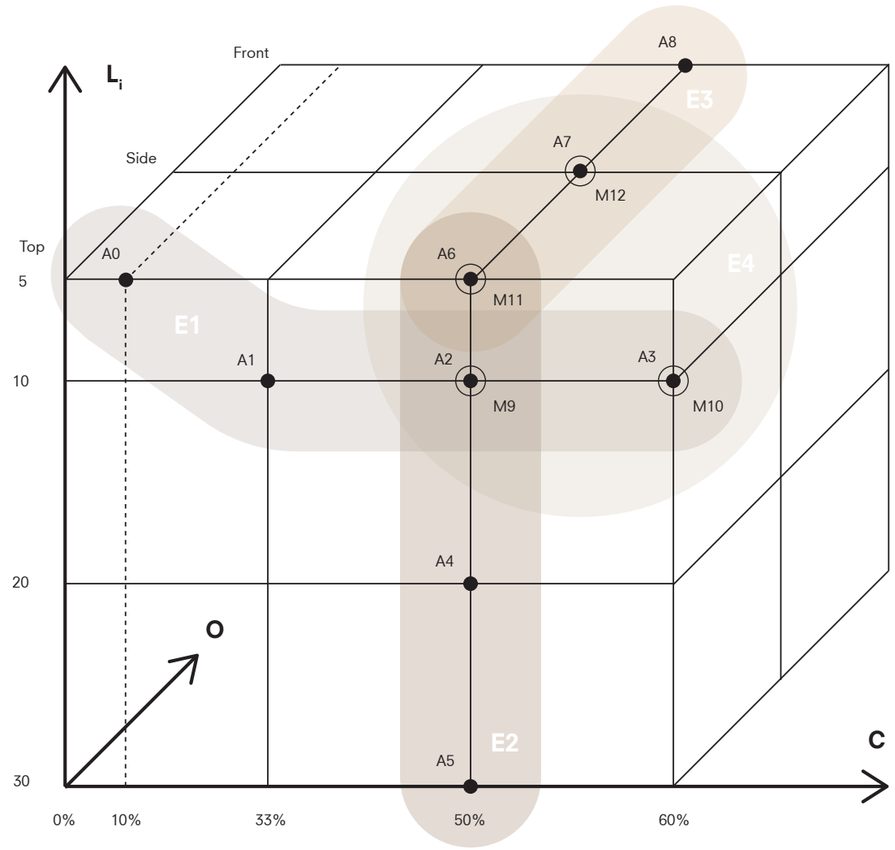

Fig 6.13 Experiment design

Configurations

Configuration	Binder type B	Orientation O	Initial layer height L_i (cm)	Compaction factor C (%)	Experiment series
A0	Air lime	Top	5	10	E1 (Baseline)
A1	Air lime	Top	10	33	E1
A2	Air lime	Top	10	50	E1, E2, E4
A3	Air lime	Top	10	60	E1, E4
A4	Air lime	Top	20	50	E2
A5	Air lime	Top	30	50	E2
A6	Air lime	Top	5	50	E2, E4
A7	Air lime	Side	5	50	E3, E4
A8	Air lime	Front	5	50	E3
M9	Mixed lime	Top	10	50	E4
M10	Mixed lime	Top	10	60	E4
M11	Mixed lime	Top	5	50	E4
M12	Mixed lime	Side	5	50	E4

Table 6.6 Configurations considered in the experiments, with corresponding variable values.

Tests

Four tests were set up to test the samples from experiments E1-E4 on thermal and mechanical properties. Each test required its own sample geometry. The full, step-by-step method for each test can be found in chapters 8, 9 10 and 11.

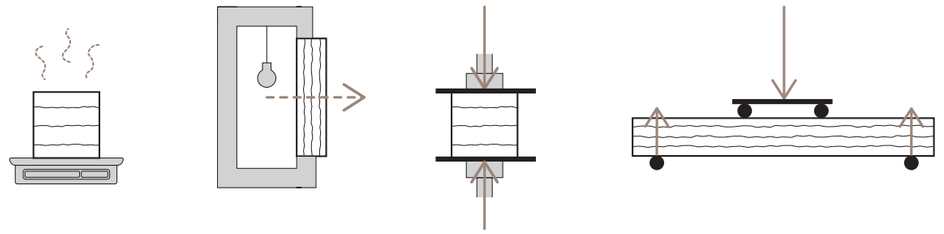

Fig 6.14 Schematic test setups, LTR: Drying,, hotbox, compressive strength, 4 point bending

Test	Purpose	Sample geometry (cm)	Output parameter	Symbol	Unit
Drying	Verify that process water has evaporated: Reference for further testing. Determine final densities.	Cube (15x15x15)	- Air-dry equilibrium bulk density - Drying curve	$\rho_{dry,eq}$ -	kg/m^3 -
Hotbox	Measure thermal resistance	Panel (27x9x27)	Thermal conductivity	λ	W/mK
Compressive strength	Measure load-bearing capacity in compression	Cube (15x15x15)	- Stress-strain curve - Young's modulus - Yield strength	- E σ_y	- MPa MPa
4 point bending	Measure flexural behavior	Column (90x9x9)	- Young's modulus - Bending strength	E σ_f	MPa MPa

Table 6.7 Test matrix

Summary

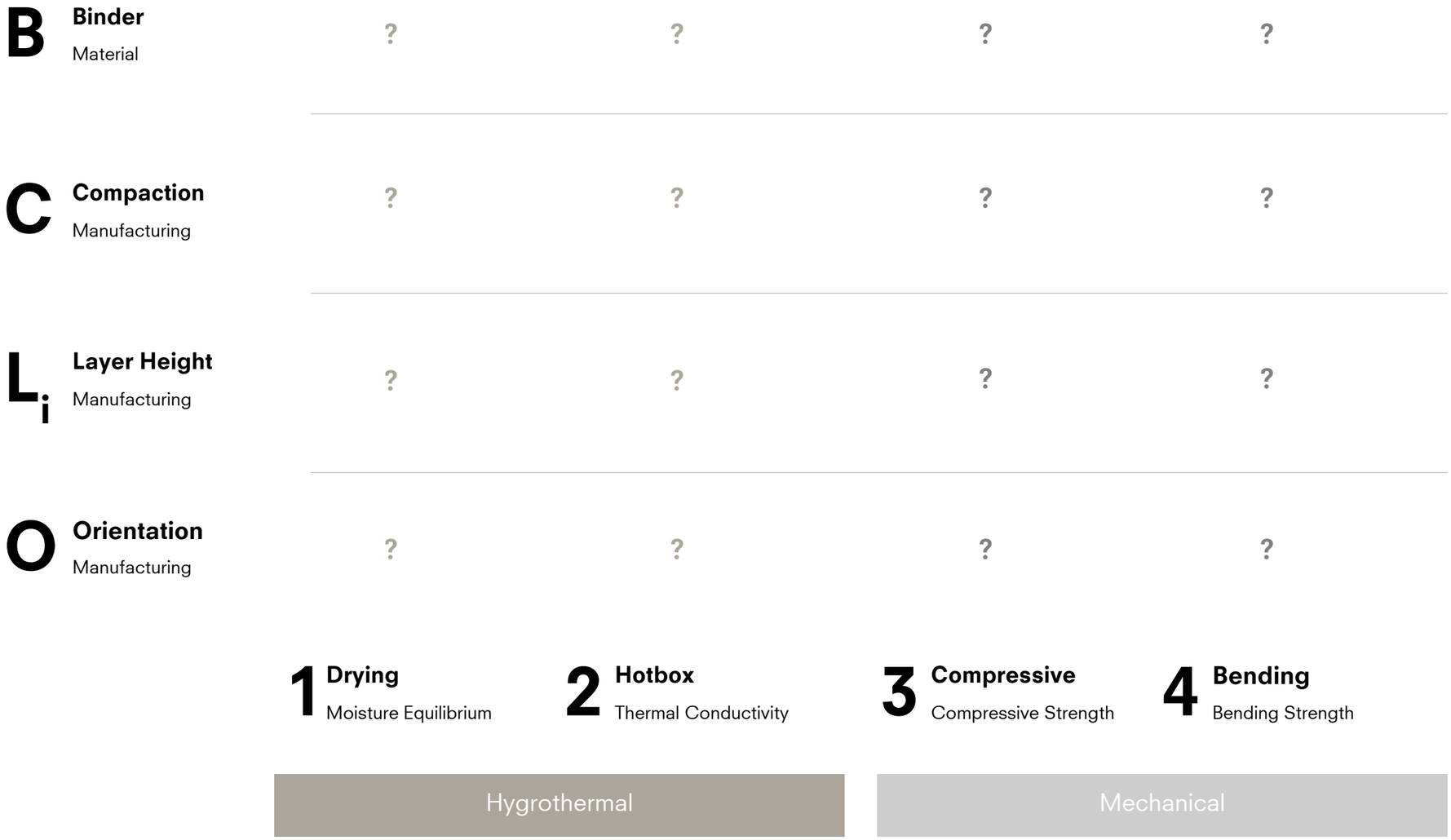

Fig 6.15 Observation Matrix

Observation Matrix

The main objective of this experiment is to produce a self-standing and insulating hempcrete wall while using an automated ramming system.

By sitting in between material characterization and manufacturing methods, this experiment examines how changes in manufacturing parameters influence the wall's hygrothermal and mechanical performance. Six considerations came up, of which four are used as the experiments variables: binder type (B), compaction (C), initial layer height (L_i) and orientation of compaction (O).

The next chapter describes the fabrication of test specimens in which these variables are systematically varied. Performance is then measured with four tests: drying and hot-box tests for hygrothermal behaviour, and compression and four-point bending for mechanical behaviour.

After testing, the matrix in figure 6.15 will mark whether an effect is observed per variable.

Sample Production

This chapter describes how the samples were produced. It specifies the location of the experiment and the tools and equipment used. It than maps the entire production workflow, including timeline and curing conditions, under which every samples was made.

Fig 7.1 Demoulding five cubic samples M9

Production Site

Location

All samples were produced (mixed, cast and cured) in a temporary workshop set up in the basement of the Keilepand, Rotterdam: an industrial hall converted into maker space.

Environmental Monitoring

During the full length of the experiment, the environmental conditions were monitored by a FL Fresh wireless datalogger, provided by the Dutch company Factorylab.

The FL Fresh was placed 60 cm above the floor, directly beside the curing setup. It uses an NDIR sensor to measure:

- Temperature (0 - 50 °C, ± 0.3 °C)
- Relative humidity (0 - 100 % RH, ± 2 % RH)
- CO_2 concentration (300 - 10000 ppm, ± 30 ppm).

Measured data was logged every 5 minutes to Factorylab's online portal via a Wirnet iStation LoRaWAN gateway (Kerlink). This provides a constant reference for the basement environment during mixing, casting and curing of the samples.

Graphs of the complete environmental data are provided further in this chapter.

Fig 7.2 Back of the Keilepand with its entrance to the basement

Fig 7.3 'Weather station' with FL Fresh datalogger (left) and Kerlink gateway (right)

Fig 7.4 Samples curing in workshop setup in the basement

Tools and Equipment

Moulds

The different test protocols in this experiment each required a different sample geometry, and therefore mould needed to be designed accordingly.

For the compression test, cubes measuring 15 x 15 x 15 cm were produced. The same cubes were used for the density monitoring. For the 4 point bending test, columns measuring 90 x 9 x 9 cm were produced. To achieve statistically reliable test results, and to cover the risk of breakage during the process, five copies of each sample configuration were produced for both tests. The hotbox test is nondestructive and can be repeated on the same sample, so only one panel measuring 27 x 9 x 27 cm was required for each configuration.

Three reusable concrete plex moulds were designed te be 20 cm taller than the target sample height to give the ramming tool enough clearance. Each time, one side functioned as permanent “lost” formwork, providing a stable surface for the samples to dry and cure.

Since some configurations shared test results, 113 unique samples were produced. The detailed sample matrix is provided in chapter 6.

Test	Sample geometry (cm)	Samples per config.
Density monitoring + compression	15 x 15 x 15	5
4 point bending	90 x 9 x 9	5
Hotbox	27 x 9 x 27	1

Table 7.1 Sample Sizes

Fig 7.5 Betonplex moulds. LTR: Single panel mould, five-fold column mould and five-fold cube mould

Fig 7.6 Several tools and equipment

Fig 7.7 Dosing Containers

Fig 7.8 Rammers

Fig 7.9 100 L electric pan mixer

Dosing Containers

To ensure that every layer is dosed with the same volume of fresh hempcrete, two custom dosing containers were designed:

Large container (2.25 L)

This container equals the volume of a 10 cm layer height in the cube mould (10 x 15 x 15 cm).

Small container (0.81 L)

This container equals the volume of a 10 cm layer height in the column mould (10 x 9 x 9 cm). Three small containers also make one 10 cm high layer for the panel mould (10 x 27 x 9 cm).

Filling a container exactly flush with the rim guarantees the correct layer height. By pouring whole, half- or double fills, the required initial layer heights (5, 10, 20, or 30 cm) are dosed quickly and repeatable for every sample geometry.

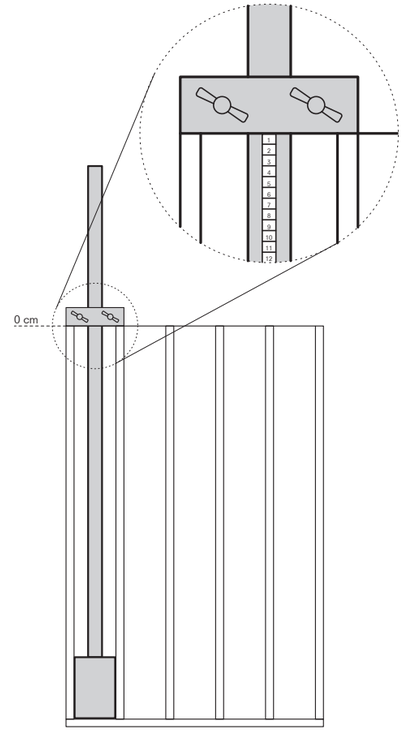

Fig 7.10 Schematic drawing of rammer with sliding clamp

Rammers

Custom rammers were designed to ensure each layer is reduced to its target layer thickness. In other words: Each layer is reduced with the same compaction factor.

A measuring tape is fixing along a wooden stick with a square foot (of either 9 x 9 cm or 15 x 15 cm). When the rammer is placed in an empty mould, the rim of the mould aligns with the zero mark. This means the tape reading at the rim always shows the distance from the bottom of the mould to the face of the rammer.

A sliding clamp with wing nuts is then locked at the target compacted layer height (e.g. 5 cm for C = 50 %). During compacting, ramming stops once the clamp touches the rim of the mould. In this way, the same thickness, and therefore same compaction factor, is ensured for every layer.

Mixer

A 100L electric pan mixer is used to mix the ProKalk Lime binder, process water and Hempbag shivs into a uniform hemp lime mixture.

Additional Tools

Several additional tools were essential for sample production:

- Electric drill and screwdriver
- Bar clamps and screws
- Mixing tubs
- Shovel
- Garden trowel
- Putty knife
- Folding rule
- Mould cleaning supplies
- Protective gloves

Fig 7.11 C_{max} test for 5x initial layer height L_i = 5 cm

Fig 7.12 C_{max} test for 4x initial layer height L_i = 10 cm

Fig 7.13 C_{max} test for 3x initial layer height L_i = 20 cm

Fig 7.14 C_{max} test for 3x initial layer height L_i = 30 cm

Preliminary Testing

Before producing any experimental samples, two preliminary tests were carried out to define the compaction limits of the CaNaCrete mix.

C_{max} test

Layers of 5, 10, 20 and 30 cm were placed into an 9 x 9 cm OSB mould and manually rammed with maximum force, until the rammer could no longer move vertically, or the mould broke.

Although thicker layers required more rams and greater force to reach this point, the maximum compaction was essentially the same for all heights. Increasing L_i only slightly decreased C_{max}. As a result, a single maximum compaction factor of C_{max} = 60 % was taken for the entire experiment.

L_i (cm)	$L_{f,\ avarage}$ (cm)	Repetitions	$C_{max,\ avarage}$ (%)
5	2	5	60
10	4	4	60
20	8,7	3	57
30	12,3	3	59

Table 7.2 Average maximum compaction factors

C_{min} test

To determine the minimum compaction needed for the fresh mix to hold together, two batches of five cubes were cast. When not compacting, all five samples failed after careful demoulding (a screwdriver was used to prevent vibrations). When compacting 10 %, one out five cubes failed. This indicated that at least C = 10 % is required to achieve sufficient initial bond.

Fig 7.15 C_{min} test: 0 % compaction, no sufficient initial bond

Fig 7.16 C_{min} test: 10 % compaction, just enough initial bond

Production Workflow

START

Demoulding

1. Place the freshly cast mould onto trestles at working height.
2. Clamp the mould securely and unscrew the betonplex top and partition planks.
3. Lift of the top sheet and planks, leaving the bottom sheet in place for the samples to cure on.
4. Clean the mould parts with a putty knife and white vinegar solution.

Ramming

1. Use compaction factor to calculate target layer height and lock sliding clamp accordingly.
2. Compact the fresh poured layer with a rammer untill the sliding clab hits the rim of the mould.
3. Repeat for every sample in the mould

Repeat untill target height is achieved

Determine **compaction factor (C)**

10 % | 33 % | 50 % | 60 %

Casting

Depending on the determined initial layer height, fill an x amount of dosing containers and pour in the mould.

Cubes and columns:
Repeat 5 times, for every sample in the mould.

Panels:
Repeat 3 times for every layer.

Determine **initial layer height (L_i)**

5 cm	0.5x container
10 cm	1x container
20 cm	2x container
30 cm	3x container

Add pigment

Into every 42 L (one mixing tub) batch of fresh hempcrete, add a dose of 70 Rouge Venetien pigment. Manually mix with a garden trowel for a few minutes to distribute the pigment evenly.

For a more intense red, add further pigment one tablespoon at a time, untill desired color intensity is achieved.

Mixing

1. Add one bag of ProKalk Lime (20 kg) into the panmixer
2. Gradually pour 80% of the water (1 construction bucket (20 L) into the mixer.
3. Watch that the lime is taken up by the water. Take care not to overmix, avoid small “balls” forming.
4. Keep the mixer running for a few minutes until the lime thickens into a lime slurry.
5. Add 0.5 Hempbag (100 L) of hemp shivs to the mix
6. Keep mixing and add the remaining 5 L of water untill a thick mixture forms.
7. Mix no more than a few minutes to prevent baling.
8. Check the mixture by hand: when a handfull is squeezed, the mix should bind into a firm ball without crumbling or releasing excess water.
9. Open the chute of the panmixer and empty its contents into the mixing tubs.

Requirements

Ambient temperature should be in between 5 and 30°C

Mix should be cast within 30 minutes

No mixing required

Determine **binder type (B)**

Mixed lime | Air lime

ProKalk Lime | CaNaCrete

Make Mould

(Re)assemble the mould in the required orientation, using bar clamps and fastening all screws with the electric screwdriver

Determine **orientation of compaction (O)**

Top

Side

Front

Fig 7.17 Illustration of the production workflow

Fig 7.18 Preparing the mould

Fig 7.19 Adding the hemp shivs to the lime mixture in the 100 L pan mixer

Fig 7.20 Filling the mould using the dosing container

Fig 7.21 Compacting the material with the rammer until sliding clamp hits the rim of the mould

Curing and Finishing

After casting, all samples stayed in the basement workshop, so that mixing, casting and curing all occurred under comparable ambient conditions. The whole experiment had a timespan of 68 days

Experiment Timeline

Because of the extensive workflow and limited moulds (one of each geometry), not all cubes, columns and panels were cast on the same day. The air lime samples (A0 - A8) were all produced over a 10 day window. This matches the 10 day processing guideline provided by EXIE for casting CaNaCrete after delivery.

After a first attempt to cut the samples to size, halfway through the experiment (at day 32), it was noticed that the inner cores were still moist, which led to reconsidering ventilation. The natural carbonisation under the ambient ventilation of the basement seemed too slow to fit the experiment time frame. So on day 39 an industrial floor fan (Spero SPKV60, 7680 m^3/h) was installed. The fan was positioned to circulate fresh air along the samples on the curing trestles. This accelerated CO_2 renewal around the samples and therefore sped up the carbonation process. This was also the moment the mixed lime samples were introduced in the experiment. They were all cast at the same day.

The panel samples were also cast at the same day. Hotbox test rounds were carried out on 39, 40, 41, 48 and 55 day relative after casting. The mechanical tests were done at a single day. At that moment, the tested air lime samples were between 58 and 67 days old. the mixed lime samples were 22 days old. A timeline of the experiment is illustrated in figure 7.22.

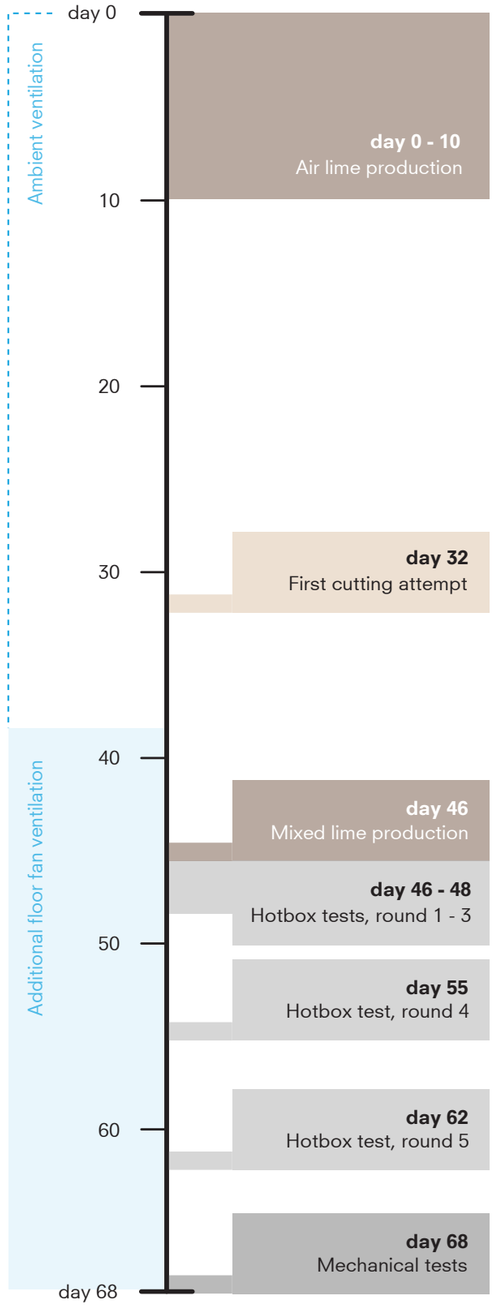

Fig 7.22 Summarized timeline of experiment

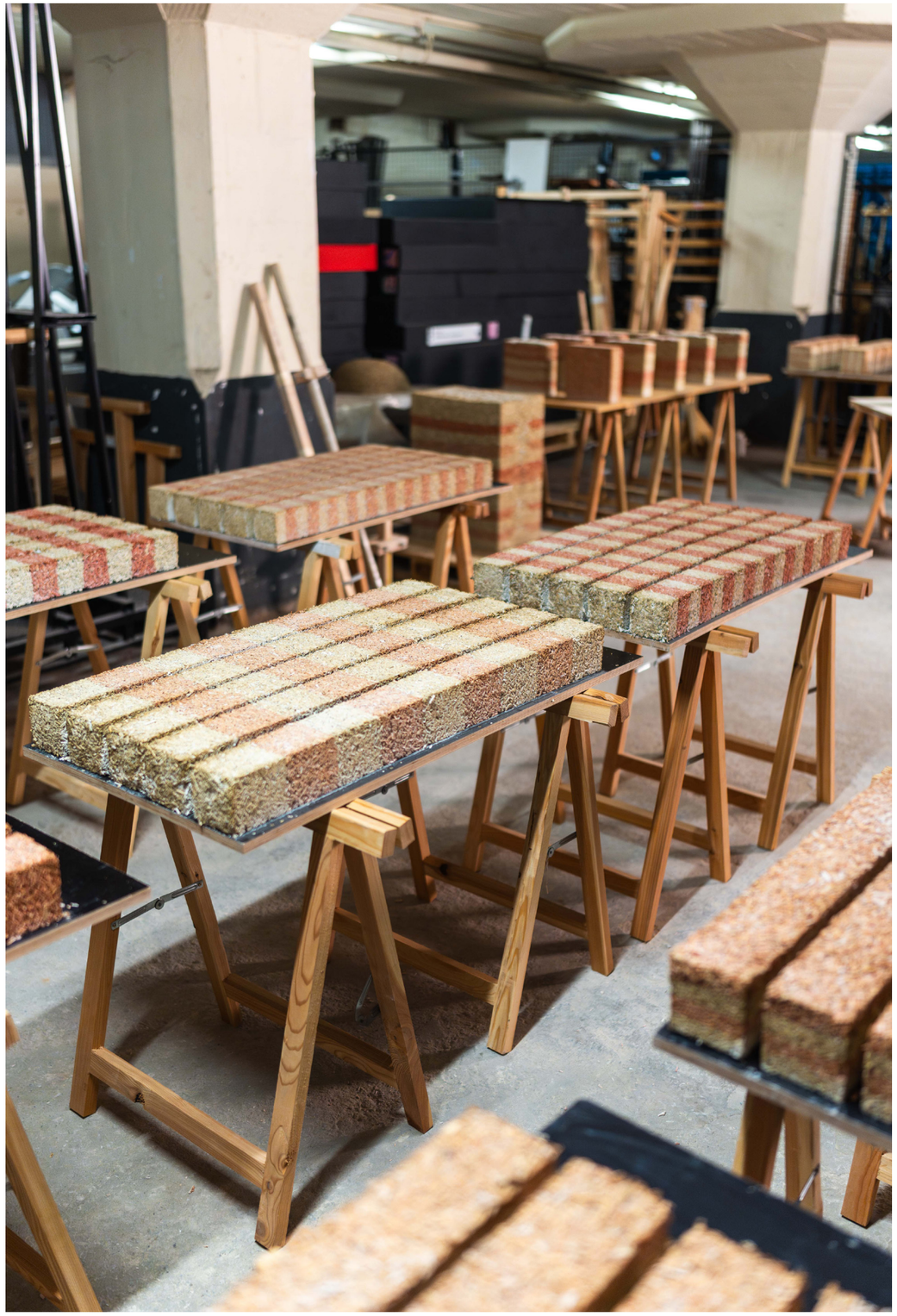

Fig 7.23 Description of Figure

Curing Conditions

The experiment took place from 1 March 2025, when the first samples were cast, to 7 May 2025, the date of mechanical testing at TU Delft. Table 7.3 lists the mean values of the 19 177 data points captured by the FL Fresh data logger. Figure 7.24 shows the complete time plots.

Temperature

In the literature, hempcrete was found to be usually cured at standard room temperature (18-22 °C). Because the average tempertature during this experiment was lower, both drying and strenght development are expected to progress more slowly than under the laboratory “sweet spot” conditions. The temperature climbed almost linearly from 14 at the start to almost 19 °C at the end of the experiment.

Variable	Mean value	Unit
Temperature	16.03	°C
Humidity	52.85	% RH
Carbon dioxide	459.68	ppm

Table 7.3 Average measurements FL Fresh

Relative Humidity

Collnart et al. (2012) found the fastest and most uniform drying at 45-50% RH, with active air movement. The mean RH in this experiment was slightly above that range but still low enough to allow moisture to escape and high enough to prevent early age shinkage cracks (< 35% RH).

Carbon Dioxide Concentration

Typical outdoor air contains about 400 ppm CO_2. The levels measured in this experiment were similar. Curing therefore took place under neutral carbonation conditions.

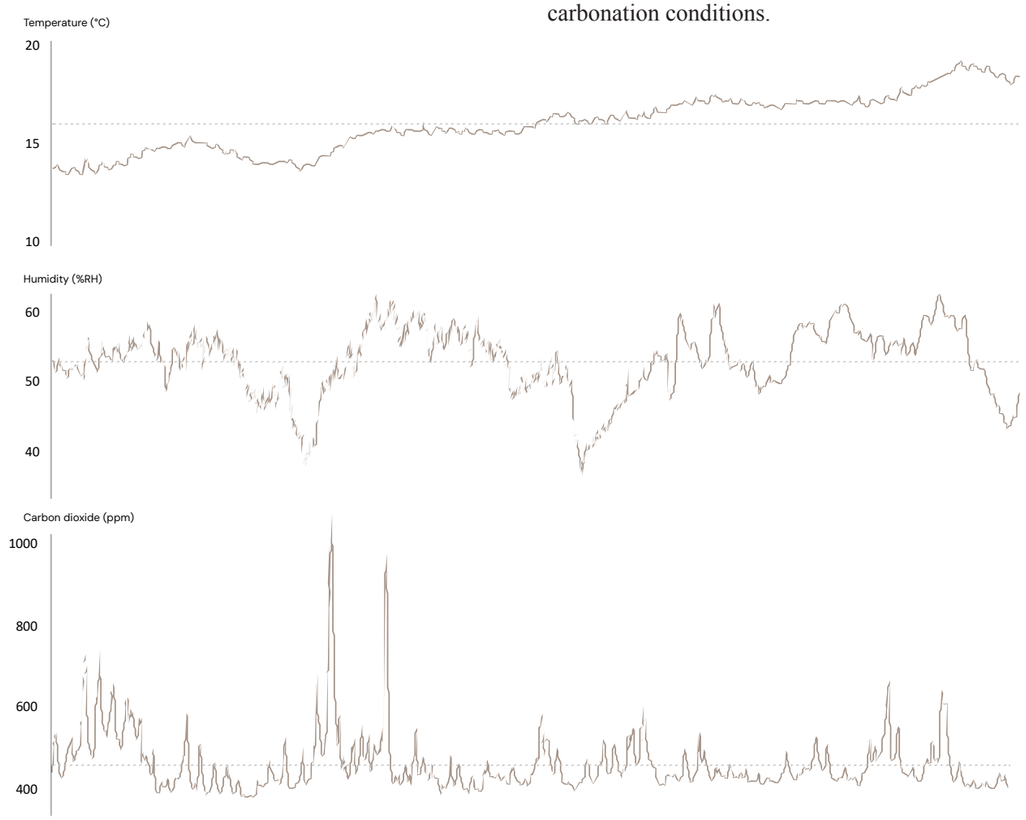

Fig 7.24 Plots of temperature, humidity and carbon dioxide in the basement. From start (1-3-2025) to end (7-5-2025)

Cutting To Size

The layer-by-layer production workflow caused most fresh cast samples to be over height. Instead of changing the dosing or compaction factor of the final layer (which would change the local density), oversized samples were trimmed to their exact target height.

The panel samples were clampted into a custom concrete plex mould and cut tot precisely 27 cm using a Japanese pull-saw. In this way, clean square edges were cut and the density of the final layer was preserved. The panels fitted perfectly into the hotbox setup.

In the compression and 4 point bending tests, height differences were not critical, as they were acounted for in normaliserd calculations. However, saw test were done to determine the inner humidity of the cubes.

Fig 7.25 Clean saw cut in cured cube

Fig 7.26 Cutting the samples to size with a Japanese handsaw

Full Scale Mockup

To demonstrate a monolithic hemp-lime wall element in which only the exterior is compacted for mechanical strength while the interior remains loose for insulation, a 1:1 scale mockup was produced.

Method

It measures 54 x 36 x 70 cm (L x W x H). These dimensions are all multiples of the 9 x 9 x 10 small dosing container. By dosing four filled containers across the width and six along the length, uniform initial layers of 10 cm were cast.

After pouring a layer, the 9 x 9 cm rammer was used to compact just the exterior 9 cm to a compaction of C = 50 %. This reduced the exterior layer height from 10 to 5 cm. The interior 10 cm layer remained uncompacted. So for the next run, only the exterior was filled with fresh material and compacted until the exteriors face was flush with the interior. Afterwards, a new layer could be placed over the entire wall section. This process was repeated seven times.

Properties

This mockup will be used to validate the results from the testing. In other words, to see what the real life insulation mechanical behaviour of the full wall would be.

Fig 7.27 Full Scale mockup, top view

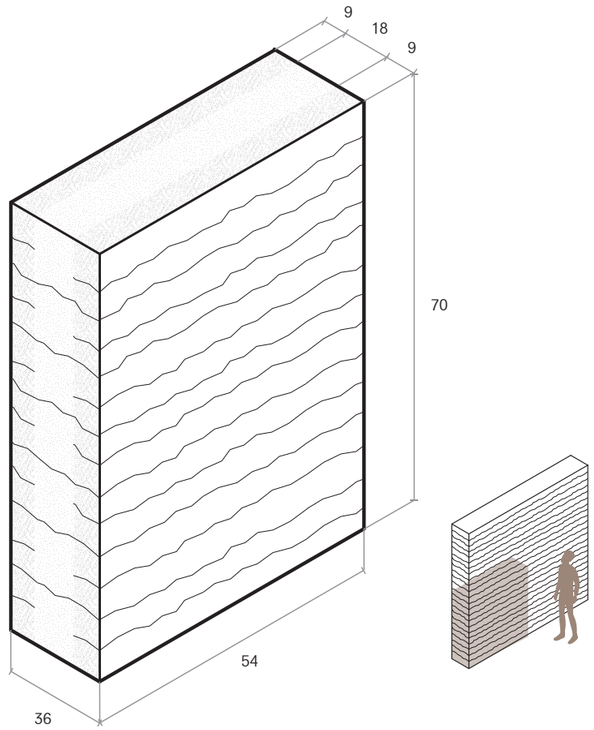

Fig 7.28 Dimensions mockup

Fig 7.29 Full scale mockup: front view

Fig 7.30 Air lime cubes (configurations A0 - A6)

Fig 7.31 Different geometries of configuration A2 for testing. LTR: Cube (15x15x15cm), panel (27x9x27cm) and column (90x9x9 cm).

Fig 7.32 Cubes presenting different compaction orientations. LTR: top (A6), side (A7) and front (A8)

Fig 7.33 Full scale mockup

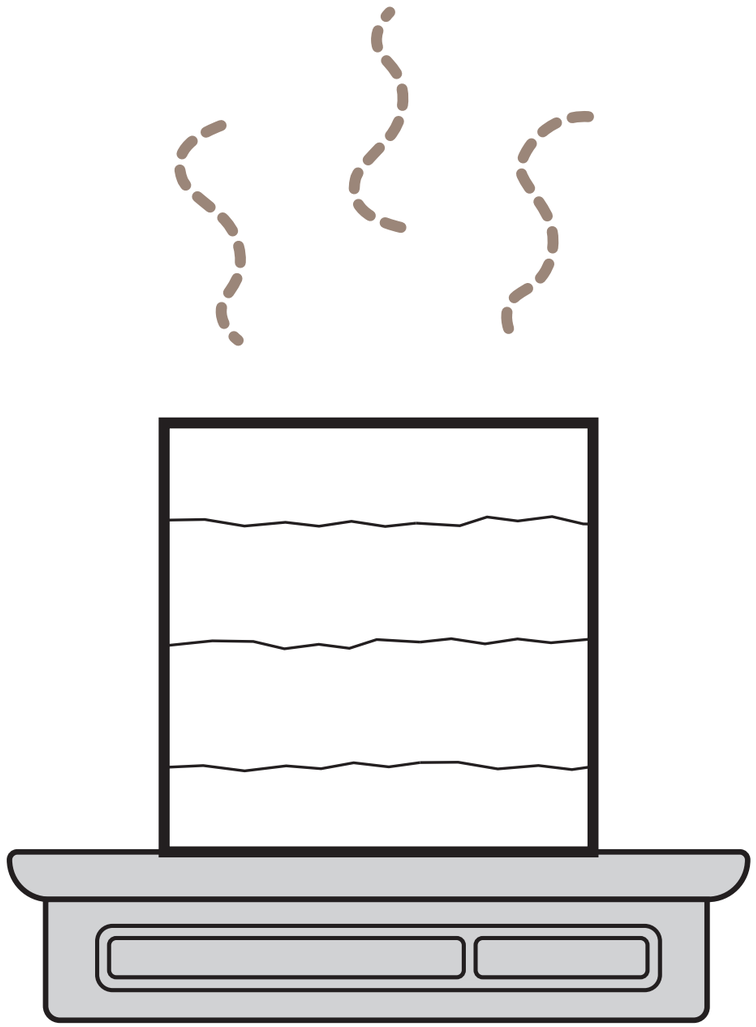

Fig 8.1 Schematic drying test

Drying Test

This chapter presents the method, results, and discussion of the drying test conducted to determine the samples' dry densities.

Method

Moisture Equilibrium

Density is the parameter that best predicts hempcrete behaviour. In earlier studies, every mix is compared by plotting its properties against its bulk density, no matter the water to binder (W/B) and binder to hemp (B/H) ratio. To position the two mixes used in this experiment within that reference field, their (equilibrium air dry) density must be known before undergoing further testing. A drying test is set up to monitor the cube samples' densities over the 68 days time frame. Because excess water would influence measurements during hotbox, compression and bending testing, the cube samples must first be proven to be "ready". Meaning having reached moisture equilibrium: all process water has evaporated, and only hygroscopic moisture remains.

Datasheets

The technical data sheets supplied by EXIE and IsoHemp list the dry bulk density of their products. For reference, the uncompacted wet (green) and dry bulk densities were measured. These values are listed in figure 8.1. The comparison to the manufacturer declared densities is not one-to-one. EXIE and IsoHemp both supply densities for their final product: a "lightly compacted" hempcrete.

The reference measurements from this experiment come from material that was not compacted at all. As a starting point, this "lightly compacted" is interpreted as 10% compaction. By taking EXIE's declared dry density and the compaction factors regarded in this experiment (10%, 33%, 50%, 60%), a theoretical "expected" dry density was calculated for every compaction factor. Figure 8.4 plots these estimates against the measured dry densities obtained at the end of curing.

Test Procedure

Although the drying rate of hempcrete wall depends on its measurements, the 15cm cubes were taken as a reference for the drying of all samples because of their workable size. Immediately after casting, the exact volume of each cube was determined. During the full experiment, one cube from each configuration was weighed every second day on a digital scale (accurate to 1 gram). These masses, divided by their volumes, resulted in bulk densities for each weighing session. After 68 days, the sequence of measurements was interpolated to draw the complete drying curve, presented in figure 8.3. The equilibrium air dry densities and the number of days required to reach them are listed in table 8.2. The drying conditions are noted in figure 7.24.

Mix	Green bulk density measured, * (kg/m³)	Dry bulk density measured** (kg/m³)	Dry bulk density, manufacturer-declared (kg/m³)
CaNaCrete	425	190	275 +/- 2.5%
Hempbag + ProKalk Lime	440	248	300 +/- 10%

**This is the fresh wet bulk density, or initial wet density. Measured right after filling the mould conditioned to 14 °C and 52.3% RH. Includes all water plus all air-voids.*

***This is the air-dry (equilibrium) bulk density. Measured after 67 days of curing and conditioned to 17 °C/ 54.9 % RH. Process water has evaporated, the rest remains as hygroscopic moisture.*

Table 8.1 Measured densities vs. datasheet values

Fig 8.2 Weighing sample on scale

Results

Configuration	L_i (cm)	C (%)	$\rho_{dry,eq}$ (kg/m³)	Days to reach $\rho_{dry,eq}$	Expected $\rho_{dry,eq}$ (kg/m³)	Note
A0	5	10	**203**	45	275	
A1	10	33	**236**	44	375	
A2	10	50	**348**	54	500	
A3	10	60	**~ 408**	> 68	625	Nearly reached equilibrium
A4	20	50	**334**	56	500	
A5	30	50	**296**	54	500	Higher volume, casting error
A6	5	50	**335**	55	500	
A7/A8	5	50	**344**	49	500	
M9	10	50	–	> 22	–	Not enough time
M10	10	60	–	> 22	–	Not enough time
M11	5	50	–	> 22	–	Not enough time

Table 8.2 Equilibrium air dry densities

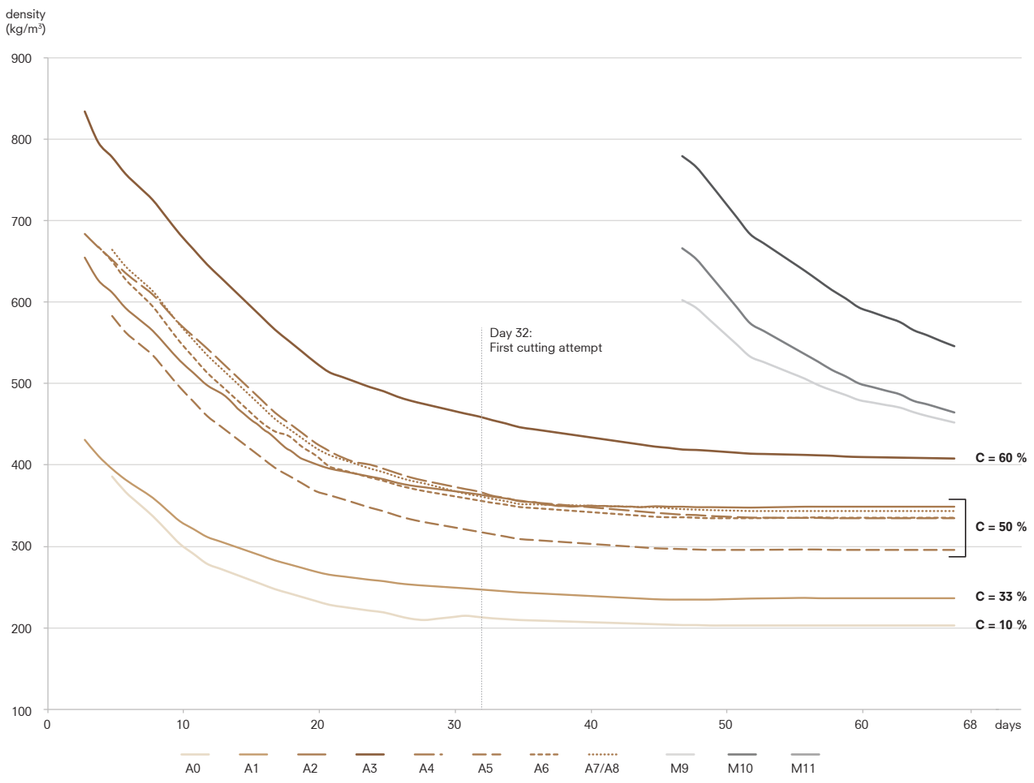

Fig 8.3 Drying curve, plotted as density decrease vs. time

Discussion

Drying Behaviour

For samples compacted between 10% and 50%, the drying curves (figure 8.3) flatten out after roughly 45-55 days. Only the most heavily rammed cube, A3 (60% compaction), was still losing mass after 68 days. This confirms that denser mixes dry more slowly. The likely explanation is because water must work its way through a tighter pore network. The drying curves did not reveal a clear influence of layer height on the overall drying rate. At day 32, the checked cubes remained moist at their cores, so further testing was postponed: the extra month they needed to cure is consistent with the drying curve. The drying curve of the hydraulic lime cubes M9-M11 never settled within the test window.

Compaction sweep

As expected, higher compaction resulted in higher final density: roughly 200 kg/m³ at minimal compaction (10%) and about 400 kg/m³ at maximum compaction (60%). The five cubes compacted to 50% clustered around 330 kg/m³, confirming a general trend.

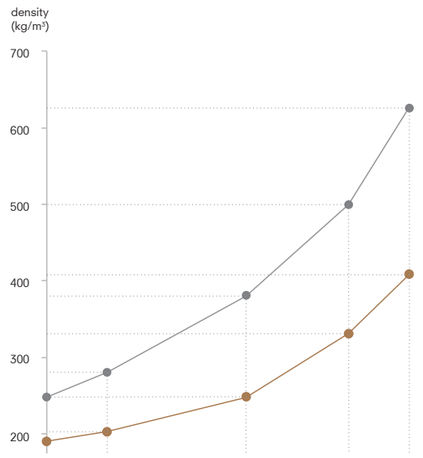

Fig 8.4 Measured vs. expected densities from datasheet

Layer height sweep

Within that 50% cluster, the outlier is A5, cast from a single 30 cm layer. To reach its target compaction, manual forces got high. The mould for A5 had no base plank, resulting in the mix being pressed out at the bottom and the sample gaining volume, leading to a lower final density. Although the final densities of the other 50% cubes are similar (334 - 348 kg/m³), visual inspection confirmed a clear internal gradient: the top of each layer being denser than the bottom. This supports the idea that thick layers compact unevenly even when the mean density of the total wall looks acceptable.

Orientation sweep

The effect of layer orientation on drying could not be isolated, because every cube was rotated regularly to promote uniform carbonation.

Binder sweep

The hydraulic lime samples did not reach moisture equilibrium at the end of the test window, so no conclusions can be drawn about the mixtures density or drying rate.

Manufacturer data sheets

Figure X.X plots the measured dry densities and compaction factor and compares those to the values predicted from EXIE's data sheet. Although both lines follow the same exponential trend (indicating high material predictability), the measured densities lie consistently lower. This offset implies that EXIE's "light-compaction" reference actually reflects a compaction level nearer to 40% - 50% rather than the assumed 10%.

Fig 8.5 Lime accumulation

Fig 8.6 Lime accumulation

Fig 8.7 Mould forming

Limitations

Non breathable mould surface

The concreteplex mould was needed for sample production because of its rigidity and smooth surface. Samples were left to cure on one side panel of the mould. Since concreteplex is non-breathable, moisture could not escape from the bottom of the samples.

Uncontrolled airflow

No constant airflow control. Without regulated air movement, stagnation parts (mostly those in between two samples) could slow evaporation and lead to inconsistent drying.

Curing environment

The drying basement is not representative of real on-site conditions. There is no natural sunlight and -heat exposure and no ventilated interior.

Observations

General

- Drying rate decreases over time
- Denser mixtures take longer to stabalise
- Dry density increases proportionally with compaction
- Mould growth and lime accumulation indicate insufficient airflow.

Sweep influence

Compaction:	observed
Layer height:	not observed
Orientation:	not tested
Binder:	inconclusive

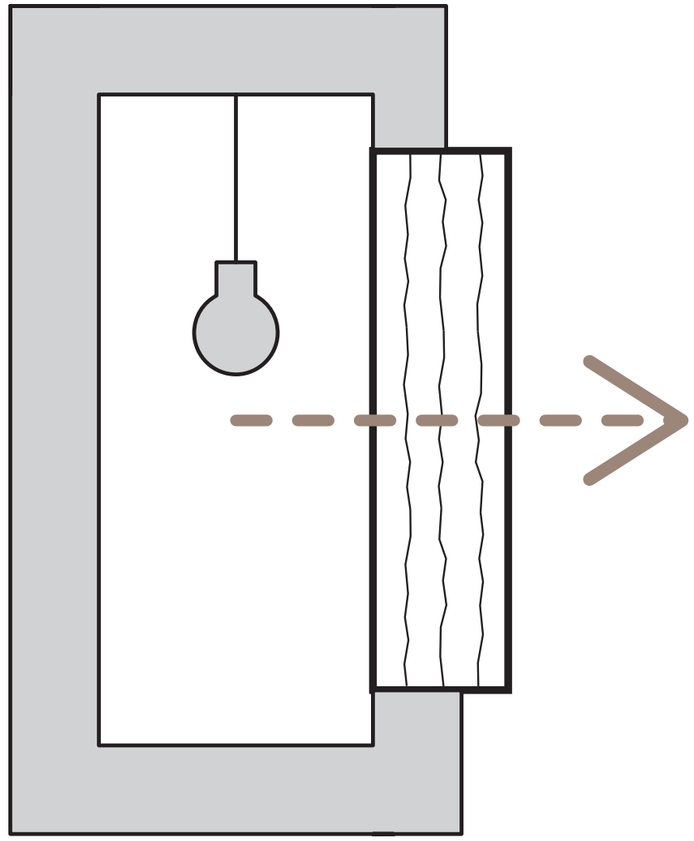

Fig 9.1 Schematic hotbox test

Hotbox Test

This chapter presents the method, results, and discussion of the hotbox test conducted to determine the samples' thermal conductivities

Method

Thermal transmission through the samples was measured using the hotbox setup at the ERiC Lab (Environmental Research in Climate) at the TU Delft Faculty of Architecture and the Built Environment. Five separate test rounds were performed so that each panel sample was measured for thermal transmission at least twice under steady state conditions.

Sample Preparation

Only the air lime based panel samples (trimmed to exactly 27 x 9 x 27 cm) were tested. Both in top and side compaction, the hemp shivs are aligned parralel to the heat flow. Front compaction would result in perpendicular heat flow to shiv alignment. Since changing the orientation from top to side does not affect the heat flow, the results for sample A7 were considered equal to those for sample A6. In total, eight panels were tested (table 9.1).

These were all produced on the same day. The hotbox testing was performed 39, 40, 41, 48 and 55 days after casting. Before testing, the dry bulk density of each panel was confirmed to be stable to ensure that all process water had evaporated and only moisture in equilibrium within the workshops relative humidity remained.

Frame

Preliminary COMSOL simulations demonstrated that a 27 x 27 cm face is big enough to not influence one directional heat flow in the middle of each sample. Slight variations in its 9 cm thickness can be normalized in the thermal conductivity calculations. To be able to test four panels simultaneously, a custom concreteplex frame was designed and built. 2 cm strokes of mineral wool were used in between the panels to both clamp them together and to prevent thermal bridging.

Configuration	B	O	L_f (cm)	C (%)	$\rho_{dry,eq}$ (rounded) (kg/m³)	Thickness (cm)	Test rounds
A0	Air	Top	5	10	205	9	3, 4, 5
A1	Air	Top	10	33	235	9	3, 4, 5
A2	Air	Top	10	50	330	9	1, 2
A3	Air	Top	10	60	405	9	1, 2
A4	Air	Top	20	50	330	9	3, 4, 5
A5	Air	Top	30	50	330	9	3, 4, 5
A6	Air	Top	5	50	330	9	1, 2
A7	Air	Side	5	50	330		Not tested, equals A6
A8	Air	Front	5	50	330	10	1, 2
M9	Mixed	Top	10	50	-		Not tested, other mix
M10	Mixed	Top	10	60	-		Not tested, other mix
M11	Mixed	Top	5	50	-		Not tested, other mix
M12	Mixed	Side	5	50	-		Not tested, other mix

Table 9.1 Sample sets tested

Setup and Equipment

Hotbox

1 cubic meter insulated box with 12 cm thick expanded-polystyrene (EPS) walls. A 63 x 63 cm opening was cut to fit the frame. The edges were sealed with duct tape.

Heating lamps

Inside the hotbox, two heating lamps were placed. A primary 60 W lamp wrapped in reflective aluminum foil to stabilize interior temperature without any direct radiation on the samples. Another 60 W lamp was used only during starting up, and turned off once the inside reached above 50 °C.

Heat flux sensors

Nine Hukseflux HFP01 Heat Flow Sensors (sensitivity 60 ± 3 μV/(W·m^{-2})) were used to measure the heat flux through the samples. One each on the interior (hot) and exterior (cold) face of the panel, plus an extra sensor on the cold face of sample A5 to investigate density-gradient effects. A steady state condition arose after the temperature on both sides on the panel had stabilised and the heat flux sensors on both sides of the samples had stablised and converged.

Thermocouples

Ten thermocouples were placed. One next to each heat flux sensor to measure surface temperatures and determine temperature difference ΔT. Two extra thermocouples were placed inside and outside the box, measuring ambient T_{in} and T_{out}.

Transmitters and dataloggers

All sensor were connected via six Eltek data transmitters to a SRV250 Squirrel receiver logger. Heat flux and temperatures were logged every 30 seconds and send to a PC running Eltek software. Realtime graphs could be read to notice whether the system was in steady state.

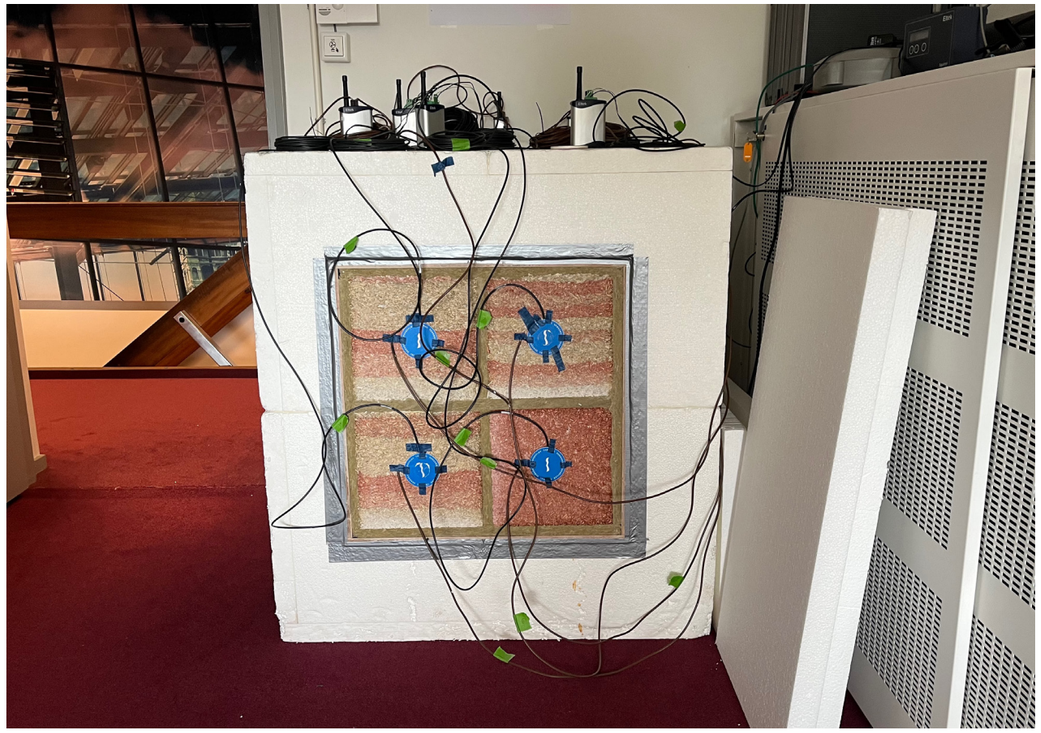

Fig 9.2 Samples in hotbox, wired with flux sensors and thermocouples

Test Simuation

Before starting the test, a COMSOL model was set up to simulate the hotbox test. In this way, one dimensional heat flow, time to steady state and the size of the panels in the frame were checked. The parameters used for this test (table 9.2) are based on the datasheets provided by EXIE and IsoHemp (table 9.3)

Parameter	Value	Unit
Thermal conductivity (λ)	0.078	W/mK
Density (ρ)	275	kg/m³
Specific heat capacity (C_p)	1200	J/kgK

Table 9.2 Material Properties entered into COMSOL

Mix	Dry bulk density ρ_{dry} (kg/m³)	λ (W/mK)
CaNaCrete	275 +/- 2.5%	0.078
ProKalk + Hempbag	300 +/- 10%	0.07

Table 9.3 Manufacturer declared properties (EXIE, 2024) (IsoHemp, 2024)

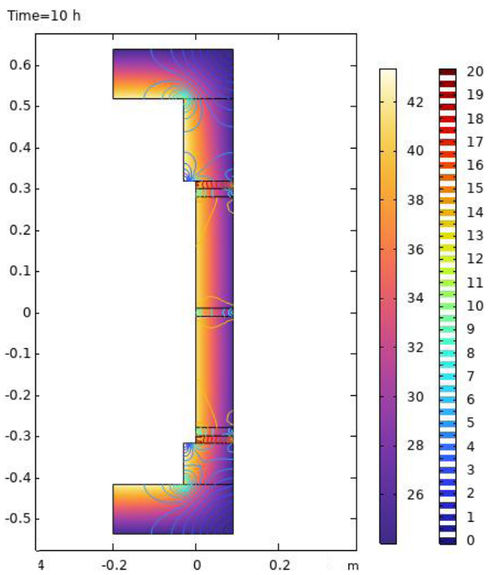

Fig 9.3 COMSOL simulation after 10 hours; The surface showing temperature (°C) and the contour lines showing total heat flux magnitude (W/m²)

One-dimensional heat flow

The contour plot of the total heat flux magnitude (the colored lines in figure 8.3) simulates all the flux streaming straight through the 27 x 9 cm panels. No lateral heat flows are observed in the centre of the test samples where the heat flux sensors will be mounted.

This validates that the 4 sample structure is truly one-dimensional in the samples center and 27 x 27 cm is big enough for reliable test results.

Time to steady state

In the heat flux vs. time plot (figure 8.4) it is noticed that the flux simulated through the hot side point probe (blue line) is peaking during the initial warm up. Afterwards it moves down towards the cold side point probe's flux (green line). After about 10 hours both curves line up at about 12 W/m². At that point, the simulated system has reached steady state thermal conduction (interior heat in = exterior heat out). This simulation shows that at least 10 hours are needed before any data can be read.

Stable temperature difference

The temperature vs. time plot in figure 9.5 shows the hot face (blue line) climbing to 46 °C, and then settling at about 42 °C after 2 hours. The cold face (green line) rises from the ambient 20 °C to 26 °C. This simulates a steady temperature difference ΔT of about 16 °C across the 9 cm panel section.

Because a larger ΔT speeds up the convergence of interior and exterior heat flux, it was decided to switch the second lamp on during the initial warm up until the hot-face temperature T_{in} reached about 50 °C. This would cause a ΔT of about 20 °C and therefore a shortened time to reach steady state.

Heat flux (W/m2)

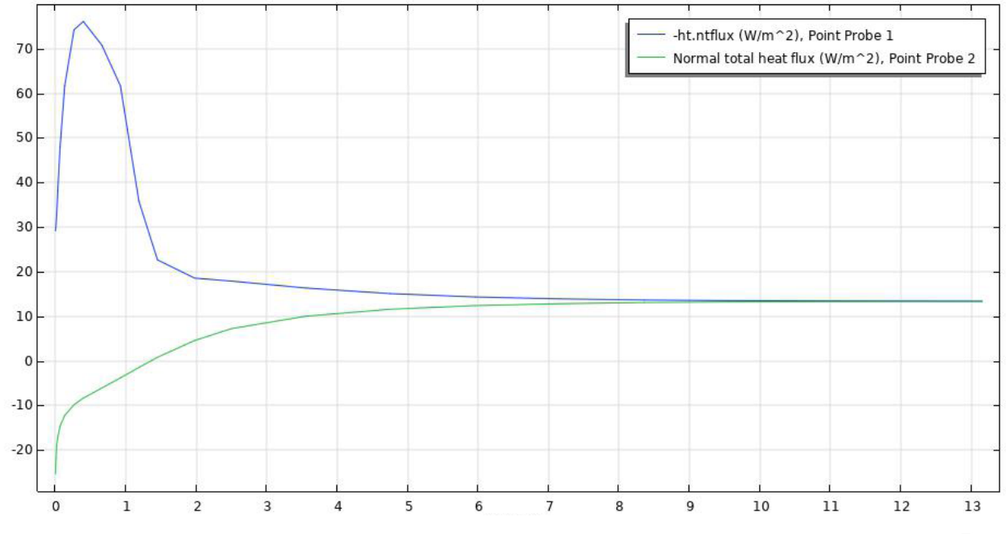

Fig 9.4 COMSOL simulation: heat flux vs. time

Temperature (°C)

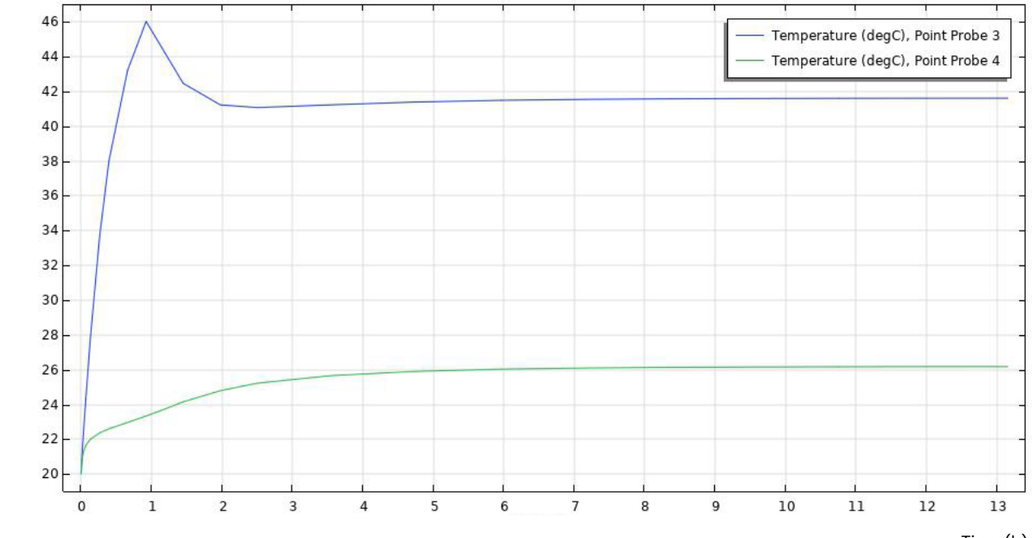

Fig 9.5 COMSOL simulation: temperature vs. time

8:00 9:00 19:00

Pre Test

1 Comfirming equilibrium state

Performing drying test to verify if all excess moisture has evaporated and sample is ready to test

2 Panel trimming

Clamp panels into sawing table cut to 27 x 27 x 9 cm with a Japanese pull saw

3 Panel framing

Seperate the four trimmed panels with 2 cm mineral wool to prevent thermal bridging.

Use bar clamps to enclose the panels and mineral wool with 18 mm concreteplex frame. Secure with screws so frame is rigid and airtight.

4 Hotbox preparation

Use a stanley knife to cut a square opening in the EPS walls of the hotbox that exactly matches the frame's outer dimensions.

5 Sensor labeling

Mark each Hukseflux heat sensor and each thermocouple with a unique number to make sure the logged data is linked to the right sample

Start Test

6 Inital warm up

Switch on both primary lamp and secondary lamp to begin heating the interior of the hotbox.

7 Sensor installation

Tape each heat flux sensor at the geomatric centre of the hot and cold faces of all four panels. Make sure the sensors have full surface contact.

Tape one thermocouple next to each flux sensor

Place two additional thermocouples to monitor ambient air inside and outside the box

8 Frame installation

Place the instrumensted frame into the cut out and seal all edges with duct tape to avoid air leaks.

Place two sheets of EPS in front of the hotbox opening to block air movement from people entering and leaving the room.

9 Data connections

Plug all flux sensors and thermocouples into the transmitters and datalogger.

10 Start logging

Start Eltek software on the PC. Logging starts at 30s intervals.

During Test

11 Temperature monitoring

Observe the hot side thermocouple. Once T_{in} > 50 °C, so that ΔT is about 20 °C, switch of the second lamp.

Observe T_{in} setteling at a constant temperature.

12 Steady state monitoring

Observe heat flux and ΔT plots to see whether hot and cold face fluxes converge and ΔT remains stable over at least 30 minutes.

13 Sensor checks

Every few hours, check visually and the on screen data to verify no sensor has shifted or fallen off.

Post Test

14 Data saving

Save the logged heat flux and temperature data files to the PC.

15 Setup shutdown

Turn of the heating lamps and loggers.

16 Frame removal

Either take the frame out of the hotbox and remove all sensors, or leave it set up for the rext round.

Fig 9.6 Timeline of one hotbox test round

Test Procedure

Fig 9.7 Constructing the frame, using two large bar clamps to clamp the panels, mineral wool and concreteplex together

Fig 9.8 Hotbox after cutting out the opening

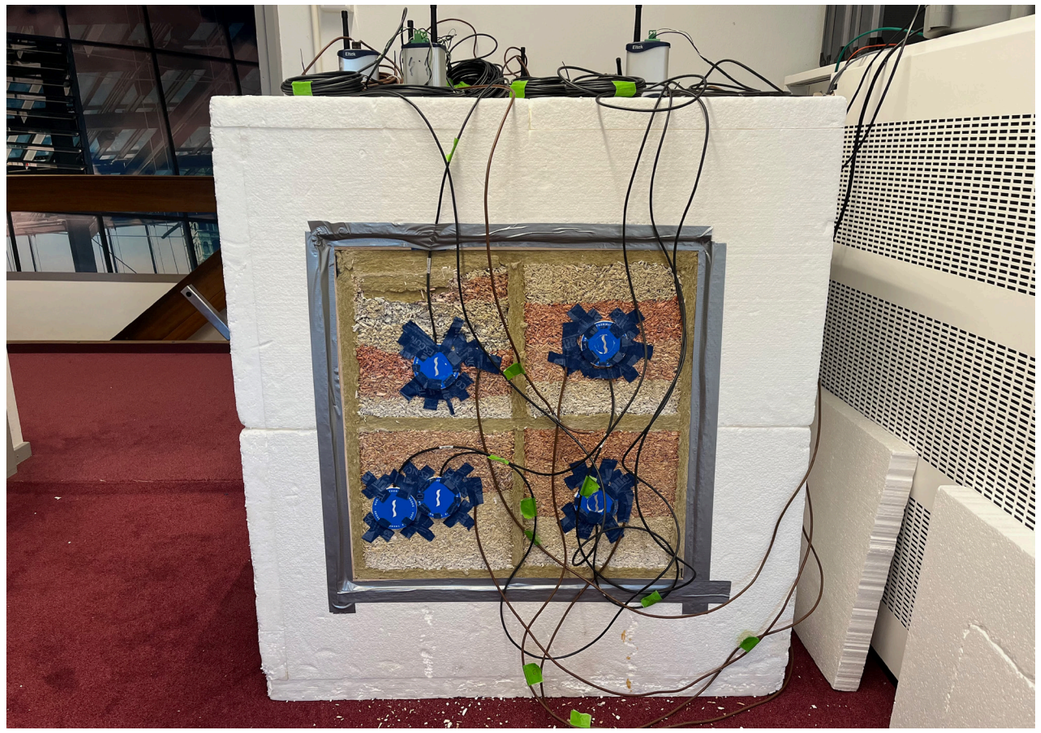

Fig 9.9 Setup for test rounds 3, 4 & 5. Two heat flux sensors on sample A5.

Fig 9.10 Setup during testing; EPS panels in front to prevent air stream, transmitters and dataloggers on top of the hotbox

Results

For each panel and test round, the thermal conductivity was estimated using the following steps:

1. Measured currents (in mV) were converted to heat flux (in W/m²) using the corresponding sensitivity values of the heat flux sensors.
2. The average heat flux was calculated for each measurement interval. This is shown in the left plot in figur 9.11 below.
3. The temperature difference (ΔT) across the sample was determined (middle plot)
4. Thermal conductivity was calculated for each interval using the following formula:

$$\lambda = (flux * thickness) / \Delta T$$

5. To ensure steady state, only the converged portion of the measurement (the final three hours) were used for averaging. This approach was necessary because the samples were not left in the hotbox long enough to reach full thermal steady state on their own.
6. As the measured thermal conductivity decreased with each next test round, only the last measurement of each panel was used for comparison between sample (printed in bold in table 9.4)

Full plots of every test in each round are included in the appendix.

Configuration	$\lambda_{(day\ 39)}$ (W/mK)	$\lambda_{(day\ 40)}$ (W/mK)	$\lambda_{(day\ 41)}$ (W/mK)	$\lambda_{(day\ 48)}$ (W/mK)	$\lambda_{(day\ 55)}$ (W/mK)	$\lambda_{estimated}$ (W/mK)	Notes
A0	-	-	0.0967	0.0856	0.0775	**0.077**	Panel broke during production. Flux Sensors lacked full surface contact.
A1	-	-	0.0888	0.0850	0.0796	**0.080**	
A2	0.1206	0.1064	-	-	-	**0.106**	People in the room; Heating turned on
A3	0.1224	0.1270	-	-	-	**0.127**	People in the room; Heating turned on
A4	-	-	0.0923	0.0888	0.0848	**0.085**	Sensor in least dense part of sample
A5	-	-	0.1145	0.1056	0.1009	**0.101**	Sensor on layer edge
A5*	-	-	0.1201	0.1086	0.1033	**0.103**	Additional Flux Sensor on cold face to check for density gradient effects.
A6/7	0.0032	0.1007	-	-	-	**0.101**	Round 1: Sensor fell off during test. Result discarded in average calculation.
A8	0.1103	0.1039	-	-	-	**0.104**	Bigger thickness is normalised in lambda calculation
M9	-	-	-	-	-	-	Not tested
M10	-	-	-	-	-	-	Not tested
M11	-	-	-	-	-	-	Not tested
M12	-	-	-	-	-	-	Not tested

Table 9.4 Thermal Conductivity results of very round

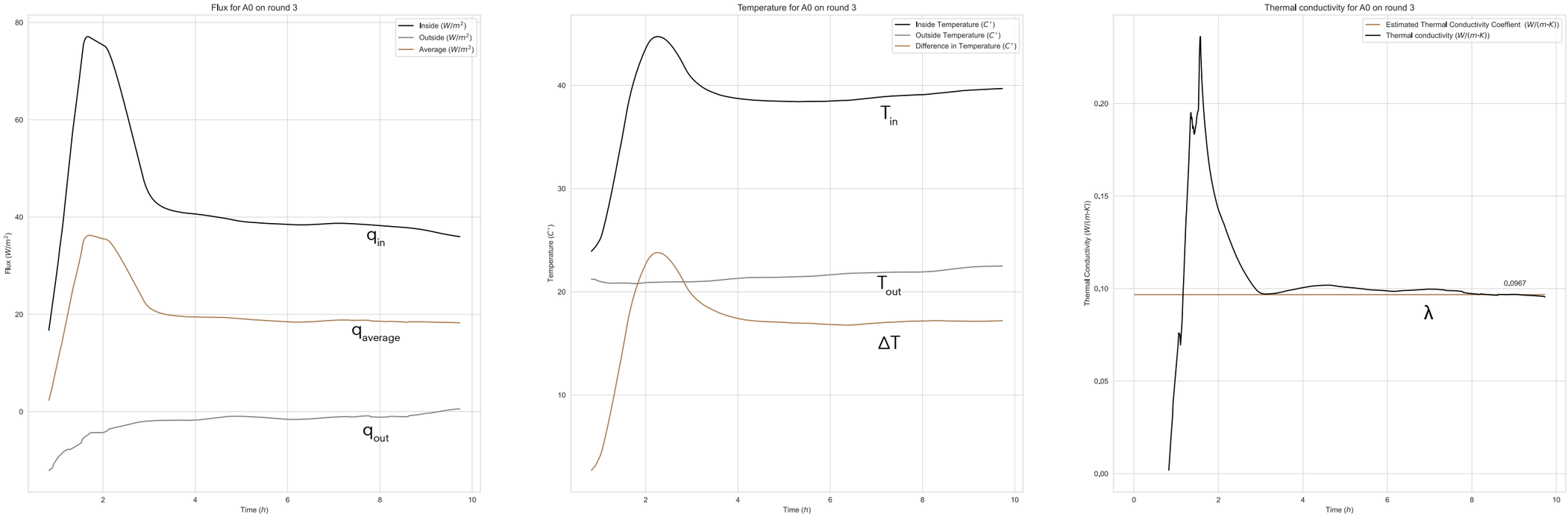

Fig 9.11 Example of output hotbox test (sample A0, round 3)

Discussion

Measured λ drop

The measured thermal conductivity decreased with each successive testing day. This likely resulted from additional drying due to heat from the lamps. Although the samples had reached moisture equilibrium (confirmed by the drying test in chapter 7), the heat exposure appears to have evaporated remaining moisture, bringing the material closer to an oven-dry state. This is advantageous, as thermal conductivity values in literature and data sheets are typically based on oven-dry conditions, making the results more comparable.

Compaction sweep

The plot in figure 9.12 presents the results of the compaction sweep. As the compaction factor increased from 10% to 60%, the bulk density of the samples rose almost linearly. In line with the literature, this rise in density led to a corresponding increase in thermal conductivity (λ). The results confirm the expected relationship: greater compaction leads to higher density, and consequently, higher thermal conductivity.

The λ value and corresponding density provided by EXIE in their datasheet are also included in the plot for comparison. As this value is based on oven-dry conditions, its slightly lower position on the graph is expected and can be attributed to the absence of equilibirum moisture.

C (%)	ρ_{dry} (kg/m³)	λ (W/mK)	Min. thickness (cm)
10%	205	0.077	36
33%	235	0.080	38
50%	330	0.106	50
60%	405	0.127	60

Table 9.5 Compaction increase measurements

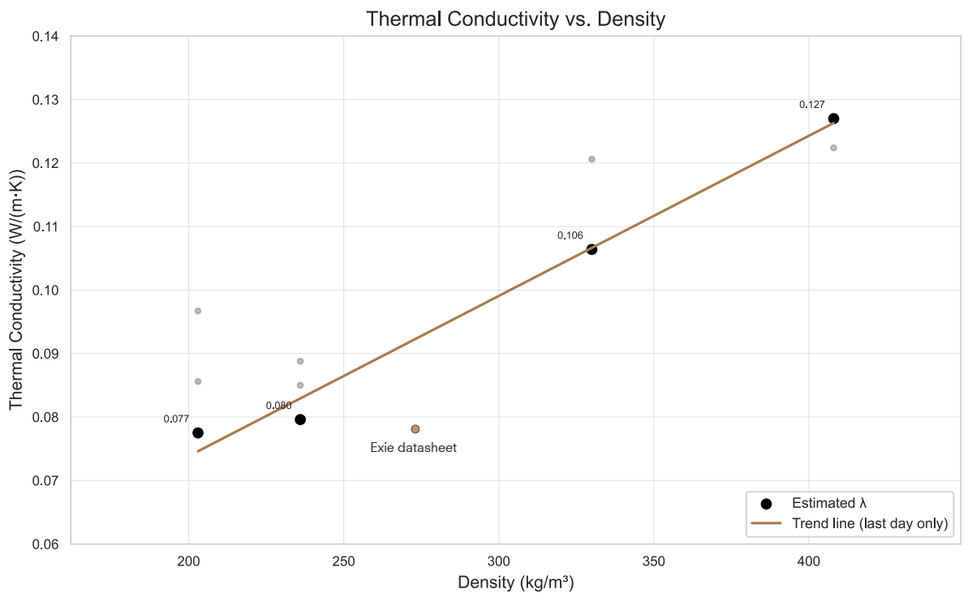

Fig 9.12 Density Sweep

Wall thickness

Table below shows the required wall thickness for each compaction factor to meet the Dutch building code requirement for outer walls (R_c value of 4.7 m^2K/W). At lower compaction levels, only 36 cm is needed to achieve the target R_c.

In contrast, a compaction factor of 60% requires a wall thickness of 60 cm due to the higher conductivity of the denser material. Further testing is needed to determine the minimum compaction level that still ensures sufficient structural strength and to assess how a monolithic wall can be effectively constructed.

Layer height sweep

The plot in figure 9.13 below shows thermal conductivity against increasing the layer height. Thicker layers produce a non-uniform density profile, with the top half becoming denser than the bottom. Since the hotbox measures one-dimensional heat flow, it is expected to be strongly influenced by the denser upper zone. The trend line in the plot remains nearly flat, indicating no clear correlation between layer height and λ within the tested range. Panel A4 shows a noticable lower, this is because the low density zone is exactly in the middle of the sample, where the sensor was placed. It was excluded from the trend line te avoid skewing the result. This deviating result showed further analysis of the density gradient is needed.

Sensor position and density gradient

To check whether the position of the sensor within the internal density gradient affects the λ, an additional sensor (A5*) was placed in the highest-density zone of panel A5, alongside the original sensor located at the interface between two layers.

In other words, while the overall trend line appears stable, this test checks whether increasing initial layer height, and the resulting density gradient, leads to thermal leakage influencing the measurement.

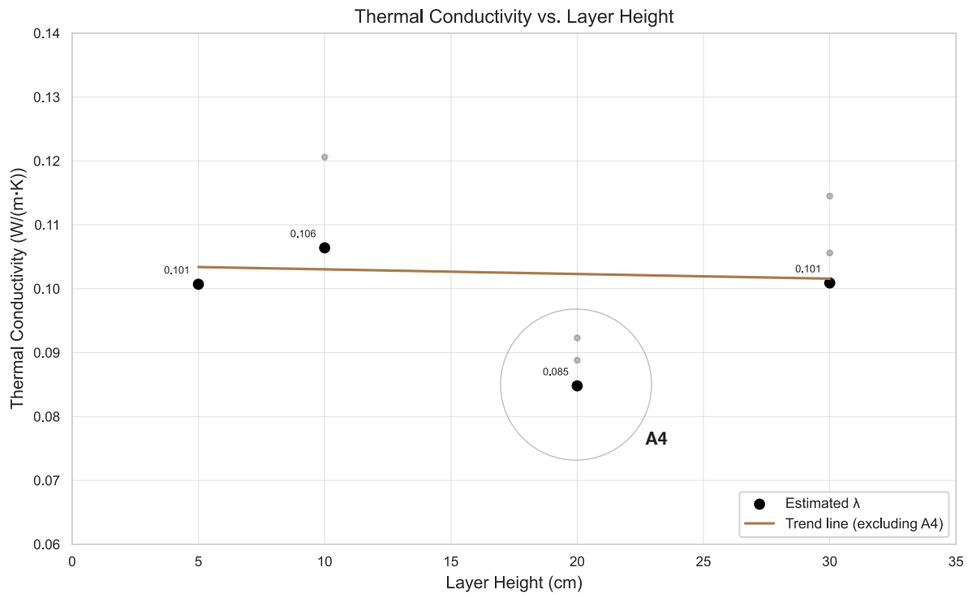

Fig 9.13 Layer Height Sweep

Fig 9.14 Left: Sensor in lowest density zone (A4). Richt: Sensors in interface zone (A5) and highest density zone (A5*)

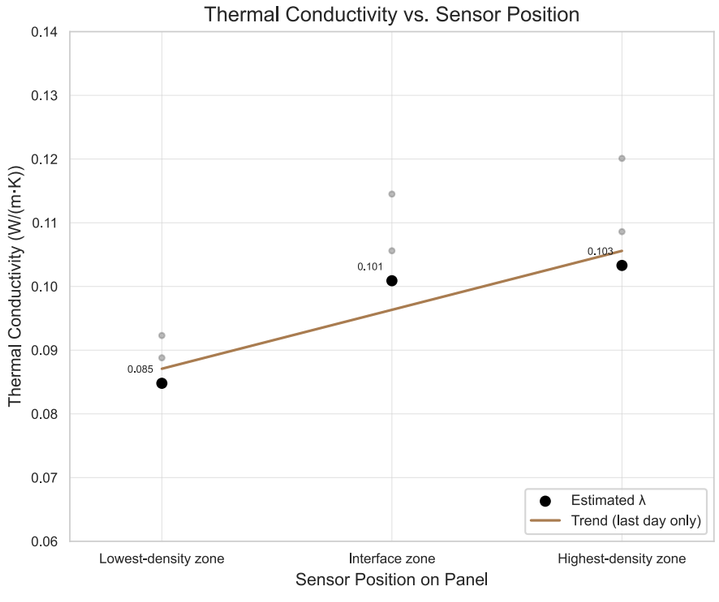

Fig 9.15 Density gradient check

The additional sensor placed in the highest-density zone of panel A5 showed a clear increase in thermal conductivity compared to the sensor at the layer interface. This supports that internal density gradients within thicker layers affect measured λ-values. The result aligns the earlier trend showing that higher density leads to higher thermal conductivity.

This finding indicates that sensor placement plays a crucial role in samples with non-uniform compaction. In practice, it suggests that thicker layered monolithic walls may under perform thermally if denser regions dominate the heat flow path. To better understand the thermal performance, it's important to either reduce these gradients during construction or measure conductivity in more than one place.

Additionally, it raises the question of how to design or compact thicker monolithic walls to reduce thermal bridging caused by denser regions.

Orientation sweep

Due to the anisotropic, layered microstructure of hempcrete, it was expected that panel orientation relative to the direction of heat flow would influence λ. In the top and side orientations, heat travels along the aligned shiv and binder layers, while in the front orientation, it crosses multiple vertical interfaces. Therefore, a higher λ was expected in the top and side orientations, and a lower λ in the front orientation.

However, the measured value in the front orientation was slightly higher. This suggests that the effect of orientation on thermal insulation may be less strong than expected.

Binder sweep

The mixed lime panels are not tested on thermal conductivity. However, literature suggests hydraulic component rich binders show a slightly higher λ than air lime binders at the same density (Nguyen et al., 2009).

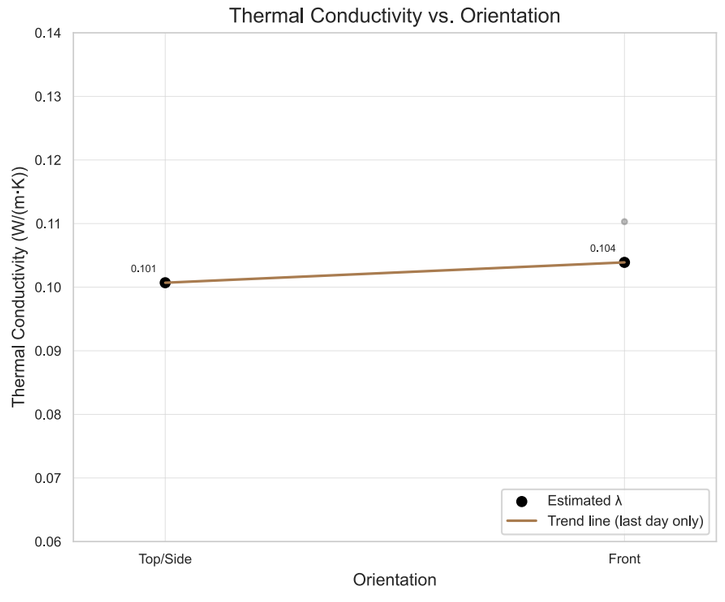

Fig 9.16 Orientation Sweep

Limitations

Steady state convergence

The hot- and cold-face heat-flux readings never fully converged, so the value of λ was estimated from the “stabilised” one-hour average instead of a true steady-state.

Residual radiation

Even though the infrared lamp was wrapped in aluminium foil, some extra radiant energy may still have reached the specimens, influencing the hot-side flux and calculated λ.

Room- and sunlight

Additional radiant heat came from the room’s ceiling lights and direct sunlight through the window.

Lab traffic

Door openings and people moving in and out of the laboratory caused pressure and temperature fluctuations, adding noise to both flux and surface-temperature measurements.

Sensor contact

Panel A0 cracked during frame assembly, causing poor sensor contact. Several other flux plates were also not perfectly flush, possibly lowering thermal resistance.

Observations

General

- Measured λ dropped with each testing day, indicating additional drying by heat.
- Density rise leads to corresponding λ increase.
- Measurements vary with sensor placement: observing density gradient influence
- Data correspond to an equivalent monolithic wall thickness between 36 and 60 cm.

Sweep influence

Compaction:	observed
Layer height:	observed
Orientation:	not observed
Binder:	not tested

Fig 9.17 Panel samples A6/7 (left) and A8 (right

Fig 9.18 Measured thermal conductivities applied to 1:1 mockup wall.

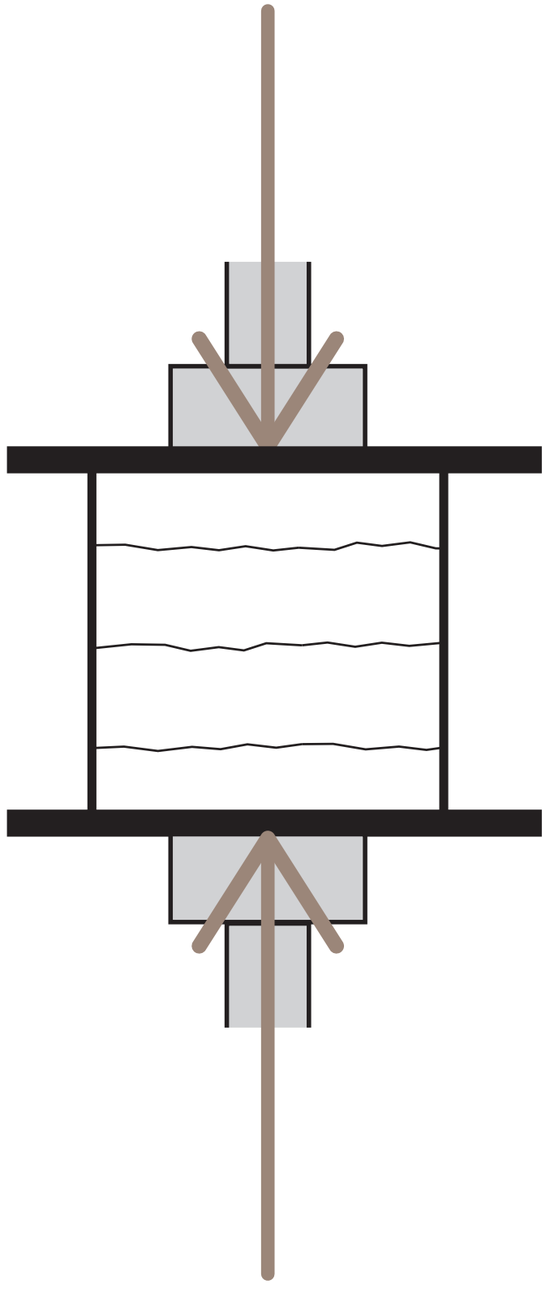

Fig 10.1 Schematic compressive test

Compressive Test

This chapter presents the method, results, and discussion of the compressive test conducted to determine the samples' yield strength and stiffness in compression

Method

The resistance of the samples to compression is measured using the Zwick Z100 universal materials testing machine at the Materials Science & Engineering (MSE) Lab at the TU Delft Faculty of Mechanical Engineering. Four replicate cubes were tested for each configuration (exept A0) to minimize standard error and increase the accuracy of the measurements.

Sample Preparation

Geometry

Several considerations led to the selection of a 15 cm cubic geometry size for the compression tests. First, standards for concrete testing specify 15 cm cubes. Adopting the same geometry makes the hempcrete results directly comprehensible to structural engineers. Second, most studies found in the literature review that deal with hempcrete of similar density ranges (200 - 400 kg/m^3) also perform their compressive tests on 15 cm cubes. For example: Nguyen et al. (2010), Williams et al. (2017), Brzyski et al. (2021). Those cubes fail at 0.2 - 0.6 MPa. This means 15 cm cubes reach ultimate loads of 4 - 14 kN. This is well below the 100 kN range of the Zwick Z100 while still high enough for accurate force measurements. Third, hempcrete is a coarse, heterogeneous material. Hemp shivs lengths used in this experiment vary between 2 and 30 mm. A 15 cm edge ensures that the sample contains many particle layers (> 5 x the maximum shiv length). Isolated air voids or shiv clusters will not influence the measured strength. Finally, a cube with equal height and width eliminates slenderness effects and potential buckling.

Curing state at test day

The air lime samples had cured in between 64 and 67 days. The mixed lime samples had only cured for 22 days, and had not yet reached equilibrium density. These were just tested to provide reference: their results should therefore be interpreted with caution rather than as definitive strengh values.

Config.	B	O	L_i (cm)	C (%)	$\rho_{dry,eq}$ (rounded) (kg/m^3)	Age at day of testing	Test repetitions
A0	Air	Top	5	10	200	64	2x (two broke)
A1	Air	Top	10	33	235	67	4x
A2	Air	Top	10	50	330	67	4x
A3	Air	Top	10	60	410	65	4x
A4	Air	Top	20	50	330	65	4x
A5	Air	Top	30	50	330	64	4x
A6	Air	Top	5	50	330	64	4x
A7	Air	Side	5	50	330	64	4x
A8	Air	Front	5	50	330		Not tested, equals A7
M9	Mixed	Top	10	50	-	22	4x
M10	Mixed	Top	10	60	-	22	4x
M11	Mixed	Top	5	50	-	22	4x
M12	Mixed	Side	5	50	-		Not tested

Table 10.1 Sample selection for testing

Fig 10.2 Sample A3 before applying pressure

Setup and Equipment

Zwick Z100

All compression tests were carried out on a Zwick Z100 universal material testing machine. It is capable of applying forces up to 100 kN.

To determine the settings of the machine, a trial run was performed on one of the A3 samples. The machine was configured with a 5N preload to smooth out the top surface of the sample, a displacement rate of 5mm/min and an automatic stop at 50mm of total displacement (vertical travel). These settings produced stable loading but reached the displacement limit before all free air was pressed out.

Therefore the settings were tuned. The preload was increased to 10 N to ensure full contact. The displacement rate was doubled to 10 mm/min to keep the tests within the day's schedule while still having a steady, controlled speed. The displacement limit was extended to 75mm so resistance after permanent deformation was also measured.

Steel plates

To distribute the load evenly over the entire 150 x 150 mm face of each cube, two 170 x 170 x 6 mm steel plates were placed between the platens and the sample before every test.

MSE Lab conditions

The tests were performed at a temperature of 21 °C and 52 % relative humidity.

Parameter	Value	Unit
Cube dimensions	150	mm
Displacement rate (platen speed)	10	mm/min
Preload	10	N
Maximum displacement	75	mm

Fig 10.3 Zwick Z100 settings

Fig 10.3 To be tested samples being transported to Delft on two pallets with a van.

Test Procedure

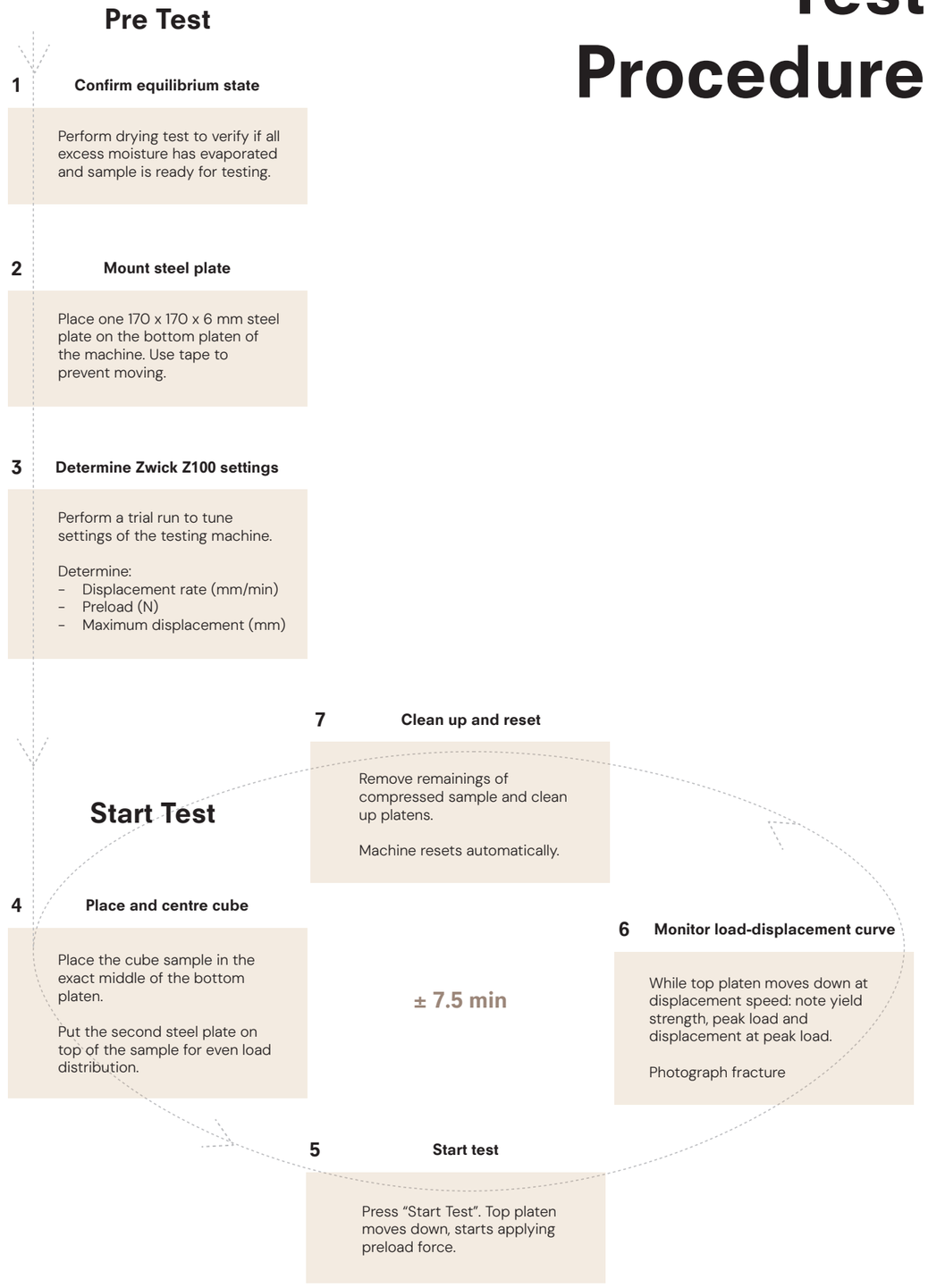

Fig 10.4 Description of Figure

Results

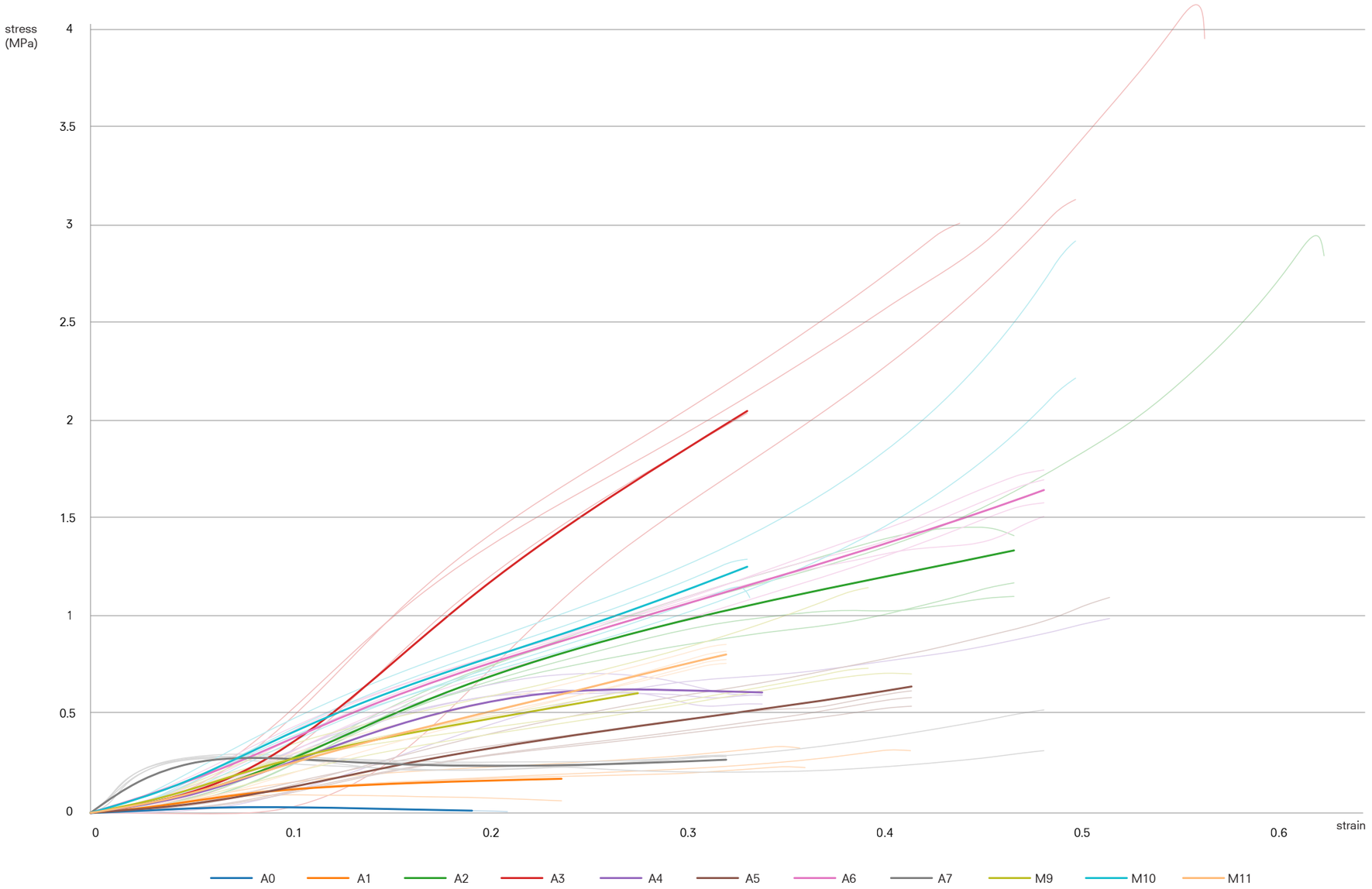

Fig 10.5 Stress-strain curves of each compressed sample. All 42 individual tests in lightened color with their average curve

Stress-strain curves

11 cubic sample configurations were evaluated on a Zwick Z100 universal test machine. Each configuration was loaded 4 times, so 44 individual force-deformation curves were plotted as output. By dividing the measured force by the samples loaded cross sectional area and the deformation by its initial height, every plot was converted to a true stress-strain curve. This is the standard format for comparing compressive behaviour across different materials and studies.

In figure 10.5 every individual curve is drawn with high transparency, while the mean curve for each configuration is over-plotted. On a first glance, two trends stand out: Configuration A3 develops the highest stresses of all and configuration A7 (tested after a quarter turn rotation) shows a noticeable steeper initial curve. This implied a higher stiffness.

This plot gives a useful overall picture, but the overlap of so many curves makes it difficult to analyse the behaviour of each configuration. The following section therefore regroups the samples according to their characteristic stress-strain behaviour and their visual deformation.

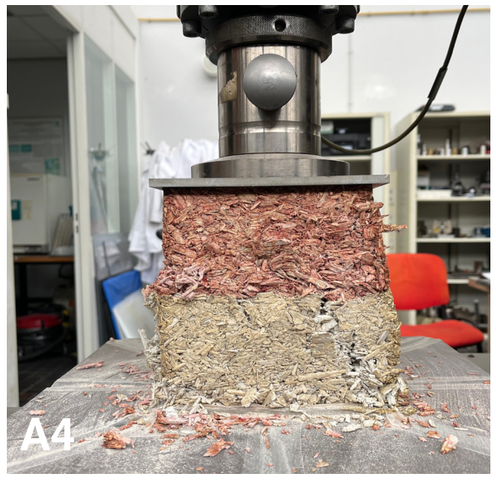

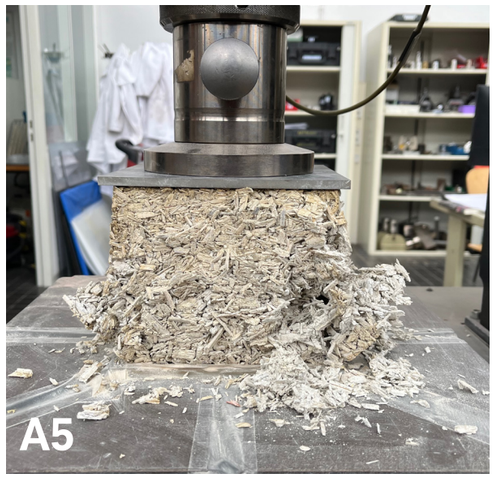

Fig 10.6 Brittle sample set

Brittle Behaviour

For the samples whose curves peak and then fall (the brittle set), the compressive yield strength ($\sigma_{c,y}$) was located at the precise point where the initially straight, steep line first breaks and starts to flatten. This is the moment the lime binder stops to control the stiffness and the shiv network starts to compact, air is pressed out. The Young's modulus (E) was calculated as the slope of that same linear segment. Because the brittle samples reach a clear maximum load and then lose capacity as they start cracking and ultimately collapse, the compressive ultimate strength ($\sigma_{c,u}$) is defined as the highest stress reached before the curve slides downward and the sample breaks down completely.

After reaching ultimate strength, the brittle samples are not able to carry any residual loads, and therefore these sample offer no safety reserve once peak stress is exceeded.

Brittle samples:

C < 50%

L_i > 10cm

O = Side/Front

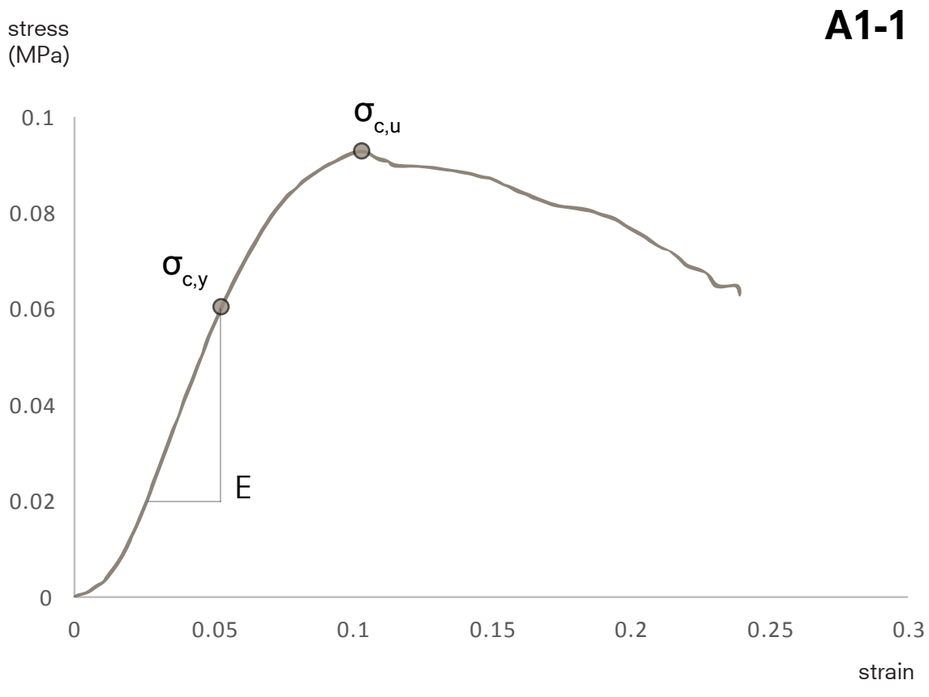

Fig 10.7 Stress strain curve of sample A1-1: Typical ductile behavior

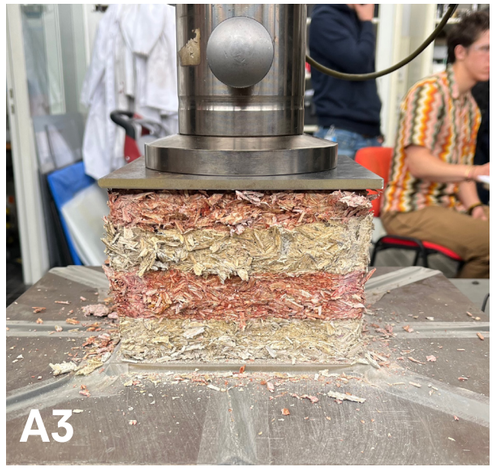

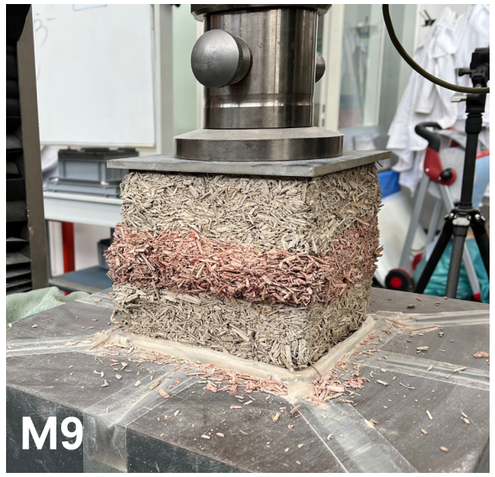

Fig 10.8 Ductile sample set

Ductile Behaviour

For the denser samples (the ductile set) the yield stress is taken at the transition point between the linear elastic and the flatter plastic region and the Young's modulus as the slope of that initial line. The ductile curves (and samples) do not collapse after yielding. Once the pores are fully closed, the slope rises again in a "strain intensification" phase (Walker et al., 2014). Here, the shivs and binder matrix re-stiffens, sometimes even steeper than its first slope. Accordingly, the ultimate strength was defined as the maximum stress reached anywhere along the curve, mostly when the test was stopped.

The ductile samples did not collapse, but only deformed vertically. This shows the materials ability to continue carrying increasing load even after permanent deformation has occurred. The post-yield hardening indicates a built-in safety margin.

Ductile samples:

C ≥ 50%

L_i ≤ 10cm

B = Mixed Lime

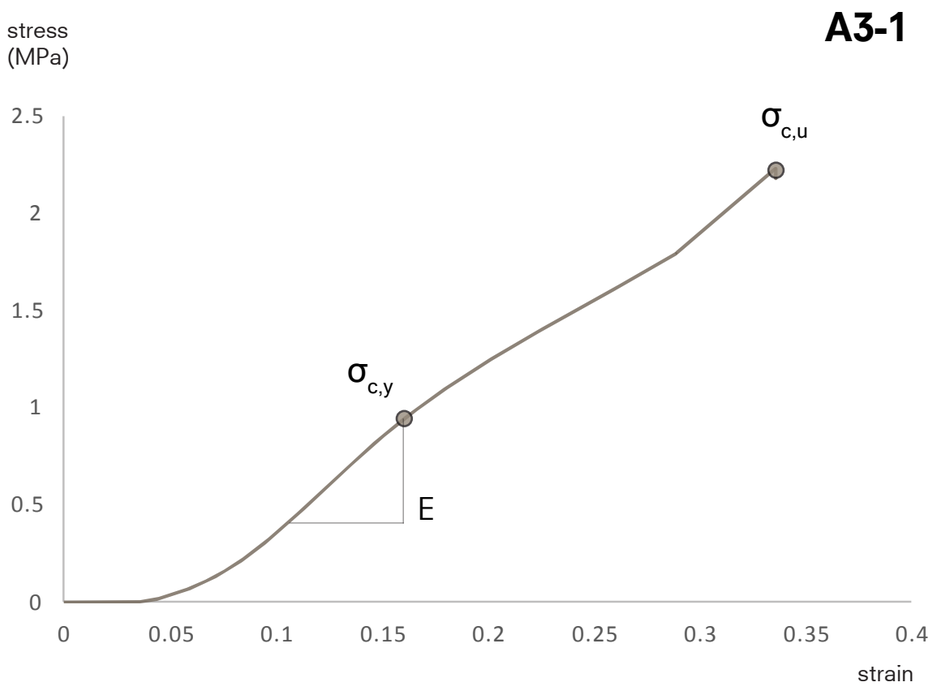

Fig 10.9 Stress strain curve of sample A3-1: Typical ductile behavior

Results Interpretation

A meaningful comparison of the results must account for curing age. The air lime samples A0-A8 were cast on different days and tested when 64 to 67 days old. Drying tests confirm they had reached equilibrium moisture content, so their recorded densities and compressive strengths represent true dry-state values.

However, literature shows that reaching final strength for hempcrete often takes longer than one year (Walker et al., 2014). Given that moisture had stabilized weeks before testing, the three-day spread in age is not expected to affect the results significantly.

The mixed lime samples, although they were cast on the same day, were tested while still well above their equilibrium moisture level. Therefore, the compressive strengths recorded for samples with this binder type resemble early stage values only and can not be taken as the materials final strength.

Configuration	Behaviour	Age at test day
A0	Brittle	64
A1	Brittle	67
A2	Ductile	67
A3	Ductile	65
A4	Brittle	64
A5	Brittle	64
A6	Ductile	64
A7/A8	Brittle	64
M9	Ductile	22
M10	Ductile	22
M11	Ductile	22

Table 10.3 Table

Table 9.4 presents the mechanical properties of all configurations in compression. A clear ultimate strength ($\sigma_{c,u}$) is hard to define (brittle set shows a noisy peak and ductile set never peak at all). Because such extreme loads will not be reached under normal operating conditions, the yield strength ($\sigma_{c,u}$) and stiffness (E) give a better picture of real-world performance. These two values are discussed in the next sections.

Configuration	Yield Strength $\sigma_{c,y}$ (MPa)	Strain at $\sigma_{c,y}$	Young's Modulus (E)	Ultimate Strength $\sigma_{c,u}$ (MPa)	Strain at $\sigma_{c,u}$
A0	0.03	0.06	0.49	0.03	0.08
A1	0.10	0.11	1.53	0.26	0.31
A2	0.51	0.15	5.01	1.71	0.51
A3	1.11	0.19	9.63	3.13	0.46
A4	0.48	0.16	3.84	0.74	0.32
A5	0.27	0.16	2.22	0.73	0.44
A6	0.52	0.13	4.76	1.66	0.48
A7/A8	0.20	0.08	9.76	0.36	0.40
M9	0.27	0.10	3.35	0.82	0.32
M10	0.46	0.11	4.91	1.93	0.37
M11	0.27	0.11	3.25	0.32	0.42

Table 10.4 Average compression measurements

Fig 10.10 Sample A4 before applying pressure

Fig 10.11 Test Setup

Discussion

Compaction sweep: Yield Strength

Prior to testing, a roughly proportional rise in strength was expected from the literature. Increasing the compaction factor C from 10% to 60% doubles the bulk density from about 200 kg/m^3 to 400 kg/m^3, so a similar doubling of yield strength was considered thinkable.

Figure 10.12 plots the measured yield strengths against equilibrium-dry bulk density. All individual tests are shown in light gray, the black markers represent the mean value at each density level. An exponential trend line has been fitted through those means.

Below about 300 kg/m^3 the increase in σ_y is little and the gray points are widely scattered. Above this level the fitted curve bends sharply upward; a small extra gain in density now produces a much larger rise in strength. The data are best described by an exponential trend rather than a linear one.

At lower densities the material still contains many large voids, so load is carried by a limited number of lime-bonded hemp shiv contacts and by the brittle binder itself. Compacting during manufacturing to above 300 kg/m³ closes these voids and presses the shiv particles into much closer contact. Each next increase in compaction seems to multiply the number of contact points inside the material, and not only adds mass. Making strength rise faster than density.

Right now, the upper limit in compaction factor is 60% (405kg/m^3): the maximum that could be reached manually. If ramming with a machine pushes the exponential trend beyond this present upper limit, even higher strengths could be reached.

However, the drying test showed this would cause longer drying times and hotbox test predicts a loss in thermal performance.

Compaction sweep: Stiffness

The Young's modulus (E), taken as the slope of the initial linear part of each stress strain curve, follows the same exponential rise when increasing density. This can be explained, because stiffness depends on how continuous the shiv-lime bond is. At low density, only a few contact points exist and the material deforms easily. Compacting during manufacturing forces the shiv and binder closer together, and the number of contact points (and paths the applied load can take) grows quickly.

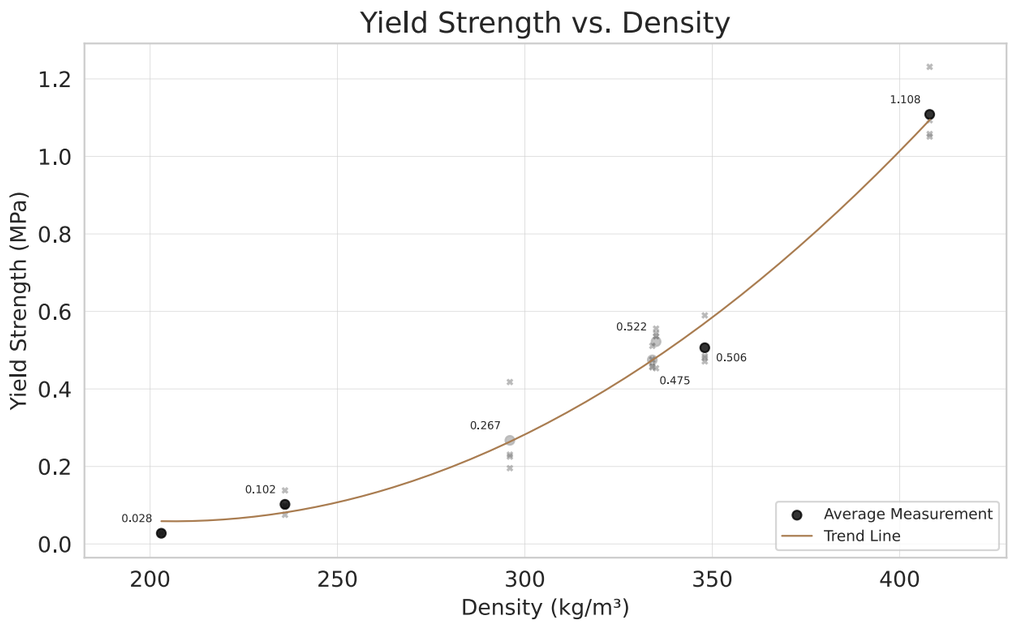

Fig 10.12 Yield strength vs. dry density

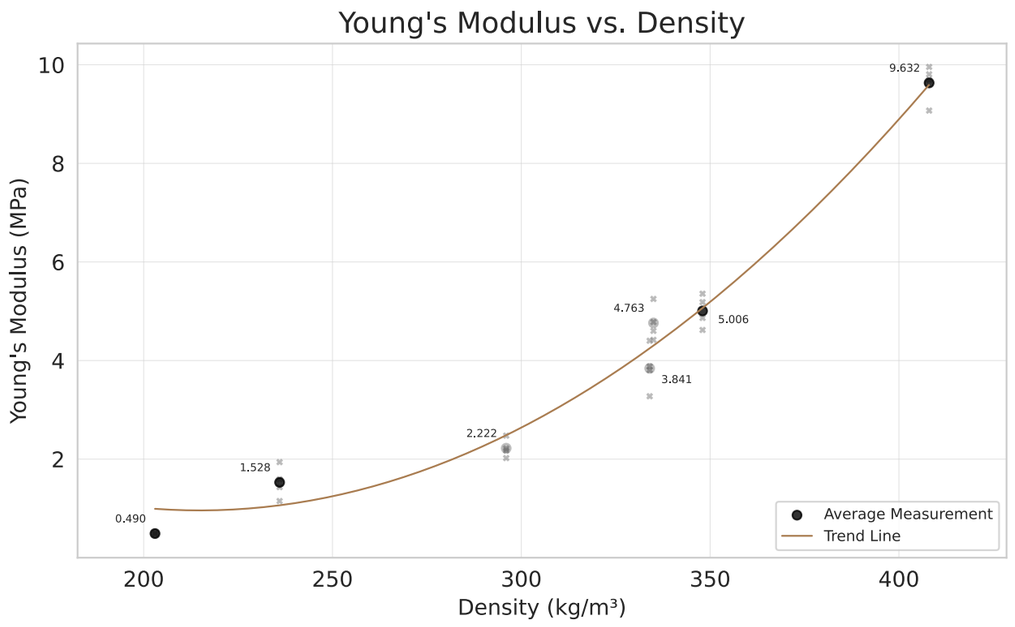

Fig 10.13 Young's modulus vs. dry density

Layer height sweep

Placing the fresh mix in thicker layers was expected to create a vertical density gradient: the top zone receives the full ramming force, while the lower zone receives less. The weaker, less dense zone should limit the compressive capacity of the sample. This means a thicker initial layer would give lower yield strength and lower stiffness than a thinner layer with the same overall density.

Figure 10.14 compares samples made with the same compaction factor (50%) and similar equilibrium-dry bulk density (330 kg/m^3), but different layer heights (L_i) during casting. Sample A5 (circled in the plot) lies below the trend line of the other three. The drying test revealed that A5 had lower density than the other cubes, a result of formwork leakage during casting.

As discussed in the previous pages, reduced density lowers both yield strength and stiffness. Including A5 in the trend would have skewed it.

It was therefore excluded from the trend fit, which slopes downward, confirming the expected drop in compressive strength and stiffness as layer height increases. Casting in thinner layers (below 10cm for this experiment) produces a more uniform micro structure, improving the materials compressive properties.

Density Gradient

Visual inspection confirmed that samples cast in layers thicker than 10 cm developed a clear density gradient through their height (figure 10.15) During compression, failure consistently happened in the lowest-density region: the material's weakest link.

To verify this, one sample was turned 180 degrees during testing. Figure 10.17 shows that, although both orientations reach the same yield strength, failure begins in the zone with the lowest density, whether that zone is at the top or the bottom of the sample.

Fig 10.15 Failure at weakest link: lowest density region

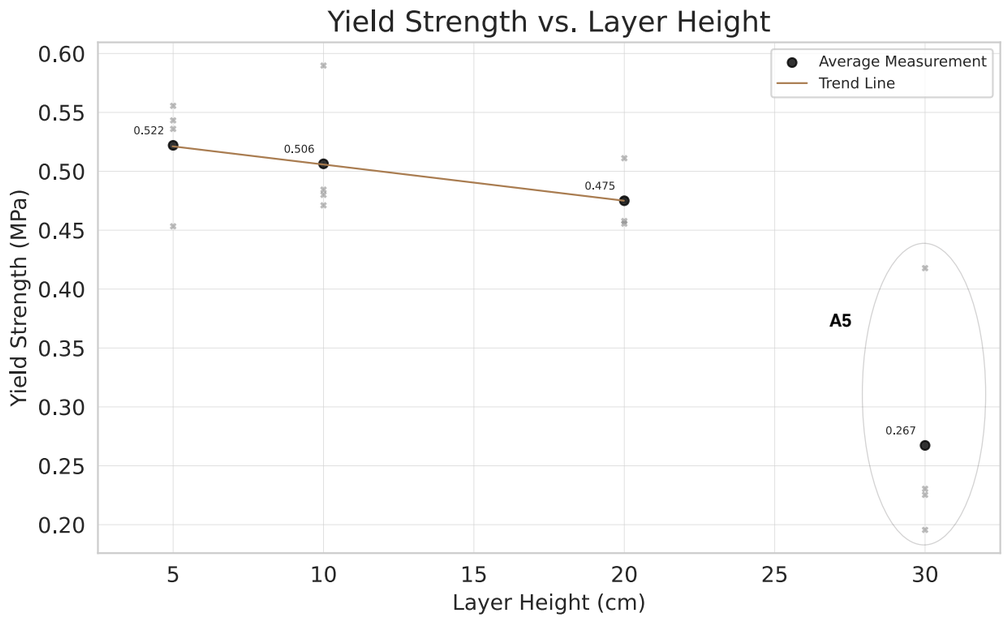

Fig 10.14 Yield Strength vs. layer height

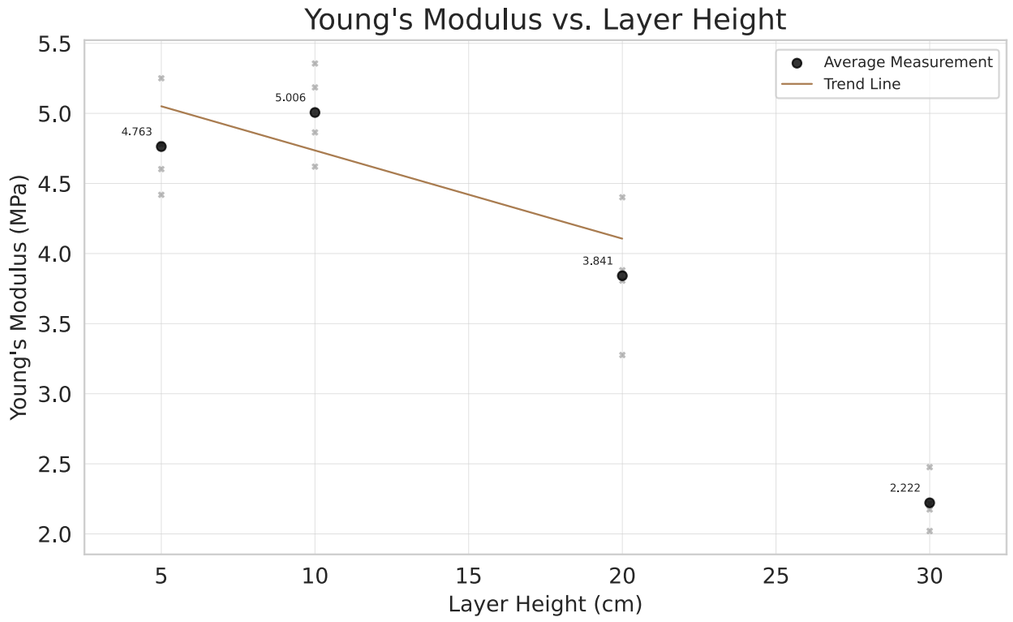

Fig 10.16 Young's modulus vs. layer height

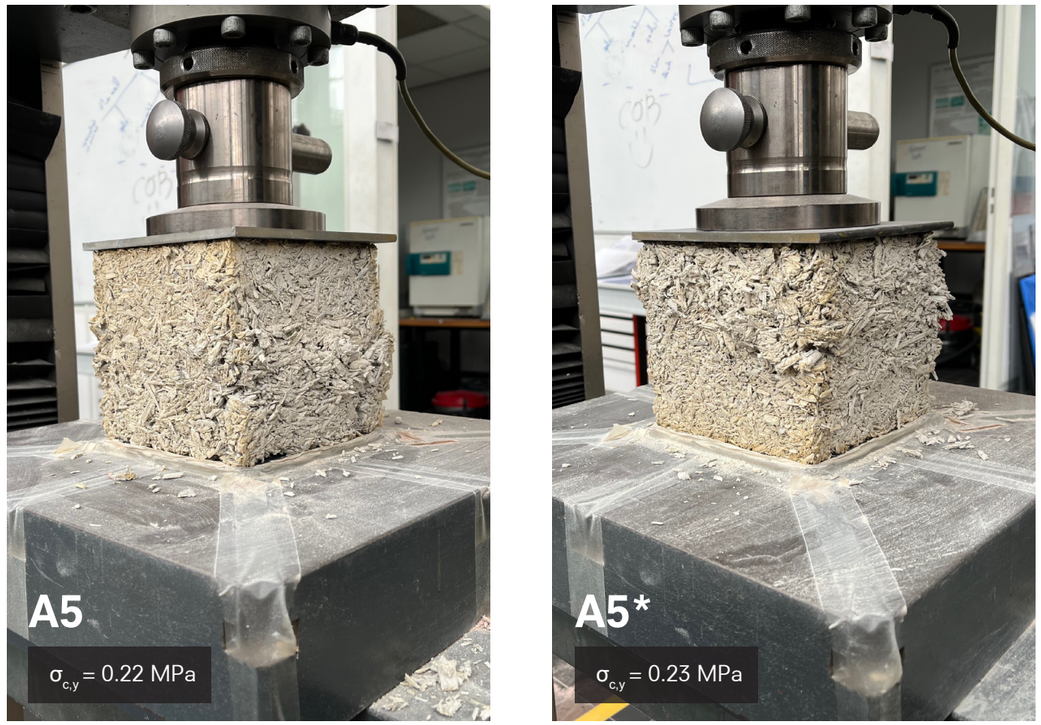

Fig 10.17 Layer height sweep: 180 degrees rotation

Fig 10.18 Orientation sweep: 90 degrees rotation

Orientation sweep

Figure 10.18 contrasts two identical configurations that differ only in orientation: samples of configuration A6 were compressed perpendicular to the layers (Top compaction), whereas samples from A7 were compressed parallel to them (Side/Front compaction). Turning the material by 90° results in the behaviour that was expected.

In the parallel case (A7) the applied load moves across every layer interface, so the layers begin to separate almost as soon as the lime binder yields: a delamination crack forms and the sample reaches its yield stress much earlier than in the perpendicular case (A6). Here, the interfaces are kept in compression, no early separation is seen, and the yield strength is therefore higher.

An interesting contradiction is seen when calculating the stiffnesses: because the hemp shiv fibers are oriented parallel to the load in A7, they brace the material during the very first strains, giving that orientation a steeper initial slope and a higher Young's modulus.

Once those aligned shivs start to buckle, however, the stress–strain curve of A7 flattens and drops at a lower stress, whereas A6 continues to carry loads. It is observed that rotating the samples shows a clear trade-off: parallel loading provides slightly stiffer initial behaviour but the material fails at much lower yield stress through layer delamination.

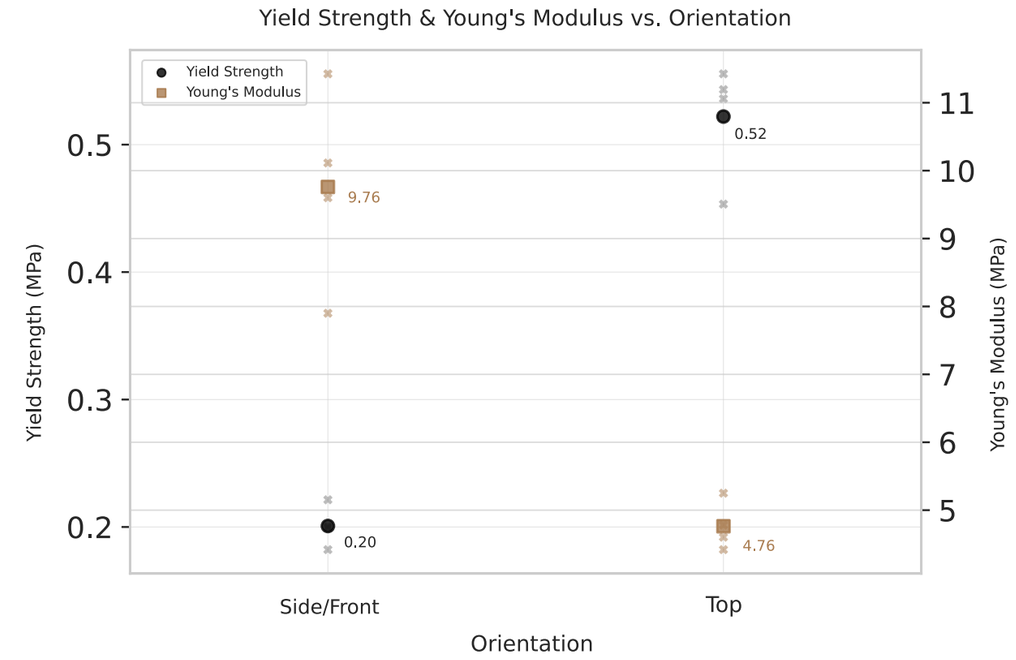

Fig 10.19 Yield Strength and Young's modulus vs. orientation

Binder sweep

EXIE and Isohemp both supply no mechanical strength on their data sheets. This makes these compression data the first benchmarks for these mixes. However, the mixed binder (Isohemp) samples were tested before moisture equilibrium was reached. They were still drying.

Figure 10.20 compares the air lime mix (in grey) with the mixed lime mix (in brown) for the same three casting configurations. The upper graph shows the yield strength, where every air lime column has higher measurements than its mixed lime copy. This indicates that air lime cubes are stronger at test age. But since the mixed lime samples were loaded before their hydraulic reaction was complete, their lower strength can be related to excess moisture and incomplete curing. Their measurements can not be interpreted as final strength.

In both binders the yield strength and stiffness columns follow the same pattern across the three configurations. The specimen compacted to 60 % is always the strongest and stiffest, whereas changing the layer height from 10 cm to 5 cm has only a minor effect on the measured values.

Visual inspection also confirmed that the mixed-lime specimens were still moist: their surface appeared darker grey and felt tacky, unlike the fully dried air-lime samples.

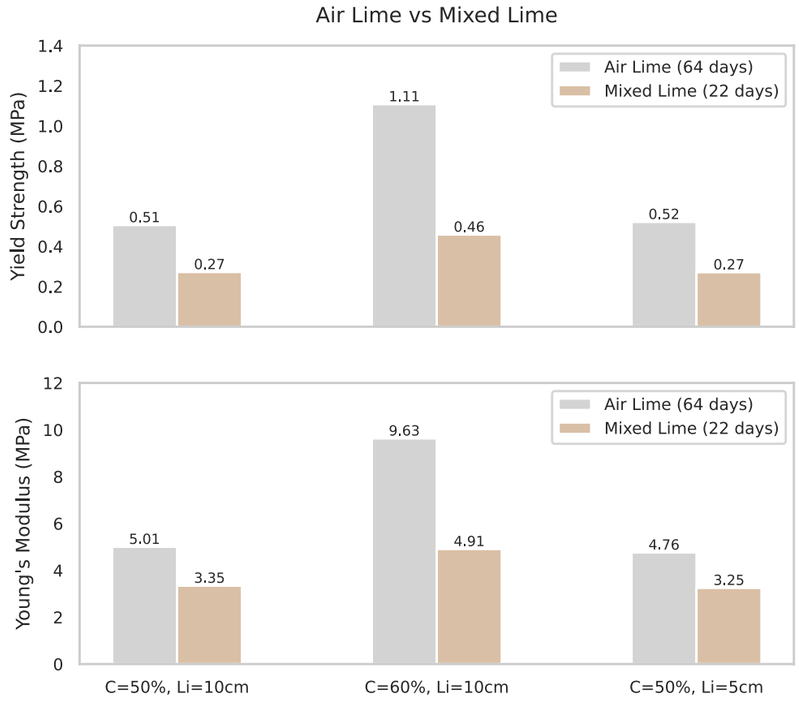

Fig 10.20 Description of Figure

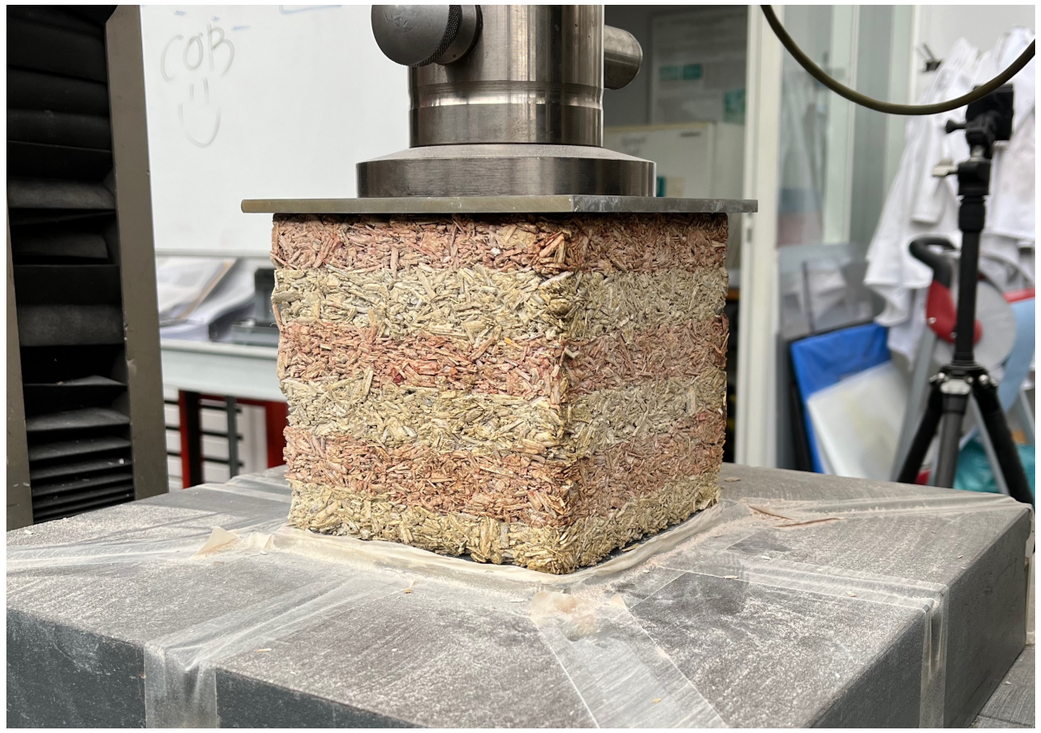

Fig 10.21 Air lime sample A6

Fig 10.22 Mixed lime sample M11

Limitations

Number of repetitions

Each configuration was tested only four times, which is too few to confirm firm statistical trends, though the results provide a useful first indication.

Moisture variability

The specimens were not oven-dry, and the laboratory's relative humidity at the first day of testing influenced their moisture content, so the measured strengths reflect the environmental conditions at the time of testing, just as they would in real life.

Binder condition

Because the mixed-lime cubes were still wet, the strength and stiffness data presented here are strictly applicable only to the air-lime (EXIE CaNaCrete) mix.

Curing age

The air-lime samples were between 64 and 67 days old at the time of testing, making comparisons slightly uneven.

Cross section dimension

Slight swelling after casting changed the cross-sectional areas by a small amount.

Layer height range

Only four layer heights were tested. These were spaced 10 cm apart. Since density gradients begin to appear at roughly 10 cm, additional heights in between are needed to pinpoint where density gradients begin.

Sample dimension

150 mm cubes represent only a small fraction of a wall and may miss larger defects, voids, or fibre alignment patterns that happen in full-scale construction.

Observations

General

- Both yield strength and stiffness increase steeply as bulk density rises.
- High compaction gives high safety margins.
- Failure starts in the least dense zone of each sample: Internal density gradients control the overall strengtht.
- Fiber orientation shows opposing trends for yield and stiffness

Sweep influence

Compaction:	observed
Layer height:	observed
Orientation:	observed
Binder:	not tested

Fig 10.23 Description of Figure

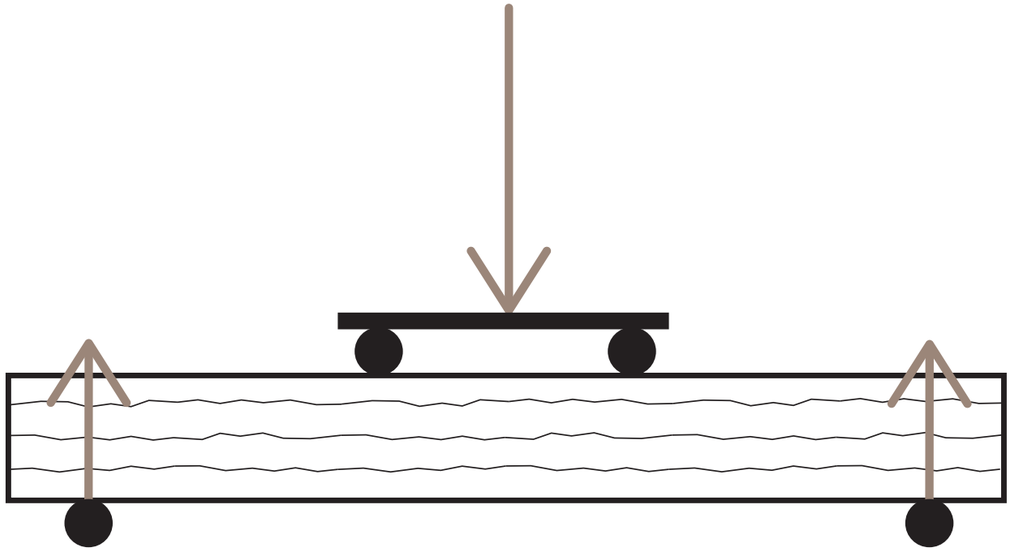

Fig 11.1 Schematic 4 point bending test

4 Point Bending Test

This chapter presents the method, results, and discussion of the 4 point bending test conducted to determine the samples' bending strength

Method

Preliminary Testing

During the 68-day curing period, attempts to lift the column samples to check their readiness revealed that most were still too fragile and fractured as soon as they were moved.

Therefore, a quick screening was carried out before testing the samples in a laboratory setup. One column of each configuration was placed as a beam across two wooden trestles spanning 800mm. First, there was no other load applied than its own weight. Columns cast at less than 50% compaction or with a layer height exceeding 10cm failed immediately under self weight. This indicated insufficient flexural capacity, due to tensile forces in the bottom of the column.

The remaining columns were then exposed to a light, “fingertip load” at mid-span (pressing the sample with one finger). Samples whose layer interfaces lay parallel to the bending load (top compaction orientation) fractured after only minimal fingertip pressure. These all broke at exactly the layer interface, falling apart into small blocks. This indicates similar delamination effects as in compression testing.

Samples compacted from the side or front (so with their layers and shiv fibers parallel to the bending load) could withstand the same manual loading without damage.

Fig 11.2 Fingertip pressure test setup

Fig 11.3 Sample failed at the layer interfaces

Fig 11.4 Side/Front compaction samples

Test Procedure

Sample selection

Only the cubes that survived the fingertip screening were taken forward. These belong to configurations A7, A8, and M12, all cast at 50 % compaction and 5 cm layer height. Consequently, the bending test focuses on orientation sweep (top vs. side/front compaction) and binder sweep (air-lime vs. mixed-lime). Variation in compaction factor or initial layer height is now outside the scope.

For each configuration, four replicate columns were tested. All air lime samples had been curing for 58 days at the testing day, and the mixed lime samples for 22 days. Like the cubes in the compression test, it is important to note that the mixed lime columns had not yet reached moisture equilibrium: they were still damp.

Lab conditions

The tests were performed at a temperature of 21 °C and 52 % relative humidity.

Setup

The flexural strength of the selected hempcrete columns was determined on the same Zwick Z100 universal testing machine in the Materials Science & Engineering Lab of TU Delfts Faculty of Mechanical Engineering. The standard compression platens used for the compressive testing were removed and replaced with a four point bending fixture. After a few trail rounds, the settings of the machine and its setup were determined to be the following:

Parameter	Value	Unit
Column dimensions	90x90x900	mm
Loading rollers distance	280	mm
Support rollers distance	700	mm
Displacement rate	5	mm/min
Preload	5	N
Maximum displacement	50	mm

Fig 11.1 Zwick Z100 4 point bending test settings

Sample	B	O	L_i (cm)	C (%)	$\rho_{dry,eq}$ (rounded) (kg/m³)	Age of day of testing	Test repetitions
A0	Air	Top	5	10	205	57	Failed at own weight
A1	Air	Top	10	33	235	67	Failed at own weight
A2	Air	Top	10	50	330	67	Failed at own weight
A3	Air	Top	10	60	405	65	Failed at fingertip load
A4	Air	Top	20	50	330	64	Failed at own weight
A5	Air	Top	30	50	330	62	Failed at own weight
A6	Air	Top	5	50	330	62	Failed at fingertip load
A7	Air	Side	5	50	330	58	4x
A8	Air	Front	5	50	330	58	4x
M9	Mixed	Top	10	50	330	-	not tested
M10	Mixed	Top	10	60	405	-	not tested
M11	Mixed	Top	5	50	330	-	not tested
M12	Mixed	Side	5	50	330	22	4x

Fig 11.2 Sample set for testing

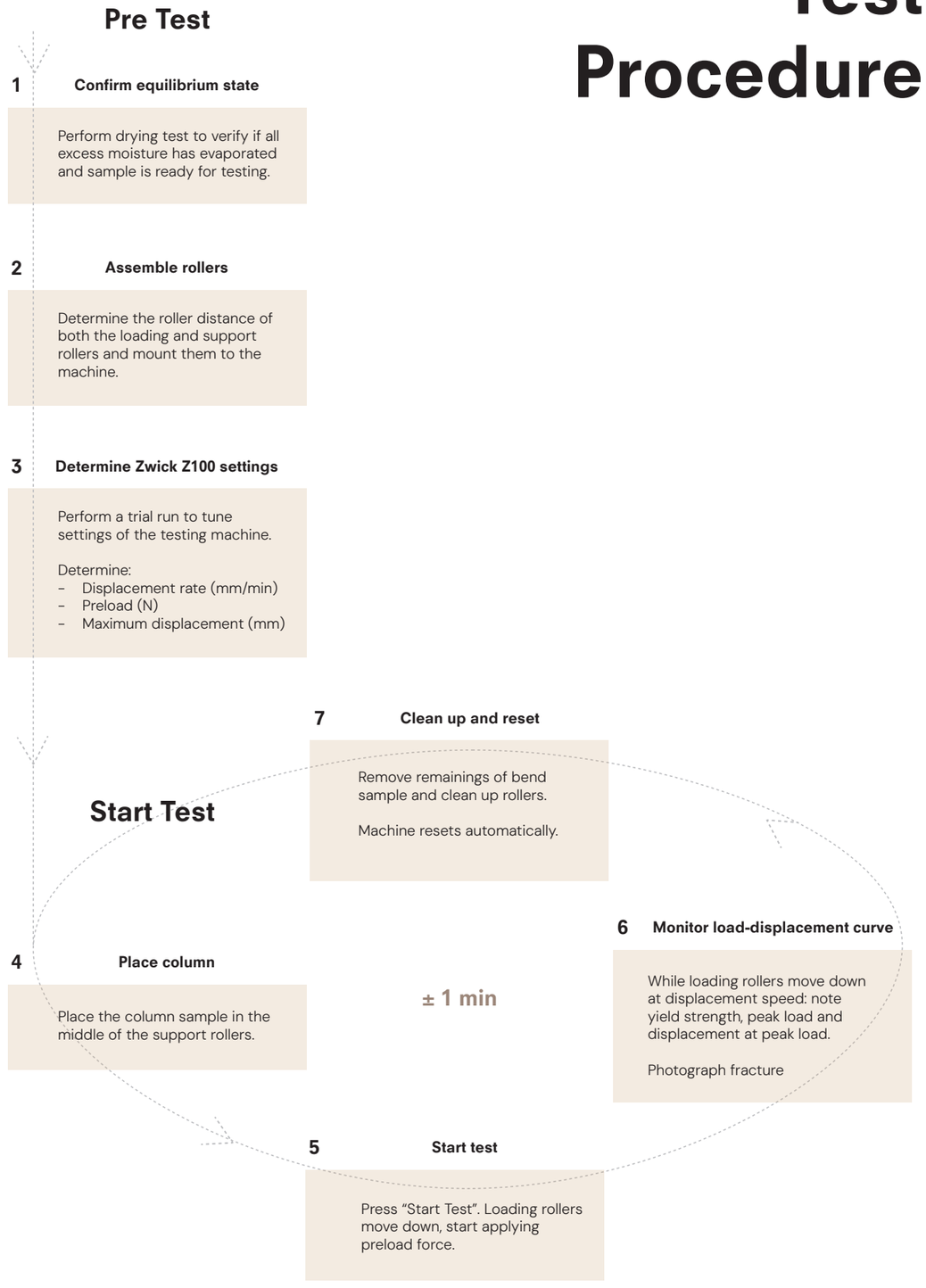

Fig 11.5 Test procedure

Results

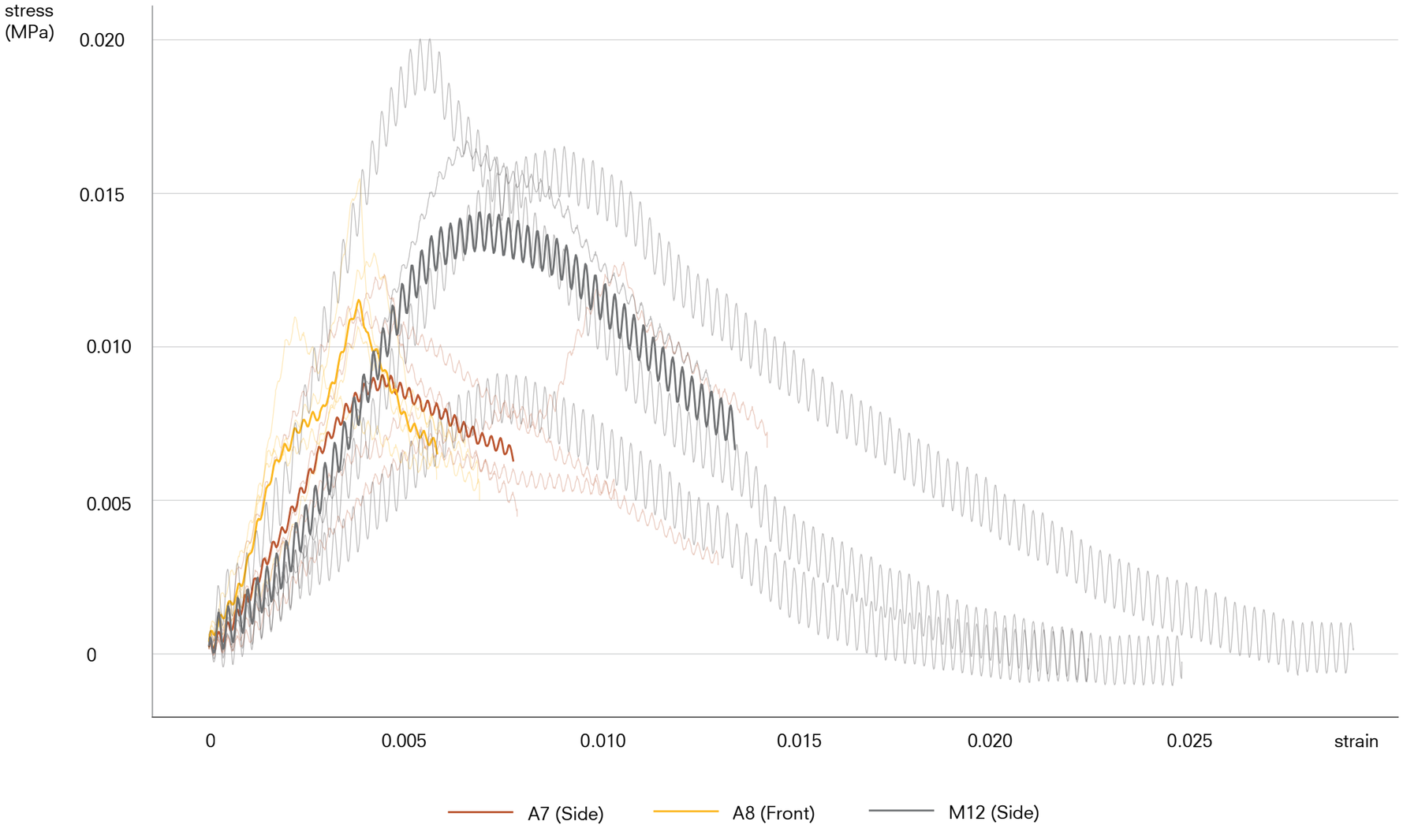

Stress-strain curves

The three sample configurations (A7, A8 and M12) were tested in four point bending on the Zwick Z100. Four replicate columns were loaded for each configuration, outputting 12 force-deflecion curves in totoal. Following the usual procedure for prismatic beams, each curve was converted to a stress-strain curve by normalising for force, supporting roller span, and the cubic cross sectional area.

In figure 11.6, all individual curves are drawn with high transparancy, and the average for each configuration is over plotted.

Fig 11.6 Stress strain curves bending tests

Discussion

Invalid Test

The resulting stress–strain curves are jagged. This roughness does not reflect real material behaviour but stems from the measurement resolution of the testing system.

Because of the heterogeneous properties of the material, the geometry of the hempcrete columns needed to be at least 3x the maximum shiv length (3 x 30mm = 90mm). For standard bending tests, the length of the sample needs to be 10x its cross section. This results in a physically large sample. For materials such as concrete (usually tested in Zwick Z100 machines), samples of this size produce big maximum loads. However, in this test, the maximum loads reached were below 120 N.

The Zwick Z100 is calibrated for forces up to 100 kN. Working three orders of magnitude below its optimal range caused testing noise and error. This resulted in the observed irregularity of the curves. For this reason the flexural stress-strain curves can not be considered reliable for comparison between A7, A8 and M12.

Observations

One observation can still be noted. Even at the largest achievable deflections the bending stress in the hempcrete remained very low. (0.020 MPa).

In other words, the material is very weak in tension for the tested geometry. Design strategies should therefore place hempcrete only in compressive zones and rely on alternative materials or reinforcement to carry tension.

Sweep influence

Compaction:	not tested
Layer height:	not tested
Orientation:	inconclusive
Binder:	inconclusive

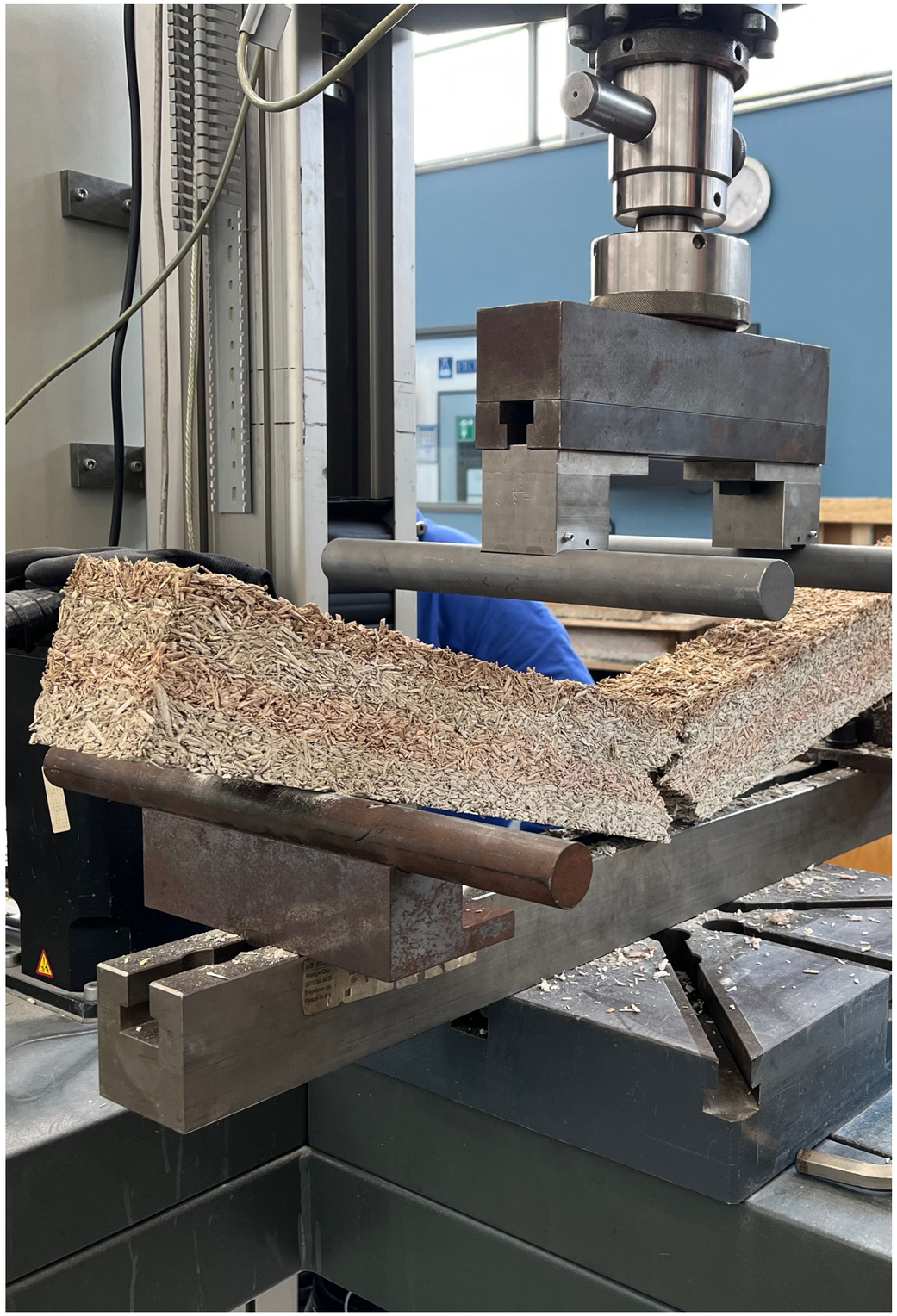

Fig 11.7 Sample after bending failure

Discussion & Conclusion

The chapter opens with a summary of the test results, then examines how manufacturing choices shaped the samples' behaviour, and concludes with the research' main findings and recommendations for future research.

Fig 12.1 Sample A2

Test Results Summary

		1 Drying	2 Hotbox	3 Compressive	4 Bending
B	**Binder** Material	inconclusive	not tested	inconclusive	inconclusive
C	**Compaction** Manufacturing	observed	observed	observed	not tested
L_i	**Layer Height** Manufacturing	not observed	observed	observed	not tested
O	**Orientation** Manufacturing	not tested	not observed	observed	inconclusive
		Moisture Equilibrium	Thermal Conductivity	Compressive Strength	Bending Strength
		Hygrothermal		Mechanical	

Observations

Because the mixed-binder specimens (M9–M11) had not reached moisture equilibrium on the test day, no observations could be made on the effect of binder type (B).

Because the four-point bending test was called invalid, no effects could be observed on the effect of any manufacturing variable on flexural strength.

Varying the degree of compaction (C) affected drying behaviour, thermal properties and compressive strength.

Varying the initial layer height (L_i) affected thermal properties and compressive strength but had no effect on drying behaviour.

Varying the compaction orientation (O) had no effect on thermal properties, yet it clearly affected compressive strength.

Fig 12.2 Observation matrix

Compaction Sweep

1 Compaction proportionally increases dry density and drying time.

2 Compaction linearly reduces thermal insulation performance

3 Compaction exponentially increases yield strength and stiffness.

Measured properties

ρ_{dry} = 205 kg/m³	λ = 0.077 W/mK	ρ_{dry} = 235 kg/m³	λ = 0.080 W/mK
$\sigma_{c,y}$ = 0.03 MPa	E = 0.49 MPa	$\sigma_{c,y}$ = 0.10 MPa	E = 1.53 MPa

Fig 12.3 Sample A0

Fig 12.4 Sample A1

ρ_{dry} = 330 kg/m³	λ = 0.106 W/mK	ρ_{dry} = 405 kg/m³	λ = 0.127 W/mK
$\sigma_{c,y}$ = 0.51 MPa	E = 5.01 MPa	$\sigma_{c,y}$ = 1.11 MPa	E = 9.63 MPa

Fig 12.5 Sample A2

Fig 12.5 Sample A3

Layer Height Sweep

1 Increasing layer height has no observed effect on dry density and drying time.

2 Increasing layer height causes density gradients which cause thermal bridges.

3 Increasing layer height slightly decreases yield strength and stiffness.

Measured properties

ρ_{dry} = 330 kg/m³	λ = 0.101 W/mK	ρ_{dry} = 330 kg/m³	λ = 0.106 W/mK	ρ_{dry} = 330 kg/m³	λ = 0.085 W/mK	ρ_{dry} = 330 kg/m³	λ = 0.101 W/mK
$\sigma_{c,y}$ = 0.52 MPa	E = 4.76 MPa	$\sigma_{c,y}$ = 0.51 MPa	E = 5.01 MPa	$\sigma_{c,y}$ = 0.48 MPa	E = 3.84 MPa	$\sigma_{c,y}$ = 0.27 MPa	E = 2.22 MPa

Fig 12.6 Sample A6

Fig 12.7 Sample A2

Fig 12.8 Sample A4

Fig 12.9 Sample A5

Orientation Sweep

1 Orientation effects were not tested for dry density and drying time

2 Orientation effects were not observed for thermal conductivity

3 Orientation strongly influences mechanical strength with opposing trends in yield strength and stiffness.

Measured properties

ρ_{dry} = 330 kg/m³	ρ_{dry} = 330 kg/m³	ρ_{dry} = 330 kg/m³
λ = 0.101 W/mK	λ = 0.101 W/mK	λ = 0.104 W/mK
$\sigma_{c,y}$ = 0.52 MPa	$\sigma_{c,y}$ = 0.20 MPa	$\sigma_{c,y}$ = 0.20 MPa
E = 4.76 MPa	E = 9.76 MPa	E = 9.76 MPa
C = 50 %	C = 50 %	C = 50 %
L_i = 5 cm	L_i = 5 cm	L_i = 5 cm
O = Top	**O = Side**	**O = Front**
B = Air	B = Air	B = Air

Fig 12.10 LTR: Samples A6, A7 and A8

Binder Sweep

No conclusive results due to premature testing of the mixed binder samples. So all results only applicable to EXIE's CaNaCrete.

Fig 12.11 Bigbag of CaNaCrete being delivered

Manufacturing Considerations

Layering

The layer height sweep makes a clear case for limiting initial layer height to under 10cm in prefabrication of hempcrete elements:

No gain in drying time

Across the tested range, thicker layers did not influence equilibrium dry density or speed up the drying process.

Thermal inconsistency

Visual inspection showed that layers thicker than 10cm develop a noticeable density gradient, with denser upper zones. The thermal hotbox (with its additional sensor in the high density zone) test showed that these zones conduct more heat: indicating that non-uniform compaction creates thermal bridges.

Mechanical degradation

The compression tests conducted show that samples cast in layers above 10 cm result in lower yield strength and stiffness and brittle behaviour. Thinner layers of equal overall density produce a more homogeneous micro structure and ductile behaviour with high safety margins.

$L_i \leq 10cm$

Taken together, these findings demonstrate that keeping layer heights below 10cm minimizes internal density gradients. This provides consistent insulation and reliable load-bearing capacity in monolithic hempcrete elements.

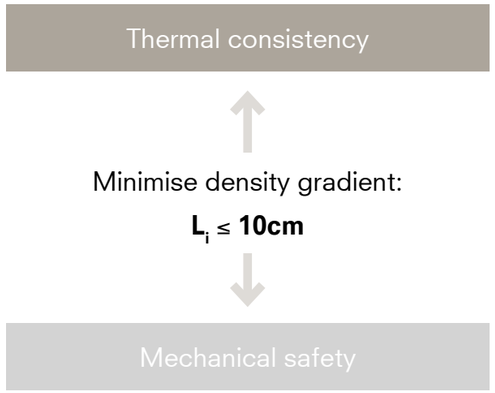

Fig 12.12 Density gradient tradeoff

Fig 12.13 Close up of density gradient

Compaction

Density control

Bulk density controls almost every property of hemp-lime. It depends on how thick each layer is placed and how firmly the mix is rammed. In this research both variables were combined into one: the compaction factor (percentage reduction in layer thickness under ramming).

Density trade off

A light mix holds more air and therefore buffers moisture and heat well; a dense mix packs more binder and develops higher compressive strength. Choosing a target density is therefore a balance between hygrothermal performance and mechanical safety.

Test results showed that once the compaction factor reached above 50%, the material changed from brittle, crumbly behaviour to ductile, crack-free behaviour. That threshold is adopted here as the minimum safe compaction level.

Wall thickness

If the whole wall is cast at one uniform compaction factor, increasing that factor pushes density (and strength) up and thermal conductivity (λ) down. To keep the thermal resistance R_c = 4.7 m²K/W, the wall must then be made thicker.

The relationship is clear: λ rises more or less linearly with density, while yield strength grows exponentially. A small extra thickness therefore results in a large gain in mechanical strength.

C ≥ 50%

For the present mix the 50% compaction setting offers the best compromise: meeting moisture and thermal targets without an excessive wall thickness and still providing a safe mechanical margin.

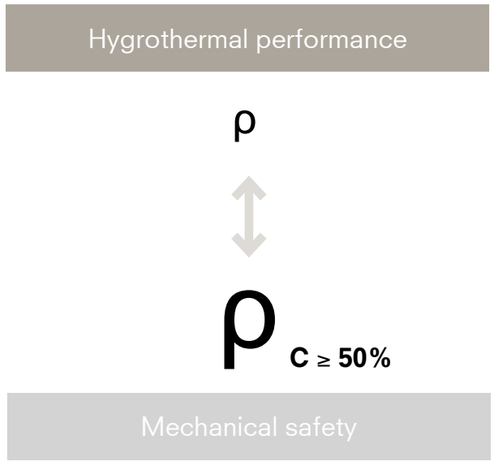

Fig 12.14 Density tradeoff

C (%)	Dry Density (kg/m³)	Yield strength (MPa)	Thermal Conductivity (W/mK)	Wall thickness (Rc = 4.7) (cm)
0	190	0	0.071	35
10	205	0.03	0.077	36
33	235	0.10	0.080	38
50	330	0.51	0.106	50
60	405	1.11	0.127	60

Table 12.1 Compaction factors, properties and wall thicknesses

Orientation

The thermal and mechanical tests on the three compaction orientations resulted in the following insights:

Thermal conductivity

No significant difference was found between top-, front- and side-compacted samples. All three orientations resulted in nearly identical λ-values in the hot-box test. This indicates that from a thermal-insulation standpoint, in this experiment, layer orientation is irrelevant.

Compressive Yield strength

Orientation had a strong effect on compressive performance. Samples compacted from the top sustained nearly three times the yield stress of those compacted from the front or side, which delaminated along their horizontal layers, already at very low loads. This suggests that aligning shiv layers horizontally under the load during prefabrication (the top-compaction method) optimizes the element's capacity to carry its own weight.

Bending strength

The 4 point bending tests were inconclusive for compaction orientation, so they cannot guide preferred orientation choice for bearing wind loads.

However, the "fingertip" testing and manual handling of the column samples (intended for 4 point bending tests) revealed that those compacted from the side or front felt and behaved more robust than the top-compacted ones, which broke at their layer interfaces almost immediately with minimum force. This observation points to additional factors, such as the sample geometry, influencing the materials bending strength.

Taken together, the dead-load compression data make a strong case for factory compaction from above (the "top" orientation) as the default for prefabricated hempcrete panels. However, the real-world performance may also depend on element shape.

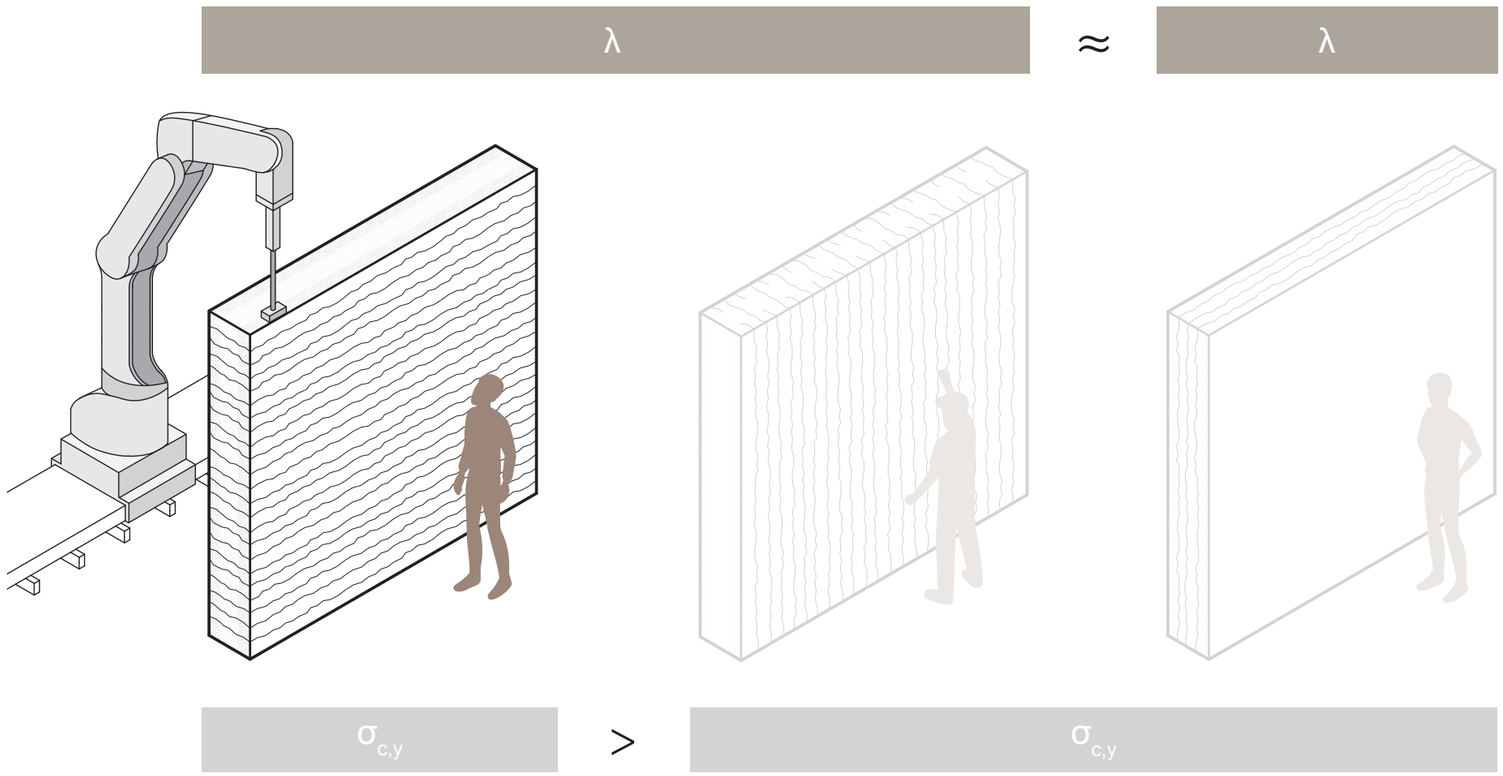

Fig 12.15 Orientation test result comparison

Transportation

The mechanical tests show that hempcrete alone does not have sufficient compressive or flexural strength to allow safe handling of bare elements.

Under a pure bending scenario, such as lifting by straps passed beneath the element, the tensile stresses at the bottom-middle section would exceed hempcrete's low tensile capacity and cause cracking or rupture. Similarly, when barrier clamps are used, the region immediately below each clamp must resist vertical tensile forces during lifting. The material's inability to carry those tensile loads means the panel would likely delaminate or fracture at the clamp line.

Any prefabricated hempcrete element requires an additional support structure or reinforcement, such as embedded wooden or steel frames to distribute stresses and ensure safe transport (figure below)

Fig 12.16 Rammed earth element: supported lifting straps

Monomateriality

If the proposed layer height is 10cm to make sure no inner layer density gradients appear, the compaction factor is 50% so brittle behaviour is ruled out, and top orientation is assumed to be the most favorable, it is interesting to see what would happen if this frame-free wall is installed against a load-bearing structure, mounted to the floors at top and bottom. The following parameters are taken, and a sketch of the scenario is shown in figure X.X.

Parameter	Value	Unit
Own weight (mean density)	275	kg/m^3
Element height	3	m
Wall thickness	0.36	m
Wind load (NEN1991-4)	1	kN/m^2

Table 12.2 Parameters

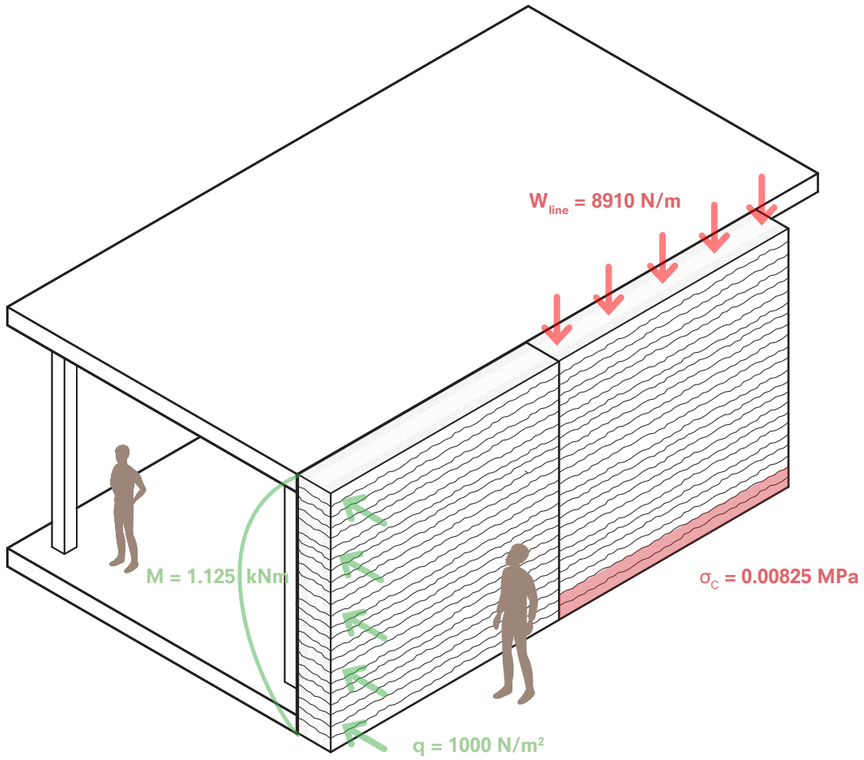

Fig 12.16 EPD comparison: CaNaCrete vs. proposed mix

Dead load

The density of the wall is taken as the average over the multi-density section. The weight per volume material is about 2750 N/m^3

This means single 3 m-high panel 0.36 m thick carries a line load of:

$W_{line} = 2750\ N/m^2 \times 3\ m \times 0.36\ m = 2970\ N/m$

Over its 0.36 m² cross section, this produces a compressive stress at the base of:

$\sigma_C = 2970 / 0.36 = 0.00825\ MPa$

This is well below the yield strength of the densified exterior, which is subjected to all the dead load, since the compressive strength of the interior is ignored. From the stress–strain curve of A2 (Figure 12.17), 0.00825 MPa correlates to 4.5 % axial strain.

This means a 3 m tall element would shorten by roughly: $0.045 \times 3 = 135\ mm$

Dead load: conclusion

0.00825 MPa is far under A2's crushing limit, so this provides a large safety margin. The wall will not fail or crack. However, the resulting 135 mm elastic settlement over a single element can not be ignored. In the design of the elements, this needs to be accounted for.

Dead load: possible strategy

Normally, wooden studs prevent this settlement, but in a fully monolithic hemp–lime wall an alternative strategy is required. One approach is to pre-load each panel in the factory to the expected dead-load stress, allow it to compress, and ship it at its "settled" height, to match the project's required wall elevation. In other words, initially build it 4.5% taller, and let it settle under its own weight.

Wind load

For the wind load of 1 kN/m² on the wall, the maximum bending moment of the wall would be:

$M = (1/8) \times 1\ kN/m^2 \times (3000mm)^2 = 1.125 \times 10^6\ Nmm$

This results in a section modulus of :

$W = (1/6) \times 1000\ mm \times (360\ mm)^2 = 21.6 \times 10^6\ mm^3$

This means the bending stress of the wall is:

$\sigma_f = M/W = 0.052\ MPa$

Wind load: conclusion

So a 3 m panel subjected to 1 kN/m² wind pressure receives about 0.05 MPa of tensile stress on the back (inside) and an extra 0.05 MPa compressive stress on the front (outside) at the outer most fibers.

Combined with the dead-load compression (0.00825 MPa), the total stress range is still well below hempcrete's compressive capacity but above its low tensile strength. This research did not succeed in finding a bending (or tensile) strength, but literature states that is typically <0.02 MPa (Nguyen et al., 2010).

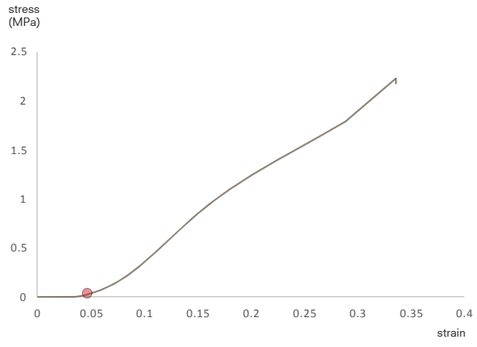

Fig 12.17 Stress strain curve sample A2 (proposed exterior)

Wind load: possible strategy

This suggests that, in this suggested form, bare hempcrete wall elements would struggle to resist wind-caused bending without additional support. Possible strategies to improve their flexural capacity include:

- Increasing the binder content in the mix (B/H ratio)
- Using a stronger binder type
- Increasing the elements wall thickness
- Introduce simple ribs along the face to increase stiffness

However, any adjustment to the (B/H) ratio, binder type, section geometry or compaction strategy will alter hygrothermal properties: affecting dry densities, drying times, R_c-values and required wall thicknesses. This means every mechanical enhancement must be balanced against insulation performance and moisture control requirements.

In practice, this would mean re-running hygrothermal simulations and laboratory tests for each new mix or density profile iteration, so that the optimal compromise between strength and hygrothermal function can be found.

Environmental Impact

Using the same carbon factors from the B-EPD of EXIE's CaNaDry (detailed discussion in chapter 3.7), we can redo the carbon calculation for the wall proposed in this experiment. The following parameters were known and recalculated for:

Since the Rc requirement in Belgium is lower than in the Netherlands, this difference needs to be accounted for in the FU. Also it is important to note that the mass per FU is much higher, because of the higher density (through higher C)

Parameter	Symbol	CaNaDry B-EPD	Proposed mix	Unit
Dry density	ρ_{dry}	175	**275**	kg/m³
B/H ratio	B : H	0.54	**1.09**	-
Thermal conductivity	λ	0.054	**0.078**	Wm/K
Hemp mass per m³	H = ρ / (1+ B/H)	113.6	**131.6**	kg
Binder mass per m³	B = ρ - H	61.4	**143.4**	kg
Rc value requirement	Rc	4.5	**4.7**	m²K/W
Functional Unit (FU)	t = Rc x λ x 1 x1	0.243	**0.351**	m³
Mass per FU	ρ x FU	42.5	**96.5**	kg

Table 12.3 EPD parameters of the two mixes

Carbon factors

(taken straight from the EPD)

Biogenic storage in hemp

Stored = - 1.39 $kgCO_2eq/kg$ hemp

Extraction + fuel emissions for lime

Emitted = + 1.10 $kgCO_2eq/kg$ binder

First, it is important to have a look that is happening in product module A1. Since changing the materials density and W/B ratio directly impact the raw material use and its GWP. Result in table below:

A1 (raw materials)

More density = more lime = more emissions

Although the denser mix stores more carbon due to more hemp, the larger lime fraction eats up most of the benefit.

Thermal performance matters

The lower λ value due to compaction means 44% more material is needed to reach the same Rc value, doubling the mass per FU and decreasing more of the advantage (-22 kg to -9 kg)

Contribution in A1	GWP / kg ($kg CO_2$-eq)		GWP / m³ ($kg CO_2$-eq)		GWP / FU ($kg CO_2$-eq)	
	CaNaDry	Proposed mix	CaNaDry	Proposed Mix	CaNaDry	Proposed mix
Biogenic capture (Hemp)	- 0.9	- 0.67	- 158	- 183	- 38	- 64
Emissions (Lime)	+ 0.4	+ 0.56	+ 68	+ 158	+ 16	+ 55
Net A1	**- 0.5**	**- 0.1**	**- 91**	**- 26**	**- 22**	**- 9**
	x 5.8		x 3.5		x 2.4	

Table 2.4 Results for A1

Densifying

Scaling

Changing the hempcrete mixture also impacts other modules in the LCA, mostly because more mass needs to be transported and mixed. That is in why is this comparison, the factors are scaled proportional to product mass.

Scenario

The analysis is based on the 75% reuse scenario, anticipating that, like the loose CaNaDry hemp-lime mix, the mixture studied here can also be reused for 75% in fresh hempcrete at end of life. Note that Phase D (potential for the next lifecycle) is excluded from this comparison.

Lime share

Product stage A1 remains negative but as the lime share rises, the hemp storage benefit shrinks.

Every mass linked module roughly doubles because 2.4 x more material is used and needs to be transported and handled on site.

More hydrated lime also means more long-term carbonation, so B1 is more negative. The net extra emissions of the higher lime share lime is only + 2.83 kg.

		CaNaDry	Proposed Mix	
		GWP total / FU ($kg CO_2$-eq)	GWP total / FU ($kg CO_2$-eq)	
A1	Raw materials	- 22.10	- 9.10	
A2	Transport	+ 1.14	+ 2.59	
A3	Manufacturing	+ 0.17	+ 0.39	
	Subtotal Product	**- 20.79**	**- 6.12**	
A4	Transport	+ 0.80	+ 1.82	
A5	Installation	+ 0.56	+ 1.27	
	Subtotal Cradle-to-Site	**- 19.43**	**- 3.03**	
B1	Use	- 4.28	- 14.45	
C1	Deconstruction	+ 0.18	+ 0.41	
C2	Transport	+ 0.25	+ 0.57	
C3	Waste processing	+ 9.33	+ 16.4	
C4	Disposal	+ 0.03	+ 0.12	
	Subtotal Cradle-to-Grave	**- 13.9**	**- 0.02**	**≈ 0**

Fig 12.17 LCA comparison: CaNaCrete vs. proposed mix

Carbon negative limit

With the 75 % end-of-life reuse scenario condisered, the dense, binder rich mixture used still ends up around net zero, effectively being climate neutral.

Any further increase in density, B/H ratio or wall thickness pushes up lime-process emissions faster than the extra hemp can offset them, so the balance tips to net-positive GWP.

Conclusion

Research Questions

The material

> What key fundamentals of hempcrete define its unique material performance?

Hempcrete is a unique building material that can serve as a single, monolithic exterior wall that accounts for all the roles conventionally split among multiple petrochemical and high carbon footprint layers: structure, insulation, moisture regulation, acoustics and fire proofing.

It solely combines hemp shiv and a lime binder to create a stand-alone, vapour-open and thermally resistant mass that stabilities both indoor humidity and temperature without additional membranes or foams.

Structurally, the composite is self-supporting but not load-bearing; strength, settlement and durability all rise or fall with binder type, binder-to-hemp (B/H) ratio and shiv orientation. In fire tests hempcrete meets class B-s1,d0.

Environmentally, the biogenic carbon stored during hemp growth and re-absorbed during lime carbonation can outweigh production emissions: under a 75 % end-of-life reuse scenario the CaNaDry reference hempcrete mix sequesters about 14 kg CO_2-eq per functional unit, making it carbon-negative as long as density, binder ratio and wall thickness are kept within limits.

The manufacturing

> How do current manufacturing techniques (in-situ and prefab) affect the performance of hempcrete walls?

Field work on a full-scale hempcrete wall with YOMABOUW showed that in-situ casting remains a largely artisanal workflow of framing, formworking, hand mixing, bucket transport, manual tamping and slow air curing.

The method offers unlimited form freedom, but labour demand is high, compaction consistency and quality is strongly dependent on worker fatigue and skill, and three-month, weather dependent, drying times complicate tight schedules. The resulting performance of the wall directly depends on all these factors.

Prefabrication in a controlled plant can solve those issues: consistent dosing, mechanical compaction and conditioned curing improve consistency, shorten workflow-times and reduce on-site skill requirements.

However, the trade-off; factory-made blocks or elements ask for a finishing layer that conceals the natural, layered hemp-lime surface texture and therefore sacrifice the monolithic aesthetic that makes cast in situ hempcrete distinctive.

The experiment

> How does varying manufacturing parameters affect the hygrothermal and mechanical performance of a hempcrete wall element?

Innovation in rammed earth manufacturing shows that mechanical automation speeds production and delivers uniform ramming. To test whether automated manufacturing in hempcrete could deliver uniform, self-standing and thermally insulating wall elements, an experiment was set up. It examines how varying manufacturing parameters influences the walls material performance.

Four parameters were varied compaction factor, layer height, orientation and binder type. Manual tamping simulated the constant force of a robot rammer by measuring compaction as the percentage reduction in layer height, rather than as applied force. This provided a control parameter that can be transferred directly to a robotic system.

Results show that layers kept below 10cm and compacted to at least 50% eliminate internal density gradients, maintain hygrothermal performance and supply a safe mechanical margin. Compression tests indicate that top-down compaction orientation performs best. Densifying the mix increases yield strength exponentially, but this comes with big settlement and deformation that needs to be accounted for. Wind-load analysis shows that pure, unreinforced hempcrete elements still need extra flexural capacity. Proposed strategies suggest altering mix design, section geometry or include denser ribs for stability.

Finally, life-cycle re-calculations confirm a carbon-neutral limit: the dense, binder-rich mix used for the experiment remains near net-zero under 75% reuse, but any further rise in density, binder ratio or wall thickness pushes lime emissions beyond the hemp biogenic storage and turns the balance to net-positive GWP emissions.

Further Research

Environmental Impact

The environmental impact of hempcrete, measured through its LCA, is strongly dependent on two assumptions, that still need further research.

Service life?

Current LCA results for hempcrete rely on EXIE's stated 75-year service life for the CaNaDry mix, a number derived from protected use of the material, such as cavity infill and floor insulation. The exterior-wall application proposed in this thesis exposes the material to weather, impact and animals, conditions for which no long-term performance data exist yet. Reliable LCA therefore depends on further research that investigates how hempcrete behaves in an exposed facade. Surface erosion, moisture cycling, biological attack and mechanical damage over time are all important and must be taken into account to determine a substantiated service life of the material.

75% Reuse scenario?

EXIE's LCA assumes that, at end of life, 75% of the CaNaDry mix can be vacuum-recovered and reused. The denser, binder-rich formulation tested in this thesis may not behave the same way. Two questions need further research:

Exposing the wall to the elements could lower the share of material that, at the end of service life, is still clean enough for reuse. Further research needs to investigate if the 75% target is still realistic or if only a smaller percentage can be reused. And even when clean rest material is available, it is expected that only a certain ratio can be mixed back into fresh hemp-lime. Further performance testing with altering mix ratios is needed to quantify how much fresh shiv and binder must be added.

Monomateriality

This research focused on pure hemp and lime: monolithic walls with no added materials or structures.

Reinforcement?

Compating the mix shows that higher density results in compressive strength gains. However, questions remain about long term deformation under self-weight and resistance to wind loads. Further research is needed on reinforcement strategies or mix modifications that improve rigidity, but not compromise the materials hygrothermal performance.

Multi-density?

Mechanical tests in this thesis were limited to samples with a single, uniform density. The full-scale prototype wall relied on a three-zone density profile: Denser exteriors for strength, a lighter interior for insulation.

Additional work is needed to interpret the current test data and to validate the multi-density concept. The dimensions of the interior and exterior zones, as well as the compaction factors chosen for each, should be optimised.

Scaling?

Scaling up is another unknown: Hemp shiv size does not scale with wall dimensions, so full-height elements may behave differently in compression, bending and creep. The shear bond between the density layers must also be tested to ensure the composite acts as a single structural unit, and not delaminates. Testing at element scale will give insights to the real-world performance of multi-density hempcrete walls.

Prefabrication

Important considerations regarding prefabrication are not discussed in this research, but are important for further research.

Element transport?

Mechanical testing confirmed that bare hempcrete elements lack the compressive and flexural strength needed for the movement of bare hempcrete, yet safe handling methods were not part of this study. Future work should define transport solutions, temporary timber or steel frames, edge stiffeners, lifting rigs, or alternative curing regimes, that protect elements without adding permanent high-impact materials.

Element connections?

Connecting adjacent elements while preserving monomateriality remains an open question. Further research is needed to develop joints that transfer shear and bending, limit air leakage, and use either hemp-lime itself or minimal, low-impact inserts so the wall continues to function as a single breathable layer.

Mounting to the building?

The final prefabrication step is connecting to the primary structure of the building. Mounting systems must resist wind loads and accommodate movement, but also keep the facade vapour-open and thermally sound. Designing and testing such fixings, and assessing their long-term durability, needs to be done before prefabricated hempcrete walls can be implemented in quick, efficient construction workflows.

Fig 12.18 A proud author and his samples

Bibliography

References

Books

Dhondt, F., & Munthu, S. S. (2021). Hemp and sustainability. Springer. http://www.springer.com/series/16490

Minke, G. (2013). Building with earth: Design and technology of a sustainable architecture (2nd ed.). Birkhäuser.

Robinson, R. (1995). The great book of hemp. Park Street Press.

Sparrow, A., & Stanwix, W. (2014). The hempcrete book: Designing and building with hemp-lime. UIT Cambridge.

Sturgis, R., & Davis, F. A. (2013). Sturgis' illustrated dictionary of architecture and building (Vol. 1). Dover Publications. https://www.hoopladigital.com/title/11605786

Van Balen, K., Van Bommel, B., Van Hees, R., Van Hunen, M., Van, J., & Van Rooden, M. (2003). Kalkboek: Het gebruik van kalk als bindmiddel voor metsel- en voegmortels in verleden en heden. Delft University Press.

Articles

Amziane, S., & Arnaud, L. (2013). Bio-aggregate-based building materials: Applications to hemp concretes. John Wiley & Sons. http://ebookcentral.proquest.com/lib/delft/detail.action?docID=1124006

Arnaud, L., & Gourlay, E. (2012). Experimental study of parameters influencing mechanical properties of hemp concretes. Construction and Building Materials, 28(1), 50–56. https://doi.org/10.1016/j.conbuildmat.2011.07.052

Bing, L., Ma, M., Liu, L., Wang, J., Niu, L., & Xi, F. (2023). An investigation of the global uptake of CO2 by lime from 1930 to 2020. Earth System Science Data, 15(6), 2431–2457. https://doi.org/10.5194/essd-15-2431-2023

Brzyski, P., Gładecki, M., Rumińska, M., Pietrak, K., Kubiś, M., & Łapka, P. (2020). Influence of hemp shives size on hygro-thermal and mechanical properties of a hemp-lime composite. Materials, 13(23), Article 5383. https://doi.org/10.3390/ma13235383

Colinart, T., Glouannec, P., & Chauvelon, P. (2012). Influence of the setting process and the formulation on the drying of hemp concrete. Construction and Building Materials, 30, 372–380. https://doi.org/10.1016/j.conbuildmat.2011.12.030

Collet, F., Chamoin, J., Pretot, S., & Lanos, C. (2013). Comparison of the hygric behaviour of three hemp concretes. Energy and Buildings, 62, 294–303. https://doi.org/10.1016/j.enbuild.2013.03.010

Collet, F., & Pretot, S. (2014). Thermal conductivity of hemp concretes: Variation with formulation, density and water content. Construction and Building Materials, 65, 612–619. https://doi.org/10.1016/j.conbuildmat.2014.05.039

de Bruijn, P. B., Jeppsson, K. H., Sandin, K., & Nilsson, C. (2009). Mechanical properties of lime–hemp concrete containing shives and fibres. Biosystems Engineering, 103(4), 474–479. https://doi.org/10.1016/j.biosystemseng.2009.02.005

Elnagar, E., Düvier, C., Batra, Z., Christoffersen, J., Mandin, C., Schweiker, M., & Wargocki, P. (2024). Creating a comprehensive framework for design, construction and management of healthy buildings. Energy and Buildings, 324, 114883. https://doi.org/10.1016/j.enbuild.2024.114883

Glé, P., Degrave-Lemeurs, M., & Hellouin de Menibus, A. (2018). Acoustical properties of hemp concretes for building thermal insulation. Proceedings of Inter-Noise 2018 (pp. xxx–xxx).

Ingrao, C., Lo Giudice, A., Bacenetti, J., Tricase, C., Dotelli, G., Fiala, M., Siracusa, V., & Mbohwa, C. (2015). Energy and environmental assessment of industrial hemp for building applications: A review. Renewable and Sustainable Energy Reviews, 51, 29–42. https://doi.org/10.1016/j.rser.2015.06.002

Jami, T., Karade, S. R., & Singh, L. P. (2019). A review of the properties of hemp concrete for green building applications. Journal of Cleaner Production, 239, 117852. https://doi.org/10.1016/j.jclepro.2019.117852

Kinnane, O., Reilly, A., Grimes, J., Pavia, S., & Walker, R. (2016). Acoustic absorption of hemp-lime construction. Construction and Building Materials, 122, 674–682. https://doi.org/10.1016/j.conbuildmat.2016.06.106

Kloft, H., Oechsler, J., Loccarini, F., & Gosslar, J. (2019). Robotische Fabrikation von Bauteilen aus Stampflehm. In Proceedings of the 3rd International Conference on Additive Fabrication in Construction (pp. xxx–xxx). https://www.researchgate.net/publication/334193576

Nguyen, T.-T., Picandet, V., Amziane, S., & Baley, C. (2009). Influence of compactness and hemp hurd characteristics on the mechanical properties of lime and hemp concrete. European Journal of Environmental and Civil Engineering, 13(9), 1039–1050. https://doi.org/10.3166/ejece.13.1039-1050

Nguyen, T. T., Picandet, V., Carre, P., Lecompte, T., Amziane, S., & Baley, C. (2010). Effect of compaction on mechanical and thermal properties of hemp concrete. European Journal of Environmental and Civil Engineering, 14(5), 545–560. https://doi.org/10.1080/19648189.2010.9693246

Niyigena, C., Amziane, S., & Chateauneuf, A. (2018). Multicriteria analysis demonstrating the impact of shiv on the properties of hemp concrete. Construction and Building Materials, 160, 211–222. https://doi.org/10.1016/j.conbuildmat.2017.11.026

Piot, A., Béjat, T., Jay, A., Bessette, L., Wurtz, E., & Barnes-Davin, L. (2017). Study of a hempcrete wall exposed to outdoor climate: Effects of the coating. Construction and Building Materials, 139, 540–550. https://doi.org/10.1016/j.conbuildmat.2016.12.143

Pretot, S., Collet, F., & Garnier, C. (2014). Life cycle assessment of a hemp concrete wall: Impact of thickness and coating. Building and Environment, 72, 223–231. https://doi.org/10.1016/j.buildenv.2013.11.010

Sassoni, E., Manzi, S., Motori, A., Montecchi, M., & Canti, M. (2014). Novel sustainable hemp-based composites for application in the building industry: Physical, thermal and mechanical characterization. Energy and Buildings, 77, 219–226. https://doi.org/10.1016/j.enbuild.2014.03.033

Van der Werf, H. M. G. (2004). Life cycle analysis of field production of fibre hemp: The effect of production practices on environmental impacts. Euphytica, 140(1–2), 13–23. https://doi.org/10.1007/s10681-004-4750-2

van der Werf, H. M. G., & Turunen, L. (2008). The environmental impacts of the production of hemp and flax textile yarn. Industrial Crops and Products, 27(1), 1–10. https://doi.org/10.1016/j.indcrop.2007.05.003

Walker, R., Pavia, S., & Mitchell, R. (2014). Mechanical properties and durability of hemp-lime concretes. Construction and Building Materials, 61, 340–348. https://doi.org/10.1016/j.conbuildmat.2014.02.065

Williams, J., Lawrence, M., & Walker, P. (2016). A method for the assessment of the internal structure of bio-aggregate concretes. Construction and Building Materials, 116, 45–51. https://doi.org/10.1016/j.conbuildmat.2016.04.088

Williams, J., Lawrence, M., & Walker, P. (2017). The influence of the casting process on the internal structure and physical properties of hemp-lime. Materials and Structures, 50(2), Article 97. https://doi.org/10.1617/s11527-016-0976-4

Reports and guidelines

ATG. (2020). ATG technical approval with certification. Approval and Certification Body. https://www.bcca.be

Bisschop, P., Leguit, M., de Ruyter, J., & de Waal, L. (2023). Vezelrijke verduurzaming: Toepassing van vlas en hennep biedt kansen voor landbouw en bouw [White paper].

BKZ. (2023). Nationale aanpak biobased bouwen [Policy document].

Carbonlab, & HCVA. (2024). Hoe willen wij bouwen M4H 2030: 200 years of construction culture.

Centre for Alternative Technology. (2010). Zero carbon Britain 2030: A new energy strategy.

International Energy Agency. (2022). Buildings: A source of enormous efficiency potential. https://www.iea.org/energy-system/buildings

Knapen, E., Janssens, B., Vandoren, B., Claes, I., Neelen, N., De Mets, T., & Hilderson, W. (2020). Kalkhennep: Ontwerp- en uitvoeringsondersteuning (Guideline).

Snauwaert, E., & Ghekiere, G. (2011). Industriele hennep. Groene Grondstoffen.

Tilstra, F., & Beatrice, G. (2024). The European market potential for hemp apparel. CBI. https://www.cbi.eu/market-information/apparel/hemp-apparel/market-potential

United States Environmental Protection Agency. (2024). Volatile organic compounds' impact on indoor air quality. https://www.epa.gov/indoor-air-quality-iaq/volatile-organic-compounds-impact-indoor-air-quality

Theses

Evrard, A. (2008). Transient hygrothermal behavior of lime-hemp materials (Doctoral thesis). Université catholique de Louvain. https://www.researchgate.net/publication/283568943

Nguyen, T. T. (2010). Contribution à l'étude de la formulation et du procédé de fabrication d'éléments de construction en béton de chanvre (Doctoral thesis). Université de Bretagne-Sud. https://theses.hal.science/tel-01017510v1

Vontetsianou, A. (2023). The effectiveness of hempcrete in the reduction of the environmental and financial costs of residences (Master's thesis). [University name].

Online sources

Bernard, L. (2024, January 11). Why construction in the Netherlands has gone to pot. Construction Briefing. https://www.constructionbriefing.com/news/why-construction-in-the-netherlands-has-gone-to-pot/8034118.article

Gosslar, J., & Kloft, H. (2023). Robotgestützte Stampflehmproduktion – Tradition trifft auf technischen Fortschritt. In Proceedings of the 2nd Conference on Clay and Earth Materials

Hempflax. (n.d.). Applications. Retrieved January 18, 2025, from https://www.hempflax.com/en/applications/

Hens, H. (2012). Passive houses: What may happen when energy efficiency becomes the only paradigm (CH-12-032). ASHRAE Transactions, 118(1), 121–132.

IBN Germany. (n.d.). Building biology course. Retrieved January 18, 2025, from https://www.baubiologie.de

Junte, J. (2020, May 6). Architectenbureau Werkstatt realiseert eerste hennephuis. Architectuur NL. https://www.architectuur.nl

Léonard, A. (n.d.). IsoHemp hempcrete blocks. Faculté des Sciences Appliquées. http://chemeng.ulg.ac.be

Risinger, M. (2020, February 18). Hemp concrete walls (R-30 + fireproof) – You won't believe how they built this house! [Video]. YouTube. https://www.youtube.com/watch?v=cm23l_VLyp4

Rotmans, J. (2022). Omarm de chaos: What does it mean for the building sector? Spectrum.

List of Figures

If not otherwise specified, figures were made by the author. Unspecified photographs were taken by the author or by Hidde Grootes on behalf of the author.

Fig 1.2
Photograph by John Henebry

Fig 1.3
Figure by CarbonLab (2024)

Fig 1.4
Photograph by Sia, Iwanderlista

Fig 1.5–1.6
Photograph by Simon Metselaar

Fig 1.7
Photograph from Kunakair.com

Fig 1.8
Photograph by Joost van der Waal

Fig 1.9
Photograph by Twee Snoeken Architects

Fig 1.12
Figure by Healthy Materials Lab (2020)
Modified by the author

Fig 1.13
Render by de Urbanisten & GroupA

Fig 2.2
Photograph by Barbetorte

Fig 2.3–2.4
Photograph by Kirsten van den Berg

Fig 2.5
Figure by Healthy Materials Lab (2020)
Modified by the author

Fig 2.7
Photograph by Matteo Fil

Fig 2.8
Figure by Thomas James Hartnell (2023)

Fig 2.9–2.12
Images from Sparrow & Stanwix (2014)

Fig 2.13
Photograph by Hempitecture

Fig 2.15
Photograph by Hempitecture

Fig 3.2
Figure from Sahin (2022)

Fig 3.3–3.4
Figure from Knapen et al. (2020)

Fig 3.7
Figure from Bath University (2010)

Fig 3.8
Figure from Collet et Pretot (2014)
Modified by the author

Fig 3.9
Figure from Ansari et al.,, 2025
Modified by the author

Fig 3.11
Figure by the author. Data from b.epd.be

Fig 4.1
Photograph by Micheal Cerrone

Fig 4.5
Figure from Knapen et al. (2020)
Modified by the author

Fig 4.6–4.7
Photograph by Micheal Cerrone

Fig 4.8–4.9
Photograph by Perry Klootwijk

Fig 4.10–4.13
Photograph by IsoHemp

Fig 4.14
Photograph by Perry Klootwijk

Fig 4.26
Photograph by Giesen Architectuur

Fig 4.17
Photograph by BC Materials

Fig 4.18
Photograph by Emma Carroll

Fig 4.19
Photograph by Hanno Makowitz

Fig 4.20
Photograph by Sasha Schade

Fig 4.21
Photograph by Harold Kloft

Fig 4.22–4.23
Photograph by Hanno Makowitz

Fig 6.11
Photograph by Salem Mostefaoui

Fig 12.13
Photograph by Pia Fischer

Fig 12.16
Photograh by Rammtec International

Appendix

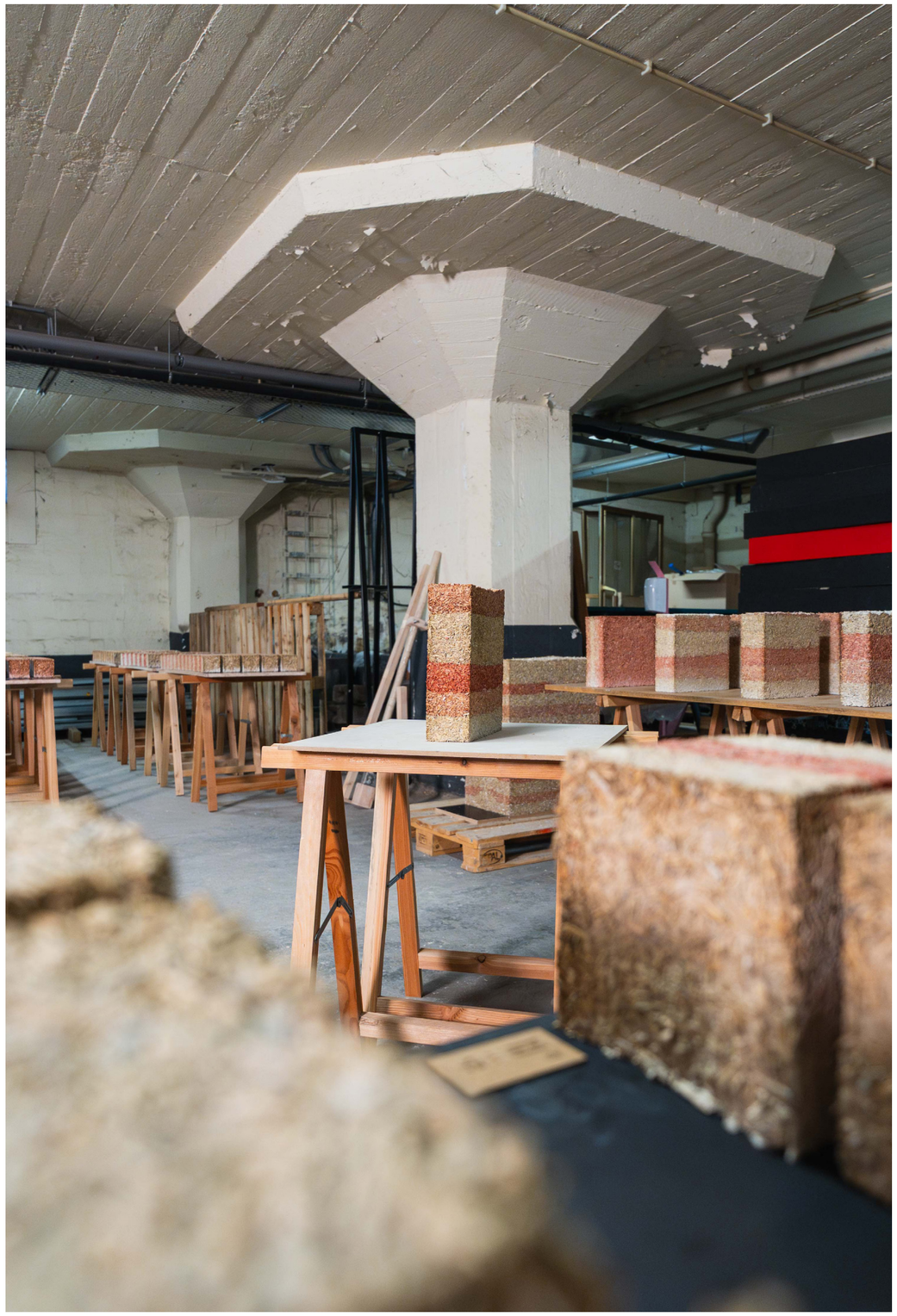

Fig A.1 Basement view

A0

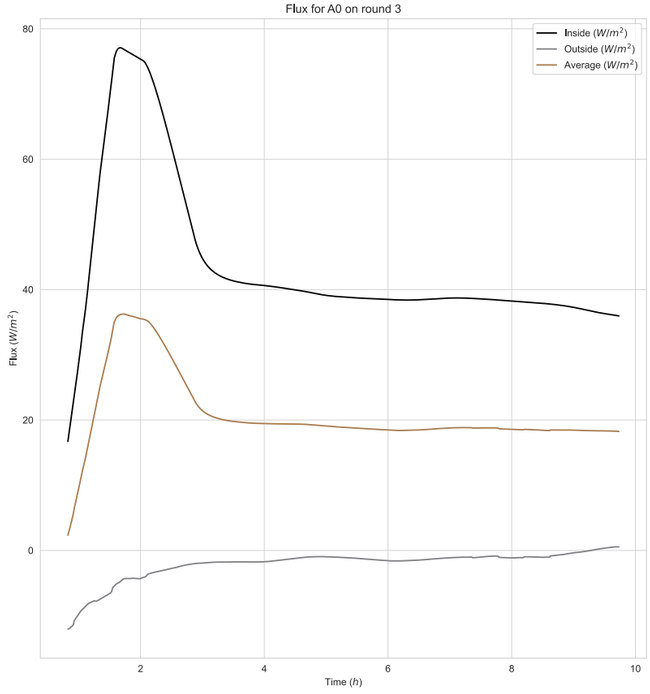

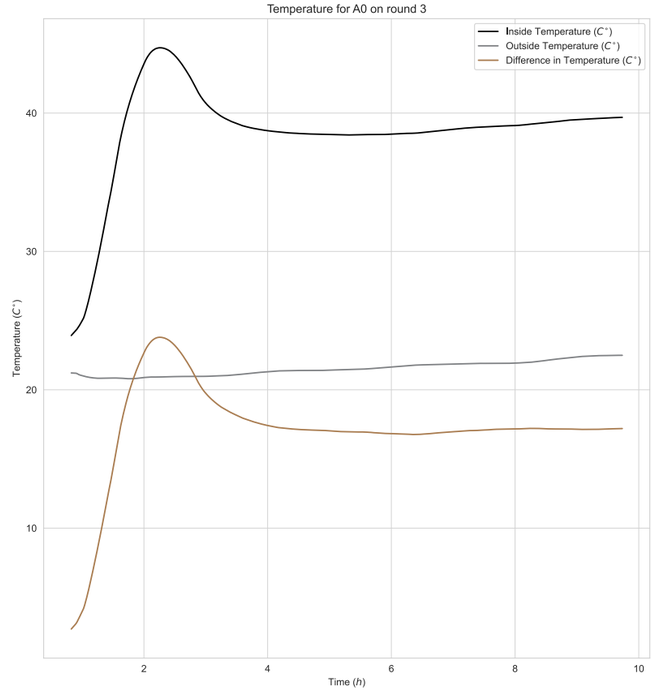

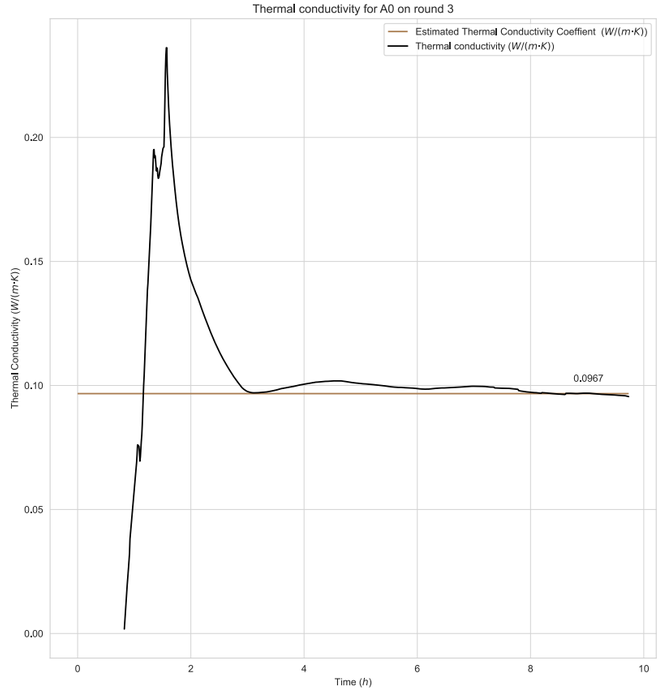

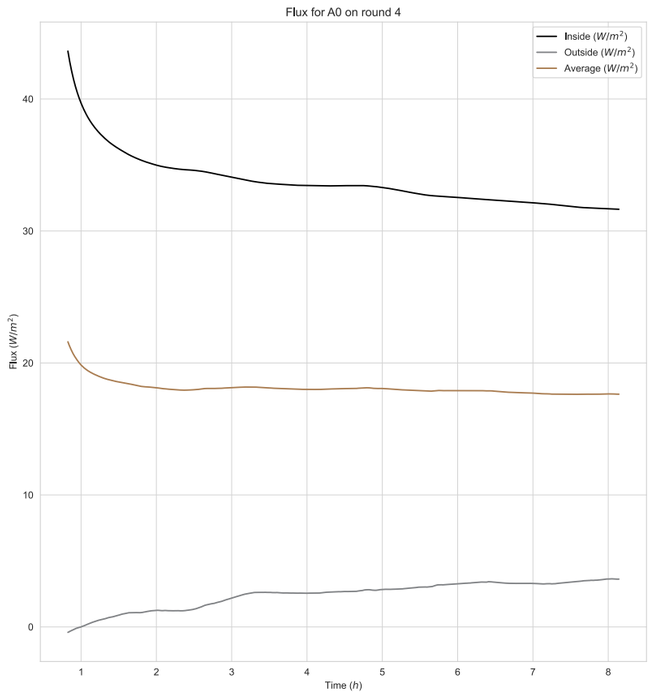

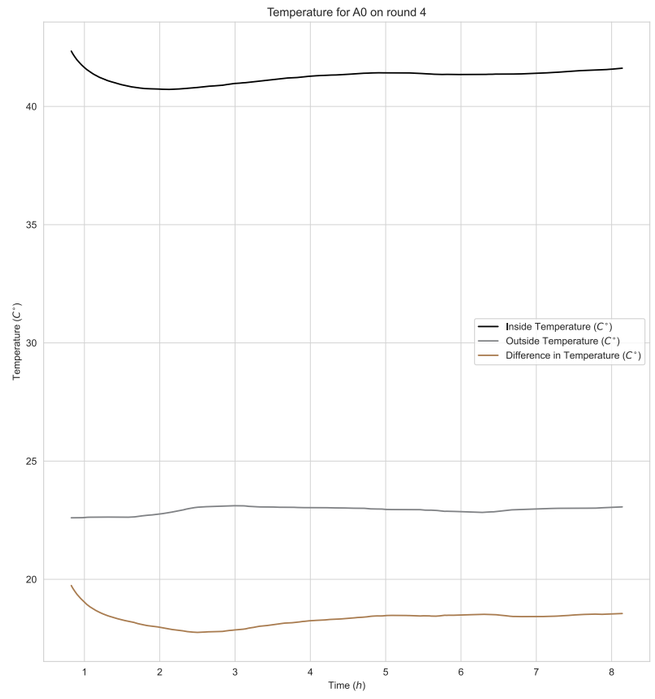

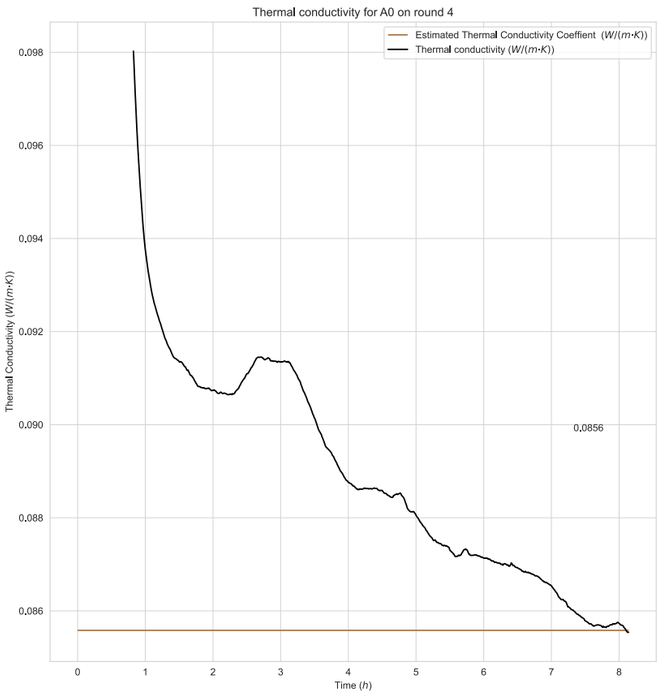

Fig x.x Hotbox measurements (flux, temperature and thermal conductivity) for sample A0. Top: round 3, bottom: round 4

A0

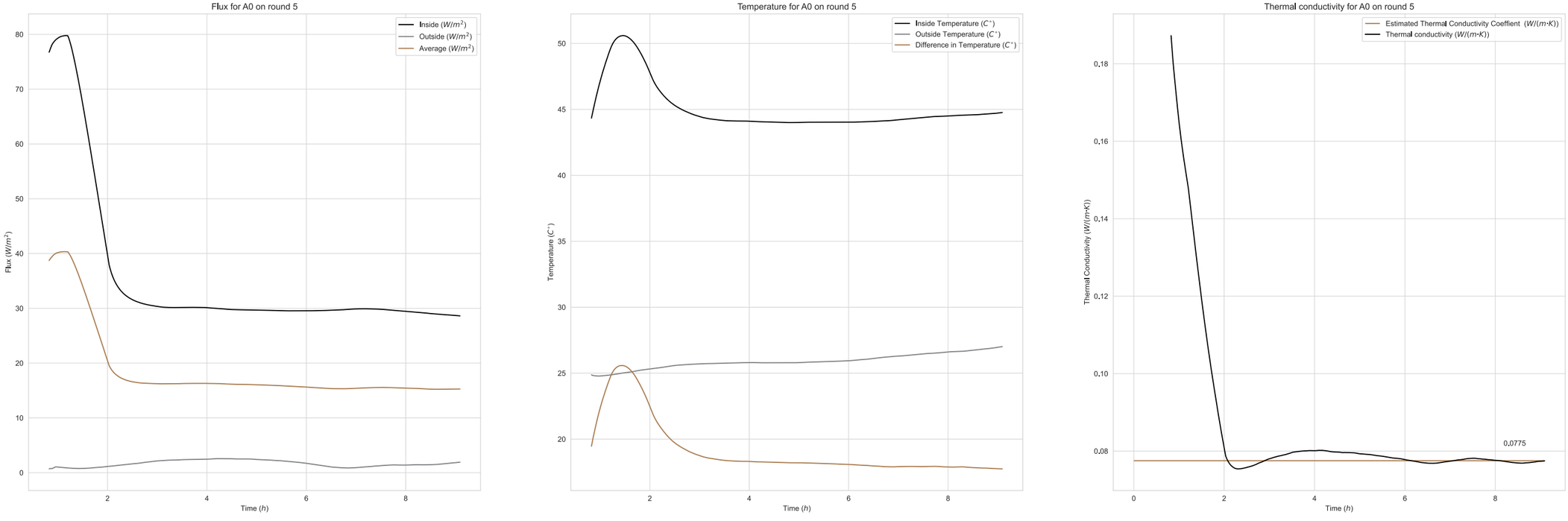

Fig x.x Hotbox measurements (flux, temperature and thermal conductivity) for sample A0 on round 5

A1

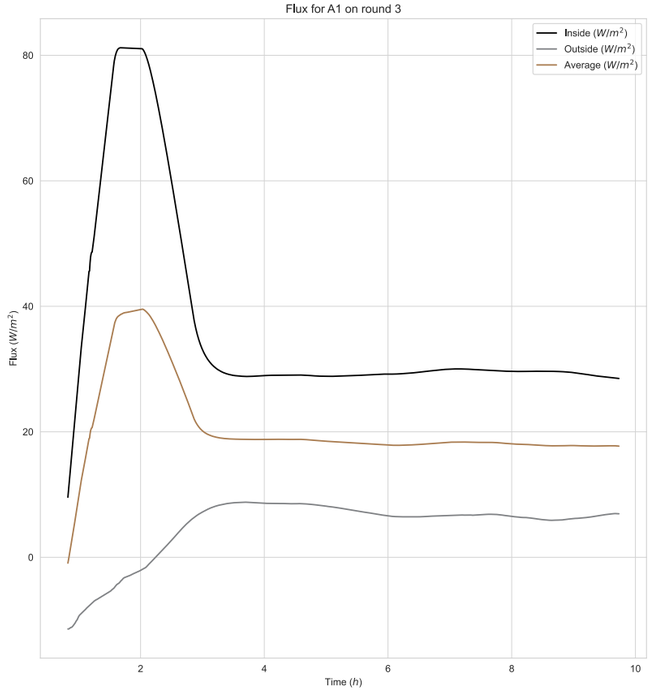

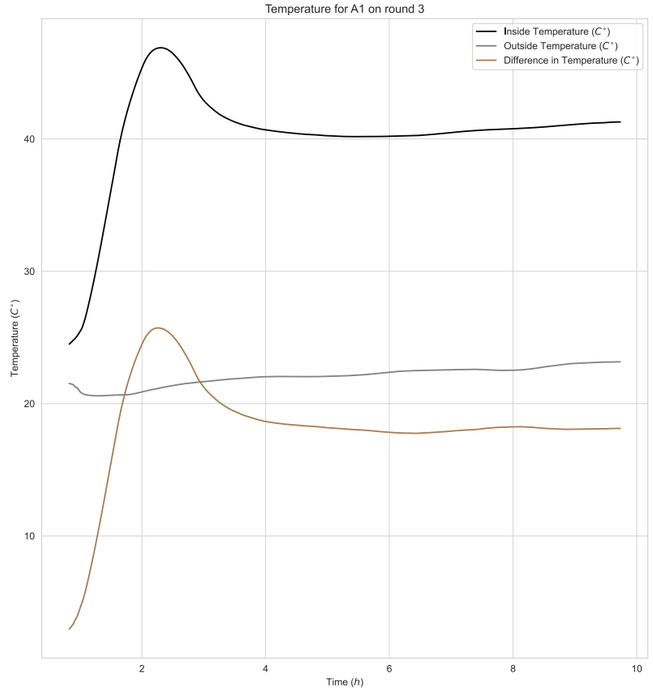

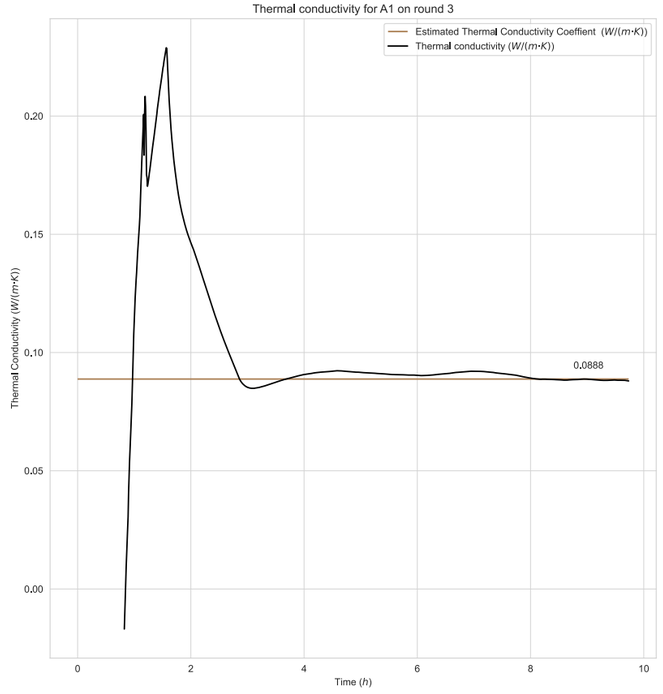

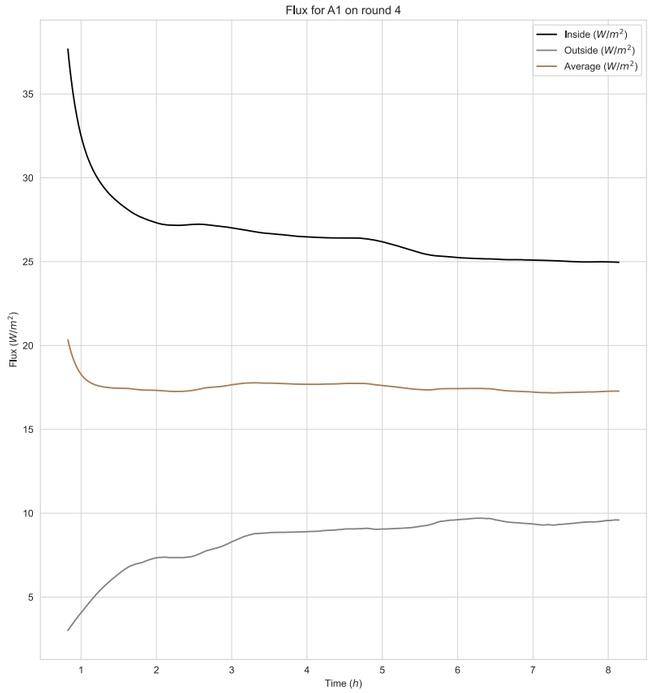

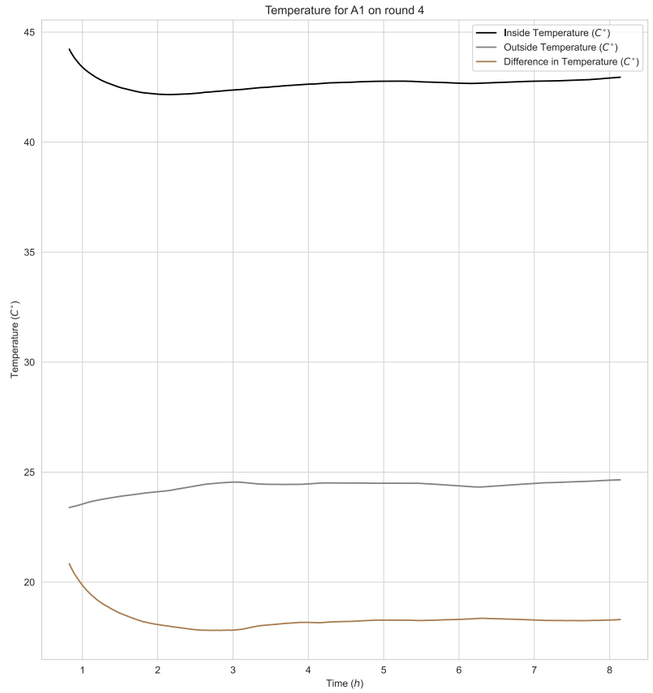

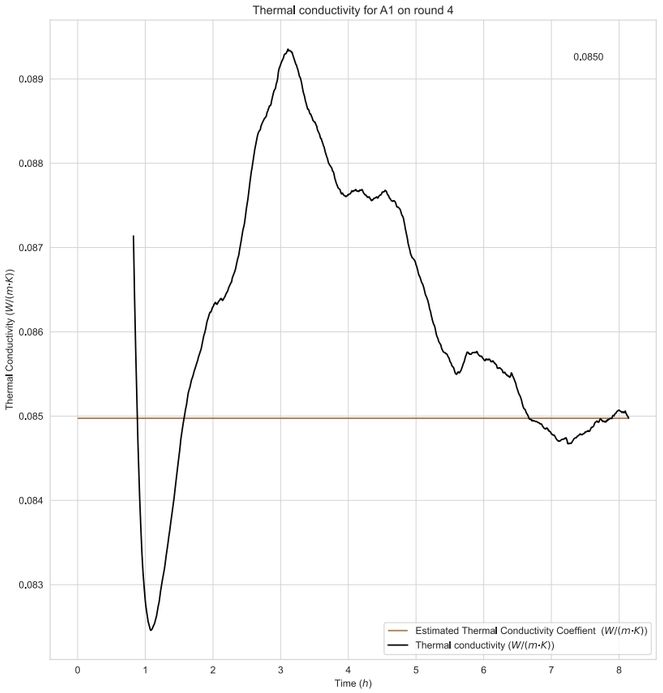

Fig x.x Hotbox measurements (flux, temperature and thermal conductivity) for sample A1 Top: round 3, bottom: round 4

A1

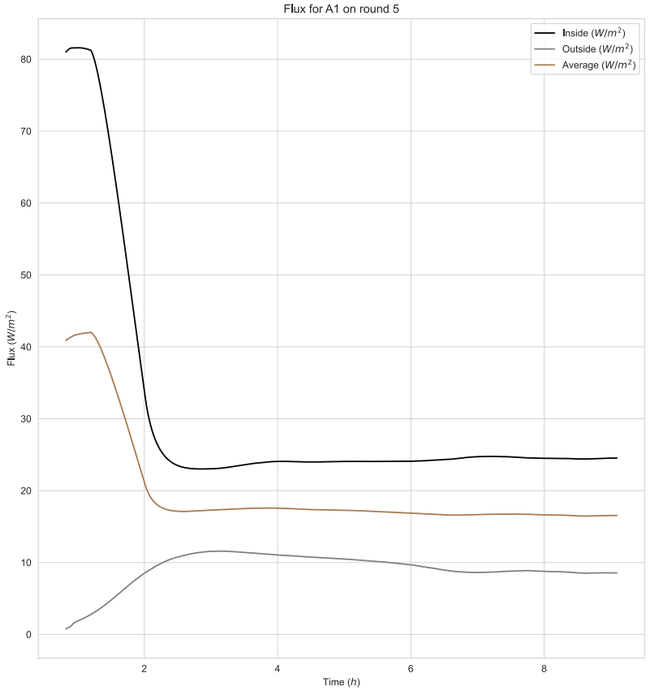

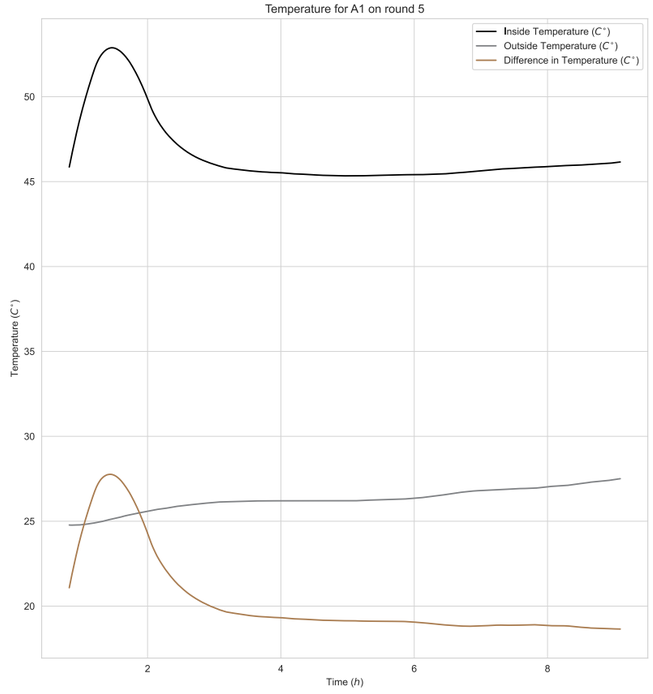

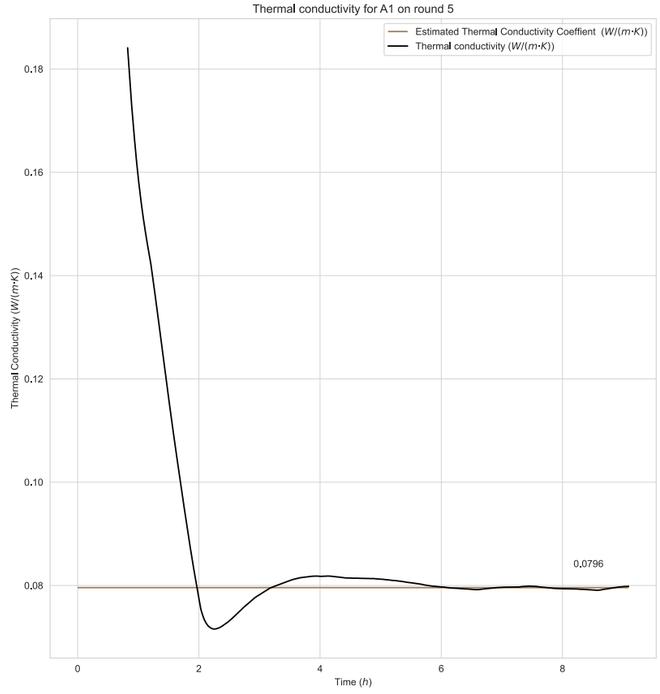

Fig x.x Hotbox measurements (flux, temperature and thermal conductivity) for sample A1 on round 5

A2

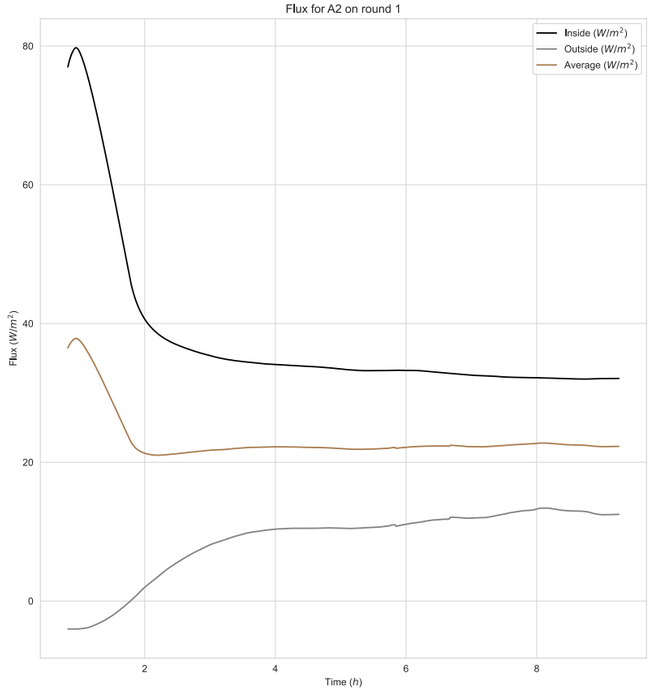

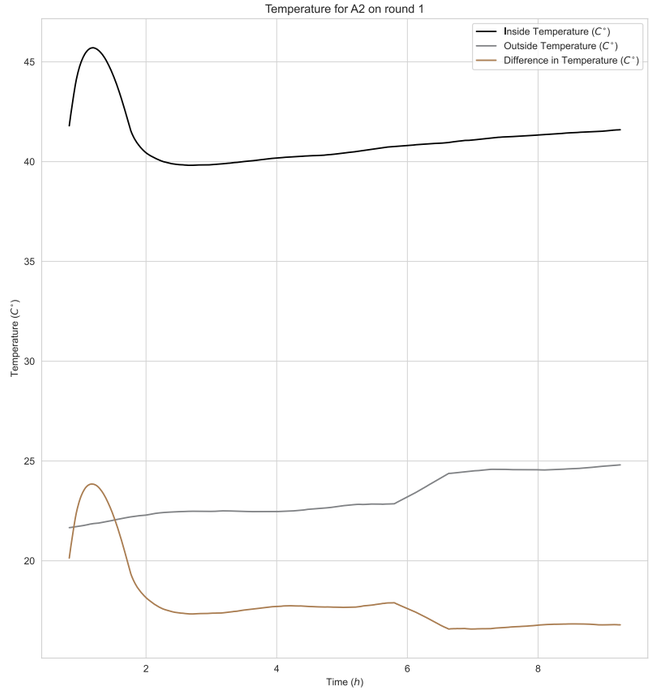

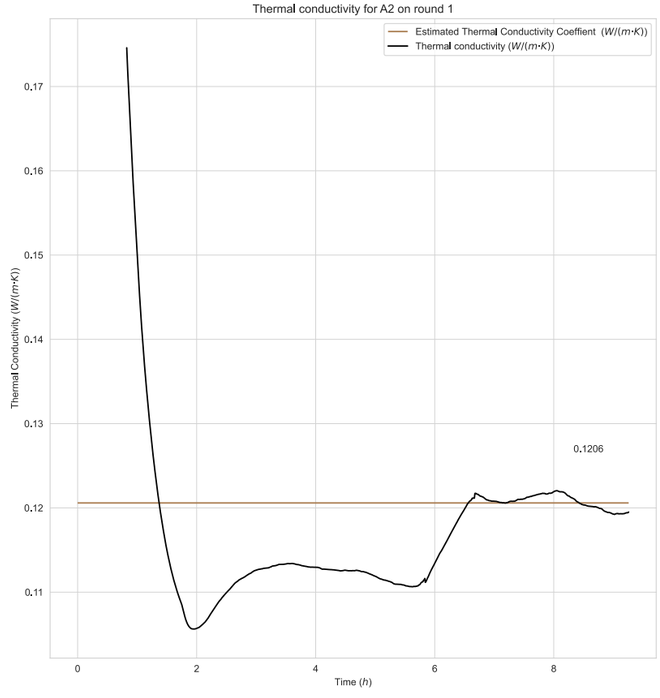

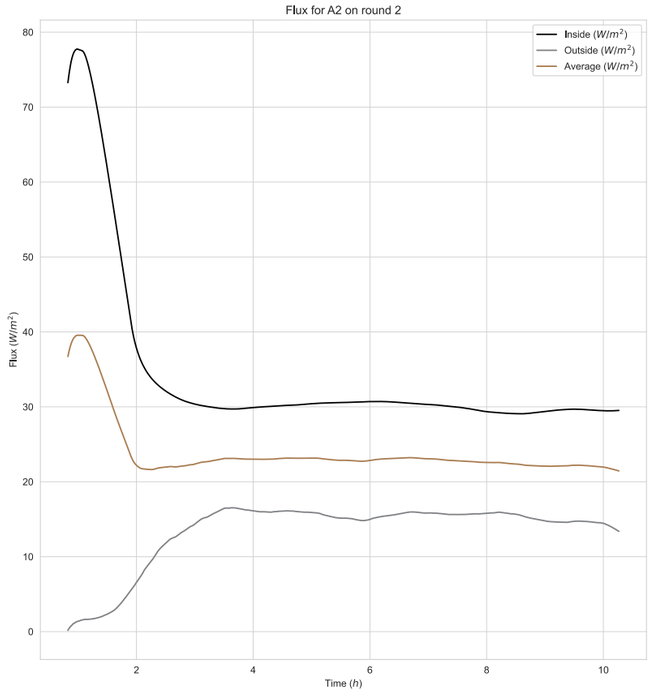

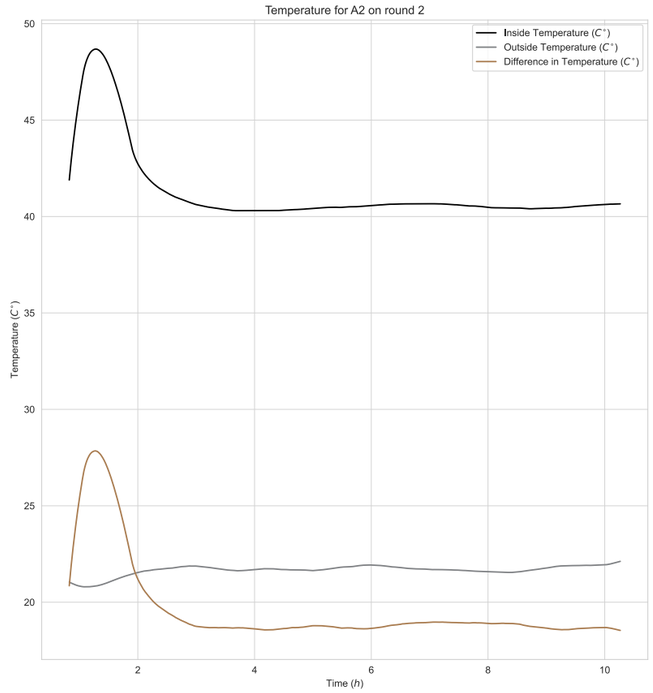

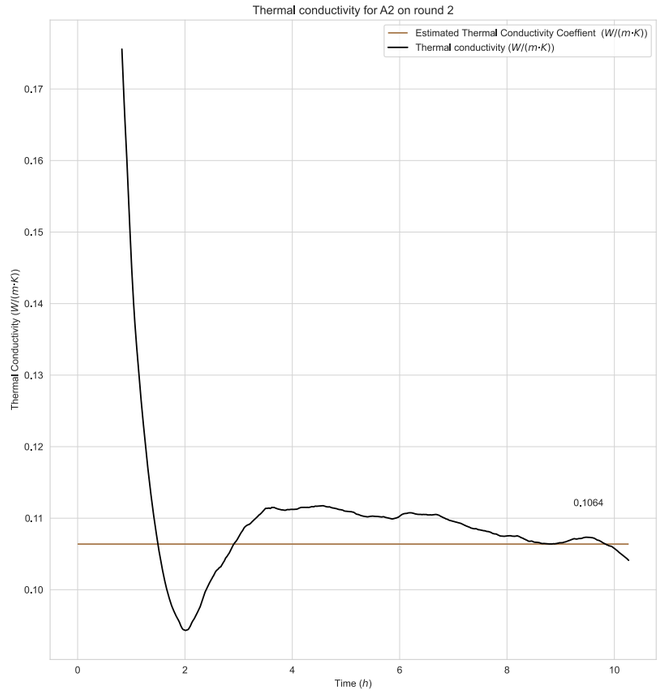

Fig x.x Hotbox measurements (flux, temperature and thermal conductivity) for sample A2. Top: day 1, bottom: day 2

A3

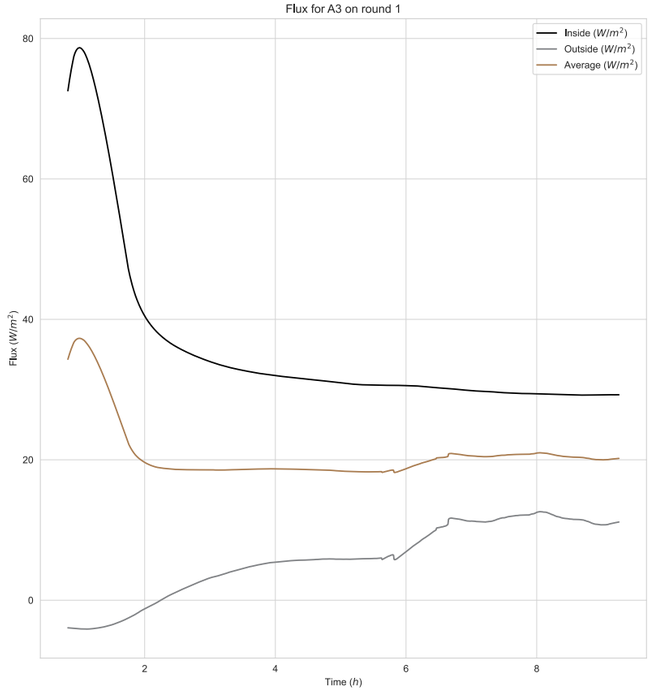

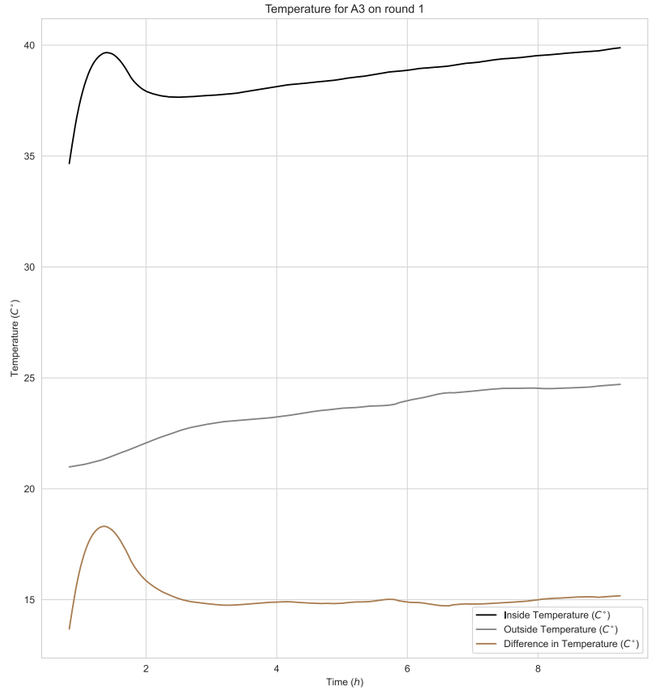

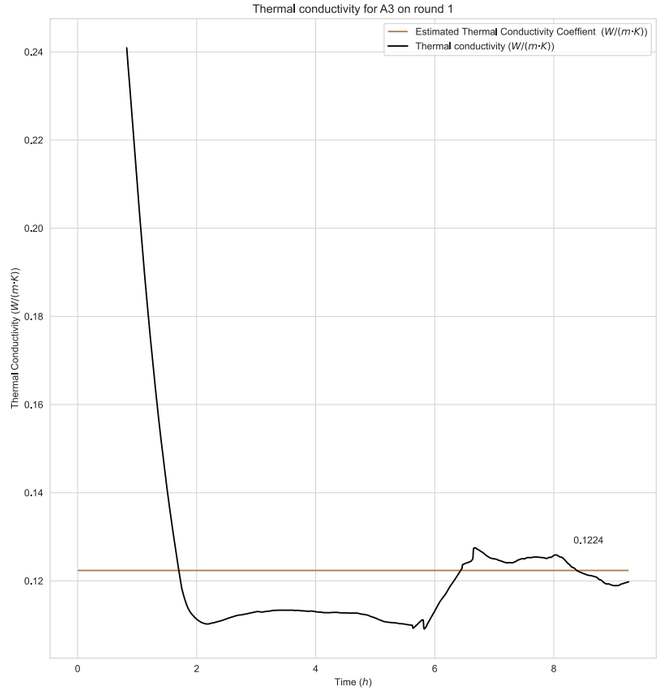

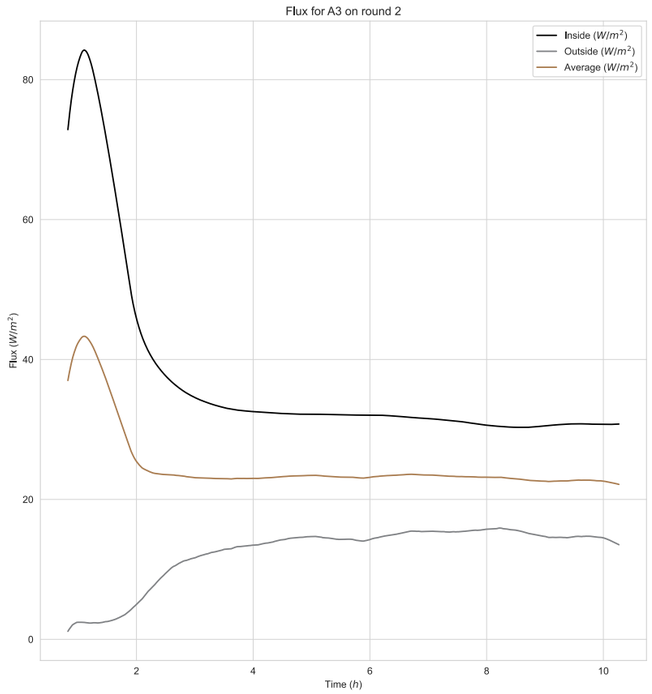

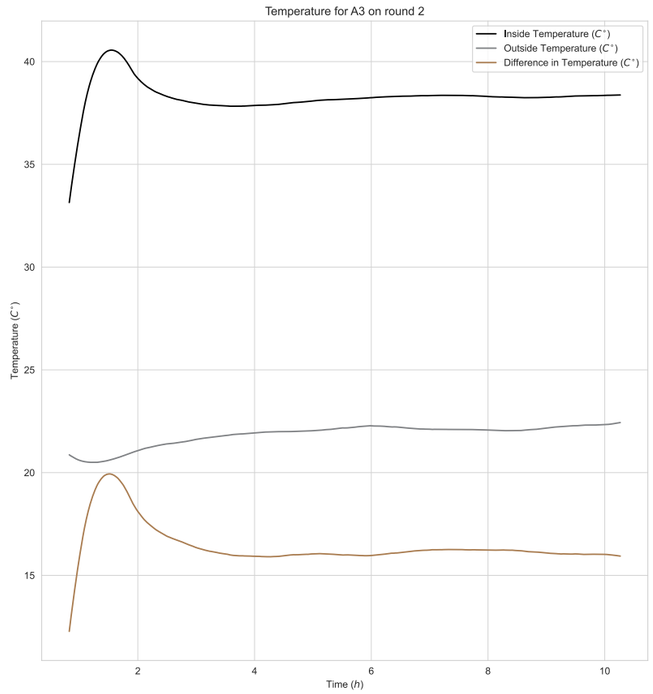

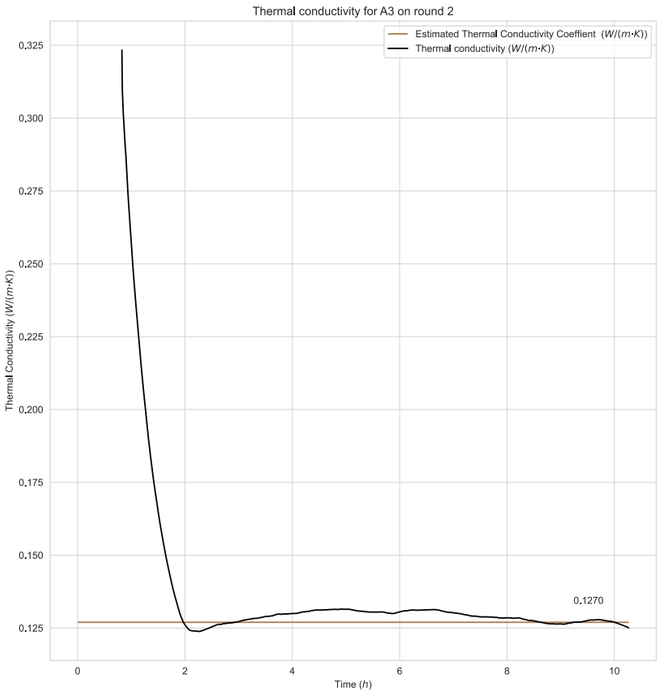

Fig x.x Hotbox measurements (flux, temperature and thermal conductivity) for sample A3. Top: day 1, bottom: day 2

A4

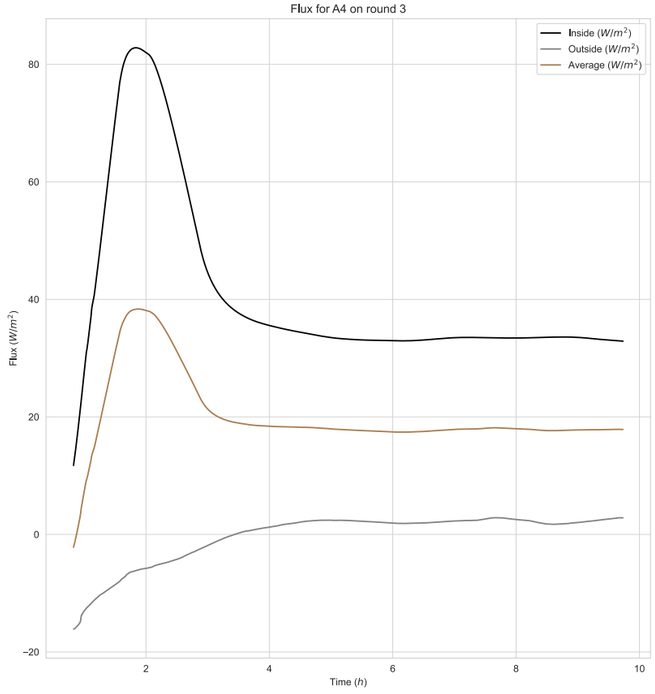

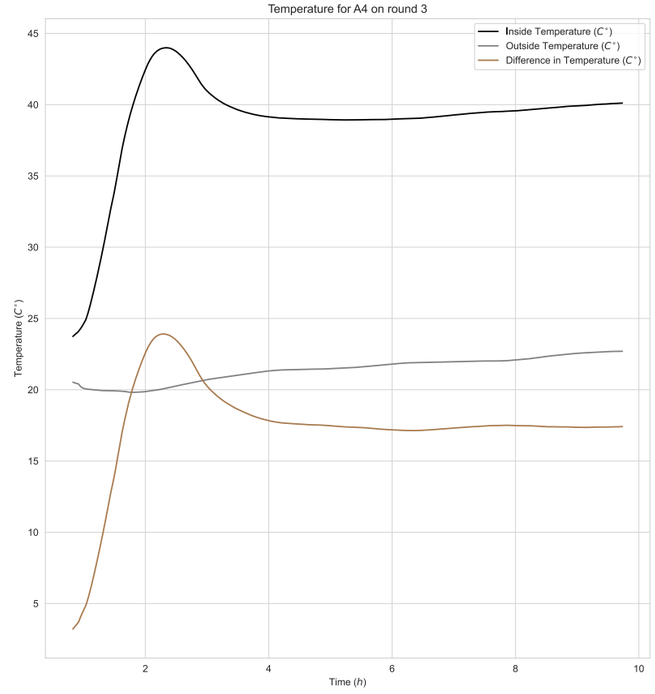

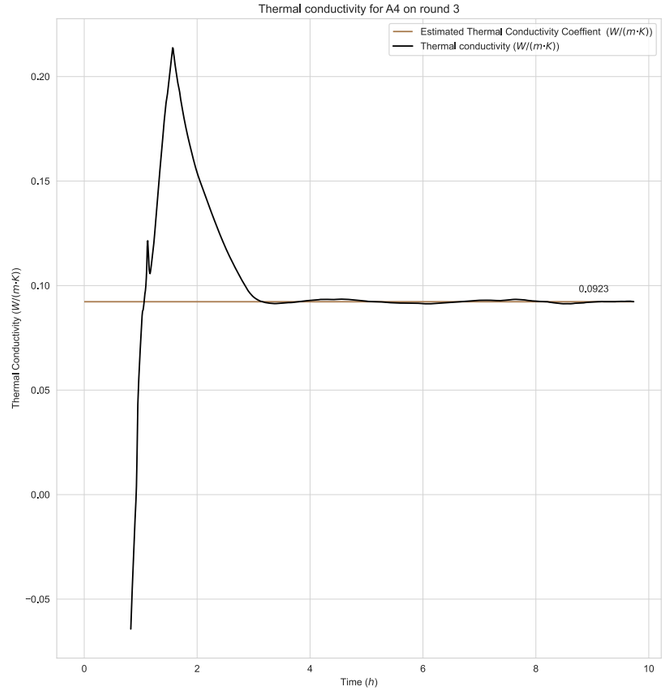

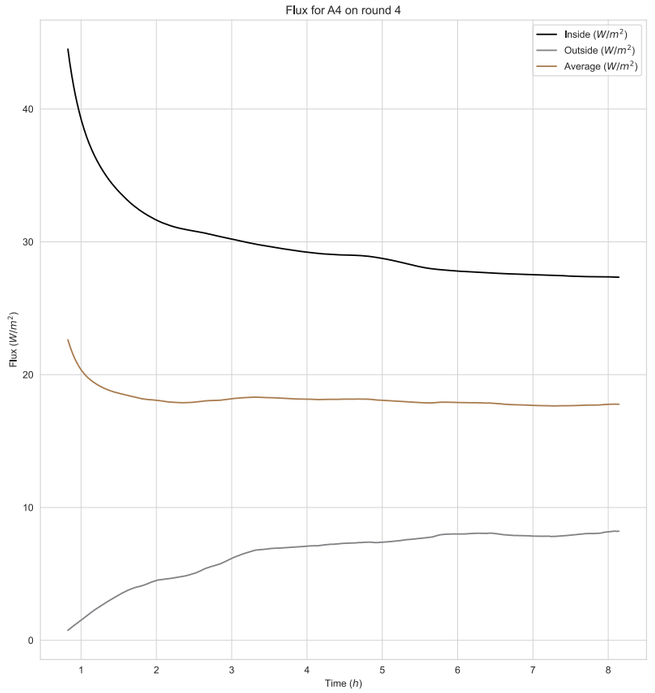

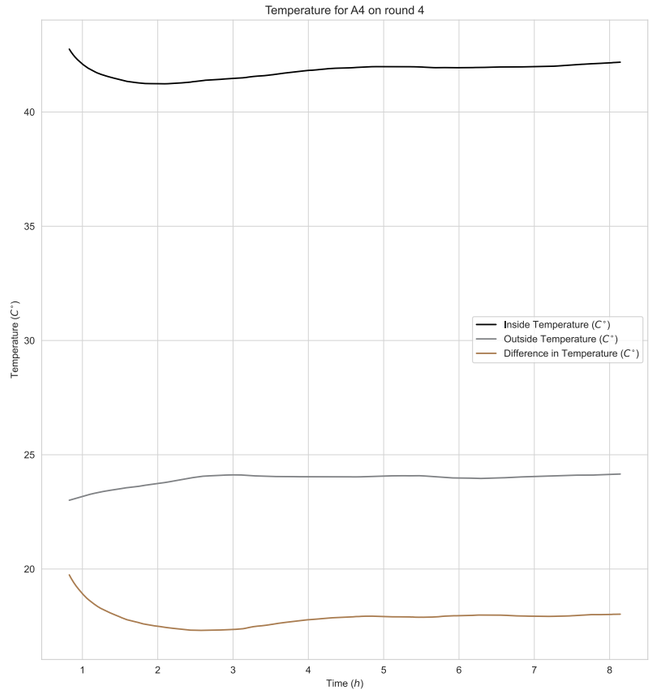

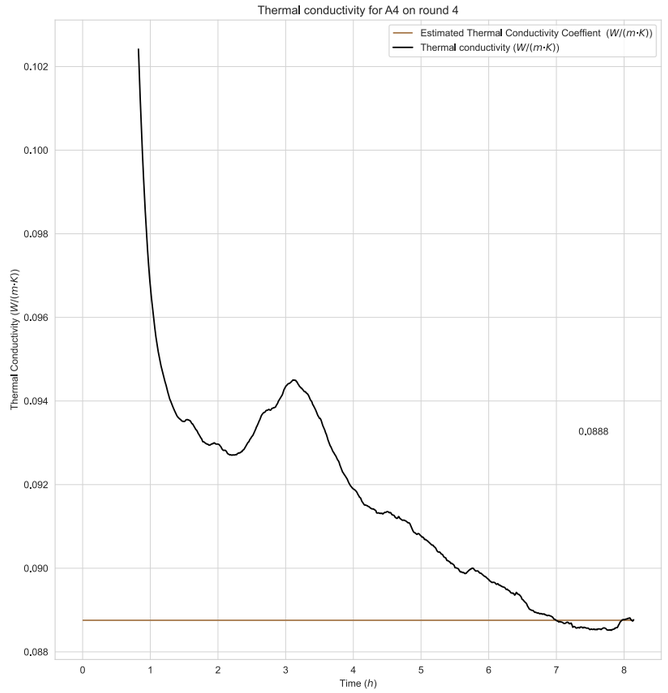

Fig x.x Hotbox measurements (flux, temperature and thermal conductivity) for sample A4. Top: round 3, bottom: round 4

A4

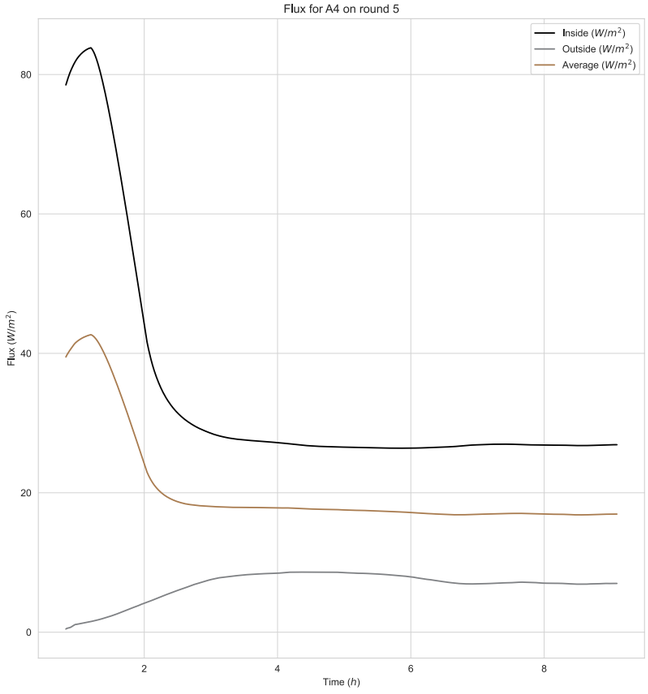

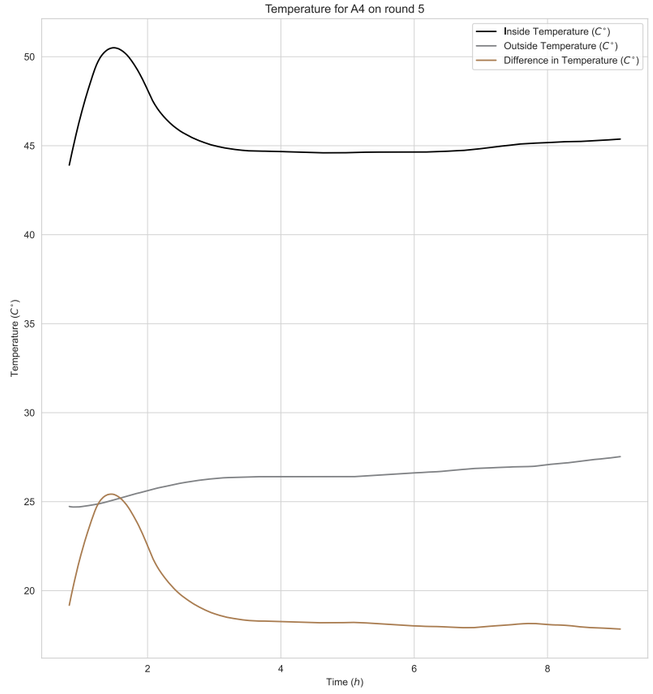

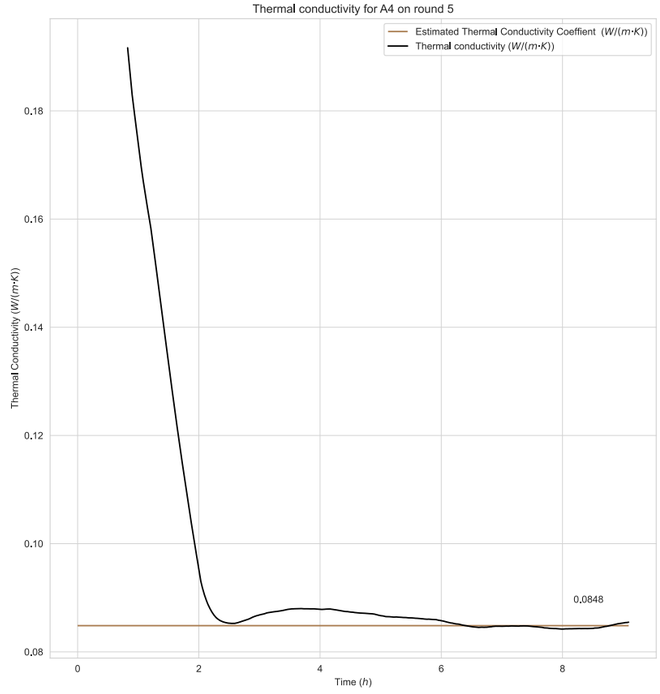

Fig x.x Hotbox measurements (flux, temperature and thermal conductivity) for sample A4 on round 5

A5

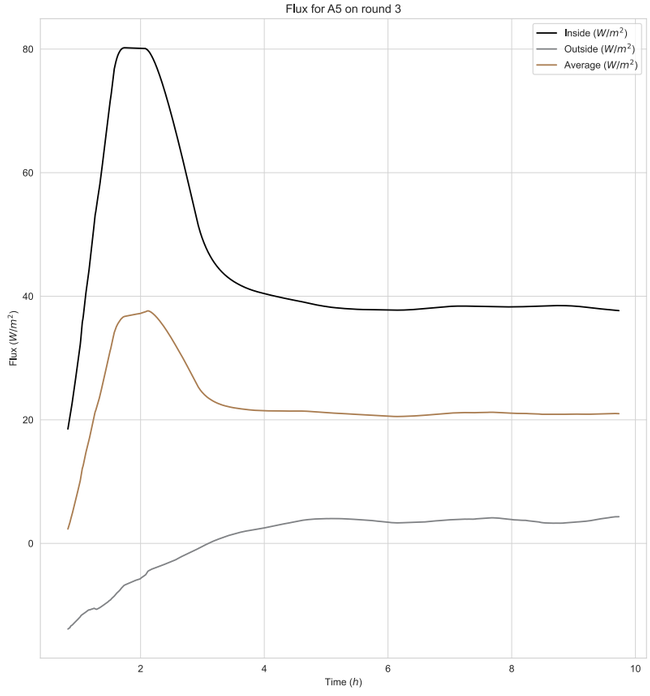

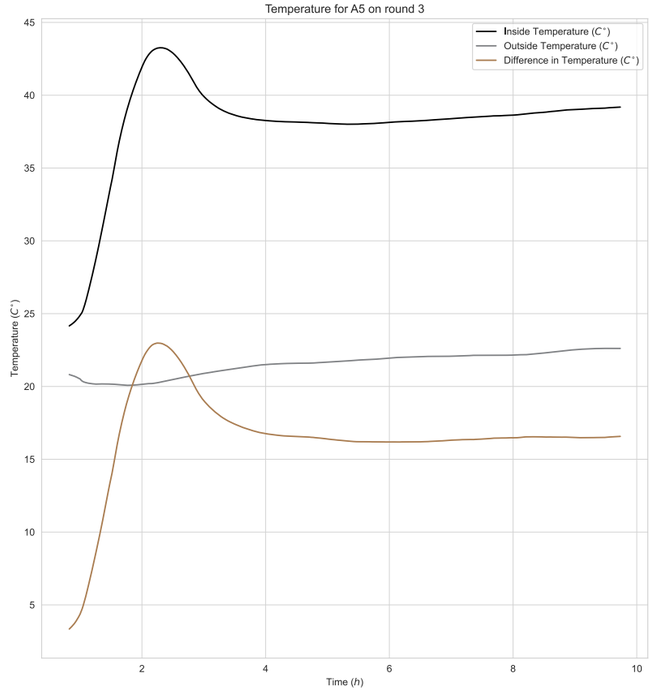

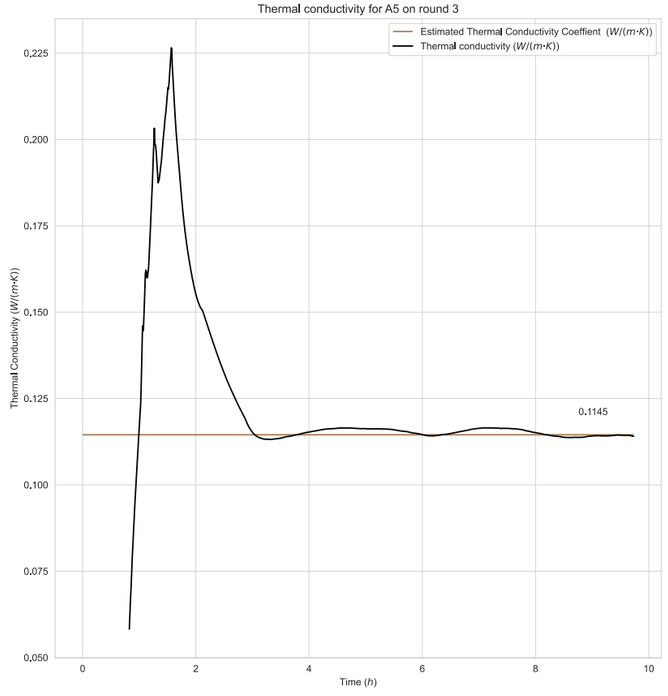

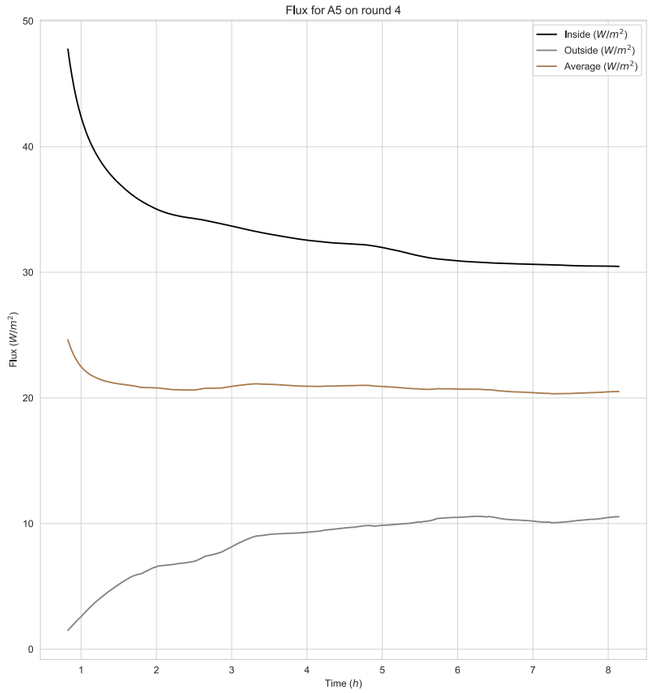

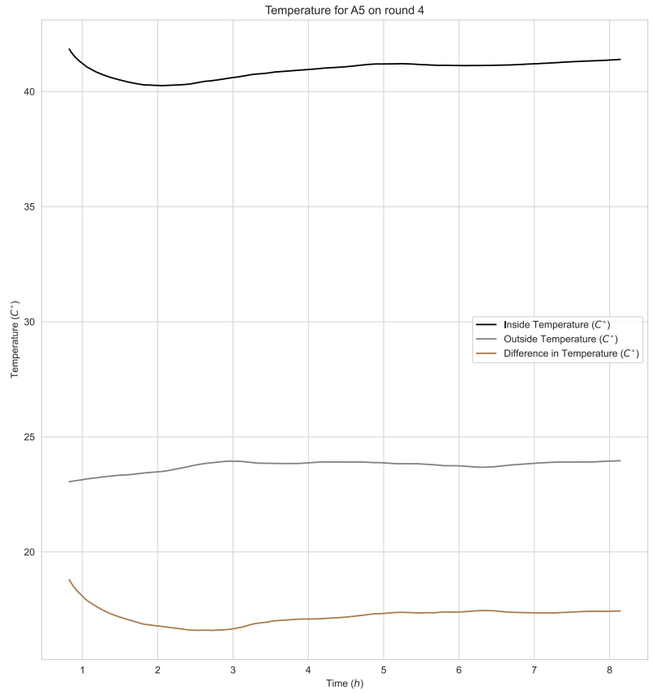

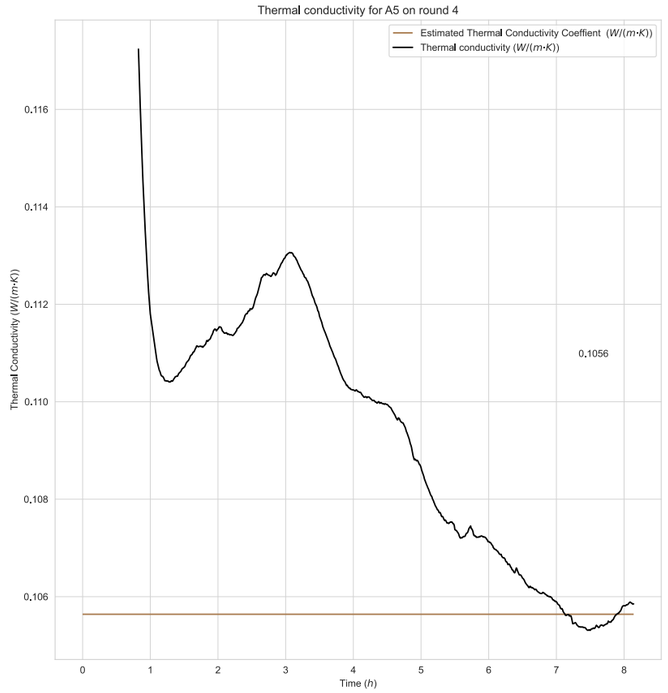

Fig x.x Hotbox measurements (flux, temperature and thermal conductivity) for sample A5. Top: round 3, bottom: round 4

A5

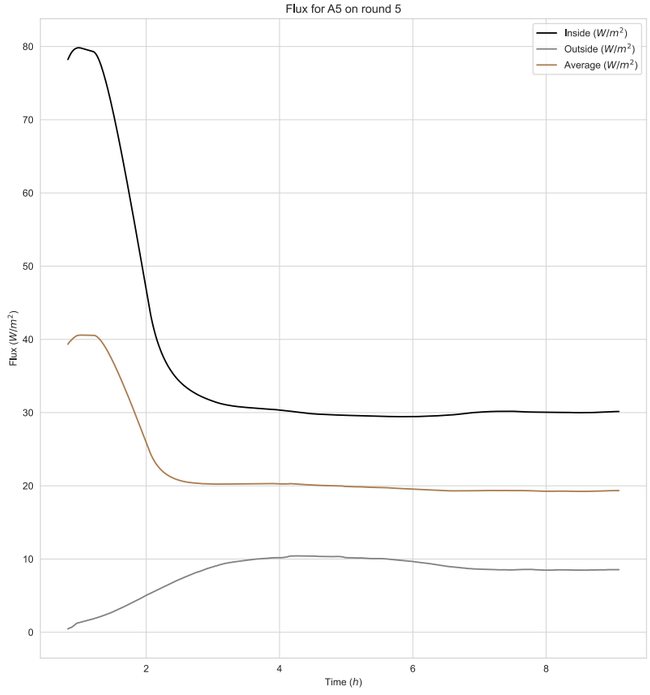

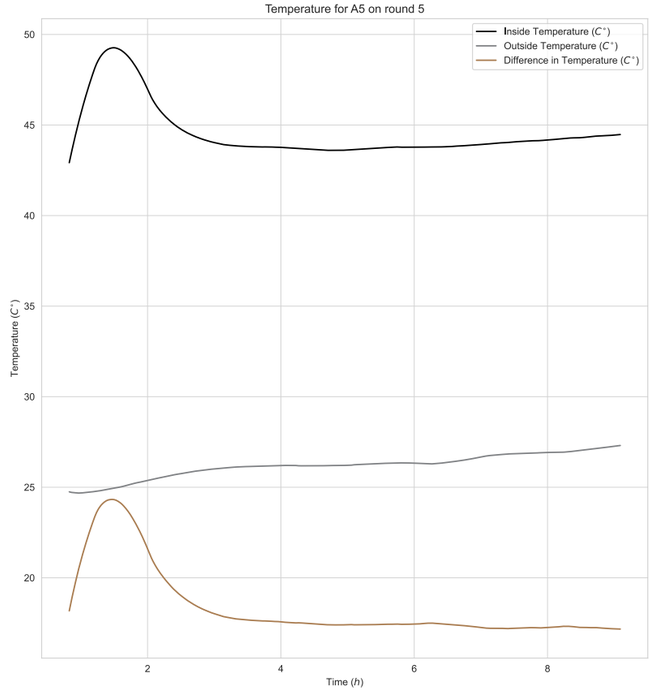

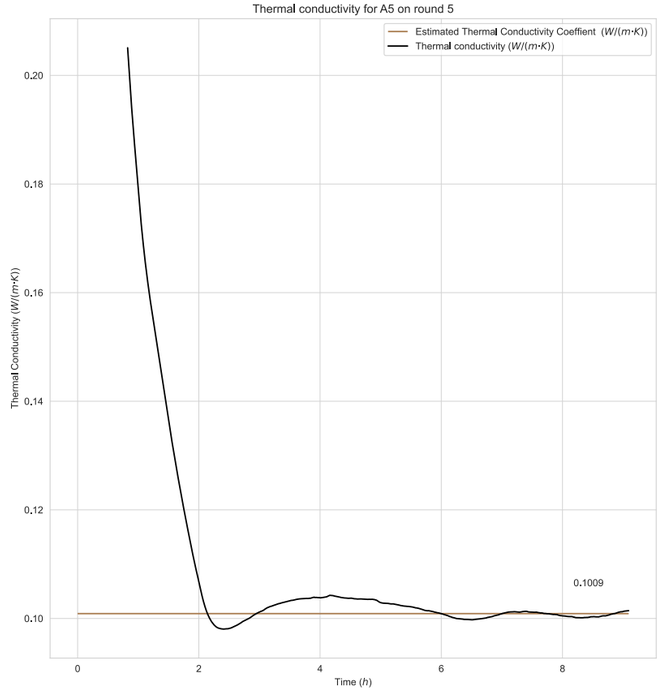

Fig x.x Hotbox measurements (flux, temperature and thermal conductivity) for sample A5 on round 5

A5*

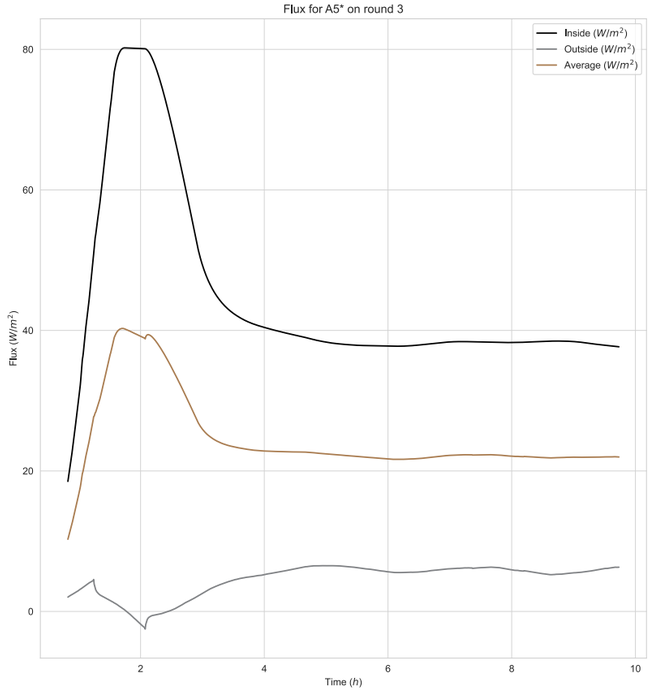

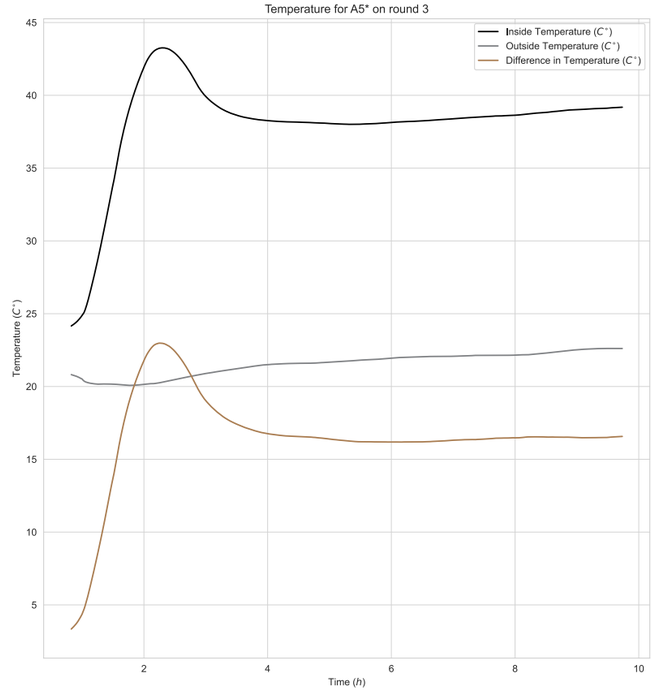

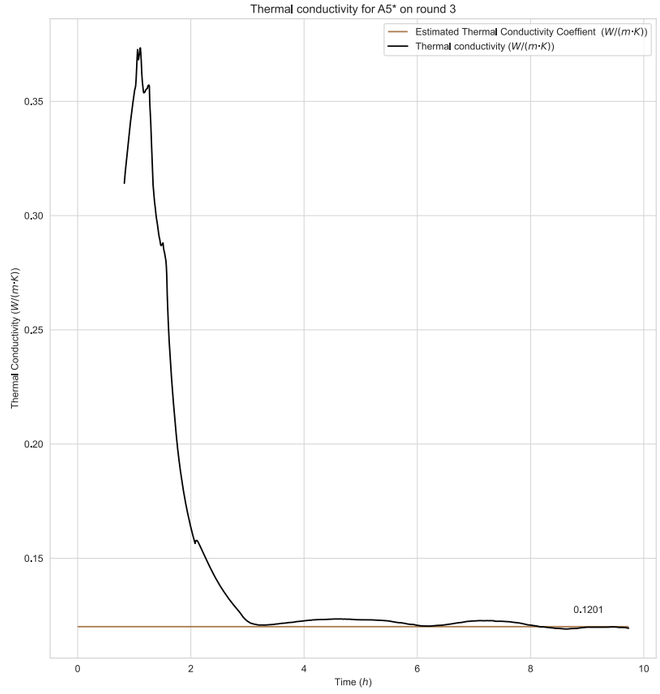

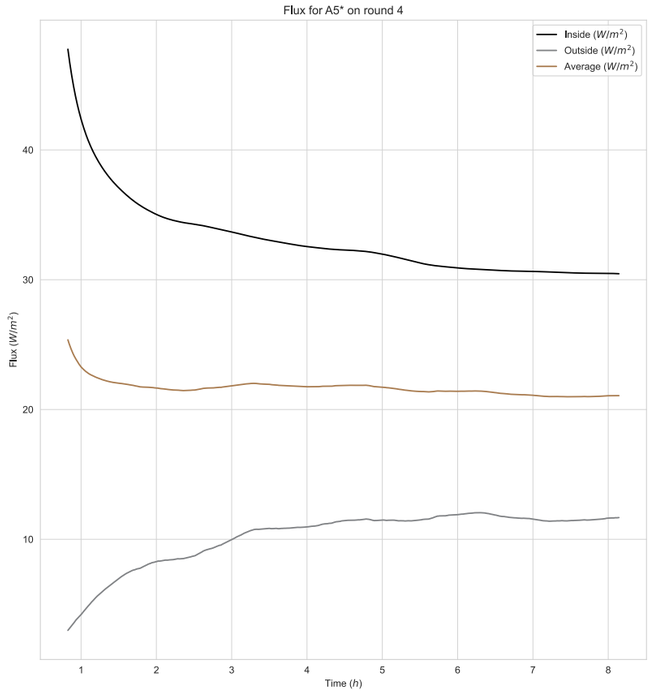

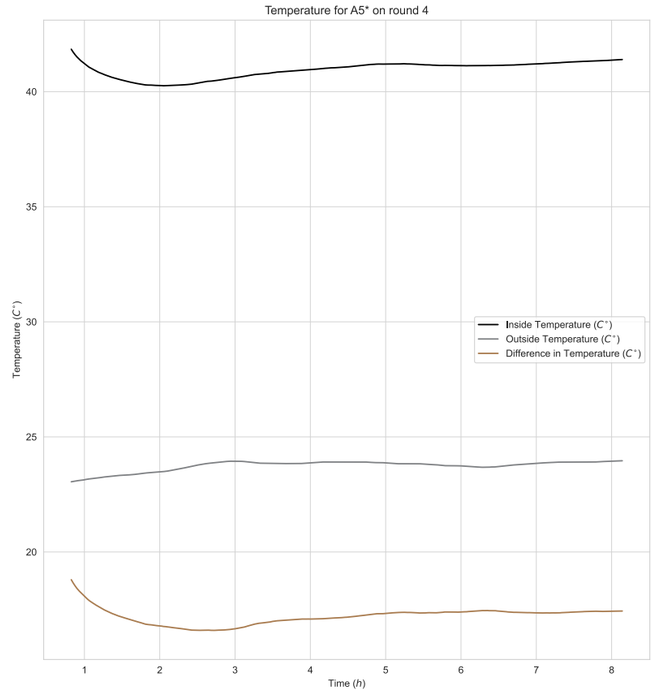

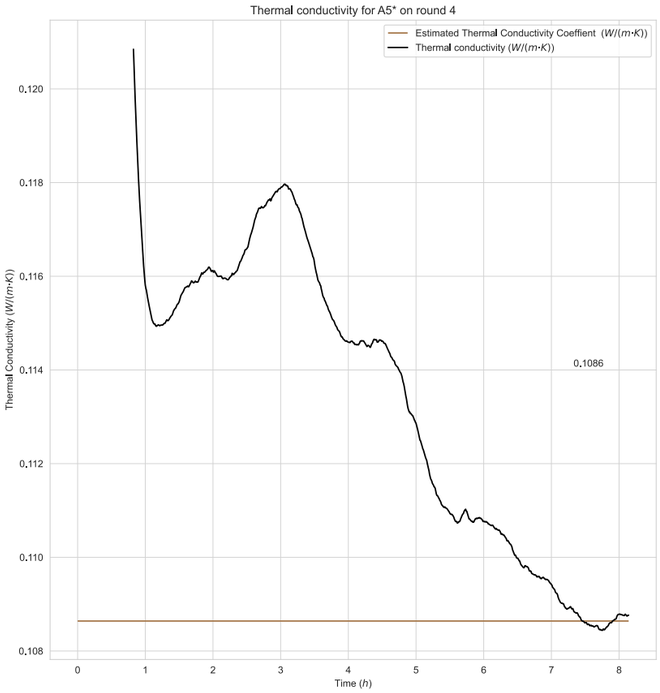

Fig x.x Hotbox measurements (flux, temperature and thermal conductivity) for the second sensor on sample A5*. Top: round 3, bottom: round 4

A5*

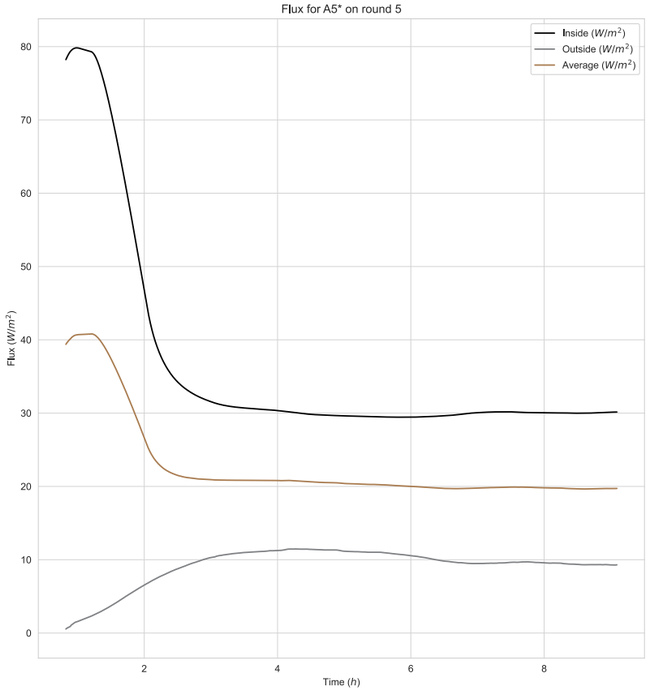

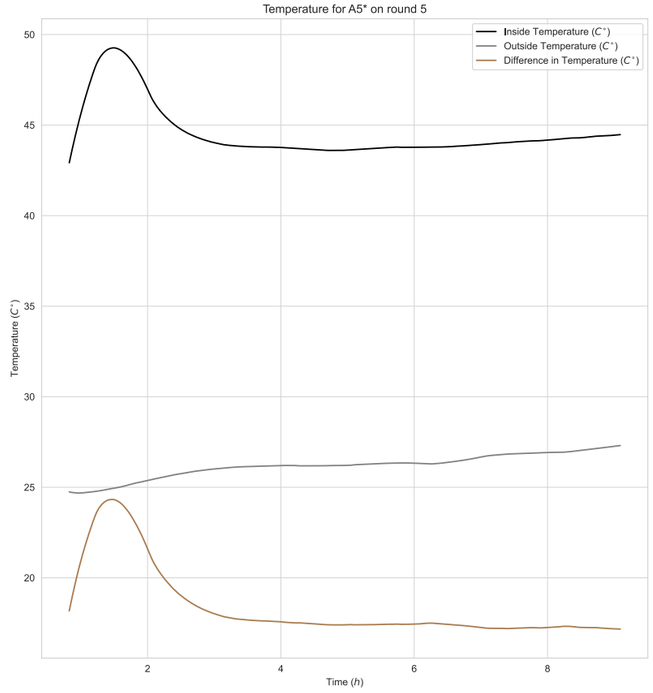

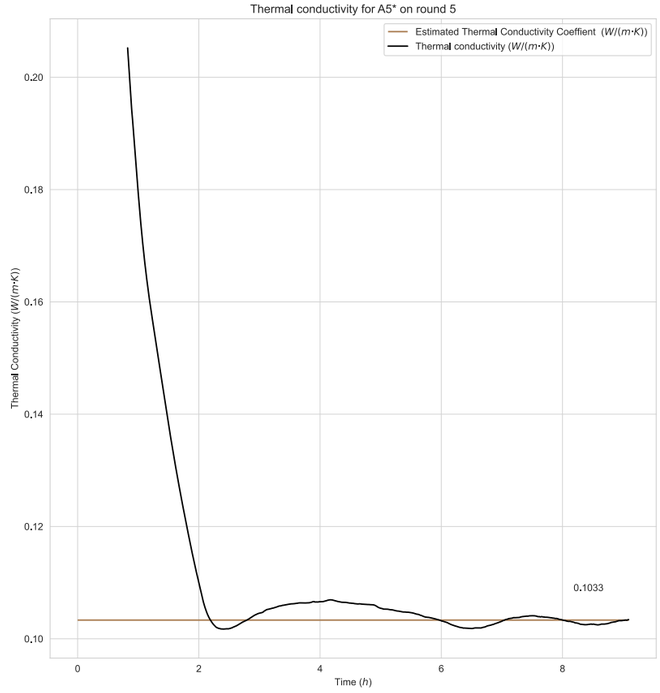

Fig x.x Hotbox measurements (flux, temperature and thermal conductivity) for sample A5* on round 5

A6/7

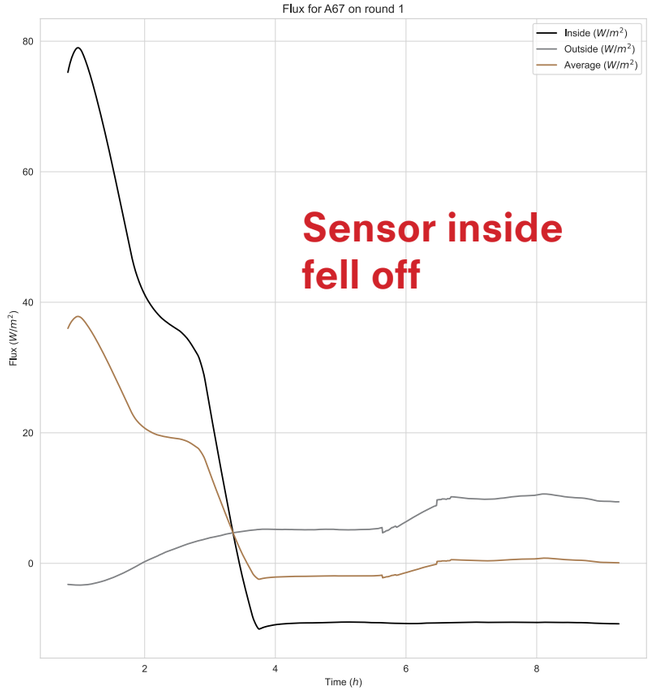

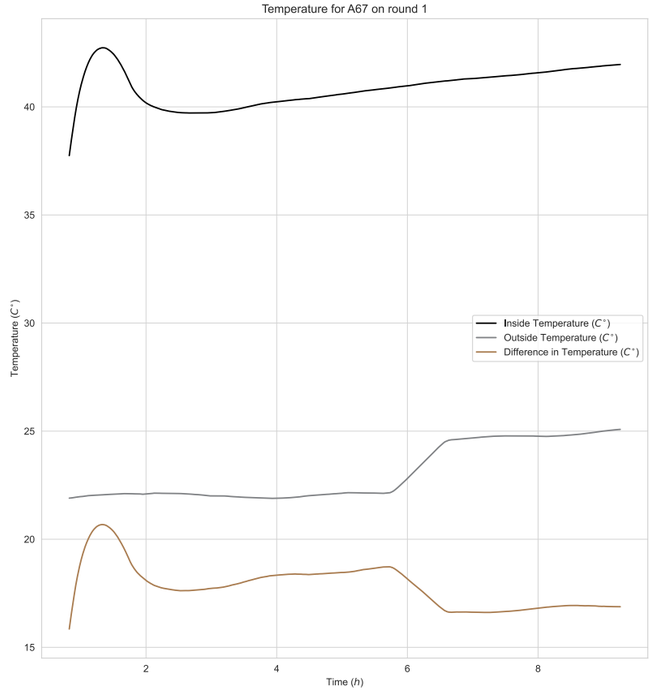

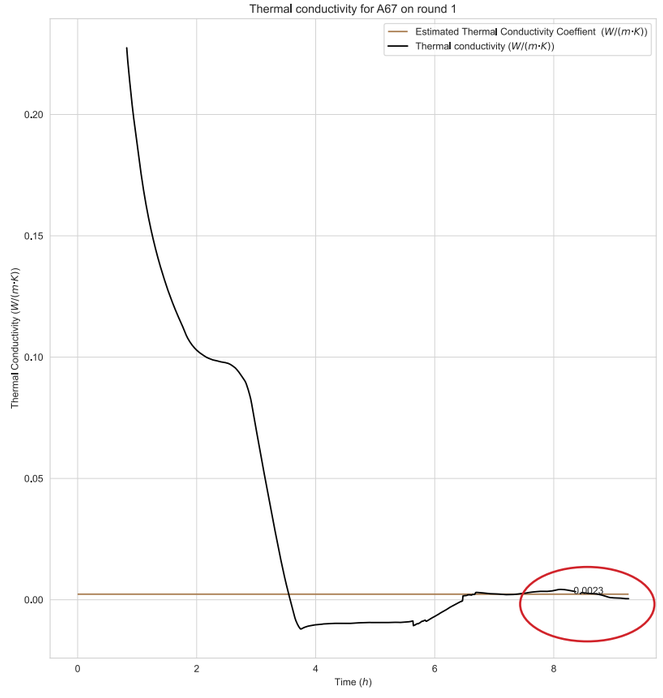

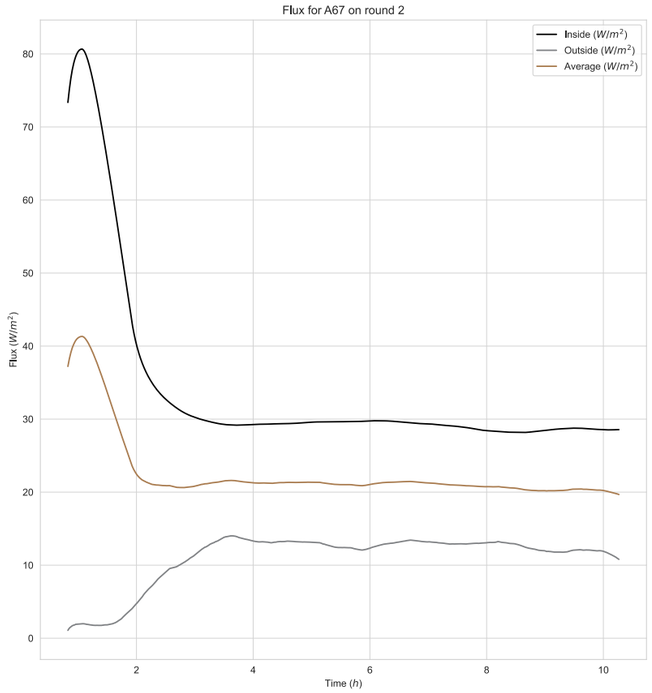

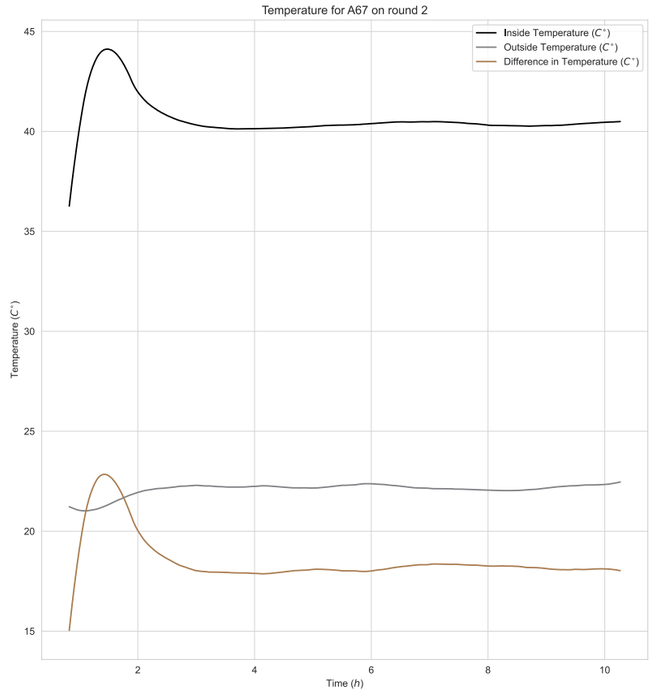

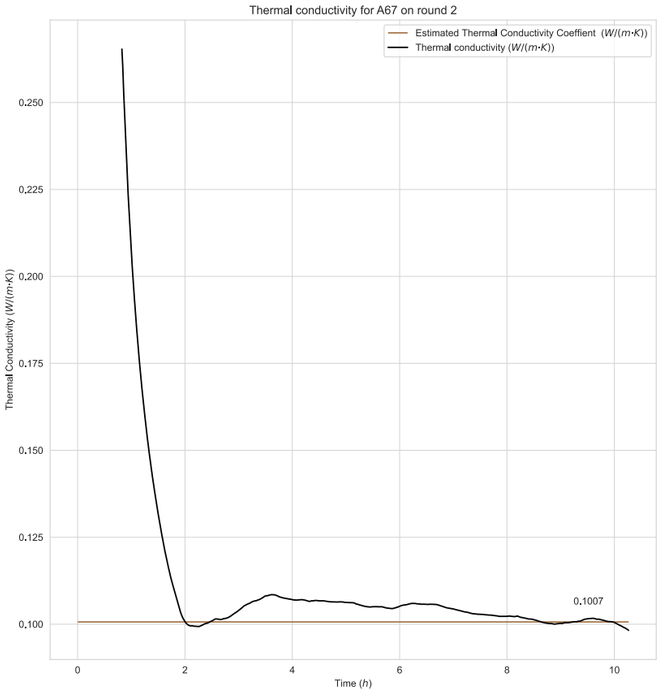

Fig x.x Hotbox measurements (flux, temperature and thermal conductivity) for samples A6 and A7. Top: round 1, bottom: round 2

A8

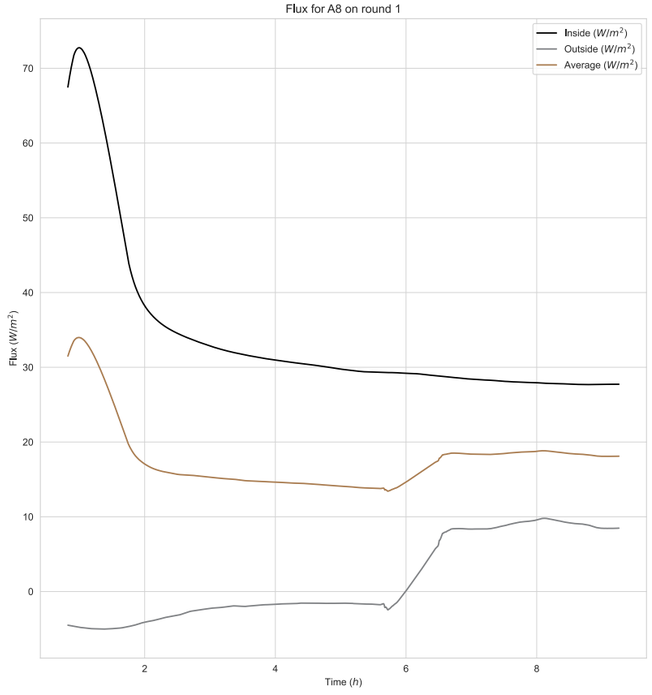

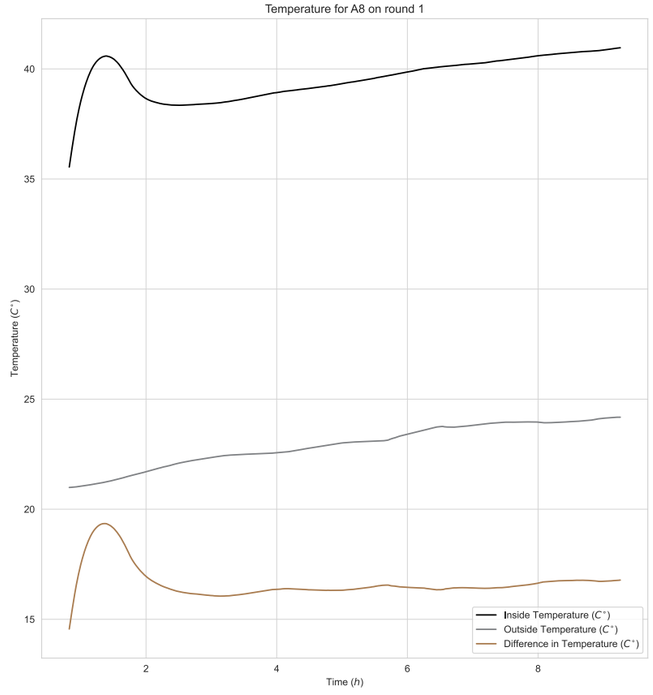

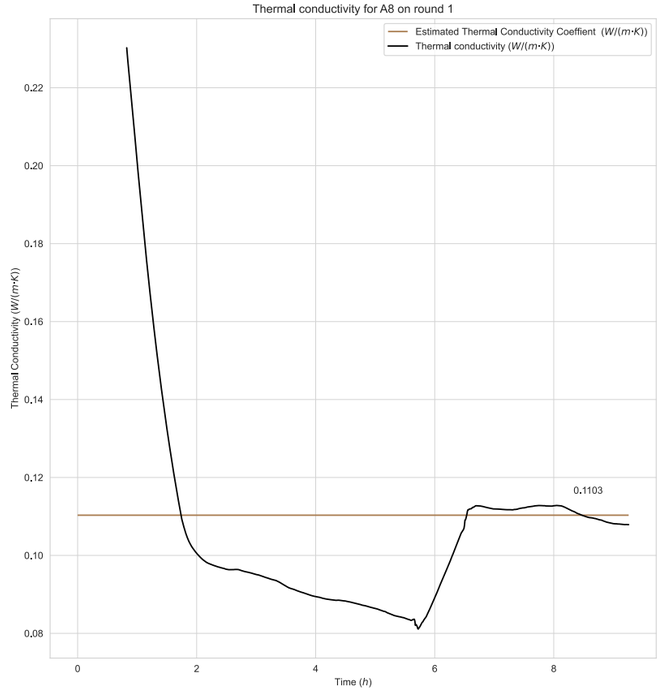

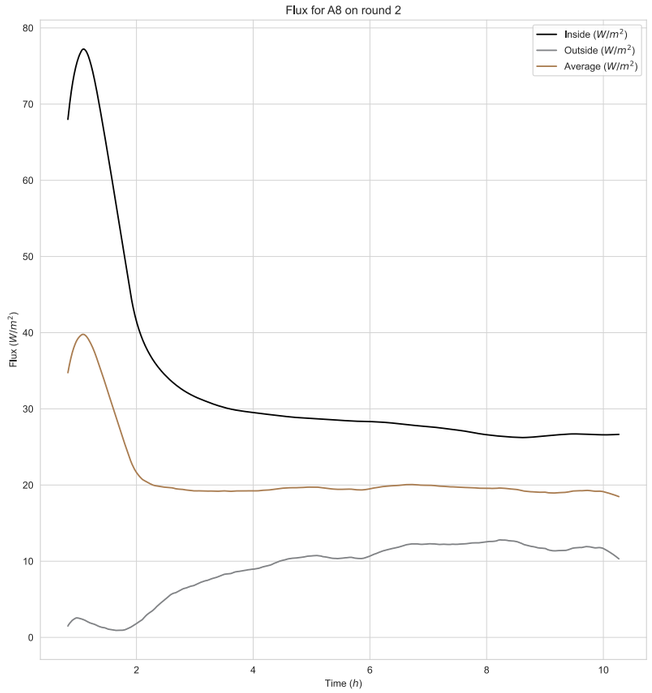

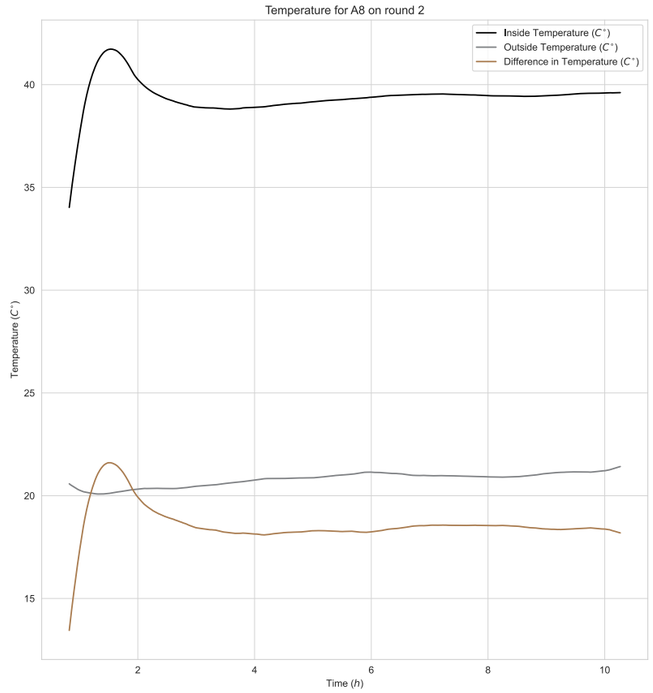

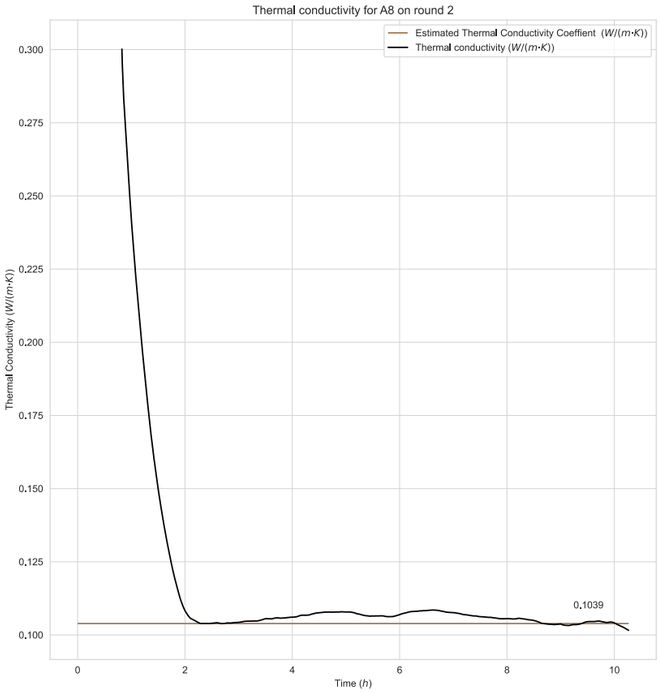

Fig x.x Hotbox measurements (flux, temperature and thermal conductivity) for sample A8. Top: round 1, bottom: round 2

Reflection

Graduation Process

Topic position in the studio

The BT master track focuses on the design of innovative and sustainable building components and their integration into the built environment. This thesis aims to turn hempcrete, a low carbon, age old, artisan material into an industrially manufactured building element. By eliminating the traditional timber frame method and relying on density alone, the project proposes and introduces a new strategy in hemp lime construction.

Results of research approach

By defining the four variables (compaction, layer height, orientation, binder) and linking the four experiments to these variables, the test matrix and result interpretation was kept clear. The material did not behave according to prediction. Curing took longer than expected. Hydraulic lime samples were not ready for testing. The geometry for bending seemed not suitable.

Relation research and design

The outcomes of this research ultimately give the design constraints. The manufacturing variables are directly seen in the design of the hempcrete wall. More importantly, this research shows that building with hempcrete asks for a totally different approach to designing facades.

Moral/ethical issues or dilemmas

The undisclosed mix additives. Hempcrete suppliers treat their additives as trade secrets, so it was not possible to know the exact ingredients and goal of the additives.

Societal Impact

Applicability of results in practice

The findings can be adopted immediately. Each thermal and mechanical measurement reported links back to four controllable production parameters (compaction factor, layer height, orientation and binder type). The first two can be hard coded into a robotic ramming system, the orientation and binder can be integrated into the suggested, prefab manufacturing workflow. Even without the automation, the companies contributing to this research (Yomabouw, EXIE and IsoHemp now have quantified performance data that helps them fine tune their existing product or workflow.

Innovation

The ultimate goal, demonstrating the full wall assembly with a working robot, was not reached. Instead, the target configurations were reproduced by hand. Only separate configurations are tested, combinations are not yet produced and evaluated on performance. Future work can combine these in multiple ways and test them.

Sustainable development

Hemp lime construction can offset the embodied CO2 of more intensive materials elsewhere in the building. In addition, the monomaterial approach reduces demolition waste and simplifies reuse.

Impact on sustainability

Hemp lime walls emit no VOCs and regulate indoor air quality, giving healthier spaces for people. It also offers a sustainable alternative for Dutch and EU farmers.

Socio-cultural and ethical impact

The project links all actors in the chain: fibre hemp farmers, hemp lime manufacturers, architects and contractors. There is a clear need that these all need to work together closely to make this material work.

Wider social context

Dutch and EU policy asks for more biobased and circular materials and projects. This project form the basis for a market ready building element that fits those targets.

Architecture / the built environment

If adopted, architects gain a monolithic wall system that eliminates the need for multi layer facades. This asks for a different approach to designing and building. It results in a modern reinterpretation of a traditional construction practice, which expands the options of bio based design.

Master's Thesis | Building Technology

MSc. Architecture, Urbanism and Building Sciences